THE AMERICAN MINERALOGIST

JOURNAL OF THE MINERALOGICAL SOCIETY OF AMERICA

Vol. 42 NOVEMBER–DECEMBER, 1957 Nos. 11 and 12

THE ROLE OF LEAD AND EXCESS OXYGEN IN URANINITE[1,2]

ROBERT M. BERMAN, *Harvard University, Cambridge, Massachusetts.*[3]

ABSTRACT

It has long been known that uraninite varies widely in both composition and properties. This paper is an attempt to describe and explain the variation in properties in terms of the variation in composition. Analyzed samples of uraninite were *x*-rayed, annealed by heating to 550° C. and 900° C. for various times in a nitrogen atmosphere, and *x*-rayed again. A decrease in unit cell size was generally observed. Calculations on the basis of Vegard's Law showed that the ordering of the interstitial oxygens could account for the decrease in cell size on annealing. The interstitial oxygens are not necessarily completely disordered before annealing. The degree of original disorder is dependent on the Rare Earth/ThO_2 ratio; for high ThO_2 and low rare earths, the interstitial oxygens are completely disordered. The degree of disorder apparently depends solely on the composition, and not on the past history of the sample; this implies that the oxygens are being continuously disordered, perhaps by alpha particles, to an equilibrium point determined by the R.E./ThO_2 ratio. The degree of ordering of the interstitial oxygens also accounts for the difference in cell size between vein pitchblendes and those from the sediments of the Colorado Plateau.

A study was also made of the degree of oxidation of uraninites. Although the uranium in many pegmatitic uraninites is more oxidized than can be obtained with the cubic UO_2 phase in the laboratory, if the atoms proxying for uranium are calculated into the structural formula, and the lead is assumed to be radiogenic and calculated as original uranium, almost all pegmatitic uraninites fall into the range of interstitial oxygen content obtainable in the laboratory. This fact supports the auto-oxidation hypothesis.

Many of the vein and sedimentary pitchblendes have compositions close to U_3O_8, although they are cubic. They may have crystallized as U_3O_8, then decomposed to the cubic phase and an amorphous phase. This suggests that the stability range of U_3O_8 includes only very exceptional natural conditions.

Vegard's Law calculations, differential leaching, and other lines of evidence indicate that lead, including radiogenic lead, is exsolved from uraninite. A study of *x*-ray line

---

[1] Contribution from the Department of Mineralogy and Petrography, Harvard University, No. 375 This paper is a condensation of a Ph.D. thesis prepared under the direction of Prof. Clifford Frondel. The original thesis contains detailed descriptions of specimens, equipment and technique, and extensive summaries of the literature, which have necessarily been greatly reduced or eliminated in this condensation. Copies of the thesis are available in the Harvard Library.

[2] Published by permission of the Director, U. S. Geological Survey.

[3] Present address, Westinghouse Bettis Plant, Pittsburgh 30, Pa.

intensities indicates that it exsolves as oriented monomolecular layers of orthorhombic PbO (massicot) along cube planes in the uraninite, separating the uraninite crystallites so that the *x*-ray reflections interfere destructively to different degrees for different directions.

SUMMARY OF RELATIONSHIPS BETWEEN CERTAIN URANIUM OXIDES

At least twenty-two different phases have been reported in the uranium-oxygen system. Quite possibly as many as thirteen actually exist. One is known to occur in nature. This section is intended as a partial synthesis of the data available in the chemical literature on this system.

U_4O_7, $UO_{1.75}$

The list of phases pertinent to the present discussion, in order of increasing oxidation, begins with U_4O_7. Zachariasen announced this phase in a still-classified report issued in 1947. Katz and Rabinowitch (1951) report that they found a cubic phase intermixed with UO_2, but with the somewhat larger unit cell $a_0 = 5.488$ Å. Zachariasen called it $UO_{1.75}$ on the basis of extrapolation of the cell size from UO_2. Katz and Rabinowitch discuss the possibility of a continuous series between $UO_{1.75}$ and UO_2. Wasserstein (1951) postulated that certain uraninites may have crystallized as $UO_{1.75}$, and been oxidized from there. More recently, in a controversy with Wasserstein (1954), Katz and Hoekstra pointed out that the evidence for the existence of $UO_{1.75}$ rests entirely on *x*-rays, that no chemical data are available, and the relationship between composition and cell dimensions in the cubic UO_2 phase is not well established or understood. The extrapolation to $UO_{1.75}$ is unwarranted, and the existence of this phase is extremely doubtful.

α-UO_2

α-UO_2 is usually obtained as a fine, brownish-black powder by reducing a higher oxide with hydrogen or ammonia. It was found by Goldschmidt and Thomassen (1923) to have a fluorite-type structure. Rundle (1948) gives the unit cell edge as $a_0 = 5.4692 \pm 0.0005$ Å at 25° C. UO_2 takes up additional oxygen without changing its structure when heated to 200–300° C. in air. This oxidation has been studied by Biltz and Muller (1927), Grønvold and Haraldsen (1948), Jolibois (1947) and many others, but the most complete and reliable data were obtained by Alberman and Anderson (1949). They found that pure UO_2 remained cubic as it oxidized, until a composition of $UO_{2.2}$ is reached. Above $UO_{2.2}$, one of the axes gradually became longer than the other two, and the material became tetragonal. The tetragonal phase continued to $UO_{2.32}$. Any attempt to oxidize it further at one atmosphere causes the appearance of a second phase, related to U_3O_8.

When Th is present, the tetragonal phase is suppressed, and the cubic phase continues to $(U, Th)O_{2.32}$. The subscript 2.32 remains virtually constant, until Th substitutes for half the U. At the mid-point of the series, it is possible to oxidize to $(U_{0.5}Th_{0.5})O_{2.34}$. The rare earths may behave similarly. The highest subscript for the oxygen which can be reached in a laboratory experiment, as the end of a continuous series with UO_2, will be referred to as the laboratory limit. As the series moves from the mid-point toward thoria, the laboratory limit falls from 2.34 to 2.0.

The effect of increased pressure on the oxidation limit has not been studied. However, R. Collette (pers. comm.) in an attempt to synthesize coffinite, subjected U_3O_8 and silica in a sealed gold capsule to pressures of 4000 atm., and a temperature of about 700° C. The capsule was recovered in a sealed condition; there was no opportunity for hydrogen generated by the steel bomb walls, or any other reducing agent, to affect the sample. The *x*-ray pattern of the run showed quartz and a cubic phase which evidently must have had the composition $UO_{2.67}$. U_3O_8, which is stable under atmospheric pressure, cannot react to high pressure by emitting oxygen gas. Increased pressure favors a reaction that decreases volume. The specific gravity of U_3O_8 is 8.39, and that of UO_2 is 10.96.

The excess oxygen is interstitial. The fluorite-type structure has holes approximately the diameter of the oxygen ion, at the $(\frac{1}{2}, 0, 0)$ and $(\frac{1}{2}, \frac{1}{2}, \frac{1}{2})$ positions. If all these holes could be filled, the composition would be UO_3. However, the interstitial oxygens are surrounded by eight other similarly charged oxygens. The mutual repulsions set up probably represent the structural control that determines the laboratory limit.

In α-UO_2, the interstitial oxygen has little or no effect on the cell size. The repulsion of the oxygen ions around it is balanced by the shrinkage of the U^{+4} to the U^{+6} ion. Alberman and Anderson could not detect any significant change in the dimensions of the unit cell from $UO_{2.0}$ to $UO_{2.2}$. Biltz and Muller (1927) did not use *x*-ray diffraction, but their chemical and specific gravity data show that the mean molar volume did not change. And finally, the unit cell size of pegmatitic uraninites can be predicted from the composition if one assumes (among other things) that the state of oxidation does not affect the unit cell size.

Under atmospheric conditions, as the temperature increases above 300° C., the cubic phase will tolerate less and less oxygen. At 1000° C., it departs very little from stoichiometric UO_2. If the material already has a composition between UO_2 and $UO_{2.25}$, and it is heated to 1000° C. in vacuum, it decomposes into UO_2 and U_4O_9. This was observed in synthetic samples by Alberman and Anderson, and in natural samples by Brooker and Nuffield (1952).

Tetragonal $UO_{2.2}$–$UO_{2.32}$

At $UO_{2.2}$, Alberman and Anderson found that the cubic form began to develop anisotropy, and became tetragonal. The axial ratio c/a reaches a value of about 1.04 at the laboratory limit. When this tetragonal phase is heated above 300° C., samples less oxidized than $UO_{2.25}$ decompose into appropriate amounts of UO_2 and U_4O_9. Above $UO_{2.25}$, U_4O_9 and Hoekstra's $UO_{2.6}$ phase appear.

U_3O_7 ($UO_{2.33}$)

In 1947, Jolibois reported the results of heating UO_2 at various temperatures in a heating balance. He found that UO_2 oxidized to $UO_{2.33}$ at 210° C. No further oxidation took place until a temperature of 300° wa reached, at which a phase related to U_3O_8 began to form. The $UO_{2.33}$ was tetragonal, and Jolibois concluded that it was a new compound with the composition U_3O_7. The observations are not in conflict with the data given by Alberman and Anderson for their tetragonal phase. A comparison of the *x*-ray data given in the original references leaves little doubt that the phases are identical.

Delta Phase

Grønvold and Haraldsen (1948) reported a tetragonal 'delta phase' formed by oxidation of UO_2 at 200° C. They noted that it decomposed at 270°, and ascribed to it a "narrow range of homogeneity around $UO_{2.40}$." The subscript 2.40 does not seem to represent a chemical analysis, but rather a blank region in which a hitherto unknown stability field could be fitted. The following table compares the cell dimensions of Alberman's tetragonal phase at $UO_{2.303}$ and Grønvold's delta phase, and shows the two are almost certainly the same phase.

TABLE 1. LATTICE PARAMETERS OF TETRAGONAL PHASES

	a_0	c_0
$UO_{2.303}$	5.396 Å	5.564 Å
Delta Phase	5.37	5.54

β-UO_2 or U_4O_9

When the oxidized cubic or tetragonal phase is heated to 1000° C. in an inert atmosphere, it decomposes, and the lines of a cubic phase with a cell edge $a_0 = 5.435$ Å appear on the *x*-ray photographs. For compositions above $UO_{2.25}$, the $UO_{2.6}$ phase also appears. Compositions below $UO_{2.25}$ decompose into the new phase and UO_2. Alberman and Anderson called this new cubic phase "β-UO_2" in their original paper, and later (1954) refer to it as U_4O_9. In their opinion, it is an ordered phase, with the interstitial oxygens occupying the ($\frac{1}{2}$, $\frac{1}{2}$, $\frac{1}{2}$) positions only. In this case, the forces of attraction and repulsion do not balance out, as was the case with the randomly distributed excess oxygens of the alpha phase. The unit cell is contracted inward upon itself, while still remaining isometric. U_4O_9 has the U_4O_8 unit cell of UO_2 with an extra oxygen in the center. The 'unknown oxide *X*' of Brooker and Nuffield (1952) is almost certainly U_4O_9.

Phases Related to U_3O_8

In an article entitled "The Uranium-Oxygen System: $UO_{2.5}$ to U_3O_8," Hoekstra, Siegel, Fuchs and Katz (1955) describe research leading to conclusions which can be summarized as follows.

1. U_2O_5, which had been reported by many earlier authors, does not exist as a phase.
2. From $UO_{2.52}$ to $UO_{2.64}$, there is an orthorhombic phase, with b/a slightly above $\sqrt{3}$.
3. When heated in air, this phase absorbs oxygen and becomes U_3O_8. At room temperature, U_3O_8 is orthorhombic; however, on heating, or on further oxidation toward one of the forms of UO_3, b/a reaches $\sqrt{3}$, at which point the phase becomes hexagonal.
4. The transition from the $UO_{2.6}$ phase to U_3O_8 is apparently continuous at higher temperatures. However, Milne (1951) gives evidence of a mixture of $UO_{2.6}$ and U_3O_8, intergrown in parallel position, in a sample that had stood for a while at room temperature.

A tentative phase diagram for the U-O system at one atmosphere is presented as Figure 1.

SPECIMENS USED IN THIS STUDY

Reference will be made to individual specimens by means of the capitalized portions of the locality names given below. Most of the specimens were taken from the Harvard collection, or were kindly loaned by Dr. George Switzer of the U. S. National Museum; in these cases, the museum numbers are given. The specific gravity and number of the analysis in the appendix are also included. More complete descriptions are available in the original thesis. Some of the uraninite samples analyzed by Hillebrand (1891) were included in Dr. Switzer's gift. These are indicated below.

URANINITE SPECIMENS FROM PEGMATITES

BOQUEIRAO, Rio Grande do Norte, Brazil. H105716. G=7.80. Large, rough crystal, with purple fluorite.

BRANCHVILLE, Conn. USNM 83567. G.=9.733. Anal. 2. Vitreous. Hillebrand (1891).

ELVESTAD, Norway. USNM 83568. G.=9.14. Anal 7. Shows xl. faces. With quartz, muscovite. Hillebrand (1891).

GORDONIA, South Africa (HOLMES) H 92341. G.=8.876. Anal 39, quoted in Holmes (1934). Sub-vitreous, with brownish alteration products.

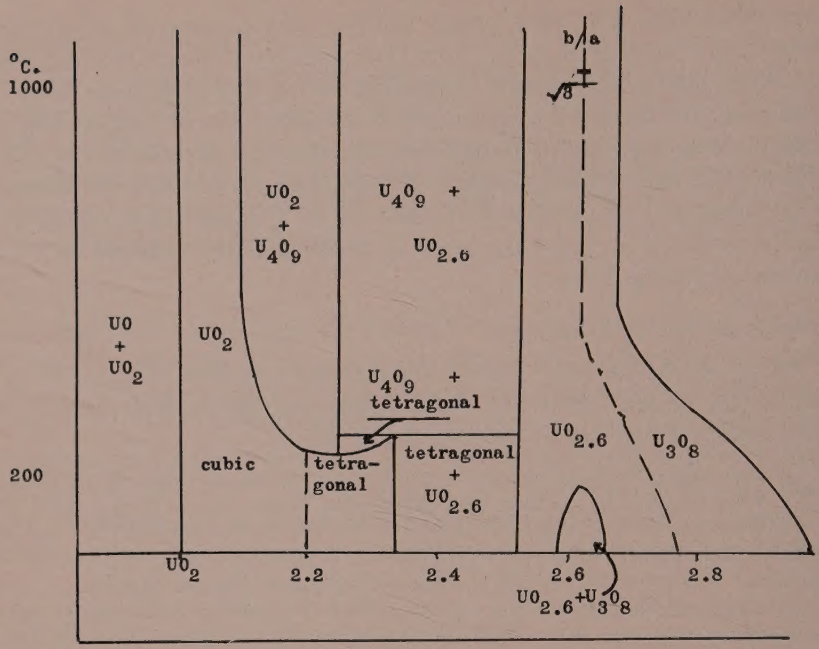

FIG. 1. Tentative phase diagram of the UO_2-UO_3 system.

GORDONIA, South Africa (USNM) USNM 103596. G.=7.32. Anal 42. Sub-hedral xls, sub-vitreous, imbedded in plagioclase.

GRAFTON, New Hampshire. H 105756. Anal 36. Altered to secondary mins. along cracks.

HALE'S QUARRY, Portland, Conn. USNM 83566. G.=9.139. Anal 27. Sub-vitr. with feldspar, muscovite. Hillebrand (1891).

HUGGENÄSKILEN, Norway. USNM 83570. G.=8.930. Anal 10. Vitreous. Hillebrand (1891).

KARELIA, Soviet Union. H 106038. G.=8.41. Vitreous. With microcline.

MOROGORO Dist., Tanganyika. USNM 93290. G.=9.09. Anal 44. Cube coated with yellowish-brown alteration products.

NEWRY, Me. H 103038. G.=9.58. Anal 33. Sharp octahedral faces. Lustre sub-metallic.

PORTLAND, Conn. H 16214. G.=10.15. Anal 32. Vitreous lustre.

SPRUCE PINE, N. Car. H 105712. G.=6.17. Anal 45. Vitreous. Conchoidal fracture. Bluish iridescence.

STRICKLAND Quarry, Portland, Conn. H 106052, Anal 24. Small crystals embedded in orthoclase.

SUDBURY Dist., Ont. G.=8.6. Anal 43. Vitreous, with quartz, biotite.

WILBERFORCE, Ont. H 105711. G.=10.25. Anal 59 and 60. Dull, earthy. With purple fluorite. Pitted crystal faces.

VEIN PITCHBLENDES

GREAT BEAR LAKE, Eldorado Mines, N.W.T. H 106051. G.=7.19. Anal 52. Botryoidal, on quartz, chalcopyrite.

JOACHIMSTHAL, Czech. G.=7.28. Anal 41. Vitreous. Seams in dolomite. Conchoidal fracture.
KATANGA. USNM 94710. Anal 40. Dull matte lustre, with yellow alteration products in cracks and crusts.
Lac PIED DES MONTS, Que. H 105713. Anal 38. Powder.
PRZIBRAM, Czech. H 105714, G.=7.82. Anal 61. Vitreous botryoidal groups, with galena, pyrite.
RIX ATHABASKA mines, Lake Athabaska Dist., Sask. H 105717. G.=7.33. Fills cracks in brecciated reddish limestone.
SCHMIEDEBERG, Silesia. Bergfreiheits Mine. H 104907. G.=7.46. Anal. 63. Vitreous veinlet in cleavable pink calcite.
THEANO POINT, Algoma Dist., Ont. H 105710. G.=7. Anal 55. Sub-vitreous, in calcareous redish quartzite. With uranophane.
WÖLSENDORF, Bavaria. Anal 37. Dull, with purple fluorite.
WOOD MINE, Central City, Colo. USNM 100453. G.=6.77. Anal 62. Grayish porous chunks. With pyrite.

SEDIMENTARY PITCHBLENDES

BIG INDIAN Wash, San Juan Co., Utah. Continental Uranium Co. Mine. H 106050. Anal 35. Grayish, dull material, permeated by calcite.
HAPPY JACK Mine, White Canyon, Utah. Lent by L. Stieff and T. Stern. G.=9.1. Anal 25. Fine powder.
MI VIDA Mine, San Juan Co., Utah. H 106040. G.=6.84. Anal 34. Massive, with seam of calcite, few grains chalcopyrite.
SHINARUMP NO. 3 mine, Sevenmile Dist., Grand Co., Utah. H 106039. Dull, pulverulent, in gray sandy limestone.
ROYAL CLAIMS, Indian Creek, San Juan Co., Utah. H 106037. Grayish, earthy material permeated with calcite.

Many of the samples had already been chemically analyzed, and analyses were obtained on some of the others. *X*-ray diffraction patterns were made of all the samples, using a ThO_2 internal standard. The *x*-ray film was measured on a spectrographic comparator equipped with a metric scale.

C. Frondel and E. Berman have collected the unit cell measurements of many uraninites. To these the author has added his own data, and the resulting distribution bar graphs are shown in Fig. 2. The median value for the pegmatitic uraninites is 5.470 Å. The median for vein uraninites is very considerably lower; 5.437 Å. The median cell size for uraninite from sedimentary occurrences is 5.406 Å, which is smaller than the smallest unit cell of the 105 pegmatitic uraninites measured. Differences in composition cannot fully account for the variation in unit cell sizes. There are apparently three different relationships between composition and cell size for the three modes of occurrence. It is therefore convenient to retain the varietal term 'pitchblende' to refer to the vein and sedimentary occurrences.

In an inert atmosphere, uraninite heated to the vicinity of 550° for

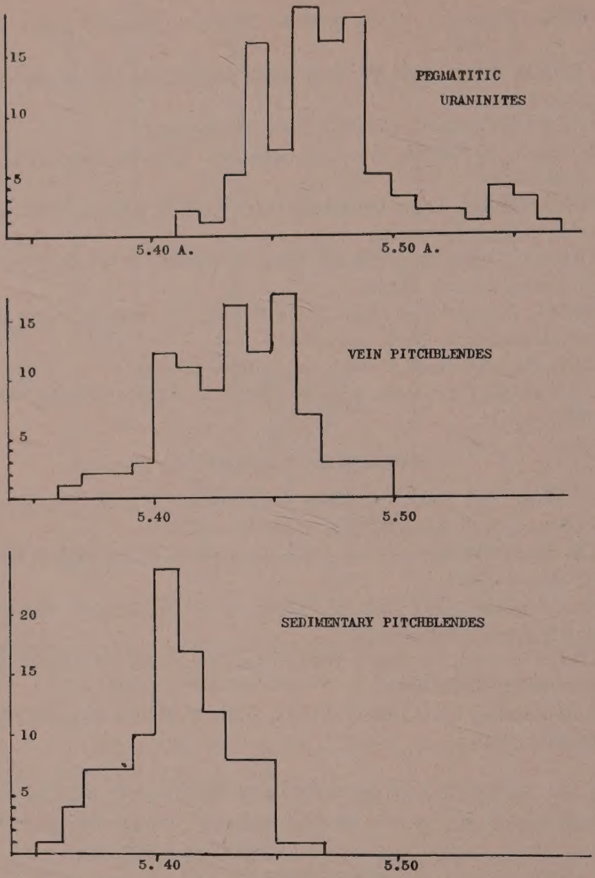

Fig. 2. Distribution of unit cell sizes in uraninites according to occurrence. (In part after C. Frondel.)

several hours undergoes a change that will be called 'annealing.' The lines of the powder pattern sharpen, and the unit cell decreases as much as 0.04 Å. The duration of heating necessary to complete the operation (i.e. until the unit cell stops changing) varies considerably from sample to sample, but 24 hours is usually safely in excess. In certain of the more oxidized samples, U_3O_8 lines appear, particularly on long runs. These may actually be the lines of the $UO_{2.6}$ phase, but Hoekstra *et al.* (1955) failed to include the powder pattern of $UO_{2.6}$ in their original description of the phase, and the criteria are therefore lacking for distinguishing the two phases in an ordinary powder photograph.

When the samples are heated to 900°, more of the samples decompose into a cubic phase and an orthorhombic one related to U_3O_8. The results depend on the state of oxidation, and perhaps on the content of thorium and other elements. The annealing studies described in this paper were done in a muffle furnace through which a constant stream of prepurified nitrogen was passed.

In certain of the calculations given later, it was necessary to adopt a value for the atomic weight of the 'average rare earth.' A value of 130 was chosen, largely on the basis of the compilation of geochemical data by Green (1953).

PEGMATITIC URANINITES

The degree of oxidation was computed for all available pegmatitic uraninite analyses which distinguish between U^{+4} and U^{+6}. The degree of oxidation is expressed as the subscript of the oxygen in the formula. The term 'm value' will be used to denote the subscript UO_m; 'n' is used for the subscript of $(U, Th)O_n$; 'p' is used for $(U, Th, R.E.)O_p$, and 'q' is used for $(U, Th, R.E., Pb)O_q$. A distribution bar graph of 'm,' 'n,' 'p' and 'q' is shown as Fig. 3.

The 'm' value is the best indication of the actual state of oxidation of the uranium atom—that is, to what extent the average uranium atom has adjusted its electron configuration and its ionic radius. Of course, the thorium, rare earth, lead, and even to some extent the oxygen ions make some adjustment, but the major change as oxygen increases is the reduction in ionic radius of uranium ions as U^{+4} changes to U^{+6}.

As will be shown, the thorium and rare earth ions occupy uranium positions in the structure. The amount of interstitial space in the structure is indicated by the total amount of uranium, thorium and rare earths. Therefore it is the 'p' value which indicates the stability or the degree of oxygen saturation of the structure, as it indicates the amount of oxygen actually in the interstitial spaces.

It will also be shown that the lead is not in the uranium positions. However, if auto-oxidation is the explanation for the uraninites that are oxidized above the laboratory limit, then the 'q' subscript would indicate the original oxidation state of the uraninite, the oxidation state that was in equilibrium with the environment when the uraninite crystallized. However, if non-radiogenic or previously existing radiogenic lead was incorporated into the sample when it crystallized, the 'q' value will be lower than the original oxidation state—perhaps even lower than 2. Non-radiogenic lead is a more serious problem in pitchblendes than in pegmatitic uraninites.

In general, the 'm' values are distributed from 2.14 to 2.80, with a decrease in frequency of occurrence above 2.50. A very considerable portion is above the laboratory limit of $UO_{2.33}$. In the calculation of 'p' values,

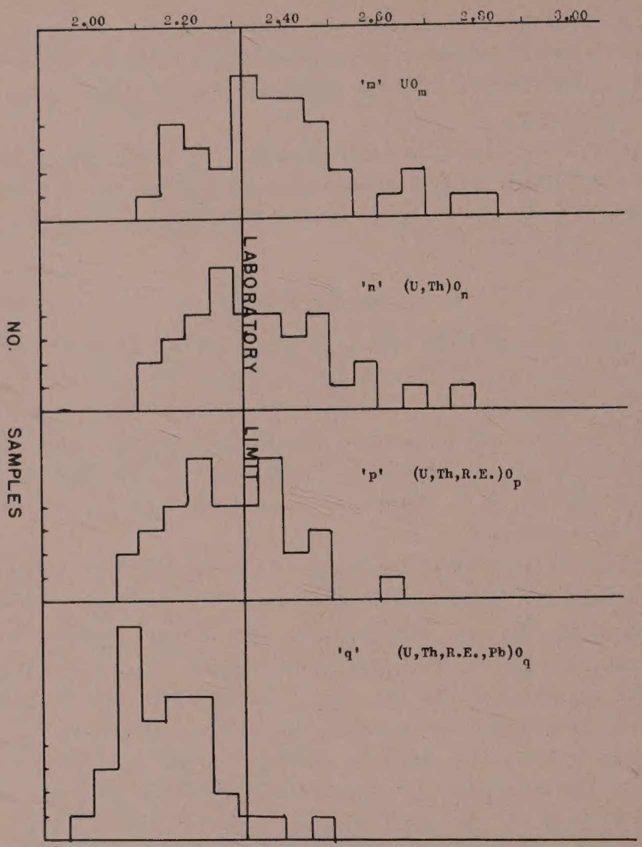

FIG. 3. Formula subscripts calculated for available pegmatitic uraninite analyses.

however, many of the more oxidized samples are shown to be structurally near or slightly above the laboratory limit; only five pegmatitic uraninites out of 34 have 'p' values above 2.40. In other words, as all the impurities proxying for the uranium are taken into account, the subscripts edge closer to permissible values.

The process is virtually completed by the 'q' values. 30 out of 34 pegmatitic uraninite analyses have 'q' values between 2.00 and 2.33, the laboratory stability range. Of the exceptions, one is slightly below the range and two are slightly above. The Spruce Pine sample, with a 'q' value of 2.488, is the only sample that still remains deep in forbidden territory.

Ellsworth (1924) proposed a process, which he called auto-oxidation, to explain the oxidation of uraninites above the laboratory limit. As each UO_2 formula unit disintegrated to PbO, it released an oxygen atom which was available for oxidizing additional UO_2 to UO_3. The data of the present study indicate that most pegmatitic uraninites crystallized within the limits of the stability field of the cubic form, as outlined in the laboratory. Auto-oxidation can satisfactorily account for the additional oxidation which places some analyses outside these limits.

Unit Cell Size Before and After Annealing

X-ray powder photographs were taken of the samples before and after annealing. Table 2 lists the furnace runs and the resulting unit cell size of the cubic phase. If lines belonging to a phase related to U_3O_8 appeared, their intensity is given, relative to the cubic phase.

These observations agree in general with those of Brooker and Nuffield (1952) and Robinson and Sabina (1955). They can be summarized as follows: in pegmatitic uraninites with relatively large unit cells (5.47 to 5.49 Å), the unit cell decreases 0.03 to 0.035 Å on annealing in an inert atmosphere. For those with smaller unit cells, the decrease is less, but the difference is not sufficient to wipe out the very considerable range in unit cell sizes.

Table 2 also shows a great disparity in the ease of annealing. The Gordonia (USNM) sample had virtually completed its annealing after 2 hours at 500° C., whereas the Wilberforce sample had not completely annealed after 26 hours at 550° C. The difficulty of annealing seems to vary as the ThO_2 content, and inversely as the rare earth content.

Calculated Values for the Unit Cell Sizes

If the uranium-oxygen system, as studied in the laboratory, is examined for behavior comparable to this annealing effect, a striking parallel is found in the transition from oxidized α-UO_2, with random oxygens in the interstices, to β-UO_2, or U_4O_9, in which the interstitial oxygens are ordered. The transition is brought about under the same range of conditions—heating the sample above 500° in an inert atmosphere or vacuum. The transition is characterized by a contraction of the unit cell of 0.34 Å, from 5.469 to 5.435 Å. These values are strongly reminiscent of many of the annealing results.

As a possible hypothesis, it is suggested that natural uraninites correspond to α-UO_2, and on annealing become the ordered phase β-UO_2. Using Vegard's Law (Vegard and Dale, 1928), it is possible to calculate a theoretical unit cell size from the analysis, first assuming that the uranium is present as α-UO_2, then as β-UO_2. Certain other assumptions must be made; they are discussed at some length in the thesis, but here their main justification must be that they work. The assumptions are as follows.

1. The validity of Vegard's Law.

TABLE 2. UNIT CELL SIZES OF PEGMATITIC URANINITES, BEFORE AND AFTER ANNEALING RUNS

Sample	Time, hr.	Temp., ° C.	a_0, Å	Δa_0, Å	U_3O_8 lines
Boqueirao	unheated		5.488		
	12	540	5.474		
	2½	900	5.455	.033	
Branchville	unheated		5.476		
	21	550	5.448	.028	
Elvestad	unheated		5.484		
	5½	500	5.465		
	5½ + 8	500 650	5.455	.029	Weak
Gordonia (Holmes)	unheated		5.491		
	21	550	5.474		
	2	900	5.463	.028	
Gordonia (USNM)	unheated		5.454		
	2	500	5.438		
	4½	500	5.438		
	10	500	5.438		
	28	500	5.438		
	2½	900	5.435	.019	
Grafton	unheated		5.443		
	4	440	5.433	.010	
	20	540			Exclusively
Hale's Quarry	unheated		5.484		
	2	900	5.451		
	7	500	5.451	.033	
Huggenäskilen	unheated		5.470		
	6	500	5.454		
	6 +20	500 650	5.447	.033	Weak
Karelia	unheated		5.491		
	24	540	5.490	.001	Weak
	4	900	Cubic pattern, lines too broad		
Morogoro	unheated		5.445		
	24	540	5.435	.010	Moderate
Newry	unheated		5.480		
	25	550	5.446	.034	
Portland	unheated		5.478		
	24	550	5.448	.030	
Spruce Pine	unheated		5.431		
	6	500	5.422	.009	
Strickland	unheated		5.488		
	12	570	5.448	.040	
Sudbury	unheated		5.437		
	6	500	5.428		
	23	650	5.429	.008	
Wilberforce	unheated		5.486		
	26	550	5.467		
	2	900	5.460	.026	
Mean probable error, ±	¼	20	0.002		

2. The cell edges of the pure end members: α-UO_2, 5.469 Å. β-UO_2, 5.435 Å. ThO_2, 5.601 Å.

3. For the putative end member (R.E.)O_2, the cell size, for purposes of calculation, is 5.38 Å.

4. Excess or deficiency of oxygen does not affect the unit cell size of α or β-UO_2.

5. Lead, including radiogenic lead, is not in the uraninite structure.

In Table 3, the results of these calculations are compared with the measured unit cell sizes of analyzed pegmatitic uraninites, before and after annealing.

The measured value after annealing and the calculated value assuming β-UO_2 agree extremely well. Indeed, considering the complexity of the substance, the difficulties of analysis, and the limitations of *x*-ray measurement, the agreement could hardly be any closer.

The author therefore maintains that pegmatitic uraninites after annealing are β-UO_2. The interstitial oxygens, which were more or less randomly arranged, order themselves on heating. The oxygen ions are similarly charged and repel each other. When thermal motion provides the opportunity, they tend to follow Pauling's rule and move as far apart as possible.

The interstitial positions they take up tend to be evenly spaced, so that, perhaps for distances of several unit cells, they can be considered as occupying the middle of the unit cell. The result is the β-UO_2 or U_4O_9

TABLE 3. CALCULATED AND MEASURED UNIT CELL SIZES, Å

Sample	Calculated assuming α-UO_2	Measured before annealing	Calculated assuming β-UO_2	Measured after annealing
Hale's Quarry	5.482	5.484	5.452	5.451
Branchville	5.479	5.476	5.448	5.448
Elvestad	5.479	5.484	5.450	5.445
Portland	5.475	5.478	5.442	5.448
Newry	5.475	5.480	5.442	5.446
Strickland	5.474	5.488	5.442	5.448
Wilberforce (outer)	5.487	5.486	5.460	5.460
Huggenäskilen	5.477	5.470	5.446	5.447
Gordonia (USNM)	5.468	5.454	5.438	5.438
Sudbury	5.458	5.437	5.430	5.429
Morogoro	5.466	5.445	5.433	5.435
Gordonia (Holmes)	5.478	5.491	5.450	5.474
Spruce Pine	5.463	5.431	5.434	5.422

structure, perhaps with an excess or deficiency of oxygens. The annealing process is therefore a disorder-order transformation.

Before annealing, some of the samples have unit cell sizes corresponding to α-UO_2; these are the first group listed in Table 3. Presumably, the interstitial oxygens are completely disordered in these samples. The second group of samples in Table 3, before annealing, have values intermediate between α- and β-UO_2. When they are annealed, they complete the rest of the journey to the calculated value for β-UO_2. It is reasonable to assume that these samples reach us in a partially ordered condition.

The samples in the second group have smaller cells after annealing than those of the first group; the more ordered a sample is in its original condition, the lower the unit cell after annealing. But the unit cell after annealing is entirely a function of the composition. In Table 4, the degree of disorder, as indicated by the measured contraction of the unit cell divided by the theoretical calculated contraction, is compared to the rare earth/ThO_2 ratio.

The degree of ordering of a sample as it is found in nature is apparently determined by the R.E./ThO_2 ratio—in other words, by the composition, and not to any great extent by other factors. One would think, for instance, that the past history of the material would have some effect; surely samples can be annealed naturally. But there is no evidence in Table 4 that the past history influences the degree of annealing.

Radioactivity may have the effect of disordering samples which are

TABLE 4. R.E./ThO_2 RATIO AND DEGREE OF ORDERING

Sample	$\frac{\text{R.E.}}{\text{ThO}_2}$	$\frac{\text{Actual contraction}}{\text{Theoretical contraction}}$
Completely disordered samples		
Branchville	~0	0.90
Portland	~0	0.90
Newry	~0	1.03
Hale's Quarry	0.06	0.90
Strickland	0.11	1.25
Wilberforce (outer)	0.14	0.96
Elvestad	0.19	1.34
Partially ordered samples		
Huggenäskilen	0.22	0.74
Gordonia (USNM)	0.90	0.53
Sudbury	4.7	0.29
Morogoro	5.0	0.30

completely ordered. The R.E./ThO_2 ratio may fix an equilibrium in the order-disorder scale; samples more disordered than the equilibrium would be annealed as a result of radioactivity, whereas those more ordered would undergo disordering. Here again, it is inconceivable that temperature should not be a factor, but there is no evidence of it in the data. Apparently, equilibrium has been attained under surface or near-surface conditions, and this in turn indicates that geologic time is not required to reach equilibrium.

PITCHBLENDES

Pitchblende differs from pegmatitic uraninite in having low or absent ThO_2 and rare earths, high CaO, small crystal size and small unit cell size.

Table 5 shows the average ThO_2, rare earths, and CaO content for the pegmatitic uraninite and pitchblende analyses in the appendix, excluding a few known to be contaminated with calcite.

Alberman, Blakely and Anderson (1951) investigated the UO_2-CaO system. They found that CaO could be incorporated into UO_2 to the extent of 20 molar per cent at 1650° C., and up to 47 molar per cent at 2080° C. As the CaO content rose, the unit cell decreased somewhat. Calculations showed, however, that it was not enough to account for the difference in cell size between pegmatitic uraninites and vein pitchblendes. The calcium can at best be one of many contributing factors.

TABLE 5. AVERAGE ThO_2, RARE EARTH AND CaO CONTENT. WT. %

	ThO_2	R.E. oxides	CaO
Pegmatitic uraninites	6.00	4.05	0.43
Pitchblendes	0.18	0.92	1.96

In nearly half the pitchblende analyses, only UO_2 and UO_3 determinations are available, and therefore only the 'm' subscript can be calculated. A distribution graph of these 'm' values for the pitchblende analyses in the appendix is given as Figure 4.

THE $UO_{2.6}$ CLUSTER

Twenty-one out of thirty-two pitchblende analyses have 'm' values below 2.50. Only one has a value between 2.50 and 2.60; a sample from Rio Branco, Minas Gerais, Brazil has an 'm' value of 2.524. This makes a very sharp saddle in the distribution curve, for 7 samples have 'm' values between 2.60 and 2.70. U_3O_8 is $UO_{2.667}$. The samples included in

TABLE 6. ANALYSES WITH 'm' VALUES BETWEEN 2.6 AND 2.7

Anal	Locality	'm'
23	Cerro Blanco, Córboda, Argentina	2.670
37	*Wölsendorf*, Bavaria	2.636
46	Monument No. 2 mine, Apache Co., Ariz.	2.635
47	Happy Jack mine, San Juan Co., Utah	2.610
55	*Theano Pt.*, Algoma Dist., Ontario	2.667
68	Martin Lake, Lake Athabaska Dist., Sask.	2.600
61	*Przibram*, Czechoslovakia	2.610

Samples available for study italicized.

this peculiar cluster are listed in Table 6. In addition, a pegmatitic uraninite, the Grafton sample, may also be included; it has an 'm' value of 2.681. The author suggests that the samples forming this 'high' in the distribution curve crystallized as U_3O_8.

Whatever these samples may have been originally, they are not now U_3O_8. Of the eight samples, including the Grafton sample, those from Wölsendorf, Przibram, Theano Point and Grafton were *x*-rayed in the course of this study; the samples from the Happy Jack and Monument No. 2 mines were *x*-rayed by the U. S. Geological Survey in Washington, and the *x*-ray pattern of a seventh, from Martin Lake, Sask., is available in Brooker and Nuffield's (1952) article as their Fig. 5.

The seven samples of the '$UO_{2.6}$ cluster' have compositions falling in, or close to, the stability range of the phases related to U_3O_8. In the distribution curves, there is evidence that they may have been U_3O_8 at one time. Except for the Wölsendorf sample, however, the available powder patterns showed only the cubic phase. The Wölsendorf sample gave no pattern. The fact that these samples are no longer U_3O_8 seems to cast considerable doubt on the possibility of finding this phase as a primary mineral under the temperature, pressure and oxygen availability condi-

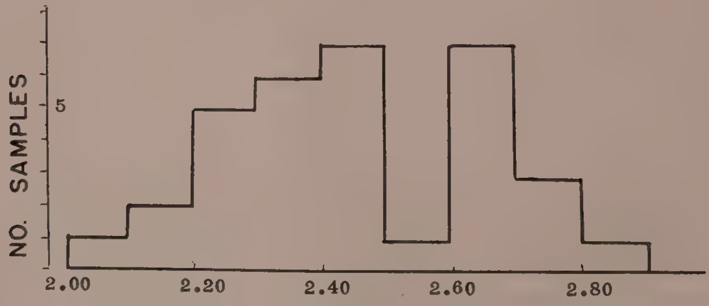

FIG. 4. Distribution of 'm' subscripts in analyzed pitchblendes.

tions of the normal geothermal gradient. High temperatures and low pressures are apparently required. U_3O_8 may possibly occur as a contact metamorphic product in areas of recent volcanic activity; even here, the usual product would probably be hydrated uranyl compounds.

Conybeare and Ferguson (1950) report some 'metamict' uraninites from Saskatchewan, presumably similar to the Wölsendorf sample. This sample was the only one examined in this study which gave no pattern. After heating in an inert atmosphere, it gave the pattern of U_3O_8. Its radioactivity is not remarkable. This sample is distinguished from most others by its composition, which suggests that it crystallized as U_3O_8 and decomposed. Other 'metamict' vein uraninites should be analyzed; it may be that the destruction of the structure was caused primarily by chemical change rather than by radioactivity. Alpha particles may be capable of disordering interstitial oxygen ions, but the structural oxygens seem to remain in place.

Unit Cell Size Before and After Annealing

As with the pegmatitic uraninites, the pitchblendes were *x*-rayed before and after heating in an inert atmosphere. The results of the furnace runs are given in Table 7.

To summarize, the vein pitchblendes have unit cell sizes of approximately 5.425 Å. On annealing, they behave much as the pegmatitic uraninites. The unit cell contracts as much as 0.035 Å, resulting in values of 5.39 or 5.40 Å. Sedimentary pitchblendes from the Colorado Plateau have significantly smaller unit cells before heating. In these cases, the values are close to 5.40 Å. On annealing, they contract comparatively little, about 0.01 Å. They behave like partially or almost completely ordered specimens. The vein pitchblendes behave like samples with random or nearly random interstitial oxygens.

After annealing, the unit cell sizes of the two types of pitchblende fall in the same range. The chemical analyses of the two types are also similar, the various determinations covering the same range. It is necessary to call upon some mechanism other than composition to explain the difference in cell size before annealing. The ordering of interstitial oxygens is both necessary and sufficient to explain the difference. When this factor is eliminated by annealing both types, there no longer is a difference. Therefore, it is possible to think of sedimentary pitchblendes of the Colorado Plateau as corresponding to annealed vein types in structure.

Table 7 shows that the Joachimsthal sample does not contract on annealing. The analysis, No. 41 in the appendix, shows that the sample contains no U^{+6}. The analysis was checked by two independent methods, one based on the reduction of ceric ion, and the other on the solubility of

Table 7. Unit Cell Size, Å., of Pitchblendes Before and After Furnace Runs

Sample	Time, hr.	Temp., ° C.	a_0, Å.	±	Δa_0, Å
	Vein Pitchblendes				
Great Bear Lake	unheated		5.425	.005	
	14	540	5.406	.002	.019
Joachimsthal	unheated		5.418	.005	
	20	550	5.418	.002	.000
Katanga	unheated		5.448	.005	
	8	500	U_3O_8		
Katanga leached 40 hr. in 0.4 N H_2SO_4	5	550	5.435	.002	.013
Pied des Monts	unheated		5.468	.005	
	7	500	5.454	.002	
	10	600	5.450	.002	.018
Przibram	unheated		5.413	.005	
	15	540	5.381	.002	.032
Rix Athabaska	unheated		5.431	.002	
	10	550	5.392	.002	.039
Schmiedeberg	unheated		5.430	.005	
	6	500	5.401	.002	.029
Theano Point	unheated		5.405	.005	
	6	540	5.390	.002	.015
Wölsendorf	unheated		no pattern		
	9	540	U_3O_8		
Wood Mine	unheated		5.448	.005	
	8	540	5.413	.002	.035
	Sedimentary pitchblendes				
Big Indian	unheated		5.39	.01	
	14	540	5.38	.01	.01
Happy Jack	unheated		5.407	.01	
	10	535	U_3O_8		
Mi Vida	unheated		5.399	.005	
	7	540	5.391	.002	.008
Royal Claims	unheated		5.40	.01	
	4	440	5.38	.01	.02
Shinarump No. 3	unheated		5.399	.005	
	7	540	5.391	.002	.008

UF_6 and insolubility of UF_4 in acid. One possible source of difficulty is the iron. The analysis reported 2.40% Fe_2O_3, which is rather high for uraninites. But even if all of this iron were Fe^{+2}, and all of it were oxidized by the ceric sulfate, and the actual amount of U^{+6} was precisely the quantity necessary to escape detection, there would still be only 4.3% UO_3, as compared to 66.1% UO_2. The 'm' value would be 2.058, and the Joachimsthal sample would still be far less oxidized than any uraninite heretofore reported. The annealing behavior seems to indicate that there are no interstitial oxygens to order or disorder. Although it is difficult to reconcile a completely unoxidized sample with the auto-oxidation hypothesis, the author feels compelled to accept the analysis as correct.

The Rôle of Lead

In Table 3, it was shown that the unit cell of pegmatitic uraninites could be calculated from the analyses, if one assumes that lead does not proxy for uranium in the uraninite structure. In itself, this is a powerful piece of evidence. It is reinforced by other, completely independent arguments.

For instance, Eckelmann and Kulp (1956) found that the various isotopic age determinations on samples of pitchblende from Lake Athabaska did not agree, and could be reconciled only if they assumed that the radiogenic lead was exsolved during two separate periods of thermal metamorphism.

Phair and Levine (1952) leached an oxidized pitchblende from Katanga, and a less oxidized sample from Great Bear Lake, in sulfuric acid of various concentrations ranging from 0.17 to 1.84 N. From time to time during the 144-hour run, solution was drawn off and analyzed, and finally the residual samples were analyzed. The results show a marked differential leaching of UO_3 from UO_2. The effect is much stronger in the more oxidized sample. Aside from this, the results also show a significant differential leaching of UO_3 and UO_2 from lead, which becomes concentrated in the undissolved portion. Of course, it is possible for a solution, solid or otherwise, to be in equilibrium with another solution with a higher, or lower, lead-uranium ratio. Methylene iodide, for instance, containing little acetone, is in equilibrium with water containing much more; therefore water can be used to remove acetone selectively from methylene iodide, even though the acetone is in solution. The mere fact of differential leaching does not prove that the lead is not in solid solution. However, in the 144 hours of Phair and Levine's longest experiment, there could not be enough diffusion in the solid state to be detected. It must be concluded that the acid acted upon an inhomogeneous surface.

The behavior of certain specimens in this study provides additional evidence that lead does not proxy for uranium in uraninite. For instance, the Huggenäskilen sample is (U, Th, R.E.)$O_{2.374}$, but (U, Th, R.E., Pb)$O_{2.215}$. On annealing, it decomposes into U_4O_9 and a smaller amount of U_3O_8. It behaves like $UO_{2.374}$ rather than $UO_{2.215}$. The 'p' subscript, rather than the 'q' subscript, also seems to control the extent of differential leaching of UO_3 from UO_2. The 'q' value provides a clue to the original state of oxidation of the environment in which the uraninite crystallized, but the 'p' value more truly represents the present structural condition of the material.

Where, then, is the lead? These specimens give the cubic uraninite pattern. There are no lines left over. If the lead is not in the uraninite structure, it seems convenient to consign it to an amorphous phase, along with excess UO_3 and other things that cannot be made to fit. In order to find if such an amorphous phase actually existed, a study was undertaken of the intensities of *x*-ray diffraction lines.

ThO_2 is isostructural with uraninite, and, since its unit cell is only a little larger, corresponding lines have Bragg angles close together. The reflectivity and absorption constants of the thorium and uranous ions are very similar. ThO_2 gives extremely sharp diffraction lines. It is a very stable, refractory substance, and it seems reasonable to assume that it is entirely crystalline. If, then, it were mixed with a chemically equivalent amount of UO_2, and the UO_2 were entirely crystalline, the *x*-ray diffractometer pattern should show pairs of peaks, close together, with almost identical areas under them. If the uraninite peak were less intense, it would indicate that the uraninite sample was not completely crystalline.

An amount of ThO_2, chemically equivalent to the uranium, thorium and rare earths, was weighed out and mixed with each analyzed sample. It was expected that the intensity of the uraninite peaks would be a definite proportion—say 85%—of the intensity of the equivalent ThO_2 peaks, and it would therefore be possible to state that the uraninite was 85% crystalline. Unfortunately, this is not the case. The measured values are astonishingly low, on the order of 25 to 50%, even for pegmatitic crystals with good external faces and sharp *x*-ray patterns. Also, the values are not uniform from line to line, so that a single percentage quoted for the whole sample would have little meaning. There seems to be a definite pattern of non-uniformity. In sample after sample, the percentage for the (111) peak was up to half again as high as those for the (200) and (220) peaks. The ratios between the peaks for (200) and (220) were almost identical. The measured values are given in Table 8.

The 'pattern of non-uniformity' has some structural significance. The

TABLE 8. AREA UNDER DIFFRACTION PEAKS, % OF AREA UNDER EQUIVALENT ThO_2 PEAK

Sample	111	200	220	311
Joachimsthal	48	35	36	
Hale's Quarry	54	37	34	34
Hale's Quarry, annealed	61	42	41	36
Gordonia (USNM)	34	28	26	15
Theano Point	42	33	31	
Sudbury	44	36	33	23
Great Bear Lake	56	50	51	
Elvestad	44	48	35	36
Pied des Monts	27	24	18	19
Spruce Pine	23	22	21	19
Happy Jack	15	16	14	
Mi Vida	17	13		
Boqueirao	75	57	52	55
Wilberforce	63	50	46	
Karelia	39	36	29	
Schmiedeberg	21	22	14	
Wood Mine	49	46	43	
Rix Athabaska	29	27	23	
Calculated (see text)	69	45	45	69

intensity of the uraninite lines has been reduced, and some reflections have been reduced more than others. There seems to have been some sort of destructive interference which is greater in some directions than in others. The author suggests that natural uraninite consists of a mosaic of crystallites in parallel position. These are separated along cube planes by 'spacers,' monomolecular layers of massicot (orthorhombic PbO), the thickness of the layer being the '*b*' axis of the unit cell. The *x*-ray reflections from two adjacent crystallites interfere destructively to different extents in different directions. The theoretical intensities calculated on these assumptions are given at the bottom of Table 8. There is good agreement with the highest of the measured intensities, such as those of the Hale's Quarry sample. The lower intensities of most of the samples can be attributed to a combination of this mechanism and the effect of amorphous material. The proposed hypothesis seems fully competent to explain the pattern of intensity variation.

Bystrom (1943) determined the structure of orthorhombic PbO. The cell dimensions are as follows: $a_0 = 5.476$ Å, $b_0 = 4.743$, $c_0 = 5.876$. Except for the *b* axis, it is similar in size to the UO_2 cell, which is cubic with $a_0 = 5.469$ Å. If the lead positions only are considered, the cell of orthorhombic PbO is very close to being face-centered. The oxygens are arranged in puckered layers between the lead layers. The lead positions in orthorhombic PbO are related to each other almost exactly as the uranium positions in UO_2, except that the '*b*' axis of the PbO is compressed. It should therefore be possible to form oriented overgrowths of PbO on UO_2, such that the Pb positions on the (010) plane of the PbO fit into the U vacancies on a cube face of the UO_2. The overgrowth is only one cell thick in this case; the UO_2 structure of the next crystallite fits on the 'back' of the layer in the same way, and continues, so that, among the (100) planes spaced 5.469 Å apart, there is one pair spaced only 4.743 Å apart, and reflections from one side of this 'spacer' are out of phase with those on the other side. Intensities calculated on this assumption agree satisfactorily with measured values, and, in combination with the other evidence, would seem to indicate very strongly that PbO is exsolved from the uraninite structure.

DIFFERENTIAL LEACHING

Some of the samples were ground and placed in 0.4 N H_2SO_4 for 40 hours in an attempt to study the differential leaching of U^{+6} from U^{+4}. It was generally not possible to spare sufficient material from the analyzed sample itself; therefore, a two-gram sample was taken from the concentrate from which the analyzed sample was picked. The resulting samples were not pure, but it is reasonably certain that uraninite was the only uranium mineral to survive the leaching process. The comparison between the material before and after leaching will be made, not by means of absolute quantities or weight per cent, but by means of the state of oxidation, as shown by the 'm' formula subscript.

It was apparent, even without analyses, that the acid attacked some

TABLE 9. 'm' SUBSCRIPTS BEFORE AND AFTER LEACHING

Sample	Before	After	Substantial differential leaching
Gordonia	2.777	2.598	+
Katanga	2.742	2.296	+
Grafton	2.681	2.328	+
Przibram	2.610	2.325	+
Morogoro	2.529	2.432	+
Sudbury	2.389	2.330	+
Great Bear Lake	2.327	2.400	?
Wilberforce	2.337	2.372	−
Schmiedeberg	2.311	2.395	−
Wood Mine	2.282	2.234	−
Pied des Monts	2.219	2.277	−

samples to a far greater extent than others. In some cases, the solution showed the yellow color of uranyl ion as soon as the sample settled to the bottom of the beaker; in others, virtually colorless acid was decanted at the end of 40 hours. The 'm' subscripts before and after leaching are given in Table 9. The analyses of leached material were made by Jun Ito.

Generally, the results in Table 9 show that samples above the laboratory limit (2.32) lose a considerable amount of U^{+6}, so that they approach $UO_{2.32}$. They do not move far past this point. Samples below the laboratory limit showed little solubility and very little, if any, differential leaching. The results indicate that samples above the laboratory limit have disproportionated into a cubic phase at the laboratory limit, sparingly soluble in acid, and an amorphous phase, high in U^{+6} and readily soluble in dilute acid.

In some of the samples, the subscripts appear to increase slightly on leaching. Apparently, the samples were oxidized slightly at some stage of the procedure.

ACKNOWLEDGMENTS

This paper is a condensation of a Ph.D. thesis prepared under the direction of Prof. Clifford Frondel of the Department of Mineralogy and Petrography, Harvard University. It is also part of a program conducted by the U. S. Geological Survey on behalf of the Division of Raw Materials, U. S. Atomic Energy Commission. The laboratory facilities were provided by contract AT(30-1)-1403 with the Division of Research, U. S. Atomic Energy Commission. The author also wishes to acknowledge the help and advice of Alice Weeks, Loren Stieff, Thomas Stern, George Phair, Michael Fleischer, Katherine Valentine, Henry Kramer, Harry Levine, and Alexander Sherwood of the U. S. Geological Survey; Professors Cornelius Hurlbut and Robert Garrels of Harvard; George Switzer, of the U. S. National Museum, who made a generous gift of chips of many of the analysed samples of uraninite; Richard Collette, Ivan Barnes, and Eleanor (Berman) Rothman of Harvard, and Jun Ito, of Harvard and the University of Tokyo.

REFERENCES

AHLFELD, F., AND ANGELELLI, V. (1948), The mineral species of the Argentine Republic. Universidad Nacional de Tucuman, Jujuy, 1948.

ALBERMAN, K. B., AND ANDERSON, J. S. (1949), *J. Chem. Soc.*, **1949**, S303.

ALBERMAN, K. B., BLAKELY, R. C., AND ANDERSON, J. S. (1951), *J. Chem. Soc.*, **1951**, 1352.

ANDERSON, J. S., EDGINGTON, D. N., ROBERTS, L. E. J., AND WAIT, E. (1954), *J. Chem. Soc.* **1954**, 3324.

BAKKEN, R., AND GLEDITSCH, E. (1938), *Am. Jour. Sci.*, (5) **36**, 95.

BERMAN, E. (1955), *Am. Mineral.*, **40**, 925.

Biltz, W., and Muller, H. (1927) *Z. für Anorg. Chem.* **163,** 257.

Brooker, E. J., and Nuffield, E. W. (1952), *Am. Mineral.*, **37,** 363.

Bystrom, A. (1943), *Arkiv vor Kemi,* **17B,** no. 8.

Chernik, G. P. (1909), *Bull. Acad. Imp. Sci. St. Petersbourg,* (6)**3,** 1203.

Conybeare, C. E. B., and Ferguson, R. B. (1950), *Am. Mineral.*, **35,** 401.

Davis, C. W. (1926), *Am. Jour. Sci.*, (5) **11,** 201.

Eckelmann, W. R., and Kulp, J. L. (1956), *Bull. G.S.A.*, **67,** 35.

Ellsworth, H. V. (1924), *Pan. Am. Geol.*, **42,** 273.

——— (1930), *Am. Mineral.*, **15,** 455.

Florencio, W., and Castro, C. de (1943), *Annais Acad. Bras. Sci.*, **15,** 19.

Foye, W. G., and Lane, A. C. (1934), *Am. Jour. Sci.*, (5) **28,** 127.

Frondel, C.: Systematic Mineralogy of Uranium and Thorium. In press.

Goldschmidt, V., and Thomassen, L. (1923), *Videnskaps Selskapets Shrifter Mat.-Naturw. Klasse,* Kristiania.

Green, J. (1953), *G.S.A. Bull.*, **64,** 1001.

Grønvold, F., and Haraldsen, H. (1948), *Nature,* **162,** 69.

Hidden, W. E., and Mackintosh, J. B. (1889), *Am. Jour. Sci.*, (3) **38,** 474.

Hillebrand, W. F. (1891), *U.S.G.S. Bull.*, **78,** p. 43.

——— (1892), *U.S.G.S. Bull.*, **90,** p. 22.

Hoekstra, H. R., and Katz, J. J. (1955), *Nature,* **175,** 605.

Hoekstra, H. R., Siegel, S., Fuchs, L. H., and Katz, J. J. (1955), *J. Phys. Chem.*, **59,** 136.

Holmes, A. (1934), *Am. Jour. Sci.*, (5) **27,** 343.

Iimori, T. (1941), *Am. Jour. Sci.*, **239,** 819.

Jolibois, P. (1947), *Compt. Rend.*, **224,** 1395.

Katz, J., and Rabinowitch, E. (1951), The Chemistry of Uranium. NNES vol. VIII-5, McGraw-Hill, New York.

Kerr, P. F. (1950), Mineralogical Studies of Uraninite and Uraninite-Bearing Deposits. Interim Technical Rept. July 1, 1949–June 30, 1950. USAEC-RMO. No Number.

Marckwald, W., and Russel, A. S. (1911), *Jahrb. Radioakt. Elektronik* **8,** 457.

Milne, I. H. (1951), *Am. Mineral.*, **36,** 415.

Nenadkevich, K. A. (1926), *Izvestia Akad. Nauk SSSR.*, (6) **20,** 767.

Nordenskiold, N. A. E. (1878), *Neues Jahrb. Min. Geol.*, **1878,** 406.

Phair, G., and Levine, H. (1953), *Econ. Geol.*, **48,** 358.

Robinson, S. C., and Sabina, A. P. (1955), *Am. Mineral.*, **40,** 624.

Rundle, R. E., Baenziger, N. C., Wilson, A. S., and McDonald, R. A. (1948), *J. Am. Chem. Soc.*, **70,** 99.

Vegard, L., and Dale H. (1928), *Zeit. Krist,* **67,** 148.

Walker, T. L. (1924), *Toronto Univ. Studies, Geol. Ser.*, **17,** 51.

Wasserstein, B. (1951), *Nature,* **168,** 380.

——— (1954), *Nature,* **174,** 1004.

Wells, R. C. (1930), *Am. Mineral.*, **15,** 470.

APPENDIX. ANALYSES OF URANINITE

This appendix contains a compilation of partial analyses of uraninite used in this study. It includes almost all available analyses starting with Hillebrand's, providing that the analyses distinguished between U^{+4} and U^{+6}. A few were omitted because the samples were stated to contain oxidized secondary uranium minerals. Some duplicate analyses were averaged, or in cases where one analysis was more detailed than another, they were combined, with averaging of comparable items. In the case of analyses performed especially for this study, the partial analysis includes all the information available.

	1	2	3	4	5	6	7	8	9
UO_2	59.93	72.25	58.51	46.56	46.13	43.62	50.74	43.03	43.88
UO_3	23.03	13.27	25.26	44.11	30.63	36.31	25.36	22.04	32.00
ThO_2		7.20	7.81		6.00	5.64	8.48	8.43	8.98
R.E.				3.04	1.56	2.80	0.47		0.53
PbO	3.08	4.35	0.70	4.53	9.04	8.41	10.06	8.58	9.46
CaO	0.11	0.18	0.84	0.23	0.37	0.30	0.77	0.37	0.36
Fe_2O_3	0.29	0.11			0.25	1.40	0.21	0.30	0.09
SiO_2	0.16	0.03	2.79	0.13	0.22	0.81	0.38	0.29	0.53

	10	11	12	13	14	15	16	17	18
UO_2	43.38	59.30	70.09	52.77	39.10	48.87	34.49	53.63	45.18
UO_3	35.54	22.33	22.69	37.54	32.40	28.58	36.94	26.32	24.90
ThO_2	6.63		0.20		10.60	2.15	0.15	3.22	11.40
R.E.	1.46		5.14	0.72	4.02	2.07	5.60	3.17	4.56
PbO	9.44	6.39	0.40	7.02	10.95	16.42	19.50	11.67	10.40
CaO	0.41	1.00	0.30	0.69	1.01	0.46	0.72	0.41	0.26
Fe_2O_3	0.32	0.21	0.10	0.15	0.43	0.30	Tr	0.17	0.58
SiO_2	0.49	0.50		0.09	0.19	0.05		0.29	0.43

	19	20	21	22	23	24	25	26	27
UO_2	47.5	55.40	41.94	23.10	28.38	75.41	52.28	42.49	59.13
UO_3	40.8	22.23	49.21	63.00	61.12	14.83	31.08	20.58	22.08
ThO_2		3.86		1.67	0.25	2.59	none	N.D.	9.09
R.E.	0.15	15.01				0.28			0.55
PbO	7.63	1.01	5.71	5.00	5.20	3.94	0.74	1.48	3.14
CaO	0.58		0.42	0.70	tr	0.30	2.22	2.40	0.08
Fe_2O_3	0.15	0.17	0.30	tr		0.53	1.21	1.93	1.21
SiO_2	0.47	0.11	0.92			0.01	2.87	4.35	1.06

	28	29	30	31	32	33	34	35	36
UO_2	44.18	23.07	19.89	44.17	74.75	76.12	64.8	52.3	26.0
UO_3	26.80	40.60	46.75	20.89	14.65	15.67	14.3	27.8	58.7
ThO_2	4.15	4.60	7.57	6.69	3.74	3.86			
R.E.	9.72	12.24	11.22	9.46	incl. in ThO_2				
PbO	10.95	10.92	10.16	10.08	4.03	5.16	0.9	1.0	2.3
CaO	0.61	0.86		0.32			3.0	4.4	0.3
Fe_2O	0.24	1.02	0.58	0.14			0.6	0.8	0.2
SiO_2	0.50			0.46			3.0	2.5	0.3

	37	38	39	40	41	42	43	44	45
UO_2	24.1	38.0	36.42	18.9	70.2	20.9	41.6	38.2	13.6
UO_3	44.5	11.3	37.94	57.7	<0.1	41.7	28.1	45.4	58.0
ThO_2		0.27	9.32	<0.03	0.08	9.18	1.53	0.4	2.93
R.E.		2.29	3.20	0.23	2.17	8.23	7.20	2.0	5.90
PbO	small	6.10	9.48	11.95	3.91	12.98	12.84	7.2	5.41
CaO	8.4	15.9	0.63	0.40	4.28	0.60	2.33	0.5	0.50
Fe_2O_3	3.4	0.5	1.86		2.40	0.65	0.42	0.7	1.01
SiO_2	2.0	1.1	0.73	0.85	4.17	1.17	0.70		0.73

	46	47	48	49	50	51	52	53	54
UO_2	31.86	31.37	36.43	40.19	36.92	44.77	48.69	42.27	41.20
UO_3	58.68	51.95	29.72	29.27	36.51	29.99	49.03	27.00	40.92
ThO_2									5.02
R.E.									1.57
PbO								13.02	8.50
CaO									0.18
Fe_2O_3									1.01
SiO_2									0.77

	55	56	57	58	59	60	61	62	63
UO_2	20.4	48.7	67.13	73.59	44.0	39.5	32.1	60.7	51.1
UO_3	43.2	25.0	23.59	16.62	23.7	27.9	53.2	25.3	24.4
ThO_2			3.80	3.78	13.5	13.4	<0.01		<0.01
R.E.	0.53		0.36	0.36	1.9	0.7	3.3		4.1
PbO	5.25	6.4	3.65	3.63	9.47	9.47	6.01	0.82	3.08
CaO	13.24	5.1	0.31	0.31	0.02	0.02	0.23	0.01	0.54
Fe_2O_3		0.8	1.00	1.28				2.49	
SiO_2	2.60	1.4							

	64
UO_2	38.71
UO_3	41.33
ThO_2	5.03
R.E.	2.61
PbO	8.39
CaO	0.35
Fe_2O_3	1.24
SiO_2	0.76

Analysis	$\frac{U^{+6}}{\text{Total U}}$
65	17.4%
66	20.2
67	40.2
68	60.0
69	78.5
70	85.0

1. Hale's Quarry, Portland, Conn. Hillebrand (1891).
2. Branchville, Conn. Hillebrand (1891).
3. Black Hawk, Gilpin Co., Colo. Hillebrand (1891).
4. Flat Rock Mine, Mitchell Co., N.C. Hillebrand (1891).
5. Gustavsgruben, Anneröd, Norway, Hillebrand (1891).
6. Gustavsgruben, Anneröd, Norway. Hillebrand (1891).
7. Elvestad, Norway. Hillebrand (1891).
8. Elvestad, Norway. Hillebrand (1891).
9. Skaatorp, Norway. Hillebrand (1891).
10. Huggenäskilen, Norway. Hillebrand (1891).
11. Johanngeorgenstadt, Saxony. Hillebrand (1892).
12. Placer de Guadalupe, Chih., Mexico. Wells, (1930).
13. Shinkolobwe, Belgian Congo. Davis (1926).
14. Wilberforce, Ont. Ellsworth (1930).
15. Ingersoll Mine, Pennington Co., S. Dak. Davis (1926).
16. Sinyaya Pala, Karelia, U.S.S.R. Nenadkevich (1926).
17. Parry Sound Dist., Ont. Ellsworth, quoted in Frondel (in press).
18. Wilberforce, Ont. Todd, analyst, in Walker (1924).
19. Shinkolobwe, Belgian Congo. Rodden, analyst, in Kerr (1950).
20. Iisaka, Abukama Range, Japan. Iimori (1941).
21. Rio Branco, Minas Gerais, Brazil. Florencio and Castro (1943).
22, 23. Cerro Blanco, Córdoba, Argentina. Chaudet, analyst, in Ahlfeld and Angelelli (1948).
24. Strickland Pegmatite, Portland, Conn. Hecht, analyst, in Foye and Lane (1934).
25. Happy Jack mine, White Canyon, Utah. G. Edgington, analyst; T. Stern, pers. comm.
26. Shinarump No. 1 mine, Sevenmile Canyon, Grand Co., Utah. G. Edgington, analyst. Weeks, pers. comm.
27. Hale's Quarry, Portland, Conn. Hillebrand (1891).
28. Arendal, Norway. Hillebrand (1891).
29. Arendal, Norway. Lindstrom, analyst, in Nordenskiöld (1878).

30. Baringer Hill, Llano Co., Texas. Hidden and Mackintosh (1889).
31. Re-analysis of above sample by Hillebrand (1892).
32. Strickland Quarry, Portland, Conn. J. Ito, analyst, ThO_2 includes rare earths.
33. Newry, Me. J. Ito, analyst. ThO_2 includes rare earths.
34. Mi Vida mine, San Juan Co., Utah. J. Ito, analyst.
35. Big Indian Wash, San Juan Co., Utah. J. Ito, analyst.
36. Ruggles mine, Grafton, N. H. J. Ito, analyst.
37. Wölsendorf, Bavaria. J. Ito, analyst.
38. Lac Pied des Monts, Que. Kramer, analyst.
39. Gordonia, SoutM Africa, Mountain, analyst, in Holmes (1934).
40. Shinkolobwe, Katanga, Belgian Congo. H. Levine, analyst.
41. Joachimsthal, Czechoslovakia. H. Levine, analyst.
42. Gordonia, South Africa. H. Levine, analyst.
43. Sudbury Dist., Ont. H. Levine, analyst.
44. Morogoro, Tanganyika. Marckwald (1911).
45. Spruce Pine, N. C. H. Levine, analyst.
46. Monument No. 2 mine, Apache Co., Ariz. A. Sherwood, analyst.
47. Happy Jack mine, San Juan Co. Utah. A. Sherwood, analyst.
48. School Section 36 mine, San Juan Co., Utah. A. Sherwood, analyst.
49. School Section 36 mine, San Juan Co., Utah. A. Sherwood, analyst.
50. Mi Vida mine, San Juan Co., Utah. A. Sherwood, analyst.
51. La Sal shaft, San Juan Co., Utah. A. Sherwood, analyst.
52. Hidden Splendor mine, Emery Co., Utah. A. Sherwood, analyst.
53. Auselmyren, Norway. Core of crystal. Bakken and Gleditsch (1938).
54. Martapoera, Borneo. Chernik (1909).
55. Theano Pt., Algoma Dist., Ont. Analyst, H. Levine.
56. Eldorado Mines, Gt. Bear Lake, N.W.T. Analyst, J. Ito.
57–58. Strickland Quarry, Portland, Conn. Analyst, Hecht, in Foye and Lane (1934).
59–60. Wilberforce, Ont. Analyst, A. Sherwood. No. 59 outer 4 mm. of large crystal. No. 60 core of crystal.
61. Prizbram, Czechoslovakia. Analyst, A. Sherwood.
62. Wood mine, Central City, Colo. Analyst, A. Sherwood.
63. Schmiedeberg, Silesia. Analyst, A. Sherwood.
64. Moss, Norway. Chernik (1909).
65. Nicholson mine, L. Athabaska Dist., Sask. Brooker and Nuffield (1952).
66. Nicholson mine, L. Athabaska Dist., Sask. Brooker and Nuffield (1952).
67. Martin lake, L. Athabaska Dist., Sask. Brooker and Nuffield (1952).
68. Martin Lake, No. 2 flow, L. Athabaska Dist., Sask. Brooker and Nuffield (1952).
69. Donaldson Group, L. Athabaska Dist., Sask. Brooker and Nuffield (1952).
70. A. B. C. Group, L. Athabaska Dist., Sask. Brooker and Nuffield (1952).

THE AMERICAN MINERALOGIST. VOL. 42, NOVEMBER-DECEMBER 1957

ABSORPTION SPECTRA OF SOME SILICATES IN THE VISIBLE AND NEAR INFRARED*

Sydney P. Clark, Jr., *Dunbar Laboratory, Harvard University, Cambridge, Massachusetts.*†

Abstract

Absorption coefficients of olivine, diopside, and three varieties of garnet have been measured in the spectral range between 0.3 and 4 microns. Olivine and diopside have absorption peaks at a wave number of about 10,000 cm^{-1}. Almandine has a strong peak at about 8000 $cm.^{-1}$ and numerous weaker peaks. A garnet between andradite and grossularite in composition showed no strong peaks. The ultraviolet absorption edge of the latter garnet lies at about 16,400 $cm.^{-1}$, and those of the other crystals lie between 27,000 and 29,000 $cm.^{-1}$. The positions of the absorption peaks can be explained by electronic transitions between a relatively small number of excitation levels.

At wave numbers between 2000 and 7000 $cm.^{-1}$ the absorption coefficient of olivine is less than 0.5 $cm.^{-1}$. and that of diopside is about 1 $cm.^{-1}$. These results support the hypothesis that radiative transfer is important in the earth's mantle.

Introduction

A recent development in geophysics is the recognition of the fact that radiative transfer may play an important role in the heat balance of the earth (Preston, 1956; Clark, 1956). In non-opaque media, the energy transferred by radiation is in addition to that carried by lattice vibrations, and the effect appears as an enhanced thermal conductivity. The term which represents the effect of radiative transfer in the expression for thermal conductivity contains one material constant, the optical absorption coefficient. The work described here was undertaken as a step towards estimating absorption coefficients in the earth.

The absorption coefficients of minerals give important information about some of their fundamental properties. The pioneer work of Coster (1948) and the careful study by Hughes (unpublished) have demonstrated that the electrical properties of silicates are similar to those of oxide semiconductors. Absorption maxima should occur at frequencies corresponding roughly to the excitation energies of the various conduction processes. Measurements of absorption spectra aid in the identification of the types of conduction mechanisms, and contribute basic data towards the understanding of the electronic structure of silicates.

Materials Studied

Most of the results were obtained from single crystals of peridot (the gemstone variety of olivine), diopside and three varieties of garnet.

---

* Paper No. 160 published under the auspices of the committee on Experimental Geology and Geophysics and the Division of Geological Sciences at Harvard University.

† Present address: Geophysical Laboratory, Washington, D. C.

Physical properties of these materials are given in Table 1, and chemical analyses of two of the garnets are given in Table 2. Measurements were also made on a single crystal of orthoclase, var. adularia, from Madagascar, and on a polycrystalline specimen of jadeite from Burma.

Flawless plates were cut from the crystals of olivine, diopside, almandine, and adularia. The grossularite was unaltered, but the specimen used in the measurements was marred by small conchoidal fractures irregularly distributed through it. The pyrope was also fresh, but it contained scattered inclusions of an opaque mineral, possibly ilmenite, and elongate prisms of a colorless mineral with refractive index less than that of the pyrope. Runs were made on two samples of pyrope; they agreed closely over most of the range of frequencies. The jadeite was milky and transmitted poorly as a result.

Compositions of the unanalyzed specimens can be estimated from the data in Table 1. The olivine contains 7–8 mol per cent fayalite according to its refractive indices, 8 per cent fayalite according to specific gravity,

TABLE 1. PHYSICAL PROPERTIES OF THE MINERALS STUDIED

Mineral	Specific gravity	Optical properties	*X*-ray properties	Thickness of specimen (mm.)
Olivine, Burma	3.31 ± 0.01	$\alpha=1.648\pm0.003$ $\beta=1.665$ $\gamma=1.686$ $(+)2V=85°$	$d_{130}=2.772\pm0.002$ Å	1.55 & 12.9
Diopside, Rotenkopf, Tyrol. Harvard Museum No. 88405	3.29 ± 0.01	$\alpha=1.672\pm0.003$ $\beta=1.680$ $\gamma=1.702$ $(+)2V=60°$ $Z\wedge C=40°$		1.56
Pyrope, Benenitra, Madagascar. Harvard Museum No. 85426	3.72 ± 0.01	$n=1.776\pm0.003$	$a_0=11.49\pm0.01$ Å	1.27_5 & 1.29_5
Almandine, India	4.16 ± 0.01	$n=1.807\pm0.003$	$a_0=11.52\pm0.01$ Å	1.56_5
Grossularite, South Africa	3.71 ± 0.01	$n=1.801\pm0.003$	$a_0=11.94\pm0.01$ Å	1.16

TABLE 2. CHEMICAL ANALYSES OF ALMANDINE AND GROSSULARITE
J. Ito, Analyst

	Almandine*		Grossularite	
	Weight per cent	Mol. Prop.	Weight per cent	Mol. Prop.
SiO_2	37.69	628	36.92	615
TiO_2	0.07	1	0.12	2
Al_2O_3	20.62	202	12.47	122
Fe_2O_3	4.30	27	14.14	88
FeO	30.80	428	1.84	26
MnO	1.97	28	0.95	13
MgO	4.40	109	—	—
CaO	—	—	33.63	601
Na_2O	—	—	—	—
K_2O	—	—	—	—
H_2O-	0.36	—	0.57	—
H_2O+	—	—	—	—
	100.21		100.64	

* Only about 300 milligrams of material were available for this analysis.

and 9 per cent fayalite according to the interplanar spacing, d_{130} (Winchell, 1933; Yoder, 1954). The diopside contains 12 per cent hedenbergite by weight according to its optical properties and about 10 per cent hedenbergite according to specific gravity. The refractive index and unit cell size of the pyrope lead to an approximate composition pyrope$_{0.44}$ almandine$_{0.55}$andradite$_{0.01}$ (Sriramidas, 1957).

EXPERIMENTAL METHOD AND RESULTS

The reduction in intensity of a beam of light in passing through a crystal is caused by three processes: absorption within the sample, reflection at its surfaces, and scattering within the sample. In the absence of scattering, the relation between absorption, reflection, and transmission is (McMahon, 1950)

$$I = I_0 \frac{(1 - R)^2 e^{-\alpha x}}{1 - R^2 e^{-2\alpha x}} \tag{1}$$

where I_0 is the intensity of the incident beam, I the intensity of the transmitted beam, R the reflection coefficient, α the absorption coefficient and x the thickness of the specimen. If R is less than 0.1, the second term in the denominator can be neglected. The reflection coefficient at normal incidence is related to the refractive index, n, by the well-known Fresnel formula

$$R = \frac{(n-1)^2}{(n+1)^2} \tag{2}$$

Expressions (1) and (2) depend on the assumptions that the sample is a clear, flat plate with specularly reflecting surfaces which are parallel to each other and normal to the beam of light. Great care in sample preparation is necessary if accurate values of the absorption coefficient are to be obtained. If the surfaces of the sample are not flat and parallel, the specimen acts as a lens, which defocuses the spectrometer. If the surfaces of the sample are not highly polished, diffuse reflection, which may be far stronger than that predicted by (2), takes place. Scattering by flaws and inclusions in the sample increases the apparent absorption coefficient. The importance of careful sample preparation cannot be overemphasized; the transmission of the grossularite sample was increased by a factor of three by repolishing after a preliminary series of measurements.

The samples used in the present work were carefully surfaced and polished, and the use of (1) and (2) in the reduction of the data is justified. Little can be done about scattering by flaws and inclusions; these were present in the grossularite and pyrope, and the absorption coefficients of these crystals are overestimated as a consequence. The error is probably not large, however, since the total cross-sectional area of flaws was only a small percentage of the areas of the crystals.

Measurements were made on a Perkin-Elmer model 12-C single-beam spectrometer, fitted with quartz optics. The transmissions of the specimens were determined by the "sample in, sample out" method, and repeat runs were made to check doubtful features of the spectra. The transmissions were reproducible to within about 2 per cent. All measurements were made at ambient temperature and covered the spectral range 0.3–4 microns.

The transmissions of the peridot, diopside, and garnets are shown in Figs. 1 and 2 as functions of wave number. (The wave number, $\bar{\nu}$, equals the reciprocal of the wave length in centimeters.) The propagation direction direction of the light was parallel to the *b*-axis of the olivine and normal to one of the cleavage planes of the diopside. The adularia showed high transmission (60–80 per cent), which decreased smoothly towards higher frequency. No peaks were found, and the results are not shown graphically. The poor transmission of the sample of jadeite precluded quantitative measurements; rough results were obtained near the ultraviolet absorption edge, which was found to lie near 29,000 cm.$^{-1}$.

The refractive indices given in Table 1 were used to determine reflection coefficients. Mean values were used for the anisotropic substances, and the dependence of the refractive index on frequency was neglected.

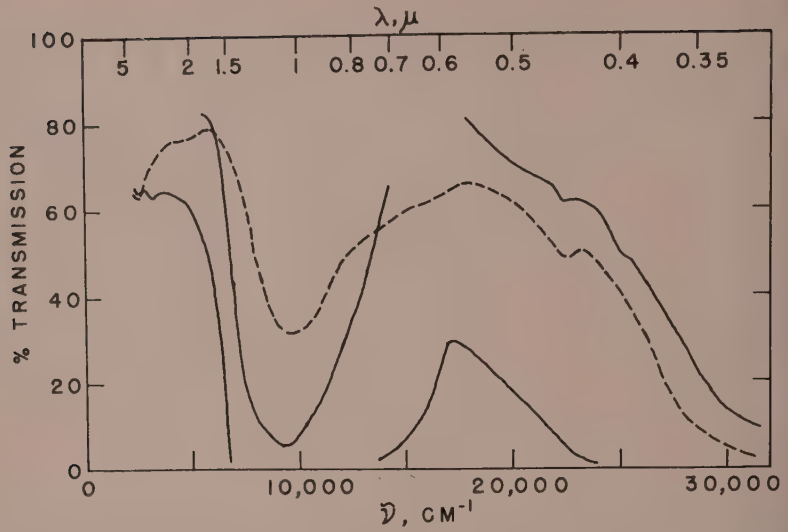

FIG. 1. Transmission curves for olivine (solid curves) and diopside (dashed curve). Results are shown for two crystals of olivine of different thicknesses.

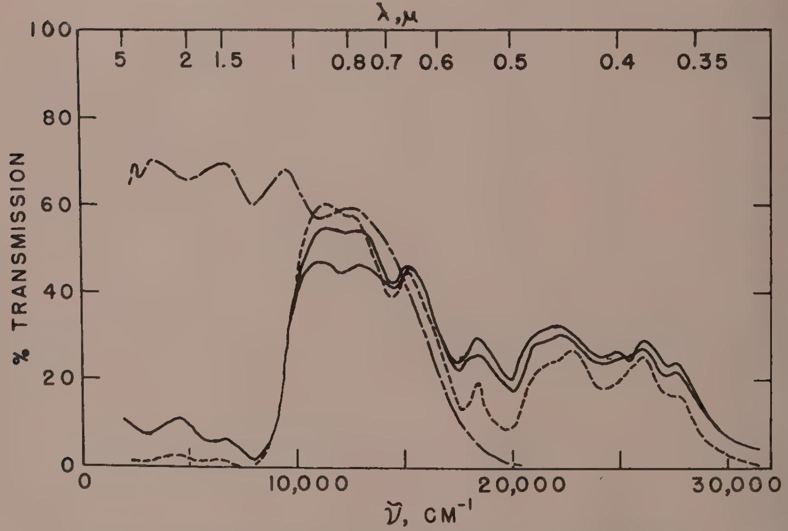

FIG. 2. Transmission curves for pyrope (solid curve), almandine (dashed curve), and grossularite (dot-dash curve).

Both of these approximations are justified, since the reflection coefficient is not a sensitive function of index for n less than 2.0. To sufficient accuracy, $R=6$ per cent for olivine and diopside, and $R=8$ per cent for the garnets.

A check on the above values of R and on the overall precision of the measurements is afforded by the results for the plates of olivine of different thicknesses. The absorption coefficients agreed to within 0.4 cm.$^{-1}$; at most frequencies the discrepancy between the two sets of data was half this. The absorption coefficients of all substances are estimated to be uncertain by no more than a few tenths cm.$^{-1}$. Results are given in Fig. 3; the absorption coefficient of adularia increased roughly linearly from about 2 cm.$^{-1}$ at a wave number of 2500 cm.$^{-1}$ to about 4 cm.$^{-1}$ at 30,000 cm.$^{-1}$.

THE RADIATIVE CONDUCTIVITY

The radiative conductivity, which relates the flux of radiant energy to the thermal gradient, was computed from the absorption coefficients shown in Fig. 3 (Table 3). Calculations were made by the methods developed previously (Clark, in press), under the assumption that the absorption is independent of temperature. For comparison with the values in Table 3, the ordinary conductivity of most silicates at room temperature is less than 0.01 cal./cm. sec.° C. With the exception of almandine and pyrope, the radiative conductivity exceeds this value at 1000° K. and increases markedly with temperature. The effect is particularly large in the cases of olivine and diopside.

It is unlikely, however, that such large values of the radiative conductivity exist in the earth. Crystals in the mantle are likely to be imperfect, and the attendant scattering may be more important than absorption in a material such as olivine. Furthermore, the absorption will increase with temperature. Both of these effects will reduce the radiative conduc-

TABLE 3. THE RADIATIVE CONDUCTIVITY

Values are given in cal./cm. sec.° C.

Mineral	Temperature (° K.)			
	1000	1500	2000	2500
Olivine	0.071	0.206	0.346	0.483
Diopside	0.016	0.057	0.106	0.173
Pyrope	0.001	0.005	0.018	0.044
Almandine	0.001	0.004	0.010	0.051
Grossularite	0.011	0.046	0.109	0.097

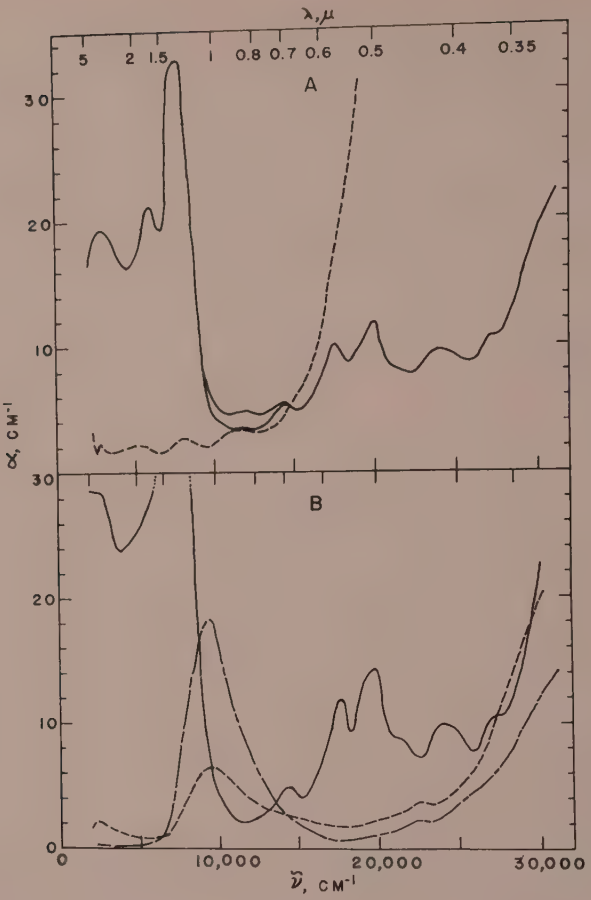

Fig. 3. (A) Absorption coefficients (α) of pyrope (solid curve) and grossularite (dashed curve). Results for the two crystals of pyrope differed appreciably between 10,000 and 15,000 cm.$^{-1}$, and are shown separately in this range of wave numbers. (B) Absorption coefficients of almandine (solid curve), diopside (dashed curve), and olivine (dot-dash curve).

tivity, since it is inversely proportional to the sum of the absorption and scattering coefficients.

Nevertheless, the measurements strongly support the hypothesis that radiative transfer is important in the earth. Any attempt to estimate the radiative conductivity in the mantle would clearly be premature, but it seems reasonably certain that an appreciable effect exists.

Discussion

The positions of absorption peaks in the visible and ultraviolet are a measure of the difference in energy between the highest filled electronic band in the crystal (the valence band) and the several excited states which may exist. The following tentative interpretation in terms of electronic energy levels is analogous to the familiar method of interpreting atomic spectra. The energies of the absorption maxima cannot strictly be combined in the simple additive manner characteristic of atomic spectra, however. The energy levels are broadened into bands by atomic interactions, and the optical selection rules in crystals require that the propagation vector of the electron be unchanged by a direct optical transition (Peierls, 1955, p. 188). Both the energy within a band and the transition probability depend on the propagation vector, and therefore the energy of that electron in a given band which is most likely to be excited depends in part on its final state.

TABLE 4. POSITIONS AND ENERGIES OF ABSORPTION PEAKS

Principal peaks are marked with an asterisk; those marked (w) are very weak

Olivine		Diopside		Almandine		Pyrope		Grossularite	
Position cm.$^{-1}$	Energy eV	Position cm.$^{-1}$	Energy eV	Position cm.$^{-1}$	Energy eV	Position cm.$^{-1}$	Energy eV	Position cm.$^{-1}$	Energy eV
2500	0.31	2500	0.31	2900	0.36	2900	0.36	2800	0.35
3200	0.40			6000	0.74	6000	0.74	5000	0.62
9600*	1.19	9600*	1.19	7900*	0.98	7900*	0.98	8000	0.99
				12,100	1.50	12,100	1.50	11,300	1.40
				14,400	1.79	14,300	1.77		
				17,600	2.18	17,600	2.18		
				20,000	2.48	20,000	2.48		
				21,500(w)	2.67				
22,600	2.80	22,600	2.80	23,900	2.96	23,900	2.96		
25,200(w)	3.12			27,200	3.37	27,200	3.37		
Ultraviolet Absorption Edges									
29,100	3.6	27,200	3.3	27,600	3.4	27,600	3.4	16,400	2.0

Ultraviolet absorption edge of jadeite at roughly 29,000 cm.$^{-1}$ or 3.6 eV.

The most intense absorption is produced by electronic transitions from the valence band to the conduction band of the crystal. These transitions give rise to absorption in the visible and ultraviolet in silicates; they lead to intrinsic semiconduction when thermally excited. Several weak peaks were found at energies less than those of the ultraviolet absorption edges; these correspond in energy to exciton absorption *i.e.* to transitions involving levels between the valence and conduction bands. They are too weak and at too high frequencies to be interpreted as due to lattice vibrations.

Positions and energies of the various peaks and of the ultraviolet absorption edges are given in Table 4. The positions of the peaks could be located within about 0.03 eV. The ultraviolet absorption edge is more difficult to locate because it is not a sharp feature. Its position was taken to be that at which the absorption coefficient reached 10 cm.$^{-1}$ This definition is arbitrary, and little importance can be attached to the exact numerical values of these particular data.

The spectra of olivine and diopside show striking similarities. The peak at about 10,000 cm.$^{-1}$ is interpreted as due to the Fe^{++} ion. It is more intense in olivine because of the higher concentration of iron atoms. This interpretation is supported by the presence of a peak at the same position in iron-bearing glasses (Weyl, 1951). Its energy corresponds to the excitation energy of "impurity" semiconduction in these minerals (Hughes, unpublished).

This peak may be the result either of an exciton level 1.19 eV above the valence band, which acts as an acceptor level, or of a donor level 1.19 eV below the conduction band. The two processes cannot be distinguished by absorption measurements alone, and ambiguity of this sort is present in all of the interpretations which follow. If the above level is 1.19 eV above the valence band, the peak at 22,600 cm.$^{-1}$ is interpreted as arising from the excitation of an electron from this level to the conduction band. Conversely, the peak at 22,600 cm.$^{-1}$ would represent a transition from the valence band to the exciton level if the latter lies 1.19 eV below the conduction band. The sum of the energies of the two peaks exceeds that of the ultraviolet absorption edge by about 0.4 eV, but the selection rules may forbid transitions from the exciton level to the bottom of the conduction band.

The peaks at 2500 cm.$^{-1}$ correspond roughly to similar peaks in the garnets. They suggest the existence of an exciton level of unknown origin about 0.3 eV above the valence band or below the conduction band. A similar peak was not found in adularia. The remaining peaks in the olivine spectrum are left unaccounted for. They did not appear in the diopside spectrum, and they may not appear in all crystals of olivine.

The results for almandine and pyrope closely resemble each other; both spectra are very complex. The positions of the peaks can be explained by exciton levels 0.36, 0.74, 0.98, and 2.48 eV above the valence band or below the conduction band. The peaks arise from transitions among these levels and between them, the valence band, and the conduction band. This scheme, however, may not account for the relative intensities of the peaks as well. With the exception of transitions to the conduction or valence band, it accounts for their positions accurately, the greatest discrepancy being 0.06 eV.

The spectrum of grossularite differs markedly from those of the other garnets; it may be explained by exciton levels at 0.35 and 0.99 eV. The peak at 11,300 cm.$^{-1}$ would then represent a transition between the valence or conduction band and the level at 0.99 eV. The discrepancy between the position of this peak and the ultraviolet absorption edge is 0.2 eV.

The peaks in the garnets at about 8000 cm.$^{-1}$ are interpreted as due to the Fe^{++} ion. The difference between the positions of this peak in garnet and olivine is attributed to the difference in coordination of the iron (six-fold in olivine and eight-fold in garnet). A similar dependence on coordination number has previously been inferred in glasses (Weyl, 1951). The peak near 20,000 cm.$^{-1}$ in almandine and pyrope is presumably due to the Fe^{+++} ion. It corresponds to the ultraviolet absorption edge in grossularite, suggesting that the narrow exciton band in almandine and pyrope is broadened by the addition of ferric iron and assumes the role of either the valence or the conduction band as the amount of ferric iron increases. The behavior of Fe^{+++} in these garnets is analogous to the behavior of Ni^{++} in glasses and in NiO (Weyl, 1951; Johnston and Cronemeyer, 1954).

The interpretations given above must be regarded as tentative. They have the advantage of simplicity, but most of them depend on the possibility of an exciton level acting simultaneously as a donor and acceptor. This is possible if the average lifetime of excited states is sufficiently long. The specimen was exposed to white light, which continually excites the electrons, during the measurements.

Uncertainties in the causes of the exciton levels can be reduced by studies of synthetic crystals ranging in composition throughout solid-solution series. The behavior of the spectra as functions of composition will yield much information about the electronic structure of silicates.

CONCLUSIONS

Perhaps the most important result of this work is the discovery that certain silicates are highly transparent to radiation in the near infrared. The fact that olivine shows this property is almost certain to influence estimates of temperatures in the earth.

Spectra of iron-bearing silicates may show considerable complexity in the visible and near infrared. An absorption peak in the spectra of olivine and diopside corresponds in energy to the excitation energy of "impurity" semiconduction in these minerals; it is tentatively ascribed to fayalite or hedenbergite in solid solution in the crystals. In such a situation, the term "impurity" should be discouraged; the term "exciton" has been substituted in this paper. Elements present in quantities amounting to a few per cent can hardly be considered impurities in the same sense as traces of other elements in silicon or germanium.

It is expected that certain exciton levels will widen as the iron content of the crystal increases. They will assume the role of either the valence or the conduction band at compositions near the iron end member. An example of this type of behavior is provided by almandine and andradite-bearing grossularite.

ACKNOWLEDGMENTS

The specimens of pyrope, diopside, and grossularite were provided from the Holden Collection of Harvard University through the kindness of Prof. Clifford Frondel. The remaining material was kindly supplied by Prof. Francis Birch. The spectrometer was made available for this work through the courtesy of Prof. William Paul. The exacting task of preparing the specimens for measurement was skillfully carried out by Mr. Harold J. Ames. I am indebted to Profs. Birch, Frondel, and C. S. Hurlbut, Jr. and to Dr. D. C. Tozer for reading the manuscript and offering many valuable suggestions.

REFERENCES

CLARK, S. P. (1956), Effect of radiative transfer on temperatures in the earth: *Geol. Soc. Am., Bull.* **67,** 1123–1124.

——— (in press), Radiative transfer in the earth's mantle: *Trans. Amer. Geophys. Union.*

COSTER, H. P. (1948), The electrical conductivity of rocks at high temperatures: *Mon. Not. Roy. Astr. Soc., Geophys. Suppl.*, **5,** 193–199.

HUGHES, H. (unpublished), The electrical conductivity of the earth's interior: Ph.D. Thesis, University of Cambridge, 1953.

JOHNSTON, R. W., and CRONEMEYER, D. C. (1954), Infrared absorption of NiO: *Phys. Rev.*, **93,** 634.

MCMAHON, H. O. (1950), Thermal radiation from partially transparent reflecting bodies: *Jour. Opt. Sci. Am.*, **40,** 376–380.

PEIERLS, R. E. (1955), *Quantum theory of solids:* Oxford University Press, 229 pp.

PRESTON, F. W. (1956), Thermal conductivity in the depths of the earth: *Am. Jour. Sci.*, **254,** 754–757.

SRIRAMIDAS, A. (1957), Diagrams for the correlation of unit cell edges and refractive indices with the chemical composition of garnets: *Am. Mineral.*, **42,** 294–298.

WEYL, W. A. (1951), *Coloured Glasses:* Sheffield, The Society of Glass Technology, 541 pp.

WINCHELL, A. N. (1933), *Elements of optical mineralogy: Part II, Description of minerals:* New York, Wiley, 459 pp.

YODER, H. S. (1954), The forsterite-fayalite series: Carnegie Institution of Washington, *Year Book No.* **53,** 119–120.

THE AMERICAN MINERALOGIST, VOL. 42, NOVEMBER-DECEMBER 1957

GEOCHEMISTRY OF GERMANIUM IN THE OXIDIZED ZONE OF THE TSUMEB MINE, SOUTH-WEST AFRICA*

CLIFFORD FRONDEL AND JUN ITO, *Harvard University, Cambridge, Massachusetts.*

ABSTRACT

The primary ores of the Cu-Pb-Zn deposit at Tsumeb contain germanium in solid solution in relatively large amounts in enargite, tennantite, renierite and germanite. Oxidation of the ores in a limestone environment has given rise to an extensive suite of secondary carbonates, sulfates, arsenates, phosphates, vanadates, and oxides. The chief cations are Cu, Pb, and Zn together with minor amounts of Ca, Mg, Fe, Ba, Cd, Mo, and Co. The germanium contained in the primary minerals is released during oxidation and is found in two valence states in the secondary minerals. It occurs very sparingly as divalent Ge in substitution for Pb in anglesite and cerussite (50–500 ppm) and in a new basic lead sulfate containing 8.18 weight per cent GeO. The bulk of the germanium in the oxidized zone is quadrivalent. It preferentially enters the early-formed arsenates, including mimetite, olivenite, and in particular bayldonite (with 500–5000 ppm Ge). The Ge^4 substitutes for As^5 in the (AsO_4) tetrahedra, with Ge^4 0.44 kX and As^5 0.47 kX, analogous to the well-known substitution of Ge^4 for Si^4 in silicates. The later-formed minerals smithsonite, cerussite, azurite, and malachite, which comprise the bulk of the upper part of the oxidized zone, are low or lacking in Ge.

The Ge^2 ion is found at the immediate interface between the sulfide zone and the oxidized zone where, in line with the known chemical and Eh-pH relations of this ion, it appears to have formed under weakly acid and reducing conditions. With increasing Eh and pH of the environment the Ge^2 is converted to Ge^4 and is housed in early-formed arsenates stable under moderately acid and oxidizing conditions. In the upper part of the zone of oxidation, under alkaline and oxidizing conditions, the germanium apparently is leached as alkali germanates in the absence of hemimorphite and other secondary silicates stable under such conditions and suited to house Ge^4 in solid solution.

INTRODUCTION

The primary sulfide ores of the Pb-Cu-Zn deposit at Tsumeb are notably enriched in germanium. We have investigated the distribution of the germanium among the various secondary minerals that have formed during the oxidation of the primary ores.

The Tsumeb mine is located in South-West Africa approximately 100 km. northwest of Grootfontein. The deposit has been described by Schneiderhöhn (1920) and Moritz (1933), and there is a large literature describing various of the primary and secondary minerals of the locality. The ore body consists of replacements along fracture zones in limestone and dolomite. The primary minerals are principally sphalerite, chalcopyrite, galena, pyrite, bornite, chalcocite, enargite, tennantite, renierite, germanite, and luzonite. The germanium is contained in solid solution largely in the enargite, tennantite, renierite, and germanite, the latter containing up to 10.2 weight per cent Ge. Single masses of germanite weighing up to 25 pounds have been found. The mine is commercially producing germanium from the primary ores at the present time. Details of the recovery of Ge from the ores are given by Ratledge, *et al.* (1955).

---

* Contribution from the Department of Mineralogy and Petrography, Harvard University, No. 376.

Surface oxidation at Tsumeb is extensive, with the formation of a remarkable variety of carbonates, sulfates, arsenates, phosphates, vanadates, and oxides (Table 1). The chief cations are Cu, Pb and Zn, together with minor amounts of Ca, Mg and Fe and trace amounts of Ba, Cd, Co, Mo and other elements. The most abundant secondary minerals are the carbonates cerussite, smithsonite, malachite, and azurite. Finely crystallized specimens are common. Secondary quartz is rare, and silicates such as hemimorphite and willemite apparently do not occur. There is also a zone of secondary enrichment containing chalcocite with covellite. The detailed paragenesis of the secondary minerals is discussed on a later page.

EXPERIMENTAL OBSERVATIONS

The present investigation would be best based on samples collected in geological context at the mine, but the oxidized ores are now entirely mined out. We have utilized a collection of about 1500 specimens of Tsumeb minerals preserved in the Harvard Mineralogical Museum. The bulk of this collection had been made by a former manager of the Tsumeb mine, and notes were available in his catalogue as to the spatial relations and association of many of the specimens.

The germanium determinations were made spectrographically on a two-meter Baird Associates grating instrument. The methods employed were basically those of Kuroda (1939) and Harvey (1947), using cathode layer excitation at 220 volts DC, continuous arc. Direct Ge determinations by wet methods were made on a few samples that contained Ge in amounts over about 0.01 weight per cent. The experimental data are summarized in Table 1. These data, taken in hand with crystallochemical considerations and chemical tests to determine valence, indicate that germanium occurs in two valence states in the oxidized zone, as Ge^4 and Ge^2, and that certain secondary minerals are separately enriched in these ions.

Distribution of Quadrivalent Germanium

The secondary heavy-metal arsenates, including olivenite, mimetite, duftite and, in particular, bayldonite are found to be notably enriched in germanium (Table 1). The six different specimens of bayldonite examined all contained Ge in the range 500 to 5000 ppm.

TABLE 1. GERMANIUM CONTENT OF SOME SECONDARY AND PRIMARY MINERALS AT TSUMEB

(Numbers refer to the number of different specimens analyzed)

Name	Composition	5000–500 ppm.	500–50 ppm.	50–5 ppm.	5–0.5 ppm.	<0.5 ppm.
Bayldonite	$(Cu, Pb)_2(AsO_4)(OH)$	6				
Olivenite	$Cu_2(AsO_4)(OH)$	1	2	1	3	
Duftite	$PbCu(AsO_4)(OH)$	1				
Mimetite	$Pb_5(AsO_4)_3Cl$		1	3	4	
Adamite	$Zn_2(AsO_4)(OH)$			1	2	
Tsumebite	$Pb_2Cu(PO_4)(OH)_3 \cdot 3H_2O$			1		
Pyromorphite	$Pb_5(PO_4)_3Cl$		1			1
Mottramite	$Pb(Cu,Zn)(VO_4)(OH)$				1	
Vanadinite	$Pb_5(VO_4)_3Cl$				1	
Wulfenite	$Pb(MoO_4)$			(Ge present, not det.)		
Anglesite	$Pb(SO_4)$	1			3	
Barite	$Ba(SO_4)$				1	
Gypsum	$Ca(SO_4) \cdot 2H_2O$				1	
Caledonite	$Cu_2Pb_5(SO_4)_3(CO_3)(OH)_5$				1	
Linarite	$PbCu(SO_4)(OH)_2$				1	
Un-named	$(Pb,Ge)_2(SO_4)(OH)_2 \cdot 2H_2O$			(8.18 per cent GeO)		
Cerussite	$Pb(CO_3)$		2		1	7
Smithsonite	$Zn(CO_3)$				3	2
Otavite	$Cd(CO_3)$			1		
Calcite	$Ca(CO_3)$			1		3
Aragonite	$Ca(CO_3)$			1		4
Phosgenite	$Pb_2(CO_3)Cl$				1	
Azurite	$Cu_3(CO_3)_2(OH)_2$			1	3	
Malachite	$Cu_2(CO_3)(OH)_2$				3	1
Rosasite	$(Cu,Zn)_2(CO_3)(OH)_2$			1		
Cuprite	Cu_2O				1	
Quartz	SiO_2					1
Chalcocite	Cu_2S					1
Enargite	Cu_3AsS_4	1				
Galena	PbS					1
Pyrite	FeS_2					1
Tennantite	$Cu_{12}As_4S_{13}$	1				

Secondary minerals known from Tsumeb but not examined in the present study: schultenite, descloizite, dolomite, siderite, rhodochrosite, plumboan conichalcite ("parabayldonite," duftite β), iron and manganese oxides.

The chief minerals of the main body of the oxidized zone at Tsumeb are smithsonite, cerussite, malachite, and azurite. These minerals all are very low in their content of Ge (Table 1). To be excepted here are certain rare specimens of cerussite and anglesite which, together with an associated new basic lead sulfate, are found on chemical tests to contain divalent Ge and which are discussed beyond. The secondary compounds of Ca, Cd, and Ba in the deposit that do not carry As or P also are very low or lacking in Ge. The correlation of the germanium thus appears to be with As^5 and not with the heavy metal cations or with the (CO_3) or (SO_4) anionic groups.

The bulk of the Ge contained in the outer crust of the Earth is dispersed in small amounts in solid solution in silicates. There is no direct evidence of the valence state of the Ge in natural silicates, but there is no doubt, from the isostructural relation of many silicates and germanates and of fluosilicates and fluogermanates, and from the existence of solid solution series between such compounds, that the Ge is present as Ge^4 in substitution for Si^4 in the tetrahedral framework. As^5 also goes in four-coordination with oxygen. Some arsenates are isostructural with silicates, such as berzeliite and grossularite, and two of the arsenates at hand, olivenite and adamite, are isostructural with andalusite. A small extent of mutual substitution of As, P, and Si also has been observed in some silicates, phosphates, and arsenates. Direct evidence of the valence state of the Ge in the arsenates at Tsumeb is lacking. It is believed to be present as Ge^4 in substitution for As^5 in tetrahedral coordination. The ionic radius of Ge^4, 0.44kX, is close to that of As^5, 0.47kX, and in fact is closer to that of As^5 than it is to that of Si^4, 0.39kX. Coupled valence compensation is required for the substitution of Ge^4 for As^5. In the case of mimetite (and pyromorphite) this may involve omissions in the halogen positions, since the apatite-type compound $Pb_5(GeO_4)(AsO_4)_2$ and solid solutions of the nature $Pb_5(Ge,SiO_4)(P, As, VO_4)_2$ have been synthesized (Wondratschek and Merker (1956)). There is no evidence for the coupling mechanism in bayldonite and the other arsenates. The coupled substitution of (OH) for O in the coordination group of the (As,Ge) is a possibility, as is the coupled substitution of a trivalent cation such as Ga^3 for Cu^2 or Pb^2 in the cation position. Ga was in fact observed in all of our samples that contained Ge, but no quantitative measurements were made. One of the samples of pyromorphite examined contained 50–500 ppm. of Ge, indicating a substitution of Ge for P analogous to that for As. We wish to emphasize that we do not have experimental proof of the valence state of the Ge in these arsenates. It is possible, although unlikely in view of the Eh-pH relations obtaining in the arsenate stage of mineralization, discussed beyond, that the Ge is divalent and then presumably substitutes in the cation positions of these minerals.

Distribution of Divalent Germanium

Although the Ge^2 ion has not hitherto been identified in minerals, the evidence for its existence at Tsumeb is clear-cut. It is present in the amount of 8.18 weight per cent GeO in substitution for Pb in a new basic sulfate of lead* and is present in the range 50–500 ppm. in the immediately associated, somewhat later-formed cerussite. Several other specimens of early-formed cerussite and a specimen of anglesite also were found to contain Ge in the range 50–500 ppm. Conclusive qualitative tests†* for divalent Ge were obtained on the anglesite, cerussite, and the basic lead sulfate. A direct wet determination of Ge in one cerussite sample gave $.015 \pm .005$ weight per cent GeO. The typical cerussite of the deposit is of a much later period of formation and is very low or lacking in Ge. Divalent germanium appears to be quite rare in the secondary minerals at Tsumeb, and will be shown to form under rather specialized conditions.

The substitution of Ge^2 for Pb^2 raises the question of the radius of the Ge^2 ion. This is given as 0.72 Å by Ahrens (1952) as calculated from ionization potentials. This value appears to be low. The only compounds of divalent germanium whose structures are known are GeI_2 and GeS. In the deformed NaCl-type structure of GeS, described by Zachariasen (1932), the Ge is in distorted six-coordination with S. The two principal Ge-S distances are 2.58 and 2.97 kX. Using the measured S-S distance of 3.55 kX, the effective radii of the Ge^{+2} are 1.20 and 0.80 kX with the average 1.0 kX. GeI_2 crystallizes in the CdI_2 structure-type (Powell and Brewer, 1938). The asymmetrical coordination in this layer-structure results in strong polarization and this is reflected in a pronounced shortening of the A–X distance as compared to the value expected from the normal ionic radii in six-fold coordination. This amounts to 8.4 per cent in CdI_2 and 13.1 per cent in PbI_2; assuming a shortening of 10 per cent in the measured Ge-I distance, 2.927 kX, the normal ionic radius of Ge^2 is 1.0 kX. The Pb^2 ion in six-coordination has a radius of 1.32 kX. This differs considerably from 1.0, but extensive solid solution series have been observed between other elements with as large a difference in size, as for example, the pair Ca-Pb in hedyphane-svabite, pyromorphite, aragonite, wulfenite and other minerals, and the pair Na-K.

---

* Formula $(Pb, Ge, Ga)_2(SO_4)(OH)_2 \cdot 2H_2O$ from the analysis PbO 63.34, GeO 8.18, (Ga_2O_3, Fe_2O_3, Al_2O_3) 0.86, SO_3 15.06, H_2O+11.35, H_2O-0.21, insol. 0.56, total 99.56. Dense white aggregates of hair-like fibers. Uniaxial (?) positive, with nO 1.747, nE∼1.78. Unit cell uncertain, apparently hexagonal with a_o 17.76 Å, c_0 10.89. DTA curve shows an endothermic break at 263° (H_2O lost) and an exothermic break at 463° (Ge^2 oxidized).

† For cerussite and the basic lead sulfate described the mineral is dissolved in HCl and lead removed as $PbSO_4$ by addition of H_2SO_4. Addition of H_2S to the weakly acid solution precipitates yellow GeS. The GeS is soluble in warm NH_4OH solution, from which, after acidification by H_2SO_4, H_2S precipitates white GeS_2. For the relatively insoluble anglesite, the very fine powder is treated with concentrated HCl. $PbSO_4$ precipitates with H_2SO_4 after dilution with H_2O_4 and GeS is precipitated by H_2S from the moderately acid filtrate.

DISCUSSION

Although germanium is markedly siderophile in its geochemical behavior, in the upper lithosphere it also shows both oxyphile and chalcophile tendencies and is found in some sulfidic ores. Here it occurs particularly in tetrahedrally coordinated sulfosalts that are structural derivatives of sphalerite, including tennantite and the related minerals renierite (with 6 to 7.7 weight per cent Ge), germanite and, in smaller amounts, in enargite, stannite, and sphalerite itself. Colusite, renierite, and germanite are essentially isostructural as shown by Murdoch (1954). We have have found by qualitative chemical tests that the Ge in germanite and renierite is divalent. The formula for germanite probably is (Cu,Ge)S. The Ge in argyrodite, Ag_8GeS_6, on the other hand, was found to be quadrivalent as expected.

When deposits containing primary sulfarsenides are exposed by erosion to chemical attack by surface waters, the S and As are oxidized to sulfate and arsenate, and the metal cations, including trace elements such as Ge, are freed to combine with oxygen or oxygenated anions available in the attacking solution. Certain elements, notably copper, may also be in part carried downward to the water table where they may be reprecipitated as sulfide. The details of the oxidation process vary widely with the mineralogy of the primary ores, climatic and other factors, and particularly with the nature of the country rock. In a limestone environment such as at Tsumeb the free acid formed during oxidation at the interface with the primary sulfosalts and sulfides is neutralized by reaction with $CaCO_3$ to produce solutions saturated with CO_2. The upper part of the zone of oxidation may then be characterized by a carbonate mineralogy.

Paragenesis of the Secondary Minerals at Tsumeb

The observed mineral association and sequence of mineralization in the oxidized zone at Tsumeb may be outlined to provide a background against which the Eh and pH relations and their control over the distribution of the Ge may be discussed.

The heavy-metal arsenates are in general the earliest formed of the secondary minerals at Tsumeb, and are developed chiefly toward the bottom of the zone of oxidation at or near the boundary with the sulfide zone. Of the several arsenates, mimetite and bayldonite appear to be first formed and often are found directly altering from sulfosalts. Olivenite occasionally is found directly deposited upon sulfosalts and chalcocite, but usually is later than bayldonite and sometimes forms pseudomorphs after that species. Adamite, like zinc compounds in general in the zone of oxidation, appears to have been relatively mobile and is found locally in the upper carbonate-rich portion of the oxidized zone. The chemistry of the oxidation of the original sulfarsenides and the reported syntheses of these arsenates, recently summarized by Guillemin (1956), indicates that the secondary arsenates at Tsumeb formed in an acid environment. Thus, duftite has been synthesized over the range pH 2.5–4, and bayldonite has been obtained from pH 5–8. Olivenite, adamite and mimetite also are obtained from acid solutions. Schultenite, which can be crystallized from boiling HNO_3, is earlier than anglesite at Tsumeb, and is associated with bayldonite. The following expressions for the oxidation of enargite and tennantite have been written by Guillemin (1956):

$$4Cu_3AsS_4 + 35\,O_2 + 10H_2O \rightarrow 12CuSO_4 + 4H_3AsO_4 + 4H_2SO_4$$
$$2Cu_{12}As_4S_{13} + 61\,O_2 + 14H_2O \rightarrow 24CuSO_4 + 8H_3AsO_4 + 2H_2SO_4$$

The dissociation constant of H_3AsO_4 is about 1/25 that of H_2SO_4. The formation of secondary copper arsenates such as olivenite by reduction of the acidity of the solution, such as by reaction with waters carrying $CaCO_3$, can be suggested by the following expression:

$$2CuSO_4 + H_3AsO_4 + 2CaCO_3 + 3H_2O \rightarrow Cu_2(AsO_4)(OH) + 2CO_2 + 2CaSO_4\cdot 2H_2O$$

At Tintic, Utah, where there has been extensive oxidation in a carbonate environment of primary ores rich in enargite, olivenite is one of the earliest of the secondary minerals. In part it is contemporaneous with chalcocite. The alteration of the enargite to olivenite and chalcocite has been represented by Lindgren and Loughlin (1919) by the following expression:

$$2Cu_3AsS_4 + 15\,O_2 + H_2O + 7CaCO_3 \rightarrow 2Cu_2(AsO_4)(OH) + Cu_2S + 7CaSO_4 + 7CO_2$$

Anglesite, at Tsumeb as elsewhere, is a relatively early mineral. It forms in an acid environment. Anglesite is developed only locally at Tsumeb, in parts of the ore body relatively rich in galena, and sometimes is found deposited upon altering galena and other sulfides. In the few specimens available where the sequence could be determined, anglesite is later than bayldonite. It is not, however, a typical mineral of the overlying carbonate stage and falls in its general position in the lower, arsenate-rich, acid portion of the oxidized zone. The one specimen of anglesite found to be rich in Ge^2 was associated with covellite and altering galena and tennantite. The anglesite was pale yellow brown in color, and was in part coated by or included black grains of an unidentified black, sulfide mineral.

The main body of the oxidized zone at Tsumeb extends upward from the arsenate stage to the surface. It is characterized by the development of carbonates, chiefly cerussite, smithsonite, azurite, and malachite. The carbonates calcite, aragonite (in large part plumboan), dolomite, otavite and phosgenite also are minerals of this stage. In detail most of these minerals show quite varied associations and sequences of formation on a hand specimen scale, at least, and in small amounts cerussite, smithsonite, and azurite are found locally throughout the zone of oxidation. In a broad way, azurite and malachite, the latter generally following azurite and often pseudomorphous after it, are uppermost and last formed.

The observed host minerals for Ge^2 apparently have formed locally in a thin zone transitional between the sulfides and the overlying arsenate zone. These minerals occur directly deposited upon altering sulfarsenide and are associated with a sooty black unidentified secondary sulfide containing much Cu and a small amount of Ge. The secondary sulfide locally coats mimetite in part, indicating some fluctuation in environmental conditions. Other specimens from the same general level in the deposit showed chalcocite associated with native copper, native silver or, more abundantly, cuprite. Chalcocite itself forms under reducing conditions, and the upper boundary of the chalcocite Eh-pH stability field (Garrels, 1954) is virtually coincident with the calculated GeO-GeO_2 boundary. The occurrence of cerussite at this level of the deposit seems anomalous, but it may be noted that the stability fields in the galena-anglesite-cerussite Eh-pH diagram (Garrels, 1954) indicate that cerussite can form in an acid environment, with the anglesite-cerussite boundary located roughly in the region from pH 5.5 to 6, with anglesite forming at lower pH. The formation of cerussite at this level would be dependent on a supply of CO_2, presumably from gangue minerals in the primary ore if the overlying arsenate zone of high acidity blocks a downward transport of carbonate ion, and on a sufficiently low concentration of sulfide ion.

The idealized Eh-pH relations in the oxidized zone at Tsumeb, based on the foregoing discussion and on the general summary by Garrels (1954), are indicated in Fig. 1. These relations are primarily dependent on the access of oxygen. Assuming access of oxygen from the surface, the minimal concentration of oxygen is reached at the interface with the sulfide zone. Below this level, which ideally is coincident with the water table, the environment is alkaline and reducing. At or slightly above the interface the supply of oxygen is adequate to completely oxidize S and As to $(SO_4)^{-2}$ and $(AsO_4)^{-3}$. The acid environment here generated passes

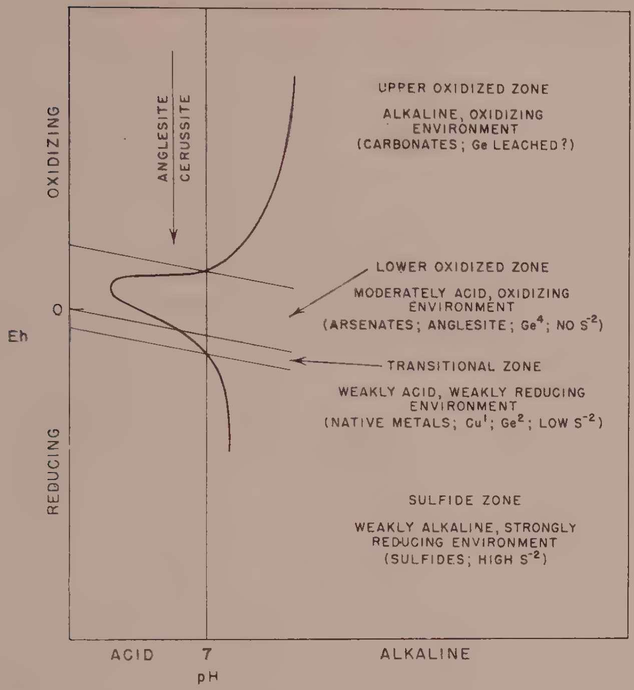
OXIDIZING
REDUCING
Eh
0
ANGLESITE
CERUSSITE
UPPER OXIDIZED ZONE
ALKALINE, OXIDIZING ENVIRONMENT
(CARBONATES; Ge LEACHED?)
LOWER OXIDIZED ZONE
MODERATELY ACID, OXIDIZING ENVIRONMENT
(ARSENATES; ANGLESITE; Ge4; NO S-2)
TRANSITIONAL ZONE
WEAKLY ACID, WEAKLY REDUCING ENVIRONMENT
(NATIVE METALS; Cu1; Ge2; LOW S-2)
SULFIDE ZONE
WEAKLY ALKALINE, STRONGLY REDUCING ENVIRONMENT
(SULFIDES; HIGH S-2)
ACID
7
pH
ALKALINE

FIG. 1. Idealized Eh-pH relations in the oxidized zone at Tsumeb.

upward, through reaction with the carbonate country rock to produce solutions saturated with CO_2, into the alkaline and oxidizing environment of the upper, carbonate zone. The actual mechanism is perhaps best envisaged as a set of essentially static Eh-pH environments, moving downward as erosion progresses, each mineralogical zone being continually reworked, rather than as one based on active circulation.

Chemistry and Geochemistry of Ge^2 and Ge^4

The Group IVb elements Ge, Sn, and Pb all form compounds in both the +2 and +4 oxidation states. With Ge, opposite to Pb, the +2 state is less important than the +4 state. In acid solutions germanous salts and the halide complex ions of Ge^2 are fairly stable in the absence of oxidizing agents. In alkaline solutions the complex ions evolve hydrogen with oxidation of the Ge^2 to Ge^4. Germanites such as Na_2GeO_2 also are known. GeO is stable in dry or moist air at ordinary temperatures, and in dry air oxidizes to GeO_2 only at elevated temperatures. Both GeS and GeS_2 are stable phases. GeS sublimes at 430° and is soluble in hot alkaline solutions. GeS_2 is soluble in excess of sulfide ion with the formation of thiogermanates. The Ge^4 ion is stable under oxidizing conditions in both acid and alkaline solutions. Ge^4 has a more acidic character than do Ge^2, Sn and Pb.

Among systems containing Ge, the Eh-pH relations have been calculated only for the system Ge-H_2O (Zoubov, Deltombe and Pourbaix (1955)). In this system at 25°, the diagram shows fields for GeO_2 (hexagonal polymorph), GeO, and Ge, with the GeO-GeO_2 boundary extending from Eh 0 at pH -2 to Eh -0.7 at pH 10. The chemistry of germanous salts in general suggests that in other systems the boundary between Ge^2 and Ge^4 would be near or below the approximate, generalized Eh-pH boundary which Garrels (1954) has indicated as separating the zone of oxidation from the zone of stable sulfides in the weathering of sulfidic ore deposits. This boundary extends from Eh 0.2 at pH 2 to Eh 0.2 at pH 10. In the case of Ge^2, in view of the very low solubility of GeS, the existence of germanous ion in this general Eh-pH region, leading to the formation of germanous oxysalts or to the entrance of Ge^2 into solid solution in oxysalts, would be dependent on a low concentration of sulfide ions.

The Ge derived from the primary ores at Tsumeb in a sense follows the Eh-pH path in the oxidized zone indicated in Fig. 1. The Ge is initially released in a more or less acid and weakly reducing environment, favoring the formation of the Ge^2 ion. The Ge^2 ion may then enter into solid solution in substitution for Pb^2 in secondary lead minerals stable under such conditions. It possibly also could concentrate sufficiently to crystallize as a germanous compound such as GeO. The downward transportation of Ge^2 and its reprecipitation in the zone of secondary enrichment as GeS is a further possibility. With increasing Eh, the Ge^2 is oxidized to Ge^4. The Ge^4 may then enter solid solution in substitution for As^5 in the secondary arsenates characteristic of the lower, acidic and oxidizing part of the zone of oxidation. When these arsenates are reworked in the passage to the alkaline and oxidizing environment of the overlying carbonate zone, the Ge^4 then released may be leached as soluble alkali germanates, in the absence of host minerals in this zone crystallochemically suited to house Ge^4. Such minerals would be secondary silicates such as hemimorphite and willemite. The studies of Schroll (1953) and others show that Ge^4 can in fact preferentially enter hemimorphite, but as noted, secondary silicates are not present at Tsumeb. Our data indicate that the carbonates of the upper part of the oxidized zone at Tsumeb are low or lacking in Ge, in line with the studies by Lopez de Azcona (1942) and others on cerussite in general, and it is presumed that Ge has been lost from this part of the deposit.

ACKNOWLEDGMENTS

We gratefully acknowledge a critical reading of the manuscript by Professor R. M. Garrels and Dr. Michael Fleischer. Mr. U. Petersen

and Mr. R. Natarajan aided in a preliminary study of the paragenesis of various of the secondary minerals.

REFERENCES

AHRENS, L. H. (1952), The use of ionization potentials. Part 1. Ionic radii of the elements. *Geochim. Acta*, **2,** 155–169.

GARRELS, R. M. (1954), Mineral species as functions of pH and oxidation-reduction potentials, with special reference to the zone of oxidation and secondary enrichment of sulfide ore deposits. *Geochim. Acta*, **5,** 153–168.

GUILLEMIN, C. (1956), Contribution à la minéralogie des arséniates, phosphates et vanadates de cuivre (I, II). *Bull. soc. min. franc.*, **79,** 7–96, 219–276.

HARVEY, C. E. (1947), A method of semi-quantitative spectrographic analysis. *Applied Res. Labs.*

KURODA, K. (1939), The occurrence of germanium in the hot springs of Senami. *Bull. Chem. Soc. Japan*, **14,** 303–304.

LINDGREN, W., AND LOUGHLIN, G. F. (1919), Geology and ore deposits of the Tintic Mining District, Utah. *U. S. Geol. Surv.* Prof. Paper **107.**

LOPEZ, DE AZCONA, J. M. (1942), Estudio geoquimico de las minerales de plomo. *Ion* (*Rev. espan. quim. apl.*) **2,** 446–457.

MURDOCH, J. (1953), X-ray investigation of colusite, germanite and renierite. *Am. Mineral.*, **38,** 794–801.

MORITZ, H. (1933), Die sulfidischen Erze der Tsumeb-Mine von Ausgehenden bis zur XVI Sohle. *Jb. Min.*, Beil.-Bd., **67,** 118–153.

POWELL, H. M., AND BREWER, F. M. (1938), The structure of germanous iodide. *J. Chem. Soc. London*, 197–198.

RATLEDGE, J. P., ONG, J. N., AND BOYCE, J. H. (1955), Development of metallurgical practice at Tsumeb. *Trans. Amer. Inst. Min. Met. Eng.*, Tech. Publ. **4011**-*B*.

SCHROLL, E. (1953), Minerals and trace elements, ore formation, and origin of the lead-zinc deposits of Bleiberg-Kreuth, Carinthia, Austria. *Mitth. Osterreich. Min. Ges.*, Sonderheft, no. **2.**

SCHNEIDERHÖHN, H. (1920), Beiträge zur Kenntnis der Erzlagerstätten und der geologischen Verhältnisse des Otaviberglandes, Deutsch-Südwestafrika, *Abhl. Senckenb. Naturf. Ges. Frankfurt*, **37,** 220–321; also *Senckenbergiana*, **1,** no. 2, 1919 and **2,** nos. 1, 2. 1920.

WONDRATSCHEK, H., AND MERKER, L. (1956), Eine Reihe von neuen Verbindungen mit apatitartiger Struktur. *Naturwiss.*, **21,** 494–495.

ZACHARIASEN, W. H. (1932), The crystal structure of germano sulfide. *Phys. Rev.*, **40,** 917–922.

ZOUBOV, N. DE, DELTOMBE, E., AND POURBAIX, M. (1955), Comportment électrochimique du germanium. Diagramme d'equilibre tension -pH du systèm Ge$-$H$_2$O at 25° C. *Centre Belge D'Etude deo la Corrosion,* Rapport Techn. no. **27.**

THE AMERICAN MINERALOGIST, VOL. 42, NOVEMBER-DECEMBER, 1957

SYNTHESIS OF TOURMALINE BY REACTION OF MINERAL GRAINS WITH NaCl-H_3BO_3 SOLUTION, AND ITS IMPLICATIONS IN ROCK METAMORPHISM*

Clifford Frondel and R. L. Collette, *Harvard University, Cambridge, Massachusetts.*

Abstract

Tourmaline can be synthesized by the reaction of a water solution of NaCl and H_3BO^3 on coarse fragments of minerals that contribute the Si, Al and Fe needed in addition to Na, B and OH for the composition of the mineral. The temperature and pressure ranged from 350° C. and 2000 bars to 550° and 700 bars. Most of the common rock-forming minerals were investigated, ranging from mixtures of magnetite, quartz and corundum to mixtures of magnetite with aluminosilicates without additional cations (such as sillimanite) or with additional cations (such as augite). In general tourmaline is not formed if the added minerals contribute alkalies to produce strongly alkaline solutions. A high content of Ca or a high ratio of Ca, Mg and Fe relative to (Al, Si) also is unfavorable.

The formation of tourmaline during the metamorphism of argillaceous sedimentary rocks is discussed from the point of view of Goldschmidt and Peters (1932) and Landergren (1945) that the boron was originally present in the sediment and not derived from igneous sources.

The ordinary black tourmaline of metamorphic and igneous rocks approximates the composition $NaFe_3Al_6(BO_3)_3(Si_6O_{18})(OH)$. Small amounts of K, Ca, Mg, Fe^3 and F usually are also present. We have found that tourmaline of this composition is formed by the reaction of a water solution of NaCl and H_3BO_3 at moderate temperatures with pieces of certain minerals that contribute Al, Fe and Si to the system. For example, corundum, magnetite and quartz contribute the Al, Fe, and Si needed for the formation of tourmaline in addition to the Na and B ions present in the solution. This particular mixture produced tourmaline when heated for 72 hours at 700 bars at 550° C. Tourmaline also is formed if NaF is used instead of NaCl. Diaspore used instead of corundum afforded tourmaline at 425°, but not at 350°.

Using a standard run composition, consisting of a water solution 0.3 N in NaCl and 3.0 N in H_3BO_3 together with fragments of magnetite, we have obtained tourmaline using the following aluminum silicates instead of corundum and quartz: sillimanite (at 500° and 460°), kyanite (at 500°), topaz (at 500°, but not 425°), kaolinite (at 550°, 500° and 425°, not 350°), "allophane" (at 550°, doubtfully at 350°) and pyrophyllite (at 550°, 500° and 350°, not 250°). The bomb pressures and run times ranged from 250 bars and 3 days at 550° to 2,000 bars and 7 days at 350°. Pyrophyllite was much more reactive than the other minerals and afforded the largest tourmaline crystals (about 0.5 mm long at 550° in 10 cc. bomb volume). Addition of quartz to these runs made no significant difference. In these and in the experiments described below the mineral fragments were only superficially attacked and products in addition to tourmaline were present in many instances.

---

* Contribution from the Department of Mineralogy and Petrography, Harvard University, No. 377.

When aluminosilicates that contained additional cations were employed it was found that tourmaline was afforded in some instances but not in others. Using the standard run mentioned above, we obtained tourmaline from staurolite (500°), zoisite (550°, scant at 500°), muscovite (550°, see below), montmorillonite (550°, not 460°), labradorite (rare at 500°, see below), and almandine (500°, not 425°). Grossularite gave negative results at 550°, 500° and 425°, with or without the addition of quartz. Labradorite did not afford tourmaline at 550° or 500°, or when quartz was added, but did yield a very small amount when Al_2O_3 was added. Orthoclase did not give tourmaline at 500°, with or without the addition of SiO_2 or Al_2O_3. Albite gave negative results at 500°. Biotite, lepidolite and muscovite did not give tourmaline at 500°, or biotite at 550°, but muscovite yielded tourmaline at 550° when SiO_2 was added.

It appears that minerals containing a relatively large amount of alkalies, that react with water to give alkaline solutions, do not form tourmaline under the conditions stated. Thus, in addition to the observations cited above, negative results were obtained from nepheline, sodalite, cancrinite, spodumene and glaucophane. This is further indicated by our (unpublished) observations made on the action of solutions on tourmaline glass and on mixed gels or oxides approximating in composition to tourmaline. Using these starting materials, tourmaline is obtained, depending on temperature and other factors, in weakly alkaline to moderately acid solutions even though alkalies may be present in amounts considerably over the requirements of the formula. The best results are obtained in acid solutions. When the solutions are moderately to strongly alkaline, however, such as by the addition of sodium silicate, sodium carbonate or sodium borates, tourmaline is not formed. It also was found in this connection that runs that produced tourmaline at 500° from pyrophyllite or kaolinite were non-productive when repeated after making the solution 0.1 N in $Na_2B_4O_7$ in addition. In the work of F. G. Smith (1949) on synthesis of tourmaline from its component oxides in water at 400°–500°, the stability field was found to be wholly in the weakly alkaline range in concentrated solutions but with one limit in the weakly acid range in very dilute solutions. The effect of pH may possibly be through an influence on the type of borate anions present in the solution, with (BO_3) groups, such as in the structure of tourmaline, present in the acid range and $[B(OH)_4]$ or other tetrahedral or polynuclear complexes present in the strongly alkaline range.

Unsuccessful results using the standard run formula were obtained with aluminosilicates relatively high in Mg or Fe^2, including clinochlore and chloritoid, and with aluminosilicates containing Ca together with these cations, including augite and hornblende. An iron-free Mg tourmaline was obtained, however, by using $MgSO_4$ in place of Fe_3O_4 with kaolinite in a stainless steel bomb. A Mg tourmaline also was obtained in a run at 500° that contained SiO_2, Al_2O_3, Fe_3O_4 and Mg borate, but not NaCl or H_3BO_3; the yield was small, and this interesting tourmaline was not further studied. The negative results obtained with some of the above minerals probably is to be connected with their relatively low content of Al or Si rather than with the content of Mg or Fe.

Stilbite, containing Ca and Na, also gave negative results. Zoisite gave positive results as noted above. Grossularite gave negative results, as did labradorite in the absence of extra Al_2O_3. A high calcium concentration, or a high ratio of calcium to aluminum, may not be favorable to the formation of tourmaline. Although the bulk of the boron in metamorphosed argillaceous rocks is carried by tourmaline, the boron in highly calcic metamorphic rocks, particularly the crystalline limestones, is distributed among a wide range of species. These include, in addition to magnesium-tourmaline, danburite, serendibite, warwickite, sinhalite, axinite, ludwigite, kotoite and others.

Our experiments suggest that tourmaline can be expected to form in the presence of Na and borate ions during the metamorphism of argillaceous sedimentary rocks, and by the action of these ions on even the high grade equivalents of such rocks. The introduction of boron from igneous sources has been a traditional explanation for the formation of tourmaline in metamorphic terranes. The tourmaline, however, also may originate from boron contained originally in the sediment itself. The work of Goldschmidt and Peters (1932) and of Landergren (1945) on the geochemistry of boron has shown that argillaceous sedimentary rocks are enriched in this element, and it is present in the average amount of 0.03–0.05 per cent B_2O_3 in marine sediments. Pieruccini (1950) found 0.03 to 0.15 per cent B_2O_3 in certain marine clays. The bulk of the boron in these sediments is not contained in accessory detrital minerals such as tourmaline, but apparently is acquired from solution in the sea water by the sediment and is held by adsorption. With increasing temperature the boron may become available to interstitial solutions, such as through desorption attending grain growth, or by recovery from solid solution in unstable phases during their recrystallization, and these solutions may then react with the aluminosilicates to form tourmaline as we have found experimentally.

This general view was first expressed by Goldschmidt and Peters (1932), and has found support in field studies of tourmaline-bearing metamorphosed sediments in central Sweden by Hjelmqvist (1938) and in Greenland by Ellitsgaard-Rasmussen (1954). Aspects of this matter have been discussed by M. C. Michel-Lévy (1953) in light of her work on the hydrothermal synthesis of tourmaline. We have synthesized tourmaline by heating shale (the Cambridge slate in the Boston area) together with magnetite and a water solution of NaCl and H_3BO_3 at 500° and at 650° C. under a pressure of 250 bars. Mme. Michel-Lévy (1949) heated schist at 400° and 10 bars in potassium borate solution and obtained sericite and tourmaline. Crystallization of tourmaline also can take place at relatively low temperatures in view of the wide occurrence of authigenic tourmaline in unmetamorphosed sedimentary rocks. Secondary polar enlargements of tourmaline grains similar to those of sedimentary rocks are readily obtained experimentally by placing seed crystals into hydrothermal syntheses of the nature described.

Tourmaline also can be produced in metamorphic or other rocks by boron introduced from outside sources, as is evidenced, for example, by the tourmaline-rich zones up to a foot or so in thickness that sometimes border large granite pegmatites in the New England area. Hutton (1939) has concluded from field evidence that the boron of the tourmaline in the Otago schists of New Zealand is not of sedimentary origin but has been derived in most instances from deep-seated granitic intrusives. Since borates in general are relatively soluble, particularly the alkali borates, the development of tourmaline during metamorphism also may be viewed as a metasomatic process in which the boron was transported from a more or less distant but not necessarily igneous source. There is, too, the possibility that boron originally present in the sediment may have been removed in solution before the metamorphism reached sufficient intensity to produce tourmaline. The boron might also become tied up in solid solution in an early-formed phase during recrystallization and rendered unavailable over the existence range of that phase. A trace element housed in solid solution in such a phase becomes available to interstitial solutions only when it is later brought into the crystal-solution interface by dissolution or recrystallization of the host crystal.

The tourmaline present in the small, discontinuous pegmatitic veinlets found in many moderate to high grade metamorphic rocks certainly in itself is not critical evidence of the introduction of these pegmatites from igneous sources. They may be authigenic pegmatites derived together with their boron content during the metamorphic process.

ACKNOWLEDGMENTS

We acknowledge with gratitude a critical reading of the manuscript by

Professor James B. Thompson. The experimental work mentioned herein was done in 1948 in connection with Contract W36-039-SC-32153, on the synthesis of tourmaline single-crystals, with the Frequency Control Branch, U. S. Signal Corps, Fort Monmouth, New Jersey.

REFERENCES

ELLITSGAARD-RASMUSSEN, K. (1954), On the geology of a metamorphic complex in West Greenland. *Medd. om Grønland*, **136,** no. 6.

GOLDSCHMIDT, V. M., AND PETERS, C. (1932), The chemistry of boron, II. *Nachr. Ges. Wiss. Göttingen, Math. Phys. Kl.*, **28,** no. 31.

HJELMQVIST, S. (1938), On sedimentary rocks in the leptite formation of central Sweden. *Sverig. Geol. Undersök.*, Sect. C, 413.

HUTTON, C. O. (1939), The significance of tourmaline in the Otago schists. *Trans. Roy. Soc. New Zealand*, **68,** 599.

LANDERGREN, S. (1945), Contribution to the geochemistry of boron, II. *Arkiv. Kemi, Min., Geol.*, **19A,** no. 26.

MICHEL-LÉVY, M. C. (1949), Synthesis of tourmaline and jeremejevite. *C. R.*, **228,** 1814.

— —— (1953), Artificial reproduction of minerals and comparison of their occurrence in metamorphic rocks. *Bull. soc. min.*, **76,** 237.

PIERUCCINI, R. (1950), Occurrence of boron in clays. *Per. Min.* **19,** 209.

SMITH, F. G. (1949), Transport and deposition of the non-sulfide vein minerals. IV. Tourmaline. *Econ. Geol.*, **44,** 186.

THE AMERICAN MINERALOGIST, VOL. 42, NOVEMBER-DECEMBER 1957

HYDROTHERMAL SYNTHESIS OF ZIRCON, THORITE AND HUTTONITE*

Clifford Frondel and R. L. Collette, *Harvard University, Cambridge, Massachusetts.*

Abstract

Zircon and thorite have been synthesized by heating admixed SiO_2 and ZrO_2 or ThO_2 gels in water over the range 150° C. and 4.8 bars to 700° and 3100 bars. Material synthesized at 150° shows strong absorption in the infra-red at 2.75 microns due to hydroxyl, and apparently contains $(OH)_4$ in substitution for (SiO_4). Zircon containing an undetermined but quite small amount of Th and of U in solid solution has been synthesized at 400° to 700° from charges containing Zr: Th or U=1:1; thorite or $(U, Zr)O_2$ are also formed. Thorite containing an undetermined amount of U in solid solution was obtained similarly. Huttonite has been synthesized hydrothermally at 300° and 700°. It is found that metamict natural thorite and zircon recrystallize when heated in water, at temperatures considerably below those needed when heated dry in air, and the presence of (OH) was verified by infra-red study in one such recrystallized sample.

Zircon

Historical

Zircon was first synthesized by Deville and Caron (1858) by the action at red heat of SiF_4 on ZrO_2 and of ZrF_4 on SiO_2. Hautefeuille and Perrey (1888) obtained crystals by the fusion of ZrO_2 and SiO_2 in lithium dimolybdate at 700°–1000°. Minute anhydrous crystals were obtained by Chrustschoff (1892) by heating a sealed bomb containing gelatinous ZrO_2 and SiO_2 to dull red heat over a Bunsen burner. Stott and Hilliard (1945) recrystallized zircon by heating zircon sand with KF at about 1525°. Crystalline zircon dissociates slowly at about 1540° and more rapidly with increasing temperature to ZrO_2 and SiO_2 or silica glass, and re-associates on slow cooling (Curtis and Sowman, 1953). Zircon also is formed by sintering ZrO_2 and SiO_2 in air at high temperatures, and this method has been employed in the preparation of $ZrSiO_4$ phosphors (Leverenz, 1950). We have found that co-precipitated ZrO_2 and SiO_2 gels do not react when heated for 24 hours in air at either 800° or 900° but that zircon is formed in the range 1000° to 1500°.

New Data

We have hydrothermally synthesized microcrystalline zircon over the range 150° to 700° by heating gelatinous ZrO_2 and SiO_2 with water in steel bombs (Table 1). The reaction is speeded by adding traces of ZrF_4. Our synthetic zircon formed at 400° and 700° gave sharp *x*-ray patterns with cell dimensions identical with those of dry-sintered $ZrSiO_4$. Material synthesized in the range 150° to 350°, however, gave rather diffuse patterns and the cell dimensions are different; with decreasing temperature the value of a_0 increases and the value for c_0 decreases slightly (Table 1). When these low temperature samples are heated in air the patterns become sharper and the cell dimensions increase to those of dry-sintered $ZrSiO_4$. The changed dimensions of the low temperature material are attributed to the presence of $(OH)_4$ in substitution for (SiO_4), for which we have additional evidence, and the change on heating to thermal decomposition:

---

* Contribution from the Department of Mineralogy and Petrography, Harvard University, No. 378.

$$Zr(SiO_4)_{1-x}(OH)_{4x} \rightarrow (1 - x)ZrSiO_4 + xZrO_2 + 2xH_2O$$

Table 1. Hydrothermal Syntheses of Zircon

Temperature	Pressure in bars	Duration in hours	Reagents	Results	Zircon	
					a_0	c_0
(1000° dry sinter)				Zircon	6.61 Å	5.98 Å
700°	1000	48	ZrO_2,SiO_2 mixed gels	Zircon	6.61	5.98
400°	1000	168	ZrO_2, SiO_2 gels	Zircon	6.61	5.98
350°	165	48	ZrO_2, SiO_2 gels	Zircon	6.62	5.97
325°	121	240	ZrO_2, SiO_2 gels	Zircon		
300°	86	120	ZrO_2, SiO_2 gels, NaCl	Zircon		
240°	34	72	ZrO_2, SiO_2 gels, ZrF_4	Zircon		
150°	4.8	500	ZrO_2, SiO_2 gels, ZrF_4	Zircon	6.64	5.96
700°	1000	48	Zr, U gel (1:1) SiO_2 gel	Zircon, (Zr, U)O_2	6.68	6.02
700°	1000	48	Zr, U gel (1:1) Na_2SiO_3	Zircon, (U, Zr)O_2		
600°	1000	24	Zr, U gel (1:1) SiO_2 gel	Zircon (U, Zr)O_2	6.67	6.02
500°	1000	48	Zr, U gel (1:1) SiO_2, Zr nitrate	Zircon, (U, Zr)O_2	6.66	6.01
400°	1000	48	Zr, U gel (1:1) SiO_2 gel	Zircon (U, Zr)O_2	6.68	6.00
700°	3100	48	Zr, Th gels (1:1) SiO_2 gel	Zircon, thorite		
700°	1000	48	Zr, Th gels (1:1) Na_2SiO_3	Zircon, thorite		

We also have synthesized zircon containing uranium and thorium in solid solution. The uranium runs were made with co-precipitated gelatinous ZrO_2 and UO_3, with Zr:U = 1:1, mixed with gelatinous silica. The products included zircon with relatively large cell dimensions (the only evidence of uranium content) and an isometric fluorite-type oxide, UO_{2+x}, with a_0 5.35 Å. The uranium content of the zircon from approximate measurements of the relative amounts of the two phases present must be very small, perhaps only a few atomic per cent. It proved impossible to isolate and separately analyze the zircon and the oxide.

The thorium runs were made from SiO_2 gel admixed with co-precipitated ZrO_2 and ThO_2 gels, with Zr:Th = 1:1. Zircon with slightly increased cell dimensions (the only evidence of thorium content) and thorite with essentially normal cell dimensions were formed in approximately equal amounts. The diffraction patterns were of very poor quality. The solubility of Th in zircon under these conditions apparently is small. It is interesting to note that in these zircon runs that the added Th crystallized as $ThSiO_4$ but that the added U crystallized as UO_2. All efforts to synthesize anhydrous $USiO_4$ have failed, although $U(SiO_4)_{1-x}(OH)_{4x}$ has been synthesized (Hoekstra and Fuchs, 1956). We have observed that natural coffinite remains stable when heated in water at 700° and 1000 bars.

Hydroxyl Content of Synthetic Zircon

The substitution of $(OH)_4$ for (SiO_4), analogous to the hydrogarnets, has been indicated in certain natural zircon and thorite (thorogummite) by Frondel (1953) and in thorogummite and the related mineral coffinite by infra-red study by Stieff *et al.* (1956). Infra-red measurements to determine the presence of (OH) were made on a number of our synthetic samples. The data were obtained on a Perkin-Elmer double-beam recording spectrophotometer, with a rock-salt prism, using mineral oil (Nujol) as the mounting medium. The region from 2 to 7 microns was scanned. Undoubted evidence of the presence of (OH) was obtained on only one sample, that of zircon synthesized at 150°. This material showed a strong absorption at 2.775 microns due to (OH), with also a weak absorption at 3.075 microns and a weak absorption of molecular water at about 6.0 microns (Fig. 1). The sample was dried at 110° before measurement. When the sample was dried at 300° the (OH) absorption at 2.775 microns remained unchanged. The unreacted SiO_2-ZrO_2 gel after drying at 110° did not show the (OH) absorption at 2.775 microns. Zircon synthesized at 400° and 500° did not show the 2.775 micron absorption, but showed weak absorption at 2.90 and 3.075 microns. The absorptions at 2.9–3.1 microns have been attributed to hydrogen bonding and to molecular water in part, but are not critical in the present work because they were observed on unreacted gels of both ZrO_2-SiO_2 and ThO_2-SiO_2 that had been dried at 110°.

THORITE

Historical

$ThSiO_4$ was first synthesized by Troost and Ouvrard (1887) by heating a mixture of ThO_2, SiO_2 and $CaCl_2$ to white heat in air. $ThSiO_4$ prepared by sintering of ThO_2 and SiO_2 at 1000°–1300° has been employed in investigations of phosphors (Leverenz, 1950). These preparations usually are referred to as tetragonal $ThSiO_4$ (thorite), but in the absence of critical evidence, they may have been the monoclinic polymorph huttonite, described in 1951, which can be synthesized similarly. Both tetragonal and monoclinic $ThSiO_4$ has been obtained by Pabst (1952), and others by heating metamict thorite in air to high temperatures. Duboin (1909) sought to synthesize $ThSiO_4$ by reaction of sodium silicate and thorium nitrate at room temperature in water but no significant results were obtained [a gel is obtained that does not give a diffraction pattern]. Britton (1927) made an electrometric titration of $ThCl_4$ solution with sodium silicate and found that the precipitate was deficient in silica for $ThSiO_4$.

New Data

We have synthesized thorite hydrothermally over the range 150° to 800° by heating gelatinous SiO_2 and ThO_2 with water in steel bombs

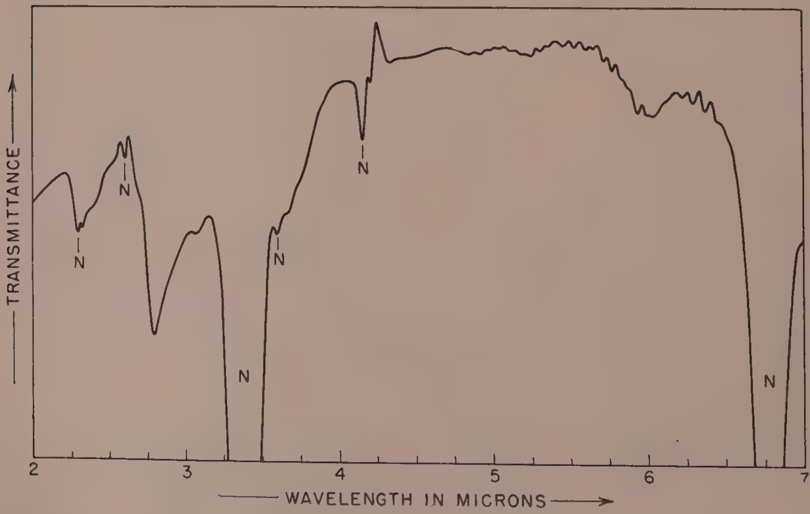

FIG. 1. Infra-red absorption curve of zircon synthesized at 150°. The chief absorptions due to the mounting medium (Nujol) are indicated by the letter N.

TABLE 2. HYDROTHERMAL SYNTHESES OF THORITE

Temperature	Pressure in bars	Duration in hours	Reagents	Products	Thorite	
					a_0	c_0
(1000° dry sinter)				$ThSiO_4$	7.08 Å	6.31 Å
800°	1000	24	Th:U=1:1 SiO_2 gel	Thorite, $(Th, U)O_2$ quartz, unident.		
700°	1000	24	Th nitrate, SiO_2 gel	Thorite	7.08	6.31
400°	1000	48	ThO_2, SiO_2 gels	Thorite	7.12	6.29
250°	40	72	ThO_2, SiO_2 gels	Thorite		
240°	34	96	ThO_2, SiO_2 gels	Thorite	7.14	6.29
150°	4.8	168	ThO_2, SiO_2 (ThF_4), SiO_2 gels	Thorite	7.18	6.28
700°	3100	24	Th:U=1:1 SiO_2 gels	Thorite, $(Th, U)O_2$ quartz, unident.	6.88	6.27
700°	1000	24	Th:U=4:1 SiO_2 gels	Thorite, $(Th, U)O_2$ quartz, unident.		
600°	1000	24	Th:U=4:1 SiO_2 gels	Thorite, $(Th, U)O_2$ quartz, unident.		
600°	3100	24	Th:U=1:1 SiO_2 gels	Thorite, $(Th, U)O_2$ quartz, unident.	7.00	6.30
400°	1000	48	Th:U=1:1 SiO_2 gels	Thorite, $(Th, U)O_2$, quartz	7.09	—

(Table 2). The products were very fine-grained. Thorite containing an unknown but considerable amount of uranium in solid solution, as evidenced by a variation in unit cell dimensions, was obtained at 400°–800° (Table 2). The solubility increases with temperature. The presence of U in solid solution decreases the cell size of $ThSiO_4$ and increases that of $ZrSiO_4$, as would be expected from the relative sizes of the ions involved. These runs were made with SiO_2 gel admixed with co-precipitated hydrous Th and U oxides, with Th:U=1:1. The products included uranoan thorite (which could not be separated for analysis), a fluorite-type oxide $(Th,U)O_2$ of variable cell size, and an unidentified phase.

The synthetic thorite showed the same features of infra-red absorption and variation in cell size as did the zircon. The material synthesized at 150° to 400° had changed cell dimensions; with decreasing temperature the value of a_0 increases and the value for c_0 decreases slightly (Table 2). On heating these samples to 1000° the patterns sharpened and the cell dimensions decreased to those of dry-sintered thorite. Infra-red absorption measurements obtained on material synthesized at 150° showed strong (OH) absorption at 2.75 microns in a sample dried at 110°. This absorption remained unchanged after the sample had been dried at 300° but disappeared when the sample had been heated to 1000°. Material synthesized at 700° did not show the (OH) absorption at 2.75 microns.

HUTTONITE

Huttonite is the monoclinic, monazite-type polymorph of $ThSiO_4$. It has been synthesized by Pabst (1952) by heating metamict thorite or a mixture of ThO_2 and SiO_2 in air to 900°–1000°, and higher. It also has been obtained by Karkhanavala (1956) by sintering ThO_2 and SiO_2 at 1500°. We have obtained huttonite by sintering poorly washed ThO_2 and SiO_2 gels at 1300°–1500°, and find that neither synthetic thorite nor crystalline thorogummite is converted to huttonite by heating for 24 hours at 1000°. We also have synthesized huttonite hydrothermally by heating very thoroughly washed ThO_2 and SiO_2 gels in water alone or in weakly alkaline water solutions at 700° and 1000 bars. If the gels are heated in dilute thorium nitrate or chloride solutions, or if uranium is present, thorite is produced. Huttonite also was obtained by heating the pure gels in water at 300° and 77 bars. Thorite is produced in this region if the gels are not thoroughly washed. The interplanar spacings of huttonite synthesized hydrothermally at 300° are distinctly smaller than those of material synthesized by sintering at 1400°.

HYDROTHERMAL RE-CRYSTALLIZATION OF METAMICT THORITE AND ZIRCON

Wholly metamict thorite and zircon can be recrystallized by heating in water at temperatures much lower than those required by heating dry in air. The metamict thorite from Hybla, Ontario, analyzed by Ellsworth (1927), does not give a diffraction pattern either when unheated or after heating in air at 600° for 24 hours; strong patterns of huttonite and ThO_2 appear only after heating to 1050° or higher. This is in general agreement with the work of Pabst (1952). The DTA measurements of Kulp, Volchok, and Holland (1952) indicate that metamict zircon recrystallizes at 890°–910°.

The Hybla thorite recrystallizes and gives a strong and sharp pattern of thorite—not huttonite—when very finely powdered and then heated with water alone for two days at 600° and 1000 bars or for seven days at 500° and 2000 bars. Lower temperatures were not investigated. Wholly metamict thorite from Arendal, Norway, and zircon from Brevik, Norway, also recrystallized in water at 600° and 1000 bars. Infra-red absorption measurements made on the unheated thorite did not show (OH) absorption at 2.75 microns but did show strong molecular water absorption at 6.0 microns and weak bands of hydrogen-bonded (?) and molecular water at 2.875–2.95 and 3.075–3.125 microns. The same material after heating in water showed a small but definite (OH) absorption at 2.75 microns. This recalls the natural alteration of metamict thorite to hydroxyl-containing thorogummite described by Frondel (1953).

ACKNOWLEDGMENT

This work was supported by contract AT(30-1)-1403 with the Division of Research, U. S. Atomic Energy Commission.

REFERENCES

BRITTON, H. T. S. (1927), Electrometric study of the precipitation of silicates. *J. Chem. Soc. London,* 425–436.

VON CHRUSTSCHOFF, K. (1892), On the artificial production of zircon in the wet way. *Jb. Min.,* **II,** 232.

CURTIS, C. E., AND SOWMAN, H. G. (1953), Investigation of the thermal dissociation reassociation and synthesis of zircon. *J. Am. Cer. Soc.,* **36,** 190–193.

DEVILLE, H. S. C., AND CARON, H. (1858), New method of synthesis of crystals of various substances. *C. R.,* **46,** 764; *Ann. Chim. Phys.* **5,** 109, 1865.

DUBOIN, A. (1909), On various compounds of thorium. *Ann. Chim. Phys.,* **17,** 354–364.

ELLSWORTH, H. V. (1927), Uranothorite from the Macdonald mine, Hybla, Ontario. *Am. Mineral.,* **12,** 368–372.

FRONDEL, C. (1953), Hydroxyl substitution in thorite and zircon. *Am. Mineral.,* **38,** 1007–1018.

HAUTEFEUILLE, P., AND PERREY, A. (1888), On the synthesis of zircon. *C. R.,* **107,** 1000–1001.

HOEKSTRA, H. R., AND FUCHS, L. H. (1956), Synthesis of coffinite $USiO_4$. *Science,* **123,** 105.

KARKHANAVALA, M. D., The synthesis of huttonite and monazite. *Current Sci.,* **5,** 166–167.

KULP, J. L., VOLCHOK, H. L., AND HOLLAND, H. D. (1952), Age from metamict minerals. *Am. Mineral.,* **37,** 709–718.

LAMBERTSON, W. A., AND MUELLER, M. H. (1953), Uranium oxide phase equilibrium systems—III. UO_2-ZrO_2, *J. Am. Cer. Soc.,* **36,** 365–368.

LEVERENZ, H. W. Luminescence of solids, New York, 1950.

PABST, A. (1952), The metamict state. *Am. Mineral.,* **37,** 137–157.

STIEFF, L. R., STERN, T. W., AND SHERWOOD, A. M. (1956), Coffinite, a uranous silicate with hydroxyl substitution: a new mineral. *Am. Mineral.,* **41,** 675–689.

STOTT, V. H., AND HILLIARD, A. (1945), Variation in the structure of zircon. *Min. Mag.,* **27,** 198–203.

TROOST, L., AND OUVRARD, L. (1887), On the silicates of thoria. *C. R.,* **105,** 255–258.

THE AMERICAN MINERALOGIST, VOL. 42, NOVEMBER-DECEMBER 1957

LUZONITE, FAMATINITE AND SOME RELATED MINERALS[1]

RICHARD V. GAINES, *Harvard University, Cambridge, Massachusetts.*[2]

ABSTRACT

A complete solid solution series extends between the tetragonal minerals luzonite, Cu_3AsS_4, and famatinite, Cu_3SbS_4. Luzonite is dimorphous with the orthorhombic mineral enargite; the solid solubility of Sb in enargite is restricted, and the orthorhombic dimorph of famatinite is not known in nature. Chemical, morphological, physical and x-ray data are given for luzonite and famatinite. The crystal structure of luzonite-famatinite is closely related to that of chalcopyrite and basically is of the sphalerite-type. Space group $I\bar{4}2m$; a_0 5.290 Å, c_0 10.465 (synthetic luzonite); a_0 5.38 Å, c_0 10.76 (synthetic famatinite); cell contents 2 $[Cu_3(As, Sb)S_4]$.

HISTORICAL SURVEY

Since first described over eighty years ago, luzonite and famatinite have been the subject of continuing controversy. The current work establishes them as a valid mineral species, forming a complete isomorphous series, with both intermediate and end compositions occurring in nature.

Zerenner (1869) made the first reference to luzonite or famatinite in noting the presence of an unknown massive brown mineral associated with enargite and chalcopyrite in a suite of ore specimens from Mankayan, Luzon, Philippines. F. W. Fritzsche (1869) analyzed the same material and reported it similar in composition to dufrenoysite, as described by Damour in 1845. Damour's "dufrenoysite" was later shown to be tennantite, and the name dufrenoysite was applied to a lead mineral by Des Cloizeaux in 1855.

Next Stelzner (1873), while studying a group of ore minerals from the San Pedro and other mines in the Sierra de Famatina, La Rioja, Argentina, noted a massive mineral of reddish black color, lacking cleavage. Chemically it was a copper antimony arsenic sulfide, with Sb:As=4:1. Stelzner named it famatinite, from the locality, and stated, correctly, that it was not isomorphous with enargite. The erroneous assumption that they were isomorphous later became deeply entrenched in the literature.

Noting the reference by Zerrenner (1869), Weisbach redescribed specimens of a "brown" material from Mankayan, Luzon, which he had put aside after a superficial examination in 1866. He stated that the new mineral, which Fritzsche had mistakenly called dufrenoysite, resembled niccolite or bornite. The chemist Winkler's analysis showed copper, arsenic, antimony, and sulfur, with a trace of iron, in proportions identical with enargite. Weisbach proposed the name luzonite for it, also after the locality, stating that it was different in appearance from enargite and was isomorphous with famatinite. Once again the original description was correct, particularly in reference to its relationship to enargite and famatinite. However, later incorrect assumptions so confused the literature that even today many do not consider luzonite a valid species.

---

[1] Contribution from the Department of Mineralogy and Petrography, Harvard University, No. 379.

[2] Present address, 2033 N. First St., Grand Junction, Colorado.

Further references were not long in appearing. Frenzel (1874) described an intermediate member from Cerro de Pasco with As:Sb=1:1, assuming it to be triclinic. Klockmann (1891) reached the same conclusions as Weisbach, using material from Sierra de Famatina, Argentina. Moses (1905) examined luzonite from Mankayan, Luzon, and, on the basis of goniometric studies, declared it crystallographically identical with enargite. He concluded that luzonite was merely a color variety of enargite. The writer, using Moses' original material, determined that he was mistaken in assuming the small enargite crystals upon which he worked to be identical with their luzonite matrix.

The sixth edition of Dana's *System of Mineralogy* states that enargite and luzonite are identical and that enargite and famatinite are isomorphous.

On the basis of nearly identical powder photographs of enargite from Silverton, Colorado and famatinite from Argentina, De Jong (1928) concluded that they had identical structures. His results were accepted by Schneiderhöhn and Ramdohr (1931) and confirmed through *x*-ray work by Waldo (1935). De Jong's "famatinite," however, was unquestionably a mixture of fine-grained enargite and some famatinite. Pure famatinite from the same mine gives a powder pattern markedly distinct from enargite.

Frebold (1927), studying ores from Mankayan, Luzon, held that luzonite was not a valid species name. An extended study by Harcourt (1937) further corroborated the work of those previously mentioned. His conclusions suffered from the fact that, although his samples of luzonite and famatinite came from five localities, the group was not large enough to be truly representative.

The wide variance of opinion held by the several investigators as to the existence and nature of luzonite and famatinite is due in a large measure to the fact that the same material has never been used for chemical analysis, polished section investigation, morphological work, and *x*-ray powder photography. Additional uncertainties arose because, as far as could be ascertained, none of the men who investigated the problem personally collected the specimens on which they worked, or visited the mines in which they occurred. Competent mineralogists visiting these localities probably would have found more luzonite-famatinite crystals. Luzonite-famatinite, moreover, are not always easily distinguishable from enargite because they usually occur more or less intergrown and because in polished section enargite often has a deceptively pink tinge.

The most recent work done on this problem has been by three Japanese: H. Imai (1943), who studied the Mankayan, Philippine Islands locality; M. Watanabé (1943), who studied luzonite from three mines in Japan and one in Formosa; and H. Sawada (1944), who made x-ray studies on luzonite crystals from Japan. Imai concluded that luzonite was a valid mineral species and that, although arsenic-rich, it did contain a little more antimony than enargite, yet considerably less than famatinite. Hence, in the series Cu_3AsS_4-Cu_3SbS_4, the mineral enargite corresponds to Cu_3AsS_4, while luzonite is an intermediate compound with a different structure (based on x-ray powder photographs). Watanabé reached a similar conclusion, even though his analysis of luzonite (intermixed with gangue) showed no antimony. Imai (1949, p. 59) refers to the fact that Sawada had determined the crystal structure of luzonite. Although Sawada's original paper, in Japanese, is not available in this country, a summary of his work was obtained by the writer via personal communication.

Using minute, imperfect, twinned crystals from the Hokuetsu mine, Japan, Sawada determined that luzonite is tetragonal, pseudo-cubic, with cell dimensions $a_1 = a_2 = 5.28$ Å; $c = 5.22$ Å. He admitted the possibility that the true cell might be a multiple of the one he determined, but had no positive evidence for this. Imai's reference to Sawada contains the misprint "$a_1 = a_2 = 4.28$ Å." His figure "$c = 10.44$ Å" is double Sawada's, with no explanation given. Imai's reference also has a discrepancy in the determination of the space group, which Sawada correctly determined to be $I\bar{4}2m$. Although Sawada's structure determination and other data are not consistent with that obtained in the present work, his is certainly the best study of the crystallography and structure of luzonite that has appeared to date. Any deficiency in his results can be attributed to the poor quality of the material with which he worked.

CRYSTALLOGRAPHY

Small crystals of luzonite were found by the writer on specimens from Mankayan, Luzon, Philippines, and Goldfield, Nevada. Interfacial angles, determined on the two-circle reflecting goniometer, indicated that the crystals are tetragonal, scalenohedral. The largest crystal observed was roughly equant and measured 2 millimeters across, but the largest dimension of those suitable for measurement was about 0.5 milli-

TABLE 1. ANGLE TABLE OF FAMATINITE AND OF A MEASURED LUZONITE-FAMATINITE CRYSTAL FROM GOLDFIELD, NEVADA

$c/a=2.000 \qquad p_0:r_0=2:1$

Forms	ϕ Meas.	ϕ Calc.	ρ Meas.	ρ Calc.	A Calc.	$\overline{M}$ Calc.
001	—	—	0–00	0–00	90–00	90–00
110	45–00	45–00	90–00	90–00	45–00	90–00
012	0–50	0–00	46–00	45–00	90–00	60–00
011	0–20	0–00	63–00	63–26	90–00	50–46
112	45–10	45–00	54–00	54–44	54–44	90–00
111	45–00	45–00	71–00	70–32	48–11	90–00
132	19–00	18–26	72–00	72–27	72–27	64–46

Doubtful forms—*q*{1·1·10}, *w*{1·3·12}, *v*{125}.

For luzonite, the axial ratio $c/a=1.978$, and $p:r=1.978:1$. Since the difference between this and the axial ratio for famatinite is small, the luzonite angle table differs only slightly from this one.

meters. All crystals measured were twins, with irregular and unequally developed faces. Fairly sharp reflections were obtained with a crystal from Goldfield, Nevada. The forms listed in Table 1 were measured on this crystal. Its analysis is shown in Table 4. It corresponds to a mineral about midway between the two end members of the series. Angles were calculated on the basis of the cell derived from precision measurement of the powder photograph of pure synthetic famatinite, shown in Fig. 5 and Table 2. Figure 1 shows a measured crystal of luzonite-famatinite from Goldfield. Portions of another crystal attached to this one as an interpenetration twin were eliminated for the sake of clarity.

Figure 2 shows an idealized crystal from Mankayan, Luzon, Philippines. Crystals from Mankayan gave poor reflections. No crystals of famatinite were observed on material from Famatina, Argentina.

STRUCTURE

The space group of luzonite-famatinite is $I\bar{4}2m$. The writer determined approximate cell dimensions by means of single-crystal *x*-ray rotation photographs of crystals from Mankayan, Luzon and Goldfield, Nevada. Later, precise cell dimensions were obtained from powder photographs of synthetic luzonite and famatinite made by hydrothermal processes. These photographs were made with filtered Cu radiation with $\lambda=1.5418$ Å. The unit cells contain two formula weights and have dimensions as follows:

Luzonite:	a_0 5.290 Å,	c_0 10.465,	$c/a=1.978$
Famatinite:	a_0 5.38	c_0 10.76	$c/a=2.000$

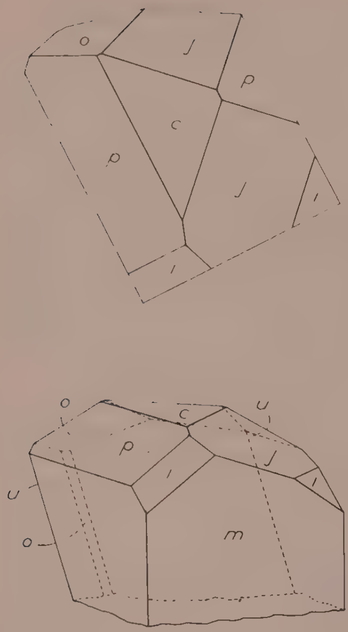

FIG. 1. Luzonite-famatinite crystal from Goldfield, Nevada.

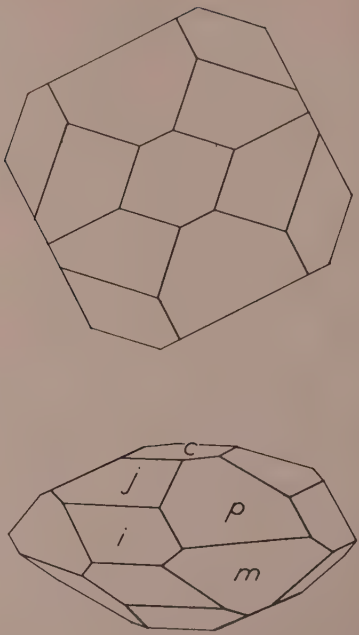

FIG. 2. Idealized crystal from Mankayan, Luzon, Philippines.

The 0-layer photograph brought out the tetragonal nature of luzonite-famatinite beyond question. Excellent zero, first, and second layer Precession photographs, shown in Figs. 3 and 4, were obtained with a fragment of famatinite from massive, coarsely crystalline material from Sierra de Famatina, Argentina. These showed that the cell is body-centered tetragonal, with no glide planes or screw axes. Eight different space groups would fulfill the criteria shown by these photographs, viz: $I\bar{4}$, $I\bar{4}m2$, $I\bar{4}2m$, $I4$, $I4/m$, $I4mm$, $I42$, $I4mmm$. $I\bar{4}2m$ was chosen on the basis of the structure as it was finally determined.

Powder photographs were taken of luzonite and famatinite from all the principal localities from which specimen material was available, and of artificial material made by hydrothermal processes. The synthetic material included the arsenian and antimonian end-members and several intermediate members of the series. Powder photographs of the natural and artificial material were in complete agreement. Careful comparison of many photographs established which lines were unquestionably due to luzonite-famatinite and which should be rejected as representing impurities.

These powder photographs were then measured and indexed, using the

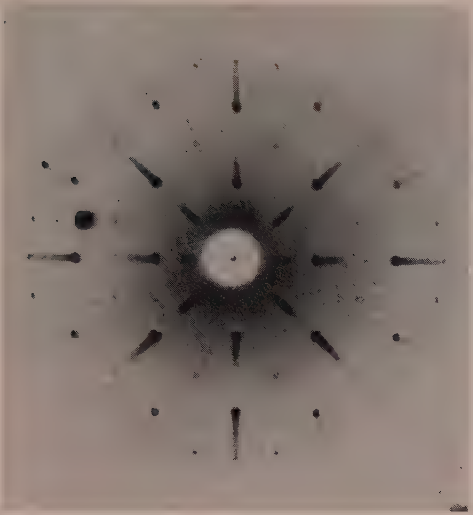

FIG. 3. Famatinite, Argentina. Precession photograph, a-axis, 0-level.

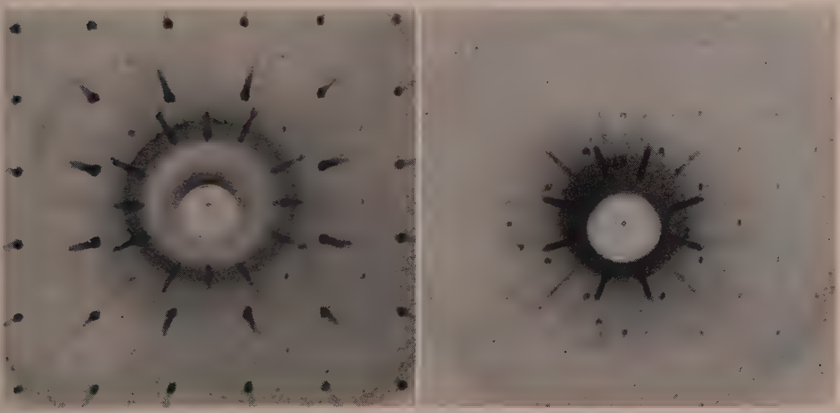

FIG. 4. Famatinite, Argentina. Precession photographs, a-axis, 1-level (left), 2-level (right).

Straumanis technique of measurement to compensate for film shrinkage and errors in camera diameter. The photographs of the two end-members and of natural luzonite and famatinite from the two type localities and from Goldfield, Nevada are shown in Fig. 5. The indexed lines of the two photographs are tabulated in Table 2. It will be noted that considerable differences in intensity exist for some of the equivalent lines of luzonite and famatinite. It was possible to obtain sharper and clearer photographs of famatinite than of luzonite. However, the most important cause of this

TABLE 2. INDEXED POWDER PHOTOGRAPHS OF SYNTHETIC LUZONITE AND FAMATINITE. CU RADIATION, NI FILTER

Luzonite				Famatinite			
Intensity	*hkl*	*d* measured	*d* calculated	Intensity	*hkl*	*d* measured	*d* calculated
1	002	5.19 Å	5.240 Å	2	002	5.261 Å	5.380 Å
3	101	4.73	4.724	3	101	4.731	4.811
10	112	3.046	3.046	1	110	3.752	3.805
4	103	2.928	2.914	10	112	3.071	3.106
4	200	2.649	2.645	2	103	2.952	2.984
3	004	2.605	2.615	5	004 200	2.664	2.690
1	213	1.954	1.959	2	202	2.390	2.405
9	220	1.855	1.870	3	211	2.336	2.348
7	312	1.592	1.592	2	114	2.181	2.197
6	116	1.578	1.581	4	213	1.985	1.997
2	224	1.520	1.522	8	220	1.895	1.903
2	321	1.448	1.452	2	006	1.787	1.793
5	400	1.321	1.323	2	301	1.763	1.768
4	008	1.302	1.308	1	310	1.693	1.701
4	332	1.212	1.213	7	312	1.614	1.622
6	316	1.204	1.207	2	303	1.597	1.603
2	420	1.179	1.183	3	224	1.547	1.553
6	424	1.078	1.078	1	206	1.485	1.492
5	228	1.071	1.072	2	321	1.469	1.477
4	512	1.018	1.017	2	314	1.434	1.437
4	336	1.014	1.014	2	323	1.373	1.377
3	1·1·10	1.006	1.008	5	008 400	1.342	1.345
2	440	.9349	.9350	1	402	1.304	1.304
4	408	.9293	.9305	2	411	1.294	1.295
4	532	.8935	.8936	1	330	1.266	1.268
4	516	.8912	.8915	6	332	1.232	1.234
4	3·1·10	.8854	.8875	1	413	1.225	1.226
4	620	.8363	.8367	4	420	1.200	1.203
4	622	.8263	.8263	1	422	1.174	1.174
4	536	.8049	.8047	1	307	1.164	1.166
3	3·3·10	.8007	.8016	1	334	1.145	1.147
				1	415	1.114	1.115
				6	424	1.099	1.098
				1	431	1.072	1.070
				1	510	1.055	1.055
				5	512	1.037	1.035
				1	521	.9960	.9948
				2	523	.9628	.9638
				4	440	.9491	.9516
				5	516	.9105	.9097
				1	600 0·0·12	.8974	.8967
				2	611	.8815	.8813
				2	534	.8736	.8730
				1	613	.8588	.8584
				5	620	.8510	.8506
				1	446 622	.8405	.8402
				1	518	.8304	.8300
				4	536	.8208	.8208
				1	624	.8120	.8112
				2	606	.8018	.8020
				1	3·1·12	.7929	.7933
				2	633	.7836	.7825
				4	448	.7768	.7767

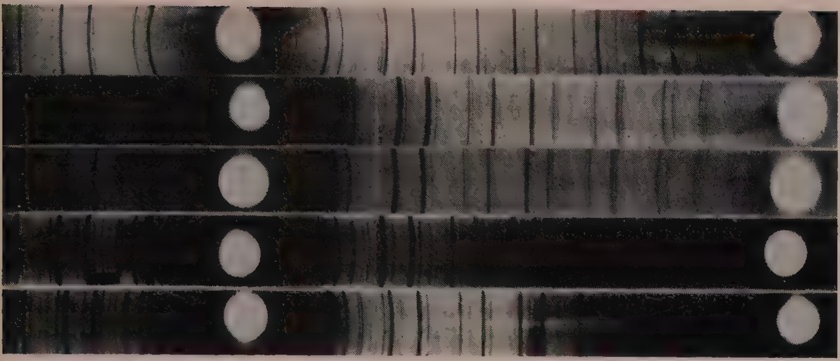

FIG. 5. X-ray powder photographs of luzonite-famatinite. Cu radiation, Ni filter. 1. Synthetic famatinite. 2. Synthetic luzonite. 3. Luzonite, Mankayan, Luzon, Philippines. 4. Luzonite-famatinite, Goldfileld, Nevada. 5. Famatinite, Famatina, Argentina.

effect is undoubtedly the large difference in scattering power exhibited by arsenic atoms as compared to antimony atoms.

Luzonite and famatinite have a sphalerite-type structure, since their powder photographs closely resemble those of sphalerite. Chalcopyrite and stannite, both of which are tetragonal, also have a sphalerite-type structure. Both, moreover, have other properties similar to luzonite-famatinite: they are almost never untwinned and in polished section show a polysynthetic type of twinning, they have similar hardness and specific gravity, and they possess closely similar cell dimensions. All four minerals have indistinct cleavages and show very limited variation in composition. A tabulation of their comparative properties follows in Table 3. Assuming, then, that luzonite-famatinite had a structure closely similar to chalcopyrite or stannite, a determination of this structure involved the distribution of the atoms in luzonite-famatinite so as to comply with a body centered tetragonal cell, and the comparison of the theoretical intensity of reflections from such a cell with the measured intensity of natural material.

The structure of famatinite can be derived from two sphalerite unit cells, one on top of the other. As there are only two antimony atoms in a

TABLE 3. COMPARATIVE PROPERTIES OF LUZONITE, FAMATINITE, STANNITE, AND CHALCOPYRITE

	Composition	Hardness	Specific Gravity	Cell dimensions		Space group	Twinning
				a_0	c_0		
Luzonite	Cu_3AsS_4	3.5	4.35–4.50	5.29	10.465	$I\bar{4}2m$	Polysynthetic, etc.
Famatinite	Cu_3SbS_4	3.5	4.50–4.65	5.38	10.76	$I\bar{4}2m$	Polysynthetic, etc.
Stannite	Cu_2FeSnS_4	4.0	4.3 –4.5	5.46	10.725	$I\bar{4}2m$	Polysynthetic, etc.
Chalcopyrite	$Cu_2Fe_2S_4$	3.5–4.0	4.1 –4.3	5.24	10.30	$I\bar{4}2d$	Polysynthetic, etc.

unit cell of famatinite, the problem of distributing these so as to give a body-centered tetragonal cell can be simply resolved by replacing the zinc atoms of the doubled sphalerite cell with antimony atoms at all the corners and at the center. The eight corner atoms contribute $\frac{1}{8}$ atom each, and the center one a full atom, for a total of two atoms. Copper atoms are then put in place of the remainder of the zinc atoms and the sulfur atoms remain undisturbed. This gives a cell containing $2(Cu_3SbS_4)$, as illustrated in Fig. 6. The derivation of luzonite and sphalerite is exactly analogous. The structure may also be derived from that of stannite by substituting arsenic or antimony for the iron atoms and copper for the tin atoms.

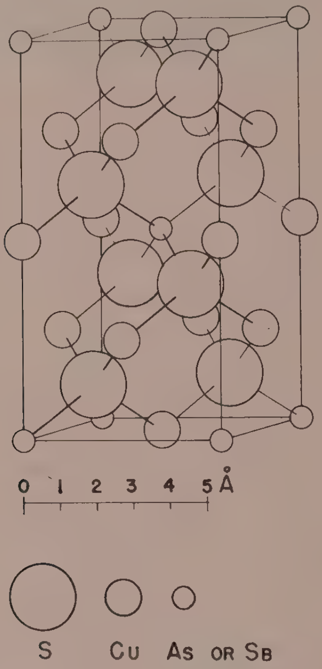

Fig. 6. Arrangement of atoms in the unit cell of luzonite-famatinite.

Confirming this structure involved making an estimation of the intensity of the spots corresponding to each *hkl* value on the precession or Weissenberg photographs, and then calculating the intensities of reflections which would theoretically be derived from the assumed structure. Estimation of intensities was made entirely by visual comparison, and the results are correspondingly approximate. The estimated intensities for luzonite-famatinite were in good agreement with the intensities calculated from the assumed structure.

HABIT

Luzonite-famatinite is usually massive and fine-grained. More rarely, it is fairly coarse-grained, and some famatinite from Argentina occurs in massive granular intergrowths with single grains attaining 5 mm. in their largest dimension. Distinct equant crystals, found in vugs and druses and not exceeding 2 mm. in size (usually less than 1 mm.) are rare. Usually crystals are rough, with some or all faces curved and etched. It is more common to find tufts, rosettes, and botryoidal crusts of indistinct crystals lining vugs and druses. Crystals suitable for goniometric or *x*-ray single crystal work are invariably inconspicuous and have not been noted except in association with massive luzonite. It is understandable that earlier workers, with the exception of Sawada, were unable to find material suitable for describing the crystal structure and habit of this mineral series.

TWINNING

As previously noted, crystals of luzonite-famatinite usually show evidence of twinning and in polished section it exhibits polysynthetic twinning, similar in appearance to that found in albite. Since twinning is invariably very fine, it is difficult to secure mineral grains for *x*-ray single crystal work known to consist of a single individual. One twin law was determined by *x*-ray work on a twinned crystal of the interpenetration type, and subsequent confirmation of this law was obtained by morphological measurements made on the same crystal. The composition plane and the twinning plane is (112). It is not known if this twin law will account for the common polysynthetic twinning of luzonite-famatinite seen in polished section.

PHYSICAL PROPERTIES

Cleavage: (101), good; (100), distinct. Cleavage is not usually observed because of the fine grain of natural material. Fracture: uneven, conchoidal. Tenacity: brittle. Hardness: about 3.5. Specific gravity: the value measured on luzonite from Mankayan, Luzon, with the Berman balance is 4.380; the value calculated from the *x*-ray data is 4.438. The value measured on famatinite from Famatina, Argentina, by pyknometer is 4.635; the value calculated is 4.660.

OPTICAL PROPERTIES

Color: deep pinkish brown. Similar to bornite, although darker and with more of a greyish tinge. Streak: black. Luster: usually dull, metallic. Opaque. In polished section pale brownish pink in color. Shows weak pleochroism and strong anisotropism. Polarization colors: greenish yellow and purplish red. Different members of the luzonite-famatinite series did not show any differences in color, luster, streak, or behavior under polarized light.

CHEMICAL PROPERTIES

Luzonite is a copper sulf-arsenide corresponding to the formula Cu_3AsS_4. Famatinite is a copper sulf-antimonide, Cu_3SbS_4. A complete solid solution series exists between the two end-members. Luzonite and enargite have identical formulas, and hence are dimorphs. There is no mineral with enargite type structure having the composition of famatinite, although a maximum of about 6% Sb will enter into the enargite structure, as determined from scores of analyses of natural crystals.

Neither luzonite nor famatinite have been found in absolutely pure masses. Even the purest obtainable material reveals, in polished section under high magnification, minor amounts of accessory materials; most commonly pyrite, tetrahedrite-tennantite, chalcopyrite, and covellite. Although the total of these impurities may be 1% or less, they serve to obscure the nature of elements which may substitute in the luzonite-famatinite structure, for they cannot be separated from material being prepared for analysis. Many of the old analyses, made on material even more difficult to purify than that used by the writer, were recalculated after subtracting anywhere from 10% to over 50% for insoluble material or pyrite.

The samples analyzed were all hand-picked under a microscope from −40 mesh material. All grains showing any foreign mineral attached or included were rejected. A representative sample of the purified material was then reserved for making a polished section, and the remainder was analyzed. Any minor recalculation of the analysis was based on the mineral impurities shown to have been present in the polished section. Analyses are listed in Table 4.

Spectrographic analysis of the purest material available, from Famatina, Argentina, showed, in addition to copper, arsenic, antimony, and iron, the following elements:

.1%–.01%–Al, Ca, Ti, Si
.01%–.001%–Mg, Na, K, Bi, Mn, Zr, Pb, Cr, Mo, V, Cb, Ta, Ag, Au, Ba

The most important point brought out by this analysis is the very small amount of such elements as Bi, Pb, and Ag present, and the spectroscopic absence of such heavy elements as Zn, Cd, and Sn, which might normally be expected to be present in traces in most base metal deposits. Actually, the mine from which this specimen came is primarily a silver-gold mine. Galena and sphalerite are minor accessories in the ore. The indication would seem to be, therefore, that the amount and

TABLE 4. ANALYSES

	1	2	3	4	5	6	7	8
Cu	48.42	47.55	48.32	43.94	45.72	45.70	42.98	43.27
Fe		.26		.48			.26	
Bi				1.79				
Sb		1.46	1.48	13.19	13.72	14.59	24.36	27.63
As	19.02	17.07	17.35	9.08	9.45	8.98	3.31	
S	32.56	32.63	32.85	30.86	31.11	30.73	28.97	29.10
Rem.		.97		.17				
Total	100.00	99.94	100.00	99.51	100.00	100.00	99.88	100.00

1) Cu_3AsS_4.
2) Mankayan, Luzon, Philippines. Gonyer analysis.
3) Analysis #2, recalculated after deduction of .97% insol. and .56% pyrite.
4) Goldfield, Nevada. Gonyer analysis.
5) Analysis #4, recalculated after deduction of .17% insol., 1.03% pyrite, and 2.20% bismuthinite.
6) $Cu_3As_{1/2}Sb_{1/2}S_4$.
7) Sierra Famatina, Argentina. Gonyer analysis.
8) Cu_3SbS_4.

kind of substitution of other elements for Cu, As, or Sb in the luzonite-famatinite structure is very limited. Probably even the iron usually reported is chiefly due to small amounts of admixed pyrite, chalcopyrite, or tetrahedrite. The chemical behavior of this group therefore contrasts markedly with that of the tetrahedrite-tennantite group, in which extensive substitution of other elements for Cu, As, and Sb is the rule.

OCCURRENCE

Members of this series are found in low to medium intensity copper deposits, particularly in the former, or in lower-intensity phases of higher intensity deposits. They are generally absent from copper deposits of the hypothermal, pyrometasomatic, or mesothermal "porphyry" type. The most common associated sulfide minerals are: enargite, tetrahedrite-tennantite, pyrite, chalcopyrite, covellite; and more rarely sphalerite, bismuthinite, ruby silvers, native silver, gold, and marcasite. Among gangue minerals barite and drusy quartz are so common as to be almost characteristic. Alunite is also found in some places.

The most important localities are Mankayan, Luzon; Famatina, Argentina; Goldfield, Nevada; Hokuetsu, and other localities in Japan; Kinkwaseki, Formosa; Cerro de Pasco, Peru; Morococha, Peru; and minor quantities are found at Butte, Montana and Cananea, Mexico.

Measurable crystals have been observed only from Mankayan, Luzon; Goldfield, Nevada; and Hokuetsu, Japan.

BIBLIOGRAPHY

BODENBENDER, G. (1922), El Nevado de Famatina: *Annales del Ministerio de Agricultura, Sección Geologia, Mineralogia y Mineria*, Republic of Argentina, **XVI,** No. 1.

DANA, E. S., *System of Mineralogy*, 6th ed., New York, 1909.

DEJONG, W. F. (1928), Die Enargitgruppe. Structur des Sulvanite, Cu_3VS_4: *Zeits. Krist.*, **68,** 522–530.

DOELTER, C., *Handbuch der Mineralchemie*, Dresden and Leipzig, Theodor Steinkopf, 1926.

FRENZEL, A. (1877), Mineralogisches aus dem Ostindischen Archipel: *Mineralogische Mittheilungen*, 302–303.

FREBOLD, GEORG (1927), Uebereinige Mineralien der Enargitgruppe und ihre paragenetische Verhältnisse in der Kupfererzlagerstätte von Mancayan auf Luzon (Philippinen): *Neues Jahrbuch für Mineralogie*, **56,** Abt. A, 316–333.

HARCOURT, G. A. (1937), The distinction between enargite and famatinite (Luzonite): *Am. Mineral.*, **22,** 517–535.

HOCART, R., AND WEIL, R. (1947), Symétrie et Reséau Structural Apparent de la Luzonite: *Comptes Rendu Academie de Science*, Paris, **225,** 194–195.

IMAI, HIDEKI (1949), The Copper Ores from the Mankayan Mine, Luzon, Philippine Islands, with special reference to the enargite and luzonite problems: *Japanese Jour. of Geology and Geography*, **XXI,** Nos. 1–4.

KLOCKMAN, F. (1891), Mineralogische Mittheilungen aus Sammlungen der Bergakademie zu Clausthal: *Zeits. Krist.*, **19,** 265–275.

LANNEFORS, N. A., *Sobre las Minas de Cobre de Famatina*, Publication No. 21, Ministerio de Agricultura, Dirección General de Minas, Geología e Hidrología, Buenos Aires, 1926.

"Las Reservas de Cobre en la República Argentina," Argentina Dirección de Minas y Geología, *Copper Resources of the World*. International Geological Congress, 16th Session, 1935, Vol. 2, pp. 443–447.

MOSES, A. J. (1905), The crystallization of luzonite: *Am. Jour. of Science*, 4th Series, **20,** 277–284.

MURRAY, G., AND BEIN, H. H. (1951), Rebuilding Leptano—The Far East's largest producer of copper: *Engineering and Mining Journal*, **152,** Nos. 3 and 4.

RANSOME, F. L., *Geology and Ore Deposits at Goldfield, Nevada*, U.S.G.S. Professional Paper #66, 1909.

SAWADA, H. (1943), *Crystallographic Study on Luzonite*, Thesis, Tokyo University.

SCHNEIDERHÖHN, H., AND RAMDOHR, P. *Lehrbuch der Erzmikroskopie*, Berlin, Borntrager, 1931, Vol. 2

SHANNON, E. V. (1917), Famatinite from Goldfield, Nevada: *Am. Jour. of Science*, series 4, **44,** 469–470.

SMITH, W. D., *Geology and Mineralogy Resources of the Philippine Islands*, Manila, 1924.

SHORT, M. N., *Microscopic Determination of the Ore Minerals*, U.S.G.S. Bulletin #**914,** 1940.

STELZNER, A. (1873), *Mineralogische Mittheilungen*, **4,** 219–262.

TALLIBART, B. (1912), *Contribución al estudio de algunos minerales de cobre del Famatina*, Thesis, University of Buenos Aires.

TOLMAN, C. F. AND AMBROSE, V. W. (1934), The rich ores of Goldfield, Nevada: *Economic Geology*, **29,** 255–279.

WALDO, A. W. (1935), Identification of the copper ore minerals by means of *x*-ray powder diffraction patterns: *Am. Mineral.*, **20,** 587, 588, 590.

WATANABÉ, MANJIRO, "Luzonite from Japan and Formosa," *Science Reports of the Tôhoku University*, Series III, Vol. IV, No. 1 (Jan., 1951).

WATANABE, TAKEO (1943), Mode of occurrence of minerals of the enargite group from the Teine Mine, Hokkaido, Japan: *Japanese Association of Mineralogists, Journal*, **30,** No. 2, 80–90.

WEISBACH, A. (1874), *Mineralogische Mittheilungen*, **3**, 257–258.

WEST, C. D. (1934), The pseudo symmetry of enargite, *Am. Mineral.*, **19,** 279.

ZERRENNER, C. (1869), Nachricht uber eine Anzahl aus verschiedenen Gebieten der Erde bei mir eingegangener interessantes Mineralien, *Berg-und Hüttenmannische Zeitung*, **28,** 106.

THE AMERICAN MINERALOGIST, VOL. 42, NOVEMBER-DECEMBER 1957

SOME FREE ENERGY VALUES FROM GEOLOGIC RELATIONS

R. M. GARRELS, *Harvard University, Cambridge, Massachusetts.*

ABSTRACT

Mineral associations in earth surface environments have been used to obtain basic thermochemical data for reactions and compounds of geologic interest. From a study of weathering processes, standard free energies of formation from the elements at 25° C. and one atmosphere total pressure have been estimated for kaolinite (−883 kcal.), muscovite (−1298 kcal.), and K-feldspar (−856 kcal.). From relations in the zone of oxidation of ore deposits a correction has been made to the published value for hydrocerussite (from −409.1 kcal. to −406 kcal.) and a new value for malachite (−217 kcal.). It is suggested that the methods used can be applied to obtain useful free energy values for many other compounds.

INTRODUCTION

Since 1952, when Latimer published the second edition of his classic "Oxidation Potentials," sufficient free energy data on compounds and ions have been easily available to calculate equilibrium relations for many low temperature-low pressure systems of geologic interest. Although these data are strictly applicable only at 25° C. and 1 atmosphere total pressure, the error in applying them to natural environments at or near the earth's surface is usually small.

Eh-pH diagrams utilizing such data were first used by Pourbaix (1949) as a convenient and provocative method of showing interrelation between solids and dissolved ionic species with special reference to problems of metallic corrosion. Since then, similar diagrams have been used to depict approximate equilibrium relations between minerals and the ions in equilibrium with them in aqueous solution, and the results have been compared to natural relations, especially in problems of atmospheric oxidation of ores, and those of primary chemical precipitation (cf. Garrels and Huber, 1953).

When such diagrams were first constructed, it was with hope that they would bear a faint resemblance to nature, and conceivably might be used like an "ideal gas" or "ideal solution"—as hypothetical models useful in showing how far complex natural relations departed from simple systems involving chemical compounds instead of minerals, and containing only those ions or other dissolved species for which thermochemical information happened to be available.

It has been a surprise to find that these naive chemical analogs of nature are directly useful in many instances. That is to say that numerous calculated solubilities fit those deduced from geologic relations, predicted assemblages of chemical compounds are reflected by identical assemblages of their nearest mineral analogs, and the environment of their occurrence, expressed on a pH-potential grid, corresponds to that found in the field. In fact, natural systems reflect the diagrams much better than most experimental ones!

The reasons for this agreement seem to be: (1) There is sufficient time available for achievement of near-equilibrium in many natural low temperature aqueous environments. Even though the low temperature activation energies for transformations of silicate structures, for example, are high, and experimental work is well-nigh impossible, the months and years during which natural systems fluctuate through a small range of conditions permit a close approach to equilibrium. (2) The amount of interaction in natural systems is less than might be anticipated from their complexity. For example, the error in calculating the free energy of formation of calcite from solubility data on sea water is small if all the currently known interactions are considered. (3) The effect of biological activity is to add complexity on the one hand, and to catalyze reaction on the other. The net effect seems to be one of increasing reaction rates of well-established reactions, and hence of helping rather than hindering the investigator. (4) In a considerable number of instances, the difference in free energy between a pure synthetic compound and its mineral analog is not large (although the difference may be extremely important for some processes!)

Because of the close correspondence between natural relations and those calculated from free energy data—that is, from experiments carefully designed to approach equilibrium, the interesting possibility arose of obtaining free energy data directly from observations on natural systems. Numerous checks were made by calculating free energies of reaction or of formation for reactions or compounds for which complete free energy data already were available. The results were so encouraging that some values for free energy of formation of minerals hitherto unknown were attempted.

CHECK CALCULATIONS

To illustrate the methods used, and to show the degree to which there is quantitative agreement between free energy values calculated from natural relations and those determined by various experimental methods, a few examples are given here of calculation of free energy of formation of substances for which experimental values already have been published.

ΔF_{CaCO_3}

The argument has raged for years as to whether the low latitude oceans are saturated or supersaturated with calcium carbonate. Thus the system seems to be one that approaches equilibrium. According to

Sverdrup *et al.* (1942, p. 205) the average calcium content of the oceans is about 0.0102 mols per liter, the average HCO_3^- is about 0.0018 equivalents per liter, the average pH about 8.2, the ionic strength is 0.7, and the temperature in the vicinity of 25° C.

Assuming equilibrium, we can write:

$$\frac{a_{Ca^{++}_{aq}}\, a_{CO_3^{=}{}_{aq}}}{a_{CaCO_{3\text{solid}}}} = k_{CaCO_3} \tag{1}$$

$$\frac{a_{H^+} + a_{CO_3^=}}{a_{HCO_3^-}} = k_{HCO_3^-} \tag{2}$$

$$\Delta F^\circ_{\text{Reaction}} = RT \ln k = -\ 1.364 \log k_{(25^\circ)}. \tag{3}$$

$$\Delta F^\circ_{\text{Reaction}} = \Delta F^\circ_{Ca^{++}_{aq}} + \Delta F^\circ_{CO_3^{=}{}_{aq}} - \Delta F^\circ_{CaCO_{3\text{solid}}} \tag{4}$$

But a_{CaCO_3} solid at 25° C. and 1 atmosphere pressure is unity by convention, and $a_{Ca^{++}} = \gamma_{Ca^{++}} \cdot m_{Ca^{++}}$, and $\gamma_{HCO_3^-} = a_{HCO_3^-} m_{HCO_3^-}$, where m represents molality and γ the activity coefficient. From Garrels and Dreyer (1952, p. 234), $\gamma_{Ca^{++}}$ in seawater is about 0.26, and $\gamma_{HCO_3^-}$ about 0.36. At pH$=$8.2, $a_{H^+} = 10^{-8.2}$.

Then, from No. 2:

$$a_{CO_3^=} = \frac{k_{HCO_3^-}\, \gamma_{HCO_3^-}\, m_{HCO_3^-}}{a_{H^+}}$$

Substituting numerical values:

$$a_{CO_3^=} = \frac{10^{-10.34}\, 10^{-0.44}\, 10^{-2.75}}{10^{-8.2}} = 10^{-5.33} \tag{5}$$

Also:

$$a_{Ca^{++}} = m_{Ca^{++}} \cdot \gamma_{Ca^{++}}$$

Using the analyzed value of calcium for $m_{Ca^{++}}$ (this assumes no important interactions of Ca^{++}) and substituting a numerical value for $\gamma_{Ca^{++}}$:

$$a_{Ca^{++}} = 10^{-2.01}\, 10^{-0.59} = 10^{-2.60} \tag{6}$$

Substituting the values from No. 5 and No. 6 in No. 1:

$$\frac{10^{-2.60}\, 10^{-5.33}}{10^\circ} = k_{CaCO_3} = 10^{-7.93}$$

Then this value of k can be substituted in No. 3:

$$\Delta F^\circ_{\text{reaction}} = -\ 1.364 \log 10^{-7.93}$$

$$\Delta F^\circ_{\text{reaction}} = 10.8 \text{ kcal.}$$

Finally, using this value, and values for $\Delta F^\circ_{Ca^{++}}$ and $\Delta F^\circ_{CO_3^=}$ from Latimer (1952) and substituting in No. 4:

$$10.8 = -\ 132.18 - 126.2 - \Delta F^\circ_{CaCO_{3\text{solid}}}$$

$$\Delta F^\circ_{CaCO_{3\text{solid}}} = -\ 269.2$$

This compares with the published value for calcite of -269.78 and of aragonite of -269.53 (Latimer, op. cit.).

The calcium carbonate-sea water system is an unusually complex one, owing to the high concentration of salts which makes it difficult to obtain reliable γ values for the ions involved. Yet the check is within one kilocalorie on the basis of a fairly crude calculation. Obviously no information has been obtained on calcite-aragonite relations, for which (Latimer, 1952):

$$\Delta F^\circ_{\text{calcite}} - \Delta F^\circ_{\text{aragonite}} = -0.27 \text{ kcal.}$$

$\Delta F^\circ_{UO_2CO_3}$

Another example is the calculation of ΔF° for UO_2CO_3 (rutherfordine). The mineral is sometimes intimately associated with various uranyl oxide hydrates, or uranyl hydroxyhydrates. The stable hydrate in water is $UO_2(OH)_2 \cdot H_2O$ (Bullwinkel, 1954, p. 7). From the reaction:

$$UO_2(OH)_2 \cdot H_2O + CO_2 = UO_2CO_3 + 2H_2O$$

it is apparent that the existence of rutherfordine at equilibrium with $UO_2(OH)_2 \cdot H_2O$ in nearly pure water at a fixed temperature can occur at a single value for the partial pressure of CO_2. Thus in the weathering environment, which is close to 25° C., the coexistence of these two species suggests that the equilibrum partial pressure of CO_2 is close to that of CO_2 in the atmosphere ($\cong 10^{-3.5}$ atmospheres). For those conditions the equilibrium constant for the reaction is:

$$k = \frac{1}{P_{CO_2}} = \frac{1}{10^{-3.5}}$$

The free energy is:

$$\Delta F^\circ_R = -1.364 \log 10^{-3.5} = 4.8 \text{ kcal.}$$

Using Bullwinkel's value of ΔF° for $UO_2(OH)_2 \cdot H_2O$ (op. cit., p. 30) and Latimer's values for the others:

$$\Delta F^\circ_R = \Delta F^\circ_{UO_2CO_3} + 2\Delta F^\circ_{H_2O} - \Delta F^\circ_{UO_2(OH)_2 \cdot H_2O} - \Delta F^\circ_{CO_2(gas)}$$
$$4.8 = \Delta F^\circ_{UO_2CO_3} - 113.4 + 391 + 94.3$$
$$\Delta F^\circ_{UO_2CO_3} = -377.1$$

Bullwinkel's listed value is -377. Actually, his value and the one calculated here have to agree, because he found experimentally that the equilibrium partial pressure of CO_2 was almost exactly that of the atmosphere, but this experimental determination does not destroy the validity of the preceding geologic reasoning.

These examples illustrate the *general* relation that geologic coexistence of two chemically precipitated phases usually indicates that the free energy of the reaction to form one from the other in their environment is about 2 kilocalories or less. The phases in question may be compatible or incompatible pairs.

Relations Deduced From Weathering Processes

Students of weathering have worked out, from various lines of evidence, a general sequence of mineral stability as follows:

$$\text{K-feldspar} \rightarrow \text{K-mica} \rightarrow \text{kaolinite} \rightarrow \begin{array}{l}\text{diaspore}\\ \text{gibbsite}\end{array}$$

$$\text{Na-feldspar} \rightarrow \text{montmorillonite} \rightarrow \text{kaolinite} \rightarrow \begin{array}{l}\text{diaspore}\\ \text{gibbsite}\end{array}$$

(c.f. Keller, 1957, Reiche, 1945, Goldich, 1938, Mohr and Van Baren, 1954).

In other words, in a system open to rain water, the rock-forming silicates tend to alter to last residue of aluminum oxide hydrates (and ferric oxide where femic minerals originally are involved). In an idealized system, we can visualize a vertical soil profile under conditions of high rainfall and continuous downward drainage as a steady state condition with zones of stability of the minerals from unaltered silicates at the bottom to aluminous residue near the top.

We have fairly good information on the free energy of formation of gibbsite and boehmite (Deltombe and Pourbaix, 1956, p. 3), at one end of the reaction series, and at the other end only a value for $\Delta H°$ for orthoclase (Yoder and Eugster, 1955, p. 262). The plan here is to start with gibbsite, and attempt to calculate the free energies of formation of the intermediate products, using $\Delta H°$ for orthoclase as an approximate check-point at the other end of the series.

Relations Among the Aluminum Oxide Hydrates

Lateritic soils contain a variety of aluminum oxide hydrates. Among the chief minerals are diaspore ($Al_2O_3 \cdot H_2O$), its dimorph boehmite; and gibbsite ($Al_2O_3 \cdot 3H_2O$). All three of these are found in important quantities, and are intimately associated. Boehmite is probably unstable relative to diaspore under geologic conditions (G. MacDonald, personal communication), but the free energy difference between these minerals is probably small, so that boehmite can form and persist. Recent work by Deltombe and Pourbaix (1956) indicates that gibbsite is stable relative to boehmite in aqueous solution at room temperature.

In summary, the geologic occurrence and thermochemical information are in harmony if it is assumed that gibbsite forms if equilibrium is attained in the presence of nearly pure liquid water, and diaspore and boehmite are the products of disequilibrium, or of heating, and drying. Gibbsite can be looked upon ideally as the product of wet leaching of silicates; boehmite and diaspore as its dehydration products. Undoubtedly there is further important control by grain size and other complicating factors, but where soil leaching takes place in well drained soils in the presence of nearly pure water, gibbsite is the expected stable phase.

RELATION OF KAOLINITE TO ALUMINUM OXIDE HYDRATES

In the weathering of feldspar, kaolinite may or may not be an intermediate product in the formation of aluminum oxide hydrates. Goldman (1955) shows convincingly that feldspar altered directly to gibbsite in the Arkansas bauxite deposits. He further interprets that gibbsite altered to cliachite (fine-grained aluminum oxide hydrates, probably chiefly monohydrate). This cliachite is, in turn, selectively altered to kaolinite. Elsewhere, as in the alteration of shales to bauxite, kaolinite is a definite precursor of the aluminum oxide hydrates. Gordon and Tracey (1951, p. 32) tie in some of the resilication of bauxite in Arkansas with waters from overlying swamps.

Thus the reaction:

$$\text{“Bauxite”} + \text{silica} = \text{kaolinite}$$

is clearly reversible under geologic conditions, going to the right when silica content of water is typical of that of swamp water, and to the left at some lower value. Furthermore, the monohydrates seem to be more easily kaolinized than the tri-hydrate, which follows from their relative stabilities in water, but both apparently can be resilicated. A reasonable estimate of the equilibrium condition would be kaolinization of gibbsite at a dissolved silica content of about 10 parts per million at 25° C. Tropical streams carry about three times this amount, average streams a little less (Clarke, 1927, Chap. III). From this the relation can be written:

$$\underset{\text{Gibbsite}}{Al_2O_3\cdot 3H_2O} + \underset{\substack{\text{10 ppm. (0.00017 } m\text{)}\\ \text{silica in solution}}}{2SiO_{2\,aq}} = \underset{\text{kaolinite}}{H_4Al_2Si_2O_9} + \underset{\substack{\text{nearly pure}\\ \text{liquid water}}}{H_2O}; \quad \Delta F = 0 \qquad (7)$$

According to Krauskopf (1956, p. 23) dissolved silica is saturated with respect to its amorphous polymers (silica glass) at a concentration of about 140 ppm. (0.0024 m) at 25° C. Thus:

$$SiO_{2\,\text{glass}} = SiO_{2\,aq\ (140\ \text{ppm})}; \quad \Delta F = 0$$

$k = a_{SiO_2} = 0.0023$ (assuming activity = molality for a molecular species in dilute solutions)

$$\Delta F^\circ_{\text{reaction}} = -1.364 \log 0.0023 = 3.5 \text{ kilocalories}$$

Therefore:

$$\Delta F^\circ_{SiO_2\,aq} - \Delta F^\circ_{SiO_2\,\text{glass}} = 3.5 \text{ kilocalories}$$

$$\Delta F^\circ_{SiO_2\,aq} = 3.5 + \Delta F^\circ_{SiO_2\,\text{glass}} = 3.5 - 190.9 = -187.4 \text{ kcal.}$$

For reaction No. 7, the equilibrium constant is:

$$k = \frac{1}{a^2_{\mathrm{SiO_2}}} \quad \frac{1}{(0.00017)^2} = 10^{7.54}$$

$$\Delta F^\circ_R = -1.364 \log 10^{7.54} = -10.3 \text{ kcal.}$$

From the standard free energy of the reaction, and the standard free energy of formation of the reactants and products, it is possible to solve for ΔF° of kaolinite.

$$\Delta F^\circ_R = \Delta F^\circ_{\mathrm{kaol.}} + \Delta F^\circ_{\mathrm{H_2O}} - \Delta F^\circ_{\mathrm{gibbsite}} - 2\Delta F^\circ_{\mathrm{SiO_2}\,aq}$$

$$\Delta F^\circ_{\mathrm{kaol.}} = \Delta F^\circ_R + \Delta F^\circ_{\mathrm{gibbsite}} + 2\Delta F^\circ_{\mathrm{SiO_2}\,aq} - \Delta F^\circ_{\mathrm{H_2O}}$$

$$\Delta F^\circ_{\mathrm{kaol.}} = -10.3 - 554.6 - 374.8 + 56.7 = -883.0 \text{ kcal.}$$

In passing it should be noted that $\Delta F^\circ_{\mathrm{kaolinite}}$ is not particularly sensitive to the value of soluble silica chosen—a tenfold larger or smaller value would change $\Delta F^\circ_{\mathrm{kaolinite}}$ by ±2.6 kcal.

INTERRELATIONS OF KAOLINITE, MICA, AND K-FELDSPAR

From the field evidence, kaolinization of feldspar seems to take place under almost any soil condition, even at pH values as high as 8 or 9, suggesting that such conditions are sufficient to convert feldspar into mica, and mica into kaolinite. If the feldspar-mica alteration is slow, and the mica-kaolin reaction fast, mica might not even be observed as an intermediate product; in fact it might not form at all as a crystalline material if conditions under which kaolinite is stable are superimposed on a feldspar grain. However, very careful work shows mica as an intermediary between feldspar and kaolin (Sand, 1956). The total evidence indicates that K-feldspar, quartz and K-mica are in equilibrium at a pH and K^+ content of the system close to but higher than those at which K-mica and kaolin are stable.

Hydrolysis of mica yields maximum pH values of the order of 9.3 (Garrels and Howard) in solutions containing K^+ ions at activity of about $10^{-3.0}$ (about 40 ppm.). The reaction involved is a surface reaction transforming K-mica to H-mica, but should be a guide to the boundary between K-mica and kaolin. At any rate the K-mica-kaolin boundary will not be at lower pH at the same K^+. Tentatively we can place the K-mica-kaolin boundary at pH 9.5 at a K^+ activity of 10^{-3}, and the K-feldspar-K-mica boundary at pH 10.5 at the same activity of K^+. These values fit geologic relations fairly well; waters at the lower limit of the zone of soil formation must represent conditions very close to equilibrium with feldspar, or at least conditions under which reaction does not take place at a finite rate over long periods of time. Not many pH measurements have been made of waters percolating through at this boundary, but values of 9 to 10 are not uncommon.

Tentatively we can write:

$$3H_4Al_2Si_2O_9 + 2K^+ = 2KAl_3Si_3O_{10}(OH)_2 + 3H_2O + 2H^+$$

$$K_{\text{Ka--mica}} = \frac{(H^+)^2}{(K^+)^2} = \frac{10^{-19}}{10^{-6}} = 10^{-13} \qquad (8)$$

$$\Delta F^\circ_R = -\ 1.364 \log 10^{-13} = 17.7 \text{ kcal.}$$

and:

$$KAl_3Si_3O_{10}(OH)_2 + 2K^+ + 6SiO_2 = 3KAlSi_3O_8 + 2H^+$$

$$K_{\text{mica--feldspar}} = \frac{(H^+)^2}{(K^+)^2} = \frac{10^{-21}}{10^{-6}} = 10^{-15} \qquad (9)$$

For (8): $\Delta F_R{}^\circ = -\ 1.364 \log 10^{-15} = 20.2 \text{ kcal.}$

$$\Delta F^\circ_R = 2\Delta F^\circ_{\text{mica}} + 3\Delta F^\circ_{H_2O} + 2\Delta F^\circ_{H+} - 3\Delta F^\circ_{\text{kaolin}} + 2\Delta F^\circ_{K+}$$
$$2\Delta F^\circ_{\text{mica}} = -\ 3\Delta F^\circ_{H_2O} - 2\Delta F^\circ_{H^+} + 3\Delta F^\circ_{\text{kaolin}} + 2\Delta F^\circ_{H^+} + \Delta F^\circ_R$$
$$2\Delta F^\circ_{\text{mica}} = +\ 170.1 + O - 2649 - 134.9 + 17.7$$
$$\Delta F^\circ_{\text{mica}} = -\ 1298 \text{ kcal.}$$

For reaction No. 9, assuming first equilibrium with silica glass:

$$\Delta F^\circ_R = 3\Delta F^\circ_{OR} + 2\Delta F^\circ_{H+} - \Delta F^\circ_{\text{mica}} - 2\Delta F^\circ_{K+} - 6\Delta F^\circ_{SiO_2(\text{glass})}$$
$$3\Delta F^\circ_{OR} = \Delta F^\circ_R - 2\Delta F^\circ_{H^+} + \Delta F^\circ_{\text{mica}} + 2\Delta F^\circ_{K^+} + 6\Delta F^\circ_{SiO_2(\text{glass})}$$
$$3\Delta F^\circ_{OR} = 20.2 - O - 1298 - 134.9 - 1145.4$$
$$\Delta F^\circ_{OR} = -\ 853 \text{ kcal.}$$

If it is assumed that equilibrium is with quartz instead of with silica glass:

$$\Delta F^\circ_{\text{orthoclase}} = -\ 856 \text{ kcal.}$$

As a check, a value of ΔH° for the formation of orthoclase from the oxides can be calculated, and compared with that cited by Yoder and Eugster (1955, p. 263). From the relation:

$$\Delta H^\circ = \Delta F^\circ + T\Delta S^\circ$$

the standard heat of formation can be obtained.

For the reaction to form orthoclase from the oxides:

$$\tfrac{1}{2}Al_2O_3 + \tfrac{1}{2}K_2O + 3SiO_2 = KAlSi_3O_8$$

the standard entropy of reaction is:

$$\Delta S^\circ_R = S^\circ_{OR} - \tfrac{1}{2}S^\circ_{Al_2O_3} - \tfrac{1}{2}S^\circ_{K_2O} - 3S^\circ_{SiO_2}$$

Using values of S° for the oxides from Latimer, and that for orthoclase (adularia) from Kelley, et al (1955, p. 11)

$$\Delta S^\circ_R = 52.5 - 6.1 - 10.4 - 30 = 6 \text{ cal/mol.}$$

For the same reaction:

$$\Delta F^\circ_R = \Delta F^\circ_{OR} - \tfrac{1}{2}\Delta F^\circ_{Al_2O_3} - \tfrac{1}{2}\Delta F^\circ_{K_2O} - 3\Delta F^\circ_{SiO_2}$$
$$\Delta F^\circ_R = -\ 856 + 188.3 + 38.1 + 577.2 = -\ 52.4 \text{ kcal.}$$

Then:

$$\Delta H^\circ_R = \Delta F^\circ_R + T\Delta S^\circ_R$$
$$\Delta H^\circ_R = -52.4 + (298 \times 0.006) = -50.6 \text{ kcal.}$$

The value cited by Yoder and Eugster (*op. cit.*) is −56.4 kcal. The check, considering the length of the "bridge" used, the uncertainty in the value for gibbsite at one end of the bridge, and the uncertainty in the value for the heat of formation of orthoclase as cited by Yoder, as well as other possible sources of error, is good.

SUMMARY

In summary, the following values have been obtained for standard free energies of reactions and of formation of compounds:

TABLE 1. STANDARD FREE ENERGIES

	$\Delta F^\circ_{298.1}$ (kilocalories)	
Reaction		
$Al_2O_3 \cdot 3H_2O_c + 2SiO_{2aq} = H_4Al_2Si_2O_{9c} + H_2O_{liq}$	− 10.3	All reaction values estimated plus or minus 2 kilocalories, with strong possibility of larger errors in values for minerals
$Al_2O_3 \cdot 3H_2O_c + 2SiO_{(glass)} = H_4Al_2Si_2O_{9c} + H_2O_{liq}$	− 17.3	
$Al_2O_3 \cdot 3H_2O_c + 2SiO_{2quartz} = H_4Al_2Si_2O_{9c} + H_2O_{liq}$	− 20.5	
$3H_4Al_2Si_2O_{9c} + 2K_{aq}^+ = 2KAl_3Si_3O_{10}(OH)_{2c} + 3H_2O_{liq} + 3H_{aq}^+$	+ 18	
$KAl_3Si_3O_{10}(OH)_{2c} + 2K_{aq}^+ + 6SiO_{2quartz} = 3KAlSi_3O_{8c} + 2H_{aq}^+$	+ 20	
Mineral	ΔF°_f	
Kaolinite	− 883	
K-mica	−1298	
K-feldspar	− 856	

The error on individual determinations is estimated at one or two kilocalories, but the possibility of cumulative errors across the "bridge" are considerable. There still is serious doubt concerning the value for gibbsite, which has been used as a base, because it is based in turn on the somewhat questionable value of αAl_2O_3. But when a firmer value for ΔF° orthoclase becomes available as a check, it should be possible to fix mica and kaolinite within narrow absolute limits.

STANDARD FREE ENERGY OF FORMATION OF $Pb_3(OH)_2(CO_3)_2$ AND $Cu_2(OH)_2CO_3$

In addition to using natural occurrence to obtain ΔF° values for compounds for which values have not been obtained experimentally, it is possible to use it to correct values already determined or to choose between data from conflicting sources.

$Pb_3(OH)_2(CO_3)_2$

Latimer estimates a ΔF° value for $Pb_3(OH)_2(CO_3)_2$ of -409.1 kilocalories. This compound corresponds to the rare mineral hydrocerussite. In nature cerussite ($PbCO_3$) is the major lead carbonate. If the reaction is written:

$$3PbCO_{3c} + H_2O_{liq} = Pb_3(OH)_2(CO_3)_{2c} + CO_{2g}$$

then the equilibrium constant, assuming that the groundwater is nearly pure water, is:

$$k = P_{CO_2}$$

$$\Delta F^\circ_R = \Delta F^\circ_{Pb_3(OH)_2(CO_3)_2} + \Delta F^\circ_{CO_2} - 3\Delta F^\circ_{PbCO_3} - F^\circ_{H_2O}$$

$$\Delta F^\circ_R = -409.1 - 94.26 + 449.1 + 56.7 = 2.4 \text{ kcal.}$$

Then:

$$2.4 = -1.364 \log k$$

$$k = 10^{-1.8}$$

Thus the equilibrium partial pressure, according to these relations, is $10^{-1.8}$ atmospheres of CO_2. This clearly cannot be the case, for $PbCO_3$ would be unknown at equilibrium at the earth's surface. Instead, because of its few occurrences, it is much more likely that it forms at a P_{CO_2} somewhat less than that commonly observed—perhaps at 10^{-4} atmospheres. In this case:

$$k = 10^{-4}$$

$$\Delta F^\circ_R = -1.364 \log 10^{-4} = 5.5 \text{ kcal.}$$

Then, assuming that the correction should be made to $Pb_3(OH)_2(CO_3)_2$:

$$5.5 = \Delta F^\circ_{Pb_3(OH)_2(CO_3)_2} - 94.26 + 449.1 + 56.7$$

$$\Delta F^\circ_{Pb_3(OH)_2(CO_3)_2} = -406 \text{ kcal.}$$

This value, 3.1 kilocalories larger than that of Latimer, has been shown to be a minimum by a prettily reasoned application of the phase rule to similar equilibria by W. L. McIntire (unpublished manuscript), but the straightforward application of known mineral occurrence probably suffices.

$Cu_2(OH)_2CO_3$

Basic copper carbonate, corresponding to the mineral malachite, occurs abundantly in the zone of weathering of copper deposits. In many instances it has been observed intimately intergrown with CuO (tenorite). From the relation:

$$Cu_2(OH)_2CO_{3c} = 2CuO_c + H_2O_{liq} + CO_{2g}$$

it is apparent that in dilute aqueous solution the equilibrium constant contains only P_{CO_2}. From the prevalence of malachite occurring alone, but in apparent equilibrium with tenorite in some deposits, it can be concluded that the equilibrium P_{CO_2} is perhaps slightly less than that of the normal atmosphere. If so:

$$k = 10^{-3.7}$$
$$\Delta F^\circ_R = 1.364 \log 10^{-3.7} = 5.0 \text{ kcal.}$$

The value of $\Delta F^\circ_{Cu_2(OH)_2CO_3}$ is not available, but accepting those for the other species as given in Latimer:

$$\Delta F^\circ_R = 2\Delta F^\circ_{CuO} + \Delta F^\circ_{H_2O} + \Delta F^\circ_{CO_2} - \Delta F^\circ_{Cu_2(OH)_2CO_3}$$
$$5.0 = -60.8 - 56.7 - 94.26 - \Delta F^\circ_{Cu_2(OH)_2CO_3}$$
$$\Delta F^\circ_{Cu_2(CO)_2CO_3} = -217 \text{ kcal.}$$

The method could obviously be used to determine ΔF° values for other basic copper salts, and work is in progress by P. Hostetler at Harvard University that will compare experimentally determined values with those deduced in this manner.

CONCLUSION

The examples given here of the use of natural mineral occurrence to obtain basic thermochemical data suggest that many useful estimates could be made to supplement current values derived almost entirely from laboratory experiment, and further that experimental values can be checked by knowledge of natural occurrence. Many geologists have gone to the laboratory to obtain data to use in explaining geologic phenomena; the possible contributions that might be made by reversing the process seem to be somewhat neglected.

ACKNOWLEDGMENTS

I want to express my gratitude to the members of the Geochemistry Seminar at Harvard University, who contributed largely to the development of the ideas presented here. I am especially indebted to P. B. Hostetler and to W. L. McIntire of that Seminar, to J. B. Thompson, and R. Siever, of the Division of Earth Sciences at Harvard, and to C. L. Christ, of the United States Geological Survey, who gave freely of their time in discussing many of the problems involved, and made many valuable suggestions.

REFERENCES

BULLWINKEL, E. P. (1954), The chemistry of uranium in carbonate solutions: U. S. Atomic Energy Commission, R.M.O. **2614,** 59 pp.

CLARKE, FRANK WIGGLESWORTH (1924), The data of geochemistry: *U. S. Geol. Surv. Bull.*, **770,** 841 pp.

Deltombe, E., and Pourbaix, M. (1956), Comportement electrochimique de l'aluminum. Diagramme d'equilibre tension-pH du system Al-H_2O, a 25° C.: Rapport Technique, **42,** Centre Belge d'Etude de la Corrosion, Brussels, 14 pp.

Garrels, R. M. and Huber, N. K. (1953), Relation of pH and oxidation potential to sedimentary iron mineral formation: *Econ. Geol.*, **48,** 337–358.

Garrels, R. M. and Dreyer, R. M. (1952), Mechanisms of limestone replacement at low temperatures and pressures: *Bull. Geol. Soc. Amer.*, **63,** 325–379.

Garrels, R. M. and Howard, Peter, Reactions of feldspar and mica with water at low temperature and pressure: in press.

Goldich, S. S. (1938), A study in rock weathering: *Jour. Geol.*, **46,** 17–58.

Goldman, Marcus I. (1955), Petrography of bauxite surrounding a core of kaolinized nepheline syenite in Arkansas: *Econ. Geol.*, **50,** 586–610.

Gordon, Mackenzie, Jr. and Tracey, Joshua I. (1951), Origin of the Arkansas bauxite deposits: In *Amer. Inst. Min. Met. Eng. Symposium* "Problems of clay and laterite genesis," pp. 12–34.

Keller, W. D. (1957), The principles of chemical weathering: Lucas Bros., Columbia, Mo., Revised Edition, 110 pp.

Kelley, K. K., Todd, S. S., Orr, R. C., King, E. G. Bonnickson, K. R. (1953), Thermodynamic properties of sodium-aluminum and potassium-aluminum silicates: *U. S. Bur. Mines R. I.*, **4955,** 14 pp.

Krauskopf, K. K. (1956), Dissolution and precipitation of silica at low temperatures: *Geochim. et Cosmochim. Acta,* **10,** 1–26.

Latimer, Wendell M. (1952), Oxidation Potentials: Prentice Hall, Inc., New York, Second Edition, 392 pp.

Mohr, E. C. J. and Van Baren, F. A. (1954), Tropical Soils: Interscience Publishers, New York.

Pourbaix, M. J. N. (1949), Thermodynamics of dilute aqueous solutions: Edward Arnold and Co., London, 136 pp.

Reiche, Parry (1945), Survey of weathering processes and products: *Univ. New Mex. Pub. in Geology*, No. **1**.

Sand, L. B. (1956), On the genesis of residual kaolins: *Am. Mineral.*, **41,** 28–40.

Sverdrup, H. U., Johnson, Martin W., Fleming, Richard H. (1942), The Oceans: Prentice Hall, Inc., New York, 1086 pp.

Yoder, H. S. and Eugster, H. P. (1955), Synthetic and natural muscovites: *Geochim. et Cosmochim. Acta,* **8,** 225–280.

THE AMERICAN MINERALOGIST, VOL. 42, NOVEMBER–DECEMBER 1957

BIKITAITE, $LiAlSi_2O_6 \cdot H_2O$, A NEW MINERAL FROM SOUTHERN RHODESIA*

CORNELIUS S. HURLBUT, JR., *Harvard University,*
Cambridge, Massachusetts.

ABSTRACT

Bikitaite, $LiAlSi_2O_6 \cdot H_2O$ is a new mineral from the lithium-rich pegmatites at Bakita, Southern Rhodesia. It occurs as a late mineral interstitial to granular eucryptite. No crystals were observed. *X*-ray study yields: monoclinic; $a_0 = 8.63$ Å, $b_0 = 4.95$, $c_0 = 7.64$, $\beta = 114°34'$ $(a_0 : b_0 : c_0 = 1.743 : 1 : 1.543)$; space group, $P2_1/m$. Colorless to white. Specific gravity 2.34 (meas.) 2.29 (cal. for two formula-units per cell). Hardness 6. Optically biaxial (−); $n\mathrm{X} = 1.510$, $n\mathrm{Y} = 0.521$, $n\mathrm{Z} = 1.523$, $2\mathrm{V} = 45°$, $r < v$, $\mathrm{Z} = b$, $\mathrm{X} \wedge c = 28°$. Analysis gives: SiO_2 55.79, Al_2O_3 26.68, Fe_2O_3 0.07, Li_2O 6.51, Na_2O 0.10, K_2O 0.17, MgO 0.33, H_2O 9.82, Total 99.47. The strongest *x*-ray powder lines are: 4.19 Å, (10), 3.48 (10), 3.40 (10), 7.84 (8). The name *bikitaite*, is from the locality, Bikita.

INTRODUCTION

The pegmatites of Bikita are located about forty miles east of Fort Victoria, Southern Rhodesia. Since the finding of cassiterite there nearly fifty years ago, they have been known as the "Bikita tinfield." From that time, the area has been a small tin producer, mostly from eluvial deposits. Shortly after the discovery of tin, tantalum was found at Bikita but little attention paid to it until World War II created a demand for the element. At present both metals are being mined on a small scale. The tantalum minerals, according to Macgregor (1946), are tantalite, simpsonite, microlite and an abnormal manganese tantalate.

The geology of the Bikita area has been mapped by Tyndale-Biscoe (1952). His map shows scattered pegmatites extending over a distance of two and one-half miles in a north-south direction. The major dike with N-S strike and easterly dip is approximately one mile long and lies in the southern part of the area, and at present is being actively mined for lithium. Development to date has shown this pegmatite to contain one of the world's great concentrations of lithium. Spodumene and amblygonite are both present but the chief lithium minerals are petalite and lepidolite, which are found in hundreds of thousands of tons. The southern half of this body is mined by Bikita Minerals, Ltd., with lepidolite the principal ore mineral. In the northern half George H. Nolan, Ltd., is mining mainly petalite.

OCCURRENCE

In 1955 the writer collected specimens of eucryptite from the Nolan property. Some of the eucryptite was in coarse crystals, others in fine-grained granular aggregates, associated with granular quartz. Present in the granular material was an unidentified mineral in extremely limited amount. In a specimen recently received from Mr. George Nolan this unknown mineral, although not abundant, was in sufficient amount to separate for study. It proved to be a new mineral and is named *bikitaite* from the locality.

---

* Contribution No. 380, Department of Mineralogy and Petrography, Harvard Unisity, Cambridge, Massachusetts.

It is almost certain that a paragenetic study of the Bikita pegmatites would be most rewarding. This at present is impossible with the limited number of specimens at hand, but age relations of some of the minerals are known. Tyndale-Biscoe (1952) states, "It is probably very difficult to obtain pure samples of petalite for analysis as it always contains relics of feldspar which it probably replaces." Eucryptite appears to replace the petalite. Bikitaite is still later for it is found in small fractures within the eucryptite and fills interstices between quartz and eucryptite grains (Fig. 1). Quartz makes up about one-fourth and eucryptite three-fourths of the aggregate.

Physical and Optical Properties

Bikitaite is colorless and transparent in the small grains available. No cleavage was observed on the fragment used for single crystal work. When crushed material is observed microscopically, most of the grains

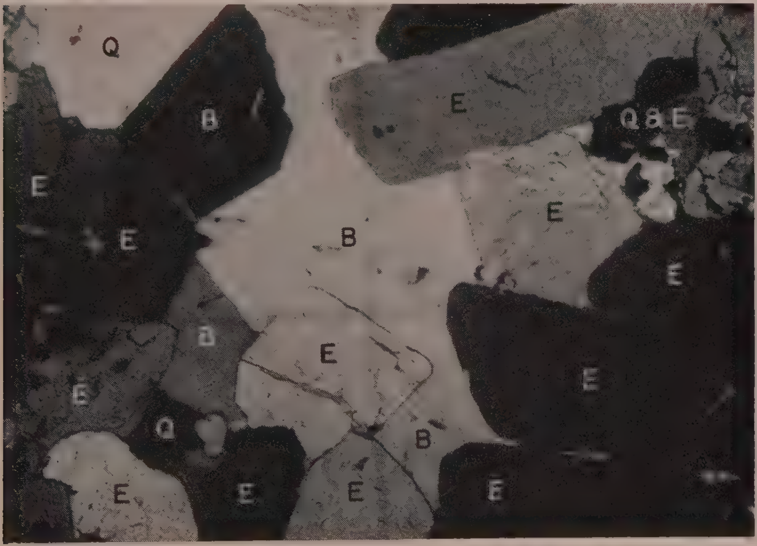

Fig. 1. Photomicrograph showing bikitaite interstitial to eucryptite and quartz. Crossed nicols. Photograph covers area of thin section 3×2.25 mm. E-eucryptite. Q-quartz. B-bikitaite.

appear randomly oriented indicating the lack of a pronounced cleavage. However, a few show parallel extinction with positive elongation. Two different orientations are observed in these grains. In one orientation the X direction is essentially across the length and in the other the Y direction. It can be concluded, therefore, that there is poor {001} and {100} cleavage. The hardness is 6. Specific gravity measured by suspension in bromoform is 2.34 ± 0.04 (calculated 2.29). The grains used for suspension were so small that it was difficult to tell when the density of the mineral was exactly matched with the density of the liquid; hence the uncertainty in the measured specific gravity. The streak is white. There is no fluorescence in either short- or long-wave ultraviolet radiation. This is in contrast to the eucryptite with which bikitaite is associated and which fluoresces pink to red. The optical properties are given in Table 1.

TABLE 1. OPTICAL PROPERTIES OF BIKITAITE

	nNa	
$X\wedge c=28°$	1.510 ± 0.001	opt. (−)
Y	1.521 ± 0.001	$2V=45°$
$Z=b$	1.523 ± 0.001	$r<v$

CHEMICAL COMPOSITION

As stated previously, bikitaite occurs in small amounts interstitial to quartz and eucryptite grains and as fracture fillings in eucryptite. To obtain material for chemical analysis it was necessary to crush the specimen to minus 150 mesh to liberate bikitaite from the eucryptite and quartz. A separation was then made in bromoform. About 40 grams of the specimen were used to obtain 400 milligrams of bikitaite.

The chemical analysis is given in Table 2 together with the contents of the unit cell. Using the measured specific gravity, 2.34 and cell volume, 296.8 Å^3, the molecular weight of the cell contents was determined as, M. = 418. This value multiplied by the atomic ratios give the cell contents as: $(Li, Na, K, Mg)_{1.89}Al_{2.20}Si_{3.90}O_{12.05}\cdot 2.3H_2O$. This can be considered essentially as $2(LiAlSi_2O_6\cdot H_2O)$ which is equivalent to spodumene plus water. An excess of alumina and a deficiency of silica over the stoichiometric proportions indicates that some alumina may be substituting for silica in four-fold coordination. The presence of Mg^{++} substituting for Li^+ makes at least a partial valence compensation for the substitution of Al^{+3} for Si^{+4}.

Bikitaite is apparently the first natural hydrated lithium aluminum silicate to be described, although several have been produced in the laboratory. In 1894 Thegutt obtained $LiAlSiO_4\cdot H_2O$ by heating a mixture of kaliophilite, lithium chloride, carbonate and water. In recent years considerable work has been done on the synthesis of lithium aluminum silicates, notably by Hatch (1943), Winkler (1947), Roy and Osborn (1949) and Barrer and White (1951). Of these, however, only Barrer and White reported hydrated compounds. They synthesized two hydrated lithium aluminum silicates: $Li_2O \cdot Al_2O_3 \cdot 2SiO_2 \cdot 4H_2O$ and $Li_2O \cdot Al_2O_3 \cdot 8SiO_2 \cdot 5H_2O$ with ion exchange properties similar to zeolites. Neither of these compounds corresponds to bikitaite in *x*-ray powder data.

A differential thermal analysis of bikitaite showed two endothermic reactions, one beginning at 190° C. and ending at 475° C. and the other beginning at 750° C. and ending at about 900° C. The first reaction is interpreted as due to loss of water and the nearly 300° C. interval over which it is given off indicates it is zeolitic type. The *d* spacings as shown by an *x*-ray powder photograph of bikitaite after being heated to 500° C. are the same as given by the mineral before heating. This also indicates that water is nonessential. The loss of water lowers the refractive index to an average value of 1.485. Apparently water is not again taken up for holding the mineral in an atmosphere saturated with water vapor or immersing it in water does not raise the refractive index. The second endothermic reaction is the result of inversion to β-spodumene. After heating to 900° C., bikitaite gives an *x*-ray powder photograph identical to that of β-spodumene taken on material supplied by R. A. Hatch and described by him (1943). The β-spodumene produced by heating bikitaite is an extremely fine aggregate of birefringent crystals with an average refractive index of 1.520. For β-spodumene Hatch gives *n*O =1.518–1.519, *n*E 1.523–1.524.

TABLE 2. CHEMICAL ANALYSIS AND UNIT CELL CONTENTS OF BIKITAITE

	Weight per cent 1	Weight per cent 2	Molecular ratios	Atomic ratios	Atoms per unit cell	Theoretical cell contents
SiO_2	55.79	56.13	.9338	(Si) .9338	3.90	4
Al_2O_3	26.68	26.84	.2633	(Al) .5266	2.20	2
Fe_2O_3	0.07	—				
Li_2O	6.51	6.55	.2192	(Li) .4384	1.83	2
Na_2O	0.10	0.10	.0016	(Na) .0032	0.01	
K_2O	0.17	0.17	.0018	(K) .0036	0.02	
MgO	0.33	0.33	.0082	(Mg) .0082	0.03	
H_2O	9.82	9.88	.5489	(H)1.0978	4.59	2
	99.47	100.00				

1. Jun Ito, *analyst*, 1957.
2. Recalculated to 100 per cent after deducting Fe_2O_3.

X-RAY STUDY

No crystals of bikitaite are available for morphological study. In fact it was difficult to obtain a crystal fragment large enough to manipulate for single crystal *x*-ray work. To do this a portion of the eucryptite-bikitaite specimen was coarsely crushed (minus 50-plus 100 mesh), separated in bromoform, and the grains of the material of lesser density examined optically. A grain 0.25 millimeters in maximum dimension and free from eucryptite and quartz was thus selected. Two orientations were effected by the precession method enabling rotation and Wiessenberg photographs to be taken about the *b* and *c* axes. From these photographs the data in Table 3 were determined.

TABLE 3. UNIT CELL DATA FOR BIKITAITE

Crystal class	Monoclinic prismatic $2/m$
Unit cell dimensions	a_0 8.63, b_0 4.95, c_0 7.64 Å, $\beta=114°34'$.
Axial ratios	$a_0:b_0:c_0=1.743:1:1.543$
Cell volume	296.8 Å^3
Space group	$P2_1/m$.
Formula units per cell	2

The only space group extinctions found were on the 0-level photographs for $(0k0)$ with $k=2n$. The space group is thus $P2_1/m$.

The *d* spacings of a powder photograph taken with copper radiation are given in Table 4. The intensities of the various lines were obtained by means of a diffractometer.

TABLE 4. X-RAY POWDER SPACING FOR BIKITAITE

Copper Radiation, Nickel Filter

I	*d*	I	*d*	I	*d*
8	9.21	10	3.40	2	1.900
6	8.04	7	3.29	2	1.895
8	7.84	8	3.22	1	1.855
6	6.95	4	3.08	1	1.615
4	6.84	2	2.93	1	1.610
3	4.39	1	2.87	1	1.565
6	4.30	1	2.79	1	1.535
10	4.19	4	2.53	2	1.465
3	4.08	3	2.52	2	1.432
1	4.03	4	2.475	2	1.350
1	3.91	1	2.320	1	1.345
2	3.82	1	2.045		
10	3.48	1	1.96		

REFERENCES

BARRER, R. M., AND WHITE, E. A. D. (1951), The hydrothermal chemistry of silicates, Pt. I, Synthetic lithium aluminosilicates: *Jour. Chem. Soc. London*, 1276–1278.

HATCH, R. A. (1943), Phase equilibrium in $Li_2O \cdot Al_2O_3$-SiO_2 system. *Am. Mineral.*, **28,** 471–496.

MACGREGOR, A. M. (1946), Simpsonite and other tantalates from Bakita, Southern Rhodesia: *Min. Mag.*, **27,** 157–165.

RAY, R., AND OSBORN, E. F. (1949), The system lithium metasilicate-spondumene-silica: *Journ. Chem. Soc.*, **71,** 2086–2095.

THEGUTT, S. J. (1894), Zur Chemie einiger Alumosilicate: *Neues Jahrb. Min.*, **B.B.9,** 555–623.

TYNDALE-BISCOE, R. (1952), The geology of the Bikita tin-field, Southern Rhodesia: *Geol. Soc. of S. Af. Tr.*, **54,** 11–25.

WINKLER, H. G. E. (1947), On the synthesis of nepheline: *Am. Mineral.*, **24,** 131–136.

THE AMERICAN MINERALOGIST, VOL. 42, NOVEMBER-DECEMBER 1957

ZINCIAN AND PLUMBIAN DOLOMITE FROM TSUMEB, SOUTH-WEST AFRICA*

CORNELIUS S. HURLBUT, JR., *Harvard University, Cambridge, Massachusetts.*

ABSTRACT

Five specimens of zincian-plumbian dolomite from Tsumeb, South-West Africa are described. Chemical analyses give a range in percentage of ZnO from 3.23 to 8.74 and of PbO from 0.58 to 4.96. DTA analyses show a progressive decrease in the temperature of the first endothermic reaction with increasing percentage of ZnO and a decrease in the temperature of the second endothermic reaction with increasing percentage of PbO. Because of several variables the indices of refraction, specific gravity and unit cell dimensions show a much less regular variation with change in composition.

INTRODUCTION

Through the kindesss of Dr. B. H. Geier and Dr. G. Söhnge of the Tsumeb Corporation, five specimens of dolomite from Tsumeb, South-West Africa were made available for study. Assays made at the mine laboratory showed that the dolomite contained appreciable amounts of zinc. Lead was also present and in two specimens in significant amounts. Only traces of zinc have heretofore been found in dolomite, with the exception of a dolomite from Blieberg, Carinthia which according to Gintl (1877) contained 1.57 per cent ZnO. In a paper describing tarnowitzite and plumbocalcite from Tsumeb, Siegl (1936) mentions a plumbodolomite from Kreuth, Carinthia, but no analysis nor description of the mineral is given. Until now this appears to be the only locality of a plumbian dolomite.

Although all of the dolomite specimens came from the 30 level and are associated with oxidized ore minerals, they differ in their physical appearance and show considerable differences in their chemical analyses. In Table 1 they are numbered from 1 to 5 and hereafter will be referred to by number.

CHEMICAL COMPOSITION

All the specimens with the exception of #5 have visible impurities intimately disseminated through them. In order to separate the dolomite from the associated minerals, the samples were ground to minus 200 mesh and a separation made with methylene iodide. The method proved fairly effective with the exception of #2 in which, after separation, could be seen tiny particles of malachite attached to the dolomite fragments.

---

* Contribution from the Department of Mineralogy and Petrography, Harvard University, No. 381.

Table 1. Appearance and Association of Dolomite

1. Flesh colored, massive; associated with chalcocite, native copper and limonite.
2. White, massive; associated with malachite and limonite.
3. Light gray, porous crystalline crusts; associated with malachite, native copper and limonite.
4. Pink, massive and in crystalline aggregates and individual rhombohedrons; associated with malachite.
5. Flesh-colored crystalline crusts; free of other minerals.

The copper reported in the analysis of #2 is, therefore, assumed to be due to malachite. The copper reported in the other analyses may also be due to malachite in particles too small to be detected.

To make the analyses conform to the dolomite type formula, $AB(CO_3)_2$, it is necessary to group Zn, Fe and Mn with Mg in the B positions rather than with Ca in the A position. Moreover, the closer

Table 2. Chemical Analyses of Zincian Plumbian Dolomite*

	1	2	3	4	5
CaO	29.33	27.74	27.77	29.74	28.13
MgO	18.30	17.78	14.34	15.03	14.78
ZnO	4.48	3.23	8.74	6.80	8.31
FeO	0.44	0.66	0.12	0.18	2.16
MnO	0.41	0.27	0.09	0.30	0.27
CoO	0.10	—	—	0.53	0.10
CuO	0.06	1.73	0.15	0.97	0.09
PbO	0.58	3.75	4.96	0.70	1.06
CO_2	45.58	43.95	43.56	45.48	44.32
H_2O	—	—	—	—	0.27
Insol.	0.69	0.94	—	—	0.40
Total	99.97	100.05	99.51	99.73	99.89
			Molecular Percentages		
$CaCO_3$	49.88	29.30	50.27	52.21	49.49
$MgCO_3$	43.28	43.87	36.10	36.71	36.19
$ZnCO_3$	5.24	3.95	10.89	8.22	10.00
$FeCO_3$	0.58	0.92	0.17	0.25	3.27
$MnCO_3$	0.55	0.38	0.12	0.41	0.37
$CoCO_3$	0.14	—	—	0.70	0.12
$CuCO_3$	0.08	—	0.19	1.20	0.10
$PbCO_3$	0.25	1.68	2.26	0.30	0.46

* Mr. Jun Ito, *analyst*.

approach of Zn, Fe and Mn in ionic size to Mg than to Ca argues for such a grouping. Also, on the basis of ionic size Pb is considered to substitute for Ca rather than Mg. For analyses 1 and 5 the formula can be written, (Ca, Pb)(Mg, Zn, Fe, Mn, Co)$(CO_3)_2$, giving almost exactly a 1:1 ratio of the elements in the A and B positions. However, in analyses 2, 3 and 4 there is a slight excess of Ca^{++} plus Pb^{++} over the amount required in the A position. In these there is presumably a substitution of Ca^{++} for Mg^{++} and the formula can be written, (Ca, Pb)(Mg, Zn, Fe, Ca, Mn, Co)$(CO_3)_2$.

DIFFERENTIAL THERMAL ANALYSES

Differential thermal analyses were made in air of the analyzed specimens. The thermal curves are reproduced in Fig. 1 together with a curve for dolomite from Binnenthal, Switzerland.

The equipment used in the thermal study was manufactured by the Robert L. Stone Co., Austin, Texas. The samples were ground to minus 60 plus 200 mesh and the temperature increased at a uniform rate of 10° per minute with a resistance of 400 ohms.

The curves show the two endothermic peaks characteristic of the dolomite structure. The first peak of the Binnenthal dolomite is at 815° C. Haul and Heystek (1952) list 12 DTA analyses of dolomite as reported by seven investigators. These data show the first peak has been variously reported from 770°–825° C. The first endothermic reaction of dolomite is due to the decomposition of the $MgCO_3$ layers in the structure and the temperature at which it takes place is influenced by the cations that have been substituted in the Mg^{++} positions. Kulp, Kent and Kerr (1951) point out that in ankerite the greater amount of Fe^{++}, the lower the temperature of the first endothermic peak. According to them a Mg:Fe ratio of 5:1 reduces this peak temperature from 815° C. (dolomite, iron free) to 760° C. Frondel and Bauer (1955) show that in kutnahorite a ratio of Mg:Mn$=$1:13 lowers the temperature of the first reaction to 774° C.

Zn substituting for Mg in the dolomite structure causes a greater effect. Mg:Zn$=$10:1 reduces the temperature of the first endothermic peak to about 740° (specimen 2). Increasing amounts of Zn tend to further lower the temperature of this reaction but the trend is not linear as in ankerite (Kulp, Kemp and Kerr, 1951). In specimen #3 with Mg:Zn$=$3.3:1, the peak temperature of the first reaction is 725° C. In these zincian dolomites the situation is complicated by cations other than Mg^{++} and Zn^{++}. In #5 the presence of 3.27 per cent $FeCO_3$ can be detected in the thermal curve by its oxidation to Fe_2O_3 and CO_2. The amount of Fe^{++} in the other samples is so small that its presence is not recorded by the thermal analyses.

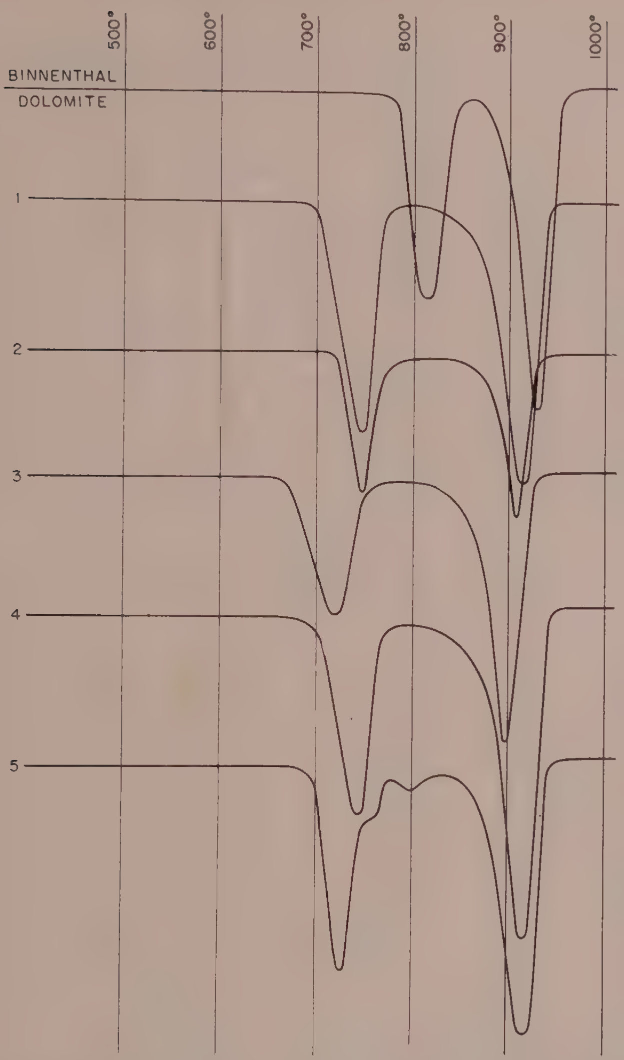

FIG. 1. Differential thermal analysis curves of zincian-plumbian dolomite.

There is no evidence that the temperature and amplitude of the second endothermic peak, that associated with the decomposition of the $CaCO_3$ layers, is affected by the presence of Zn. However, there appears to be a rough correlation between the amount of Pb and the temperature of the second endothermic peak. This peak in the Binnenthal dolomite (lead free) is at 940° C. In sample #1 with 0.25 mole per cent $PbCO_3$ it is at 925° C.; and in sample #3 with 2.26 mole per cent $PbCO_3$ at 895° C. In a similar manner the presence of lead in calcite lowers the temperature of the endothermic peak. According to Beck (1950) the peak temperature of the single endothermic reaction of Iceland spar is at 1,005° C. whereas in plumbian calcite from Bleiberg, Corinthia with 23 per cent $PbCO_3$, it is at 925° C.

PHYSICAL AND OPTICAL PROPERTIES

The refractive indices as measured by the immersion method are given in Table 3. Also given in the table are values for nO calculated from the indices of refraction of $CaCO_3$, $MgCO_3$, $ZnCO_3$, $FeCO_3$, $PbCO_3$ and $MnCO_3$, taken in the ratios of the analyses of Table 2. The specific gravities were obtained by use of the Berman microbalance and checked by suspension in methylene iodide. Specific gravities were calculated from the specific gravities of the end members taken in the ratios of the analyses. In both indices of refraction and specific gravity there is fairly good agreement between measured and calculated values.

TABLE 3. TSUMEB ZINCIAN-PLUMBIAN DOLOMITE

Indices of Refraction and Physical Properties

	Specimen No.				
	1	2	3	4	5
Measured					
nO	1.690	1.698	1.703	1.699	1.700±0.0005
nE	1.520	1.519	1.520	1.519	1.521±0.001
Calculated					
nO	1.690	1.693	1.701	1.696	1.700
Specific Gravity					
Measured	2.90	2.93	3.08	2.93	2.95
Calculated	2.91	2.97	3.07	2.94	3.01
Color	flesh colored	white	gray	pink	flesh colored
Hardness	4	3½	3½	3½	4
Fluorescence	red	none	none	none	red

The color of specimen #4, a vivid pink, is undoubtedly due to the presence of cobalt (0.53 per cent CoO). Furthermore, the flesh color of specimens #1 and #5 may also be due to the small amount (0.10 per cent CoO) of cobalt.

X-RAY STUDY

X-ray powder photographs were taken of the five specimens of zincian dolomite and of the Binnenthal dolomite for comparison. The *d* spacing of $10\bar{1}4$ and 0006 and unit cell dimensions listed in Table 4 show only slight correlation with composition. Specimens 3, 4 and 5 with greater amounts of $ZnCO_3$ have slightly larger unit cells than specimens 1 and 2.

TABLE 4. AXIAL RATIOS OF TSUMEB ZINCIAN-PLUMBIAN DOLOMITE

	d-10$\bar{1}$4	d-0006	c_0	a_0	c_0/a_0
1	2.889	2.665	15.990	4.806	3.327
2	2.885	2.668	16.008	4.804	3.332
3	2.899	2.679	16.074	4.808	3.343
4	2.894	2.683	16.098	4.816	3.343
5	2.892	2.675	16.050	4.814	3.334
Binn. dolomite	2.887	2.670	16.007	4.804	3.330

EVALUATION OF DATA

In the normal solid solution series involving two or three end-members, there can usually be shown a progressive change in the physical constants with change in the relative amounts of the substituting ions. This is true in minerals of the dolomite structure-type, $AB(CO_3)_2$, when one or two substituting cations occupy the B position. However, in the dolomite from Tsumeb, the situation is complicated not only by having as many as four elements substitute in the B position, but also having Pb substitute in the A position.

Attempts to plot specific gravity, index of refraction and d spacings against composition showed marked deviations from progressive change. Only in the differential thermal analyses is there a general correlation with composition. This is undoubtedly due to the fact that DTA separates from one another the effects due to substitution in the A positions from substitution in the B positions.

REFERENCES

BECK, C. W. (1950), Differential thermal analysis curves of carbonate minerals: *Am. Mineral.*, **35**, 985, 1013.

FRONDEL, C., AND BAUER, L. H. (1955), Kutnahorite: A manganese dolomite, $CaMn(CO_3)_2$: *Am. Mineral.*, **40**, 748–760.

GINTL, F. W. (1877), Lotos, Prag.

HAUL, R. A., AND HEYSTEK, H. (1952), Differential thermal analysis of the dolomite decomposition: *Am. Mineral.*, **37**, 166–179.

KULP, J. L., KENT, P., AND KERR, P. F. (1951), Thermal study of the Ca-Mg-Fe carbonate minerals: *Am. Mineral.*, **36**, 643.

SIEGL, W. (1936), Über Tarnowitzite und plumbocalcite von Tsumeb, *Min. Mitt.*, **48**, 286.

THE AMERICAN MINERALOGIST, VOL. 42, NOVEMBER-DECEMBER 1957

THREE OCCURRENCES OF HIGH-THORIAN URANINITE NEAR EASTON, PENNSYLVANIA*

ARTHUR MONTGOMERY, *Lafayette College, Easton, Pennsylvania.*

ABSTRACT

The geology, mineralogy and paragenesis of three occurrences of high-thorian uraninite in serpentine near Easton, Pa., are described. Seven x-ray fluorescence analyses together with three corroborative chemical analyses show this mineral to be high-thorian uraninite rather than high-uranoan thorianite as supposed. Six samples contain from about 15% to 35% ThO_2.

At the Williams quarry hydrothermal alteration of much uraninite to a sequence of secondary uranium- and thorium-rich minerals occurred. Frondel's Mineral C, thorogummite, then boltwoodite and uranophane were formed during serpentinization of fractured dolomite-diopside-tremolite contact-metamorphosed rock. Supergene coatings, chiefly hydrous uranium silicates and including boltwoodite and uranophane, formed much later.

At the reservoir site slight hydrothermal alteration of uraninite to thorogummite occurred. At the Royal Green Marble Co. quarry uraninite is found unaltered. At these localities fracturing or temperatures during later hydrothermal mineralization may have been of lower intensity.

It is concluded that thorium-rich Easton uraninite does not alter readily to secondary minerals, except when subjected to severe deformation and concomitant attack by serpentinizing hydrothermal solutions. The Th, U and Zr of this contact-metasomatic uraninite and the associated zircon originated in a granite-pegmatite magma rich in these elements, which intruded dolomitic rocks and through deformation while crystallizing yielded the hydrothermal solutions that deposited these minerals in those rocks, then serpentinized the rocks.

INTRODUCTION

High-thorian uraninite, regarded until now as high-uranoan thorianite,[1] occurs in serpentine rock at three localities just north and northeast of Easton, Pennsylvania. The two earlier discoveries were made around 1930 by George W. Gehman (1936) at the C. K. Williams quarry and at the near-by site of the College Hill reservoir. In the past few years uraninite has been found also at the quarry of the Royal Green Marble Co. about a mile northeast of the first two occurrences and on the New Jersey side of the Delaware River.

This paper reports the results of a paragenetic study made of uraninite and associated minerals from all three occurrences. One result of the study reveals that the Easton mineral generally called thorianite is actually high-thorian uraninite and that true Easton thorianite rarely exists. An early mineralogical study of this mineral from the Williams quarry was made by Wells, Fairchild and Ross (1933). The present investigation has depended on the large and unique collection of Easton uraninite specimens formerly belonging to George W. Gehman and now at Lafayette College. Mineralogy owes a debt to Mr. Gehman for making the original discovery of Easton uraninite at the Williams quarry, first identifying the mineral by chemical means, and then by unflagging effort throughout many ensuing years collecting nearly all of this material now available for study.

---

* Although not formally a contribution from the Mineralogy and Geology Departments of Harvard University, this may be considered one in view of the author's continuing work in the Berman Laboratory.

[1] The terms high-thorian uraninite and high-uranoan thorianite are arbitrarily taken for convenience at 15%-50% contained ThO_2 in uraninite and 15%-50% contained uranium oxides in thorianite.

This study was much aided by Dr. Clifford Frondel of Harvard University and Dr. Brian H. Mason of the American Museum of Natural History, to both of whom sincere thanks are given. Grateful acknowledgment is expressed for *x*-ray fluorescence analyses of uraninite specimens made in the Berman Laboratory of the Harvard Mineralogy Department by Dr. Robert M. Berman, for partial chemical analyses of three uraninite specimens made by Dr. Jun Ito at Harvard, and for photographs of two specimens taken by Dr. B. M. Shaub of Smith College. Dr. and Mrs. John S. Stevenson of McGill University kindly supplied samples of and information relative to thorianite from Pontiac County, Quebec. Dr. George Switzer kindly furnished a sample of thorianite from Betroka, Madagascar, from the collection of the U. S. National Museum. Clark C. McLean of Belvidere, N. J., generously made available for study all of his uraninite specimens from the Royal Green Marble Co. quarry.

Geologic Setting

The mineralogy and paragenesis of these three uraninite occurrences cannot be fully understood without reference to the regional geology and the sequence of paragenetic events which controlled the formation of all minerals found in the serpentine-talc deposits near Easton. The geology of these deposits has been described by Peck (1905), Fraser (Miller, 1939), Bayley (1941), and Montgomery (1955).

A zone several hundred feet wide of serpentinized dolomitic limestone, of likely correlation with the Franklin metamorphic limestone of Precambrian age, follows the lower south slope of Chestnut Hill which borders Easton on the north (Fig. 1). This prominent northeasterly-extending ridge ends about a mile east of where the Delaware River cuts through it at Weygadt Gap. The uraninite occurrences and also a number of serpentine-talc quarries are located along this zone, mainly on the Pennsylvania side of the river.

In addition to its zone of serpentinized Franklin rocks, Chestnut Hill is made up primarily of Precambrian para- and orthogneisses. The Precambrian crystalline rocks of the ridge occupy the core of an anticline formed during Appalachian folding, but they presumably owe their present position also to steep faults separating them from the flanking Cambrian limestones. Among the orthogneisses the Pochuck amphibolite and younger Byram granite gneiss predominate. The Pochuck is much infiltrated in lit-par-lit fashion by Byram granite, and at Weygadt Gap these interlayered gneisses are crosscut by veins of coarse-grained tourmaline-bearing pegmatite probably related genetically to the Byram. Very coarse pegmatite outcrops on all sides of the Williams quarry a half-mile southwest of Weygadt Gap. Some of this pegmatite has clearly intruded Franklin rocks at the quarry and has been the unmistakable cause of contact-metasomatic effects in closely adjacent rocks. It seems beyond doubt that magma of such pegmatite, or magma related genetically to such intrusive pegmatite, gave rise to the hydrothermal solutions which serpentinized an originally dolomitic limestone and formed the numerous interesting and rare-element minerals now found in the serpentine deposits (Peck, 1905; Montgomery, 1955).

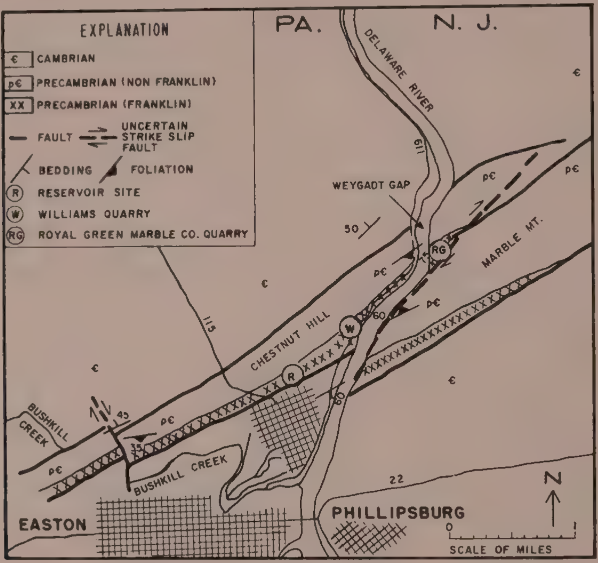

FIG. 1. Geologic sketch map of Easton area (adapted from maps of Peck (1905), Fraser (Miller, 1939) and Bayley (1941) and based on USGS Topographic Easton Sheet), showing location of three uraninite occurrences.

MINERAL PARAGENESIS

Both field and laboratory study point to a long-continued series of related structural and metamorphic events in Precambrian time. These were the factors responsible for the complex paragenetic relationships found among the minerals of these serpentine deposits. That all of these events occurred during Precambrian time is attested by age determinations on two different contact-metasomatic minerals of the deposits. One gave 800 million years for thorianite from the Williams quarry (Wells, 1933), while the second of 850 million years is a recent determination by the Larsen method (E. S. Larsen, Jr., personal communication) on zircon from the quarry of the Royal Green Marble Co.

At the Williams quarry especially there is a bewildering variety of minerals—about forty distinct species have been found here—and metamorphic rock types. Nearly all of the latter, however, have been converted more or less in the direction of one end-product, serpentine. Most common of these rock types are those rich in gray-green serpentine, which may be massive, finely to coarsely micaceous, or else streaked or mottled with interstitial patchy areas of whitish calcite or pale brown to pink dolomite. The latter two minerals vary from coarsely crystalline character to finely fibrous material partly altered to tremolite. The micaceous serpentine is rich in flakes of pearly-gray to gray-green phlogopite from fine to very coarse size. A second common rock type consists chiefly of interlacing stubby to bladed prisms of gray-white tremolite. The tremolite prisms are in part fibrous and altered to greenish serpentine. This tremolite-rich rock is much in evidence at the north end of the Williams quarry. Another rock type is coarsely foliated talc, grayish or pale pink, and occurring in large-scale schistose masses above and west of the north end of the quarry. A less common rock type, found close to pegmatite above the southwest end of the quarry, consists of splintery gray-white diopside in crudely prismatic masses largely altered to fibrous tremolite. Relic parting surfaces belonging to the original diopside still show up prominently in this pseudomorphic tremolite.

The field and laboratory evidence in support of the paragenetic sequence of minerals given in Table 1 was described in detail by Montgomery (1955), chiefly for relations found at the Williams quarry. Some of the inferred paragenetic events and the main supporting points are summarized here.

Thermal metamorphism:

Following pegmatite intrusion certain silicious dolomitic Franklin beds were largely converted by thermal metamorphism to coarsely crys-

TABLE 1. PARAGENETIC SEQUENCE OF COMMON MINERALS OF EASTON SERPENTINE DEPOSITS

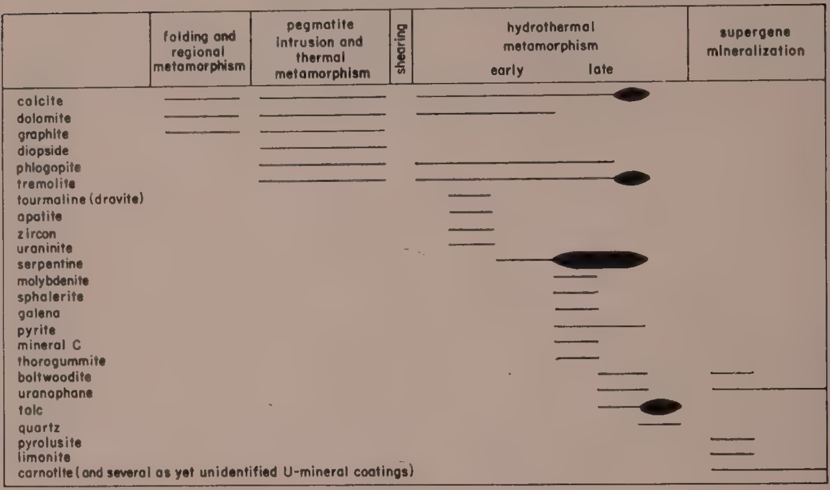

tallized diopside or tremolite. Relatively unaltered dolomite rock still occurs close to pegmatite, suggesting that the silica needed to form diopside and tremolite at this time did not come from a pegmatite source.

Early hydrothermal metamorphism:

The early diopside and tremolite formed as coarsely prismatic crystals, but even the freshest looking diopside now found is largely altered to fibrous tremolite. Beds of gray-white, graphitic and phlogopite-banded marble found above the southwest corner of the quarry also show partial alteration to fibrous tremolite. The formation of such fibrous tremolite, mainly pseudomorphic after diopside, reasonably marks an early stage of hydrothermal metamorphism. It is believed that crystals of uraninite and zircon were deposited at this time by early hydrothermal solutions. Grains of uraninite from the Williams quarry most commonly occur in massive serpentine enclosing patches of gray-white diopside partly altered to fibrous tremolite in finely gray-and-white-banded relic structures. These structures are due to selective filling or replacement by dark gray serpentine along parting planes originally developed in coarsely prismatic diopside. In a few specimens irregularly shaped grains of uraninite have unmistakably replaced diopside or fibrous tremolite pseudomorphic after diopside.

Late hydrothermal metamorphism:

Later periods of hydrothermal metamorphism were closely associated in time with powerful shearing forces. Extensive fracturing occurred and the more permeable rocks were penetrated by hydrothermal solutions. While earlier mineral formation tended to be by replacement, here it tended to follow open spaces. The formation of the sulfides, molybdenite, sphalerite, galena and pyrite, occurred during this time. These sulfides largely formed in small fractures or along grain boundaries of earlier minerals. During this later hydrothermal mineralization serpentine formed on a large scale, in part directly from strongly sheared dolomite rock. Solutions from crystallizing pegmatitic magna now carried both water and silica. Coarse to fine flakes of colorless phlogopite formed in great abundance together with much of the serpentine, derived either from shaly impurities in the original rocks or from potash-bearing hydrothermal solutions. It must have been primarily due to these episodes of intense shearing, confined to particular rocks, and the resultant strongly-penetrative, but localized hydrothermal mineralization, that alteration of some of the uraninite in rocks now found at the Williams quarry to a sequence of secondary uranium-thorium minerals took place.

During latest hydrothermal metamorphism deformational forces continued to open up the rocks to widespread penetration by hydrothermal solutions. Open fractures became filled with whitish, silky, fibrous tremolite and calcite of finely acicular habit. Some of these tremolite-calcite fracture fillings are six inches wide and many feet long. One of the last minerals in the hydrothermal sequence was talc, which in part altered directly from serpentine along zones of very late shearing when lower temperatures prevailed. Final open spaces became partly filled with drusy quartz.

Supergene mineralization:

The effects of ground-water solutions during near-surface and surface weathering of rocks found at the Williams quarry are shown by the presence of thin fracture coatings of such minerals as limonite and pyrolusite and of such alteration products of uraninite as carnotite and uranophane.

Paragenetic relations seem much the same in rocks exposed at the quarry of the Royal Green Marble Co. and in specimens from the site of the College Hill reservoir. At the first locality massive apple-green serpentine is common, enclosing partly-engulfed patchy areas of pale-pink coarsely-rhombohedral calcite and crossed by fracture fillings of snow-white, fibrous calcite and tremolite. Molybdenite in thin flakes and coarse scaly masses and also pyrite in small cubes occur abundantly in some of this serpentine rock. Uraninite is found in association with these sulfides in this type of rock. Uraninite specimens preserved from the reservoir excavations on College Hill show either grayish-green, streaky and micaceous serpentine rock, or grayish rock rich in coarsely prismatic tremolite partly altered to pale green serpentine. Some of these specimens show evidence of fracturing and shearing and marked alteration to gray-white, fine-scaly or powdery talc.

URANINITE AND ALTERATION PRODUCTS FROM THE WILLIAMS QUARRY

High-thorian uraninite from the C. K. Williams quarry (formerly called Sherrer quarry) occurs as black grains in several types of streaky or micaceous serpentine rock. Determinations of thorium-uranium content by the *x*-ray fluorescence analyzer of the Berman Laboratory in the Harvard Mineralogy Department on four "thorianite" specimens from the Williams quarry, show this mineral to be much richer in uranium than thorium in all cases. A partial chemical analysis of one of these specimens (T_4) by J. Ito at Harvard confirms the Th-U content as determined by *x*-ray fluorescence analysis. The mineral is therefore high-thorian uraninite rather than high-uranoan thorianite as formerly supposed. The original thorianite specimen from the Williams quarry analyzed by Wells (1933) and showing a ThO_2/U_3O_8 ratio of about 51/49, cannot be regarded as typical for the locality.

The most common occurrence of uraninite from the Williams quarry is in a grayish-green serpentine rock showing grayish patchy areas of fibrous tremolite pseudomorphic after coarsely prismatic diopside. This tremolite has in turn been partly replaced by encroaching massive serpentine. The encroaching serpentine may also appear micaceous from an abundance of enclosed phlogopite flakes of pearly-gray to pale-green color. A second less common occurrence is in brownish or pinkish, fine-grained dolomite rock specked with small flakes of colorless phlogopite and streaked with grayish or brownish serpentine. Gehman (1936) reports that uraninite and also zircon were mostly confined to a narrow shoot-like zone soon mined out near the north end of the quarry. This would have been in association with the tremolite-serpentine rock still remaining in the walls there. Confirmation of this occurrence comes from traces of alteration products of uraninite still to be found near the floor of the quarry in this area. Well-formed zircon crystals, dark brown to creamy-gray in color and up to a centimeter and more in length, are associated with uraninite in several specimens of tremolite-serpentine rock from the Williams quarry.

The uraninite grains usually have a round shape, suggesting rounded cubic crystals, but some are highly irregular in shape. Some grains of the latter type have been fractured and broken apart by deformation. The grain size is from small specks up to a centimeter and more, with an average size of about 0.25 to 0.5 cm. The color is jet black in freshest appearing grains, but typically this grades into dark brown or reddish-bronze shades because of slight alteration effects. The luster is resinous. The freshest material is opaque, compact, and breaks with a conchoidal fracture. In a few cases where diopside or tremolite have been partly replaced by patchy irregular grains of uraninite, the latter has a finely granular character.

The majority of uraninite grains from the Williams quarry have been altered to secondary uranium-thorium minerals to a greater or lesser degree. Although these alteration minerals have to some extent distinctive colors, they tend to grade into one another indistinguishably. The two earliest-formed secondary minerals, Frondel's Mineral *C* (Frondel, 1956a) and thorogummite have darker colors, ranging from chocolate-brown and brownish-orange in Mineral *C* to yellow-brown or pale orange-yellow in thorogummite, and have a marked resinous luster. The later-formed ones, boltwoodite (Frondel, 1956b), uranophane, carnotite, and several as yet unidentified species, are various lighter shades of yellow or yellow-green and do not possess a resinous luster.

Mineral *C* and thorogummite have largely formed within or along the edges of grains of altered uraninite, thus are pseudomorphic after those uraninite grains. The next-formed minerals, boltwoodite and some uranophane, have formed around the edges of altered uraninite grains or up to a few inches away, either by replacement of tremolite or diopside, or as fillings of small openings and along fracture surfaces. The latest-formed minerals, including boltwoodite and most of the uranophane, have commonly migrated some distance (whether in terms of a few inches or many feet) away from the grain sites of the original genetically-related uraninite, having been carried in solution to their new sites where they have been deposited as thin coatings on fracture walls or on exposed surfaces.

The alteration of uraninite from the Williams quarry to its secondary pseudomorphic products has proceeded in various ways and to a variable degree. Commonly patchy spots, irregular central cores, or narrow outer rims of dark brown, orange-brown, or brownish-yellow material appear in the grains and stand out in sharp contrast to the blacker color of relatively unaltered uraninite. Or else the original uraninite may have vanished, except for tiny scattered specks of black material, with its place wholly taken by minerals of brown or yellow colors. Where alteration of uraninite grains has progressed all the way to brownish-yellow or pale yellow material, made up chiefly of thorogummite or of boltwoodite and uranophane, the grain shapes are highly irregular due to obvious deformational effects. Deformation is especially evident where such grains are enveloped by massive serpentine. Most of the unaltered uraninite and its grains of more regular shape are associated with coarsely prismatic diopside-tremolite material, which may have helped to protect these grains from the severest effects of deformation and the most penetrating attack by hydrothermal solutions.

The various alteration products of uraninite at the Williams quarry have been identified chiefly by optical properties and *x*-ray powder photographs. In refracted light the earlier-formed of these minerals appear to be minutely-grained aggregates. The mean or diagnostic index of refraction ranges from 1.78 to 1.80 for Mineral *C* and from 1.67 to 1.70 for thorogummite, and it is close to 1.670 for boltwoodite. The *x*-ray powder patterns for all three minerals are distinctive. Translucent reddish-bronze areas in several uraninite grains from the Williams quarry are isotropic and have an index of 1.84. This may be thorite, present as a very rare alteration product of high-thorian uraninite at this locality. In two specimens there are small irregular grains of a translucent red mineral with a high luster. It is isotropic and has an index of refraction of 1.94. After heating to 1000° C., a fragment of this red mineral gave the powder pattern of uraninite.

Color and luster aid in identification of these secondary minerals, especially when studied under the binocular microscope. Mineral *C* has a distinctive orange-brown or brownish-orange color when relatively pure, breaks with smooth conchoidal surfaces, and has a highly resinous luster. Thorogummite, which varies in color all the way from gray-white to yellow-brown but is most commonly a brownish-yellow at the Williams quarry, has a less-marked resinous luster and does not break to smooth conchoidal surfaces.

Where thorogummite grades into boltwoodite, the latter can be distinguished by its dull luster, rough-granular appearance, and a paler, more translucent yellow color. Boltwoodite also occurs as finely-fibrous material and as thin coatings on fracture surfaces. It is commonly closely associated with uranophane, and where the two minerals are intimately

---

FIG. 2. High-thorian uraninite from Williams quarry showing differential alteration as controlled by serpentinization. The five black grains are rounded and deformed cubic or cubo-octahedral crystals of uraninite. They are rimmed and spotted with yellow-brown or orange-brown thorogummite and surrounded by gray fibrous tremolite with minor serpentine. Two yellow shapes near bottom center represent uraninite cubes engulfed by massive gray serpentine and almost entirely altered to brown thorogummite and yellow boltwoodite and uranophane. ×1½. Photograph by B. M. Shaub.

FIG. 3. Secondary uranium minerals from Williams quarry associated with relic parting structures after diopside (light yellow areas with dark parallel lines). The structures were developed in diopside which first altered to fibrous tremolite. Parting planes were then infiltrated by dark-gray serpentine while intervening tremolite became replaced by yellow boltwoodite and uranophane derived from altered and destroyed uraninite close by. Gray-green serpentine surrounds the structures. ×1½. Photograph by B. M. Shaub.

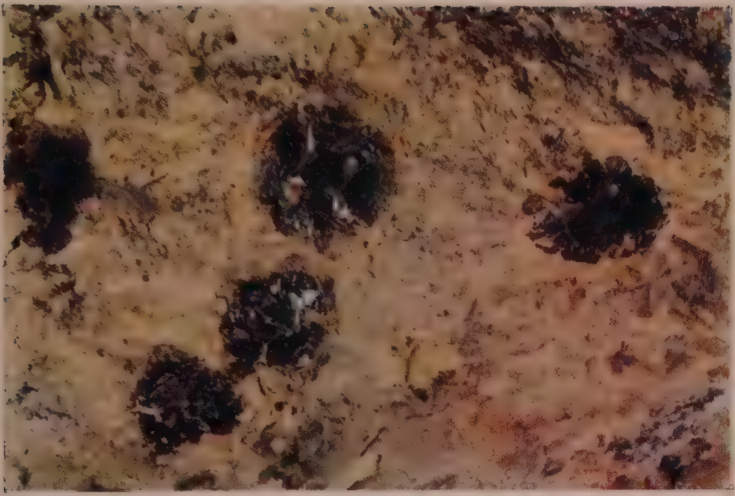

FIG. 2

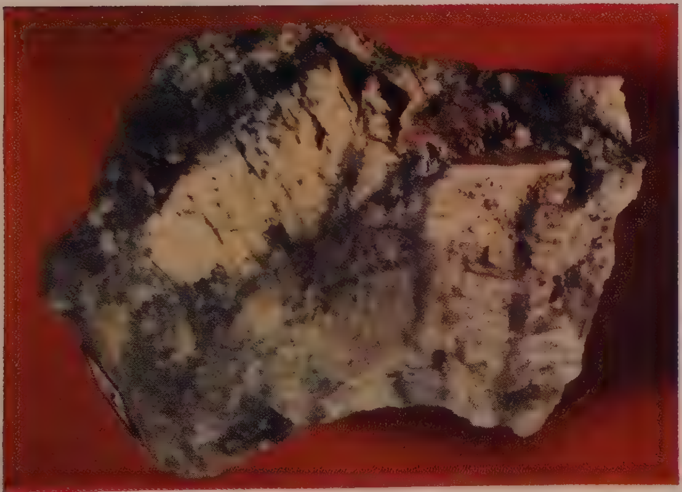

FIG. 3

mixed together as fibrous replacements of tremolite or diopside in the relic parting structures pseudomorphic after diopside, uranophane is more transparent and has a brighter lemon-yellow color than boltwoodite. Boltwoodite may be distinguished also by its rather weak yellowish fluorescence.

The later-formed secondary uranium minerals at the Williams quarry occur chiefly as thin fracture coatings or efflorescences on exposed surfaces. One of these minerals, found as a very rare coating of minute flakes of pale greenish-yellow color on phlogopite, fluoresces a bright yellow-green. Its high refractive index is 1.623 and it was first thought to be meta-autunite or uranocircite, but the *x*-ray powder photograph proves unidentifiable. A non-fluorescent mineral that occurs not uncommonly as yellowish fibrous or flaky coatings has been determined to be a new hydrous uranium silicate by mineralogists of the U. S. Geological Survey (S. Rubenstein and M. E. Staatz, personal communication). This mineral occurs with other secondary uranium minerals on the Colorado Plateau, as does boltwoodite. Carnotite occurs rarely as thin coatings of flaky aggregates with a distinctive yellow-green color. Uranophane occurs mostly as thin coatings of finely-fibrous character and pale-yellow to lemon-yellow color. An unusual occurrence of this mineral at the Williams quarry, found some years ago by John H. Bertrand, Jr., of Easton, shows tiny bright-yellow acicular crystals of uranophane intergrown with finely prismatic calcite and fibrous tremolite. The crystals are mostly aggregated in tiny prismatic bundles, but single crystals project into small cavities also. Among the specimens from the Williams quarry showing surface coatings of secondary yellowish or greenish-yellow uranium minerals, there may be additional species so far unidentified.

These alteration minerals of primary uraninite found at the Williams quarry are with one exception uranium-rich minerals with very little or no thorium present. The exception is thorogummite, which is high in thorium. It is likely that nearly all of the thorium once present in the primary high-thorian uraninite is preserved in thorogummite. Since in most cases studied Mineral *C* appears to have formed before thorogummite, it would suggest that once the primary uraninite had broken down to a secondary uranium-rich, thorium-poor mineral, the bulk of the thorium left over was used to make thorium-rich thorogummite.

Uraninite at the Royal Green Quarry

In the past several years a small number of specimens of high-thorian uraninite have been found in material excavated from the serpentine quarry of the Royal Green Marble Co. (hereafter called the Royal Green quarry). This actively working quarry is on the New Jersey side of the

Delaware River, about a mile northeast of the Williams quarry and two miles north of Phillipsburg, N. J. The discovery was made in 1952 by J. Kent Perry of White House Station, N. J., but nearly all of the specimens since found were collected by Clark C. McLean of Belvidere, N. J.

This uraninite occurs as black grains in massive apple-green serpentine, in much of which coarse scales of molybdenite and small pyrite cubes are abundant. The mineral is jet-black, massive and compact, and shows a conchoidal fracture. It is opaque and shows a weakly resinous luster on freshly broken surfaces. The grains vary in size from mere specks up to more than a centimeter across. Some grain shapes are highly irregular, but most of the larger ones possess a crudely squarish or rounded outline suggestive of cubic or cubo-octahedral crystals. One rounded crystal 0.5 cm. in size is a modified cubo-octahedron.

Some uraninite grains are cut across by narrow veinlets of fibrous calcite and tremolite; others have been fractured and somewhat deformed and broken apart. In no case are there any signs of alteration effects. A Th-U determination by the Berman *x*-ray fluorescence analyzer on a uraninite grain from this occurrence gave a contained Th/U ratio of 16%/32%. A partial chemical analysis of this specimen (T_{13}) by J. Ito confirms the Th/U ratio but reports higher Th and U. This composition is very slightly higher in Th with respect to U than in analyzed samples from the Williams quarry. The lack of alteration to secondary minerals in uraninite from the Royal Green quarry seems hardly due, therefore, to higher-thorium, lower-uranium content, but more reasonably reflects less drastic deformational effects and weaker attack by hydrothermal solutions than in the case of the altered uraninite from the Williams quarry.

The close association of uraninite at this locality with molybdenite, pyrite, and also minor sphalerite and galena is of interest. These minerals occur at the Williams quarry, but much less commonly and not in close association with uraninite. Since scales of molybdenite and aggregates of small pyrite cubes are found following grain boundaries between uraninite and the surrounding serpentine in several specimens from the Royal Green quarry, the formation of sulfides at this locality came after uraninite. Molybdenite occurs commonly in certain zones of serpentine rock at the Royal Green quarry where no traces of uraninite have been observed. A few well-formed zircon crystals of reddish-brown color and up to a length of 2 cms. are also found associated with uraninite from the Royal Green quarry. Because they formed as isolated crystals and have been partly fractured and broken apart as have uraninite crystals from this locality, they are believed to have been deposited contemporaneously with the uraninite.

URANINITE FROM THE SITE OF THE COLLEGE HILL RESERVOIR

Some years after his original discovery of uraninite at the Williams quarry, Gehman (1936) found a second occurrence of this mineral in material excavated from the site of the then-new College Hill reservoir and dumped along the banks of the Delaware River. It was already too late to examine the site of the occurrence, but Gehman managed to collect numerous excellent uraninite specimens from the excavated material. The rock proves to be similar in all respects to the typical serpentinized tremolite and dolomite rock found at the Williams quarry. The reservoir site is located on the south slope of Chestnut Hill about a half-mile west of the Williams quarry.

Nearly all of the specimens from this locality contain crude, but distinctly-formed uraninite crystals, ranging in size from about 0.25 cm. to 1 cm. Most crystals are simple cubes, but several are cubo-octahedrons. Two of the latter crystals show indistinct trapezohedral faces. The mineral is jet-black, opaque and compact, and exhibits a resinous luster on freshly broken surfaces. The occurrence is either in pale-green coarsely-prismatic tremolite, partly altered to greenish serpentine and grayish talc, or else in pale-pink to greenish-gray dolomite rock, specked with tiny white flakes of phlogopite and largely altered to olive-green serpentine and gray-white talc.

Many of the crystals have been fractured, deformed and broken apart. Powdery serpentine or talcose material thinly coats some of the broken crystal surfaces and surrounds crystal faces; in several cases this surrounding material has a reddish-brown color apparently due to staining by iron-oxide. In several specimens where the uraninite crystals are much fractured and broken apart and where the surrounding grayish matrix material is strongly talcose, the crystals show a partial alteration, especially on the outer surfaces, to a grayish or gray-brown, transluscent and highly resinous substance. Some reddish-brown limonitic staining spreads outward also from these altered crystals. The resinous alteration material proves to be thorogummite of distinctly different character from the yellowish thorogummite found in intimate association with secondary uranium minerals at the Williams quarry. This material varies from a highly-lustrous, colorless, transparent substance to translucent grayish material, and it merges indistinguishably into opaque black thorianite. The colorless, transparent material seems isotropic, with a refractive index of 1.693, but gives a sharp x-ray powder pattern of thorogummite. The grayish material is anisotropic, gives a sharp x-ray powder pattern of thorogummite, and has a variable index ranging from 1.67 to 1.70. In one specimen, thin outer zones of several thorianite crystals, which have altered to grayish thorogummite, are covered with tiny, crude, parallelorientated crystals. These crystals, suggestive of somewhat rounded tetragonal prisms terminated by the dipyramid, were probably originally crystallized thorite present on the outer surfaces of pseudomorphs of thorite after thorian uraninite, which have since altered to thorogummite.

No signs of secondary uranium-rich minerals have been observed in uraninite specimens from this locality. Determinations of Th-U content by the fluorescence analyzer on two of the freshest appearing uraninite crystals from the reservoir site show slightly higher Th and slightly lower U than found at the other two Easton localities. A partial chemical analysis of one of these specimens (T_{11}) by J. Ito confirms the Th/U ratio but reports higher Th and U. This is not enough of a difference in composition to explain the lack of alteration to secondary uranium-rich minerals at the reservoir site. The slight partial alteration of uraninite to grayish thorogummite found here in connection with strongly fractured uraninite crystals and a talcose matrix, indicates that shearing forces may have affected these crystals only during very late stages of hydrothermal mineralization when temperatures were low and talc was being formed from sheared serpentine rocks.

High Thorium Content of Easton Uraninite

Table 2 lists the U-Th compositions and percentage ratios for a number of uraninite and thorianite specimens from Easton and elsewhere. The cell dimensions are also given for these samples, wherever possible, calculated from spacings between the 311 lines in the corresponding *x*-ray powder photographs. In general there is rough agreement between increasing cell size in these samples and increasing Th content; but when the samples are plotted on a graph using cell size and Th/U percentage ratios as the coordinates, the points do not fall on the virtually straight-line curve relationship which exists between ThO_2 and UO_2 in artificial material. The discrepancy is largely due to the variable state of oxidation of uranium in these samples. It is possible, nevertheless, to plot a steeper curve through these points, which could prove a useful guide in correlating between Th content and cell dimensions in samples of thorian uraninite or uranoan thorianite, subject to variability in the amounts and kinds of other elements present, in the radioactive decay, and in the oxidation of uranium.

Despite the variability in Th/U content found in Easton uraninite, six of the seven samples analyzed in this study contain from about 15% to 35% of ThO_2. This is a high thorium content for uraninite, and the Easton mineral is noteworthy in occupying compositionally a portion of the wide central gap thought to exist between natural uraninite and thorianite.

TABLE 2. U-Th CONTENT AND CELL DIMENSIONS OF URANINITE AND THORIANITE

		X-ray fluorescence analysis	X-ray fluorescence analysis	Chemical analysis	Cell dimensions (in Å)
		% present (approx.) U:Th	% ratio (to 100%) U:Th	% ratio (to 100%) U:Th	calculated from x-ray powder photographs
	uraninite, Mi Vida, Utah			100: 0[1]	5.42
T_4	uraninite, Williams quarry	46: 7	86:14	86:14[2]	5.44
T_3	uraninite, Williams quarry	39:12.5	76:24		5.44
T_{26}	uraninite, Williams quarry	42:16	72:28		5.51
T_5	uraninite, Williams quarry	41:17	71:29		5.46
T_{13}	uraninite, Royal Green quarry	32:16	66:34	67:33[2]	5.50
T_2	uraninite, reservoir site	32:22	59:41		5.50
T_{11}	uraninite, reservoir site	29:22	57:43	54:46[2]	5.53
T_{12}	thorianite, Betroka, Madagascar			5:95[3]	5.60

[1] As generally reported for this locality.

[2] Jun Ito analyst, Mineralogy Department, Harvard University.

[3] As given for this locality in Dana's *System* (1944, **1**, p. 621).

Even the freshest uraninite found at the three Easton localities occurs in serpentinized rock, thus must have been exposed to some attack by serpentinizing hydrothermal solutions. Thorianite, in contrast to the marked alteration behavior characteristic of uraninite, does not break down readily to secondary minerals. It is likely that high-thorian uraninite, of the type found at all three Easton occurrences, yields less readily to secondary alteration than low-thorian or non-thorian uraninite.

ORIGIN OF EASTON URANINITE

The origin of the high-thorian uraninite occurring in serpentine near Easton is bound up ultimately with a granitic magma which during Precambrian time intruded rocks now widely exposed over east-central Pennsylvania and west-central and northwestern New Jersey. The pegmatite end-products of this magma are characterized geochemically by the common presence of minerals carrying zirconium, rare earths, and thorium and uranium.

Coarsely crystallized allanite and zircon, usually in close association with granite pegmatite, have been reported from numerous localities in the Precambrian crystalline rocks of east-central Pennsylvania and west-central and northwestern New Jersey. Recently rich deposits of uranoan thorite, monazite and zircon, of likely hydrothermal origin and closely associated with granite pegmatite, have been found near Chester, New Jersey (New Jersey State geologist, personal communication). Allanite occurs sparingly in coarse pegmatite collected from near the Williams quarry. Tiny zircon crystals are abundant in pegmatite stringers cutting Pochuck amphibolite a half-mile south of the Royal Green quarry.

The U and Th present in such granitic magma probably were used up in the normal case by dispersal in trace amounts throughout the crystal structures of accessory allanite and zircon formed in its intrusive bodies of granite. In the abnormal case where this magma was subjected to powerful deformational forces during crystallization following pegmatitic intrusion of dolomitic limestone, its U, Th, and also Zr, became free for transport into the intruded, strongly-sheared and highly permeable rocks by squeezed-off hydrothermal solutions which concentrated them in those rocks as contact-metasomatic crystals of Th-rich uraninite and of zircon.

Conclusions

Seven *x*-ray fluorescence analyses (supported in three cases by chemical analyses, see Table 2) of typical specimens of the primary thorium-uranium mineral from three occurrences in serpentine near Easton, Pa., show this mineral to be high-thorian uraninite rather than high-uranoan thorianite as formerly supposed. In six of the analyzed specimens the ThO_2 content ranges from about 15% to 35%, a high thorium content for naturally occurring uraninite.

Although specimens of high-thorian uraninite and its secondary minerals from the Williams quarry present a complex problem in paragenetic relationships, field and laboratory study reveal a reasonable and orderly sequence of mineralogical changes. (1) Cubic or cubo-octahedral crystals of uraninite first formed by replacement of diopside or dolomite during early hydrothermal mineralization. (2) Where these crystals became exposed to long-continued attack by silica-bearing hydrothermal solutions, they were partly or wholly altered to the first-formed brownish-orange secondary product, Mineral *C*, and then to lighter-colored brownish-yellow thorogummite chiefly around the outer edges of the altered grains. (3) The formation of lighter-yellow boltwoodite and uranophane came only after deformation had affected the altered thorianite grains and, by fracturing of the surrounding minerals, had opened the way for thorough penetration by hydrothermal solutions which strongly serpentinized much of the matrix material. These penetrating solutions made it possible for boltwoodite and uranophane to move outward from the edges of the altered and deformed uraninite grains, finding their way especially, through replacement of diopside or tremolite, into certain of the near-by relic parting structures pseudomorphic after diopside. (4) More recent near-surface attack by ground-water solutions dissolved uranium from the earlier-formed secondary uranium-thorium minerals, carried it some distance away, and redeposited it in the form of fracture coatings of pale yellow and yellow-green secondary uranium minerals that represent the final alteration products of the primary uraninite.

High-thorian uraninite from the reservoir site has altered in small part to gray thorogummite, or thorite later replaced by thorogummite. Strong fracturing promoted this alteration, but the absence of secondary uranium-rich minerals seems due to an attack chiefly by very late talc-forming hydrothermal solutions at lower temperatures than those prevailing during the hydrothermal alteration of uraninite from the Williams quarry.

High-thorian uraninite from the Royal Green quarry is found unaltered, despite exposure to serpentinizing solutions. Possibly pre-serpentine fracturing here was not sufficiently severe to expose this uraninite to a long-continued, penetrating hydrothermal attack.

It is concluded that because of its high thorium content none of the Easton uraninite alters readily to secondary minerals. Alteration to the earlier-formed secondary minerals has only occurred under exceptionally drastic, localized conditions of fracturing and concomitant attack by silica-bearing hydrothermal solutions. This alteration is known to have been hydrothermal rather than supergene, because it can be traced step by step through elucidation of the whole sequence of hydrothermally-imposed contact-metasomatic changes which affected the minerals of the associated serpentine deposits and to which the early-stage alteration of the high-thorian uraninite is inseparably linked.

The origin of the high-thorian uraninite found near Easton lies in a granite-pegmatite magma rich in thorium and uranium. This magma first intruded and thermally metamorphosed dolomitic limestones, then while subjected to powerful deformation during crystallization, yielded the rare-element- and silica-bearing hydrothermal solutions that penetrated the more permeable intruded rocks, deposited uraninite and zircon in them, and later serpentinized them on an extensive scale.

References

Bayley, W. S. (1941), Pre-Cambrian geology and mineral resources of the Delaware Water Gap and Easton Quadrangles, New Jersey and Pennsylvania: *U. S. Geol. Survey*, Bull. **920**, 8–53.

Frondel, C. (1953), Hydroxyl substitution in thorite and zircon: *Am. Mineral.*, **38,** 1007–1018.

Frondel, C. (1956a), Mineral composition of gummite: *Am. Mineral.*, **41,** 539–568.

Frondel, C. (1956b), Boltwoodite, a new uranium silicate: *Science,* **124,** 931.

Gehman, G. W. (1936), Some minerals of the Serpentine Range near Easton, Pa.: *Rocks and Minerals*, **11,** 90–91.

Miller, B. L. (1939), Northampton County, Pennsylvania: *Pa. Geol. Survey, 4th Ser., Bull.* **C48,** 159–203, 435–466.

Montgomery, A. (1955), Paragenesis of the serpentine-talc deposits near Easton, Pa.: *Pa. Acad. Sci. Proc.*, **29,** 203–215.

Peck, F. B. (1905), The talc deposits of Phillipsburg, N. J., and Easton, Pa.: *N. J. Geol. Survey*, Ann. Report, 1904, Pt. 3, 163–185.

Wells, R. C., Fairchild, J. G. and Ross, C. S. (1933), Thorianite from Easton, Pa.: *Am. Jour. Sci.*, 5th Ser., **26,** 45–54.

THE AMERICAN MINERALOGIST, VOL. 42, NOVEMBER-DECEMBER 1957

THE SILICA BUDGET IN THE SEDIMENTARY CYCLE*

RAYMOND SIEVER, *Harvard University, Cambridge, Massachusetts.*

ABSTRACT

The source, transportation, and precipitation of silica in solution on and near the earth's surface are evaluated to arrive at the silica budget in sediments. The forms of silica stable at low temperatures and their solubilities are summarized. The primary source of silica in solution is the chemical weathering of silicate minerals formed at high temperatures and/or pressures. Formation and alteration of clay minerals in soils and hot springs are other sources. Marine diagenesis of clays probably does not contribute much silica to solution. The major source of soluble silica in the early diagenesis of sediments is the dissolution of the remains of siliceous organisms. Solution of silica in deeply buried rocks is related to the pressure and temperature coefficients of solubility. Most natural waters are undersaturated with respect to amorphous silica and much of the ocean is undersaturated with respect to quartz. Hot spring and some soil waters may be supersaturated and inorganically precipitate silica, but the major mechanism for the precipitation of silica on the surface of the earth is biochemical. It is the diatoms, radiolaria, and other silica secreting organisms that are responsible for extracting silica from the sea. Crystalline quartz is precipitated from deep formation waters, given enough time. The silica cycle starts with the weathering of silicate minerals, goes through the stages of transportation and precipitation and, via metamorphism, comes back to reconstituted silicate minerals. The silica cycle in the past is discussed with reference to the development of the silica-secreting organisms and the conclusion is reached that since the beginning of the Paleozoic, and perhaps earlier, the silica cycle operated much as today.

INTRODUCTION

It is the purpose of this paper to discuss the sources, transportation, and precipitation of silica at or near the surface of the earth's crust in relation to the polymorphic forms of silica found in ancient and modern sediments. The discussion will not treat questions of silica movement, concentration, and precipitation involved in metamorphic or igneous processes other than to note that these processes are involved in the total cycle of silica in the crust.

Much of the material discussed here is built on modern chemical and crystal chemical ideas on the forms of solid and colloidal silica, the types of dissolved species in aqueous solutions, and the equilibria between solid and dissolved species at low temperatures and pressures, summarized most recently by Iler (1955). The application of these concepts to geologic situations has been covered in part by two recent papers (Krauskopf, 1956; White, Brannock, and Murata, 1956).

---

* Work done during the tenure of a National Science Foundation Senior Post-Doctoral Fellowship at Harvard University during 1956–57. I am indebted to R. M. Garrels for many stimulating discussions of the problems involved in silica geochemistry and for critically reviewing the manuscript. I have also had the benefit of discussions with C. Frondel and C. S. Hurlbut, Jr. on some aspects of the structure of the silica minerals, and W. F. Bradley on aspects of clay mineralogy.

FORMS OF SOLID SILICA

Crystalline

It is necessary to briefly summarize our present knowledge of the various forms of solid silica that are germane to this discussion and are of geological significance. The crystalline modification of SiO_2 that is stable at low temperatures and pressures, α-quartz, is the most abundant single mineral in sediments. As a detrital mineral it is present as the product of the mechanical weathering of quartzose igneous, metamorphic, and sedimentary rocks; its dominance as a detrital mineral is largely the result of its physical properties: hardness and lack of cleavage, and its chemical properties: extremely low solubility in water and non-reactivity. Quartz is also ubiquitous as a chemically precipitated constituent of sedimentary rocks; it has been observed as secondary overgrowths on detrital quartz grains, as pore fillings, as authigenic euhedra in carbonate rocks, as replacements of carbonate structures such as oolites, and as the essential constituent, as microcrystals, of many cherts and other siliceous sediments.

The crystalline silica polymorphs that are stable at higher temperatures and pressures (β-quartz, tridymite, cristobalite, coesite) are not of much interest in the consideration of normal sediments except insofar as some of these minerals do occur geologically and may be a minor source of silica in solid or dissolved form.

Chert

Some controversy has existed over the nature of the silica in chert, one of the most common siliceous rocks. There seems to be little doubt that microcrystalline quartz is present in most cherts. This conclusion is based on petrographic evidence (Pettijohn, 1956, p. 437–8) and *x*-ray diffraction patterns (Midgley, 1951; Folk and Weaver, 1952). The question at issue is whether chalcedony consists only of fibers of quartz, or as others have concluded (Sosman, 1927; Correns and Nagelschmidt, 1933; Donnay, 1936), of a mixture of fibrous quartz and amorphous silica. It is probable that the *x*-ray diffraction evidence on this point is inconclusive, for crystalline quartz has a high *x*-ray scattering efficiency and amorphous silica scatters *x*-rays very poorly; in a mixture of the two, where the quartz may be of extremely fine size, it is probably impossible to distinguish the broad, low intensity scattering maximum of amorphous silica unless it is present in amounts over 10–15%. Perhaps more refined techniques, such as the analysis of low-angle scattering, will help to distinguish the two forms of silica.

In a recent paper, Pelto (1956) sought to elucidate the structure of chalcedony and tried to explain its reactivity with alkalies (known from studies of concrete) in terms of composition and structure. Pelto drew an analogy between the chalcedony structure and the behavior of grain boundaries in metals and came to the conclusion that the properties could be explained by islands of poor fit, or dislocations, between subparallel bundles of quartz fibers. The reactivity with alkalies during the setting of concretes and solubility larger than that of quartz was explained as the result of the distortion at and around the dislocations.

Because of the finely crystalline state of the quartz in chert, and the highly variable amount of porosity (internal surface) between adjacent microcrystals or fibers, chert may have not only appreciably different mechanical abrasion characteristics from quartz but, insofar as solubility is affected by grain size, may have variable solubilities in water that are higher than quartz. Obviously, if there is interstitial amorphous silica in chalcedony, the solubility will be higher. The writer is not aware of accurate solubility measurements of cherts other than that by Pelto (1956), who immersed chalcedony in water at 95° C. for seventeen hours and observed solution of 51 p.p.m. It is likely, in the light of the known difficulty of attaining equilibrium between silica and water at low temperatures in a short time (Alexander, Heston, and Iler, 1954; Kennedy, 1950) that this time was inadequate for equilibrium to be attained.

Opal

Opal, or opaline silica, is a disordered hydrated form of silica whose properties are markedly different from the ordered crystalline quartz polymorphs. It appears to be a form of amorphous silica, more or less hydrated, that has formed from the partial dehydration and solidification of a silica gel. Opal is of some geologic significance in sediments both as a possible product of weathering in some soils, as an alteration product of volcanic ash (Frye and Swineford, 1946) and as a precipitate (opaline sinters) deposited from thermal spring waters (White, Brannock, and Murata, 1956). However, in terms of its abundance in surface and near surface rocks exposed to weathering, and as a constituent of sediments, it is relatively unimportant.

Amorphous Silica

Amorphous silica is a term used to describe materials whose composition is relatively pure SiO_2 that are in the mesomorphous state, that is, have only a transitory crystallographic order, such as that found in some liquids, and do not show the definite periodicity of atomic or ionic arrangement characteristic of crystalline solids. It is probably most nearly accurate, in the structural sense, to refer to amorphous silica as a disordered association of cristobalite crystallites of a size very little larger than one unit cell and therefore not properly designated as crystalline cristobalite (Warren and Biscoe, 1938). As a result of the extremely small size of the particles and the disordered arrangement, some of its physical and chemical properties are different from either quartz or cristobalite.

Under the classification of amorphous silica are included all of the various kinds of hydrated and dehydrated silica gels, silica glass, siliceous sinters, powders from the condensation of vapor phases, and, of greater geological importance, the skeletal materials of many silica-secreting organisms, such as diatoms, radiolaria, and siliceous sponges.

SOLUBILITIES IN AQUEOUS SOLUTIONS

Amorphous Silica

The metastable equilibrium solubilities of various kinds of amorphous silicas have been extensively investigated, most recently by Alexander, Heston, and Iler (1954) and Krauskopf (1956). The essential facts seem to be that all forms of amorphous silica have an equilibrium solubility in the range 120–140 p.p.m., and that opal may be slightly lower, about 100 p.p.m. The solubility is essentially independent of pH at pH values below about 9, and the dominant species in near-neutral and acid solutions, as measured by lowering of freezing point determinations (Weitz, Franck, and Schuchard, 1950) and diffusion rates (Jander and Jahr, 1934), is monomeric silicic acid, H_4SiO_4. In dilute solutions H_4SiO_4 is probably hydrated, with one layer of water molecules surrounding the $Si(OH)_4$ tetrahedra (Iler and Dalton, 1956). At pH of 9.8 and higher, H_4SiO_4 becomes dissociated to a significant extent (Roller and Ervin, 1940), the solubility increases greatly, and various other species in solution appear, such as silicate ions, and dimeric and higher polymeric forms of silicic acid (Iler, 1955, pp. 20–25). In the following discussions 140 p.p.m. will be used as the figure for the equilibrium solubility of all forms of amorphous silica at 25° C. in pure water, recognizing that it is not a precise figure. Krauskopf (1956) found that there were no significant differences in silica solubility between pure water and sea water.

Quartz

The solubility of quartz is much lower than that of amorphous silica. The precise determination of the equilibrium solubility of quartz at room temperatures has not yet been made, although figures varying from 6 p.p.m. (Gardner, 1938) to 30 p.p.m. (Lenher, 1921) have been reported. The laboratory determination of quartz solubility at low temperatures is difficult because of the long times necessary to achieve equilibrium and the necessity for eliminating traces of certain metals, notably aluminum, and fluoride ion from the system. However, there is a way to estimate quartz solubility from known thermodynamic quantities.

We will assume, following the discussion of amorphous silica solubility above, that the only dissolved species in pure water in equilibrium with quartz at 25° C. and at pH below 9, is monomeric, undissociated silicic acid. Then the reaction of interest is

(1) $2H_2O_{(liq.)} + SiO_{2(qtz.)}{}^{298.16^\circ K}\cdot H_4SiO_{4(aq.)}$.

If we know the standard free energy of formation of all of the reactants and products in this equation we can calculate the change in standard free energy of the reaction, and so the solubility. We know the ΔFf° of water and of quartz, but not of silicic acid. The latter, however, can be estimated from the reaction

(2) $2H_2O_{(liq.)} + SiO_{2(vitreous)}{}^{298.16^\circ K}\cdot H_4SiO_{4(aq.)}$.

For reaction (2) we do not know the ΔFf° of H_4SiO_4 either, but the free energy of the reaction can be calculated from the known equilibrium solubility of amorphous silica, 140 p.p.m., and thus the ΔFf° of H_4SiO_4. For reaction (2) we write

(3) $\frac{(H_4SiO_4)}{(H_2O)^2(SiO_2)} = K_{eq.}$ where ( ) indicates activity ("Thermodynamic concentration").

In such dilute solutions at atmospheric pressure the activity of solid silica and water can be taken as unity, and thus:

(4) $K_{eq} = (H_4SiO_4)$.

In very dilute solutions and considering the H_4SiO_4 is essentially undissociated at pH values lower than 9, we are justified in writing:

(5) $K_{eq} = (H_4SiO_4) = [H_4SiO_4]$, where [ ] indicates concentration in moles/li.

Then, knowing $[H_4SiO_4]$ from the solubility of silica, 140 p.p.m. SiO_2, we use the relation:

(6) $\Delta F^\circ_{(reaction)} = -RT \ln K$.

We thus calculate $\Delta F^\circ_{(reaction)}$ for (2) to be 3.6 kcal./mole. Substituting in the relation:

(7) $\Delta F^\circ_{(reaction)} = \sum Ff^\circ_{(products)} - \sum Ff^\circ_{(reactants)}$

we get

$$3.6 = \Delta Ff^\circ_{(H_4SiO_4)} - (-2 \times 56.7 - 190.9)$$
$$\Delta Ff^\circ_{(H_4SiO_4)} = -300.7 \text{ kcal./mole.}$$

(Free energy data from Latimer, 1952.)

With this estimate for the standard free energy of formation of H_4SiO_4, we now return to reaction (1), and, using relation (7), get $\Delta F^\circ_{(reaction)} = 5.1$ kcal. Using equation (6) we calculate K_{eq}. to be $10^{-3.64}$

$=[H_4SiO_4]$. Multiplying by the molecular weight of SiO_2 we get the equilibrium solubility, approximately 14 p.p.m. SiO_2.

An alternative method for the estimation of $\Delta Ff^\circ_{H_4SiO_4}$ is to use the ΔFf° value of $H_2SiO_{3(\text{``crystalline''})}$ given by Latimer (1952), −244.5 kcal., and assume that the free energy of hydration to make H_4SiO_4 by adding one molecule of water is negligible. Thus

$$(8)\quad \Delta Ff^\circ_{(H_4SiO_4)} = \Delta Ff^\circ_{(H_2SiO_3)} + \Delta Ff^\circ_{(H_2O)} = -244.5 + (-55.7) = 300.19 \text{ kcal./mole.}$$

From this value we may calculate the solubility of quartz in the same way as above to get 7.25 p.p.m., a figure which checks more closely with the figure of 6 p.p.m. given by Gardner (1938) and Kennedy (as quoted by Krauskopf, 1956).

It will be seen that the difference between 7.25 p.p.m. and 14 p.p.m. is dependent only on the difference between the two values for $\Delta Ff^\circ_{(H_4SiO_4)}$, −300.7 and −300.19 kcal. As Garrels (1957) has emphasized, precise solubility calculations can be made only from extremely accurate values for the appropriate thermodynamic quantities. In spite of this, however, both values, 7.25 and 14 p.p.m., are of the same order of magnitude and give us some notion as to the low solubility of quartz relative to amorphous silica.

Rates of Reaction

The attainment of equilibrium with water is a slow process for amorphous silica but can demonstrably be achieved in the laboratory (Alexander, Heston, and Iler, 1954; Krauskopf, 1956). The rate of attainment is strongly influenced by particle size, type of material (gel, powder, or other), pH, and in supersaturated solutions, by the extent of supersaturation. The rate of attainment of equilibrium in the quartz-water system at room temperature has not been measured but must be very much slower than for amorphous silica.

At room temperatures and atmospheric pressure, amorphous silica is metastable with respect to quartz, the thermodynamically stable modification of SiO_2. However, in all cases, the precipitate formed from supersaturated solutions at low temperatures is amorphous silica rather than quartz (Iler, 1955, p. 15). Solutions undersaturated with respect to amorphous silica (<140 p.p.m.) but supersaturated with respect to quartz are stable over a period of years. The studies of the synthesis of quartz crystals have shown that clear crystalline quartz, by methods so far known, cannot be formed directly from solution at anywhere near room temperatures and atmospheric pressure (Buehler and Walker, 1949; Corwin, et al, 1953). The difficulty experienced in precipitating crystalline quartz at low temperatures and pressures in the laboratory as contrasted with the obvious ease with which nature accomplishes the synthesis may be related to several different factors. Perhaps the most important need that is absent in the laboratory is sufficient time; the rate of attainment of equilibrium in the quartz-water system at low temperatures may be so slow that several thousand years may be needed to either precipitate or convert amorphous silica to quartz.

Another factor is the relative structural complexities of the various forms of solid SiO_2. Applying Ostwald's rule, or the amplification and extension of it as a "simplexity" principle by Goldsmith (1953), one may characterize amorphous silica as a close relative to the cristobalite structure, the high temperature phase that is formed more easily than the low temperature, more complex structure, quartz. On the other hand, Buerger (1935, 1954) has pointed out that the high temperature silica polymorphs may be stable by virtue of the stuffing of their more open structures by impurity cations that balance valence deficiencies produced by substitution of small amounts of Al for Si. The more close-packed quartz structure cannot accommodate these impurities and presumably any inversion from high to low temperature forms must be accompanied by expulsion of impurities.

Ionic Strength

There is little effect of ionic strength of aqueous solutions on the solubility of amorphous silica (Krauskopf, 1936), at least insofar as salt concentrations of the order of magnitude of sea water are concerned. This might be expected on the basis that monomeric silicic acid is essentially undissociated at pH lower than 9, thus electrically neutral and unaffected by the distribution of ionic charges in the solution. Solutions of high ionic strength, however, may have an effect on the solubility at high pH, where silicate ions are present, and where the activity of water is lowered significantly.

It is of interest that the amorphous silica of diatom tests is less soluble (or dissolves more slowly) than inorganic silicas. This may be because the organisms complex the silica with aluminum or other cations, such complexes being extremely insoluble (Iler, 1955, p. 16).

Sources of Silica in Solution

Weathering of Silicates

The primary source of silica in solution on the surface of the earth is the chemical weathering of silicate minerals. In the chemical degradation of these minerals by water solutions, varying amounts of SiO_2 are contributed at varying rates, depending on climate, relief, and the nature of the original material. We are probably justified in assuming from laboratory experiments that in most geological conditions, where the pH is less than 9.5, the silica in solution is dominantly undissociated H_4SiO_4. This may be an oversimplification, however, for it has been established that wollastonite treated with acid gives soluble polysilicic acids rather than monomeric (Weitz, Franck, and Schuchard, 1950) and Murata (1946) has pointed out that in aluminosilicates with a high Si:Al ratio there may remain a silica network after Al has been removed by acid. But it is probable that such open silica networks are appreciably soluble (to give monomeric silicic acid) and that eventually the polysilicic acids formed from solutions of metasilicates such as wollastonite, and other silicates in very alkaline waters will depolymerize in near-neutral or slightly acid stream waters to give monomeric H_4SiO_4.

The silicate minerals of igneous and metamorphic origin, feldspars, amphiboles, pyroxenes, etc., that break down rather rapidly under many soil forming conditions may be expected to supply the greatest proportion of H_4SiO_4. Quartz from igneous and metamorphic rocks and from quartzose sediments, considering its low solubility and slow rate of solution, probably supplies a less significant amount.

Weathering of Clays

The weathering of clay minerals may or may not yield free silica to solutions. For example, the alteration of an illitic (micaceous) clay that has the approximate composition and structure of muscovite, to kaolinite, does not yield silica, for, despite the different arrangement of Al and Si in the two structures, the stoichiometric proportions of Al:Si in the two minerals are the same. But if, under extreme weathering conditions, kaolinite alters to gibbsite (bauxite), we may expect large quantities of silica to be contributed to solution. On the other hand it may be possible for an illitic clay to weather to montmorillonite. If the montmorillonite that is formed by this alteration is one in which there is very little substitution of Al for Si in the tetrahedral layer, there will be an addition of silica to the clay, the silica being withdrawn from available solutions. Thus this transformation would be a net reducer of the quantity of silica in solution. But if the "montmorillonite" formed from weathering of mica has the tetrahedral composition of the original mica, a more probable situation,* there would be no net change in silica.

Thermal Springs

Another source of silica in solution at the surface is from thermal spring waters (see White, Brannock, and Murata, 1956). Although the absolute amount of silica in these waters is small compared with the total contribution from all surface waters, the concentration of H_4SiO_4 in thermal waters may be quite high. White and co-workers have shown that as these waters suddenly cool at the surface they become supersaturated and precipitate siliceous and opaline sinters; the remaining saturated silica solutions then merge with the general run-off of the region.

---

* W. F. Bradley, personal communication.

Marine Alteration of Clays

The marine alteration of some clay minerals that has been postulated to explain the distribution and occurrence of clay minerals in modern sediments (Grim, Dietz, and Bradley, 1949; Millot, 1949; Grim, 1953; Grim and Bradley, 1955) may be a source of silica in solution. The same considerations discussed above with reference to the weathering of clay minerals apply here. Alteration of kaolinite to illite, if such a reaction does actually occur, would involve no net change in silica. But if there is appreciable alteration of montmorillonite to illite and/or chloritic clay minerals there should be a net loss of silica in the solids, the excess presumably going into solution, at least temporarily. However, it has not yet been generally accepted that such changes in clay composition as a result of marine diagenesis (or penecontemporaneous alteration) involve any part of the structures other than cation-exchange positions (Grim and Bradley, 1955) and it is change in composition of the tetrahedral layers that affects the silica contribution. It may be that these layers are inherited intact from the source areas and it is only in the milieu of subaerial weathering that clay minerals can be a source of silica.

Water of Compaction

Johnson (1920) has suggested a source for the silica secondarily precipitated in sediments in the squeezing out of water from shales during the compaction process. This squeezing out process will give silica in solution only if the original interstitial water contained much silica in solution. Silica in solution in interstitial waters, neglecting for the moment biochemical factors, can originate from one of several sources. One possibility is from the alteration of clay minerals; as we have seen in the discussion above, this seems unlikely. Another source is the dissolution of extremely fine-grained quartz that is often found in shales. Iler (1955, p. 9) has calculated quartz solubility as a function of particle size and found that the solubility starts increasing only when sizes as fine as 10 millimicrons are approached. The question is, then, do muds and shales contain quartz particles of this size? It is known that the <0.1 micron size fraction prepared by settling of suspensions of many modern and ancient sediments normally contain practically all clay minerals and no quartz, as estimated by *x*-ray diffraction methods. Now, one might argue that such fine quartz particles are not there because they have already dissolved. But is it not much more probable that these extremely fine sizes of quartz were dissolved in the transporting waters before the detritus ever reached the depositional site? One final possibility is that temperatures attendant on burial and compaction are high enough to dissolve large amounts of silica. But Kennedy (1950) showed that below 140° C. quartz solubility remains very low and it is unlikely that temperatures above 100° C. would be reached before the shale was almost completely compacted and most of the water squeezed out. Therefore it seems that waters of compaction would not ordinarily contain more dissolved silica than the original entrapped sedimentation water.*

Biochemical

One of the major sources of silica in solution in the early diagenesis of sediments is the dissolution of siliceous organisms such as diatoms, radiolaria, and siliceous sponges. These materials are essentially amorphous or opaline silica and have a solubility of about 140 p.p.m. Bruevich (1953), Bezruhkov (1955), and Lisitsyn (1955) measured relatively high concentrations of dissolved silica in the interstitial waters of the bottom sediments of the Bering Sea and observed corroded and partially dissolved diatom shells in the sediments. Emery and Rittenberg (1952) noted concentrations of silica in interstitial waters in California basin sediments that are much higher than in the overlying sea water. The silica-secreting population can extract huge quantities of silica from sea water and, during life, can protect their siliceous parts from dissolving in sea water, which is undersaturated with respect to amorphous silica. Some time after death and the cessation of metabolic processes that protect the silica tests from dissolution, the tests slowly dissolve in the undersaturated solutions around them. This mechanism undoubtedly accounts for a large part of the silica in solution in the interstitial waters of modern sediments.

Diagenesis

The solution of quartz at depth during diagenesis of sediments may be a source of much of the silica in solution in deep underground waters, as proposed some years ago by Waldschmidt (1941).† More recently Heald (1956) has offered excellent petrographic evidence that there has been interpenetration and solution of quartz grains in a quartz-cemented sandstone, and suggested that it is the pressure of overburden borne on grain-to-grain contacts that is responsible and called such effects the result of "pressure solution." The work of Taylor (1950), relating increasing interpenetration of quartz grains to depth of burial, would seem to corrobrate this explanation. Kennedy (1950) has shown quantitatively how quartz solubility increases with temperature. To the extent that very deep burial is tied to increase in temperature due to the geothermal gradient, solution effects due to temperature should become appreciable at depths of over 10,000 feet. At shallower depths one would not expect the temperature effect to be great. The pressure effect at relatively low temperatures on the solubility of quartz that Heald (1956) inferred from petrographic evidence has not yet been adequately investigated in the laboratory, although Maxwell and Verrall (1954) suggested that temperature is more important than pressure for silica solution and precipitation. It may be that quartz solution effects observed in rocks that have never been deeply buried is to be correlated with the chemical nature of the formation waters. Walker (1957), for example, believes that quartz replaced by carbonate minerals may supply a great deal of the silica precipitated as cement.

---

* A recent article that has just come to my attention (Fothergill, 1955) suggests that there may be a mechanism involving the compacting muds behaving as a dialytic membrane and concentrating, among other dissolved species, silica.

† See Pettijohn, 1957, pp. 656–659 for an excellent summary of silica cementation.

Concentrations of Dissolved Silica in Surface and Formation Waters

It now remains to discuss the concentrations of silica in solution in natural waters to evaluate the possibilities of inorganic precipitation of quartz or amorphous silica from saturated or supersaturated solutions. Most of the data in this section are taken from Clarke (1924). The following discussion is predicated on the assumption that in most natural waters, the pH is below 9.8 and that, as a result, the dominant species in solution is undissociated H_4SiO_4 and the equilibrium solubility is approximately that measured in the laboratory. As the solubility of amorphous silica is about 140 p.p.m. at 25° C., no inorganic precipitation of any variety of amorphous silica can occur at concentrations below this value. Conceivably, crystalline quartz could inorganically precipitate from any solution with more than 6–8 p.p.m. SiO_2, given enough time and the optimum conditions (whatever they may be at low temperatures). But there is no clearcut observational evidence to show that crystalline quartz is in fact being inorganically precipitated anywhere from surface waters and this taken together with the practical impossibility of precipitating quartz in the laboratory at room temperatures makes this possibility unlikely.

Soil Waters

It is rather difficult to get a clear picture of the amount of dissolved silica in soil waters; this is mainly due to the lack of good chemical analyses of soil waters but also due to the difficulty of sampling of soil waters and interpreting the validity of the samples. Obviously, however, the concentration of silica will depend on the extent of chemical weathering, with all that that term implies in relation to climate, topography, bedrock character, and maturity of soil development, and also the amount of water passing through the soil. All one can say at the present is that a few analyses show solutions which are undersaturated with respect to amorphous silica (Mohr and Van Baren, 1954). The great amount of silica released in the extensive weathering and breakdown of silicate minerals in lateritic and bauxitic tropical soils probably leads to much higher silica concentrations than might be found in more temperate podzol, rendzina, and tchernozem soils. Indeed, the presence of amorphous silica veinlets and nodules in laterites must be taken as evidence of silica-supersaturated soil waters.

Whether soil waters are or are not supersaturated with silica, they remain so only while they are still in the soil. After they percolate through the soil profile and merge with bedrock groundwaters or drain into streams, they become diluted and so undersaturated. If the soil waters become super-saturated, gels may form and become part of the soil. But how does the soil water become supersaturated in the first place? It would seem that the most likely opportunity for supersaturation would be a change from very alkaline (pH above 9.8) conditions where minerals such as feldspar are actively hydrolizing and decomposing (Garrels and Howard, 1957) and silica is more soluble, to more neutral or slightly acid conditions lower in the soil profile, where silica is less soluble. In this case, the formation of gel from the supersaturated solution would depend on the gelling rate, which is dependent on pH, degree of supersaturation, OH^- and F^- ions, and other factors (Iler, 1955, pp. 45–55).

Rivers

Almost all streams and rivers, regardless of size, are undersaturated in silica as shown by the analyses in Clarke (1924, pp. 74–109) and emphasized by Krauskopf (1956). Of all the analyses quoted only two rivers in South America are supersaturated. Most of the others fall into a range from a few parts per million to 35 p.p.m. A very small number range from 35–75 p.p.m. Clarke, speaking with reference to the abundance of SiO_2 with respect to the other dissolved solids, made the point that, in general, silica will be highest in the upper parts of streams that drain a metamorphic and/or igneous terrain where chemical weathering is at a maximum. In these streams, silica only ranges up to 25–35 p.p.m., even though it may be the dominant constituent of the dissolved matter.

As the streams travel on to their middle and lower courses they become more and more diluted by run-off waters that are low in silica and tend to range from 8–15 p.p.m. SiO_2, very little more than the amount in equilibrium with crystalline quartz.

One may ask the pertinent question as to whether these analyses reflect SiO_2 carried in colloidal suspension, which, if it were included, would raise the total amount. As pointed out by Roy (1945) and Krauskopf (1956) this is most unlikely; in the normal range of pH values of river waters any colloidal silica should equilibrate fairly rapidly and dissolve. In addition, gravimetric and colorimetric determinations usually agree closely; as the colorimetric analysis is not sensitive to colloidal particles one infers that there is little or no colloid present.

Although lakes are not volumetrically important, they may have relatively high concentrations of dissolved silica. This is particularly true of alkaline lakes in which, due to the high pH and the consequent formation of silicate ions, the solubility of silica may be much higher than 140 p.p.m. Owens Lake, California, for example (Clarke, 1924, p. 162) has 300 p.p.m. dissolved silica. One might expect that lowering of the pH of these lakes, the consequent disappearance of silicate ions and the resultant lowering of silica solubility, would result in the inorganic precipitation of amorphous silica.

Groundwaters

Some groundwater analyses (Meents *et al.*, 1952) show that in the upper zones of fresh water there is little silica in solution and the solutions are vastly undersaturated. But the situation in the deeper groundwaters, in which there may be mixing of meteoric and connate (or more properly, formation) waters and the total amount of dissolved solids may rise to 30,000 p.p.m. or higher, may be quite different. Some of the deep formation waters have as much as 50–60 p.p.m. silica. Some of the highest values for dissolved silica in deep formation waters, exclusive of areas near hot springs, indicate that the solutions are still undersaturated with respect to amorphous silica, particularly when the temperature increase in solubility is taken into account. It may be that some very deep formation waters, very concentrated with respect to all dissolved solids, and at higher temperatures due to the geothermal gradient, have much more silica dissolved and may even reach saturation. In these cases one may expect that some change in condition, such as temperature decrease, would result in precipitation of amorphous silica.

The Oceans

According to the data in Sverdrup, Johnson, and Fleming (1942, p. 180) the oceans are undersaturated with respect to amorphous silica at all depths. The dissolved silica in most ocean waters is only a few parts or even tenths of a part per million. The maximum quoted by Sverdrup *el al* is about 8 p.p.m. A later figure that is somewhat higher was given by Bruevitch (1953), who reported concentrations up to 12 p.p.m. in bottom waters of the Bering Sea. Thus from the present ocean there is no possibility of inorganically precipitating amorphous silica from such undersaturated solutions. It is even doubtful whether most ocean waters are saturated with respect to quartz, although some bottom waters may be.

It is also possible to speculate that in some areas on the ocean floor there may be a thin unmixed layer of water just above the sediment-water interface, in which silica concentrations may be much higher due to diffusion of silica saturated waters expelled from the compacting sediment. Some bottom sediments have been reported as having concentrations up to 68 p.p.m. (Emery and Rittenberg, 1952). Unfortunately we have too little information on the chemical composition of interstitial waters of modern sediments to generalize.

PRECIPITATION OF SILICA

It is obvious that a silica solution must be supersaturated with respect to amorphous silica before inorganic precipitation of a gel or colloidal particles can take place. In the previous section we have seen that the only natural waters at or near the earth's surface that are supersaturated are thermal spring waters.

The one mechanism that seems to be responsible for precipitating amorphous silica is biochemical. It is known that diatoms, radiolaria, and other silica-secreting organisms are efficient in extracting silica from solutions under-saturated with respect to amorphous silica. The diatoms deplete such solutions to concentrations of 65–85 micrograms per liter (Iler, 1955, p. 281). In the absence of an inorganic mechanism for silica precipitation, and in view of the biochemical efficiency of silica extraction, it appears that the siliceous organisms are probably responsible for keeping the oceans so undersaturated in silica. Partial evidence for this is the increase in abundance of diatoms following volcanic ash falls, which release abundant silica in the process of glass alteration.

Another biochemical source of precipitated silica may be silica-secreting floral species. A number of land plants (horsetail, bamboo, are two examples) secrete small quantities of silica and it may be that some marine species do so also. Although the amount of silica per organism may be quite small, the absolute amount contributed by large populations may be significant.

Although many surface waters are supersaturated with respect to crystalline quartz there is no clearcut observational evidence that crystalline quartz is being precipitated from these waters. The very fact that these waters maintain silica in solution far in excess of that amount in equilibrium with quartz for long times suggests that quartz crystallizes from natural solutions extremely slowly in the range of room temperatures. As mentioned earlier, laboratory experiments have not been successful in precipitating quartz at room temperatures. Of course, one can always invoke some unknown catalyst that can make the reaction proceed at a measurable rate at room temperature but the nature of such a catalyst (if indeed, one exists) eludes us at present. We can only invoke time for this extremely slow reaction.

The time is available in the diagenetic stage of the history of a sedimentary rock. After burial the formation waters containing silica in solution may gradually equilibrate with quartz, the excess silica crystallizing as clear authigenic overgrowths on detrital quartz grains, as small quartz euhedra in limestones, or possibly as microcrystalline, chalcedonic quartz aggregates. But even in Paleozoic sandstones buried 3000–4000′ (Meents, *et al.*, 1952) there may still be more silica dissolved in the formation waters than is in equilibrium with quartz. The increased solubility of quartz due to temperature increase along the geothermal gradient is probably insufficient at this depth to account for the amount of silica found in solution. The explanation for this is either the extraordinary length of time necessary for equilibration, or more probably, to the fact that the formation waters may be much younger than the sediments that contain them. The evaluation of whether formation waters are in equilibrium with quartz at depths below about 10,000′ must wait on more precise determinations of the solubility of quartz in the temperature range 25°–150° C.

In few formation waters is there more silica in solution than is in equilibrium with amorphous silica and so it is unlikely that this kind of silica is precipitated during diagenesis.

A graphic representation, using an architectural metaphor, of the abundance of silica in various waters is shown in Fig. 1. The volumes of the buildings are crudely proportional to the total amount of water; their heights are proportional to the concentration of soluble silica. The base represents the kind of silica precipitated and at the bottoms of the buildings are representations of the amount of silica precipitated. Superimposed are two planes representing the solubilities of quartz and amorphous silica. Thus no building below its appropriate solubility plane can precipitate silica inorganically.

The sea water building has a great volume but a very low concentration of silica. At the opposite extreme is the hot springs "skyscraper," small in volume but high in silica concentration. River and formation waters lie in between. The soil waters building is of unknown height and

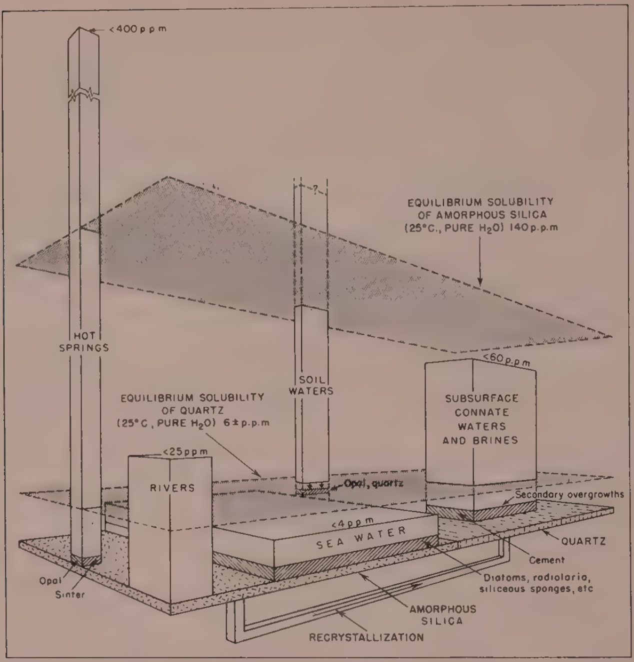

<400 p p m
?
EQUILIBRIUM SOLUBILITY OF AMORPHOUS SILICA (25°C., PURE H_2O) 140 p.p.m
HOT SPRINGS
SOIL WATERS
<60 p.p.m
SUBSURFACE CONNATE WATERS AND BRINES
EQUILIBRIUM SOLUBILITY OF QUARTZ (25°C, PURE H_2O) 6± p.p.m
<25 p p m
RIVERS
Opal, quartz
Secondary overgrowths
<4 p p m
SEA WATER
QUARTZ
Cement
Diatoms, radiolaria, siliceous sponges, etc
Opal
Sinter
AMORPHOUS SILICA
RECRYSTALLIZATION

FIG. 1. Silica abundance in natural waters. Volume of "buildings" roughly proportiona to absolute amounts of silica in solution. Height of "buildings" roughly proportional to concentrations of silica in solution.

relatively small volume. All of the buildings except that of formation waters and part of soil waters rest on an amorphous silica base, i.e., this is the material primarily precipitated. The formation waters building and part of the soil waters building rest on a quartz base signifying that crystalline quartz is precipitated directly from these waters. The amorphous silica is converted to quartz in the "sub-basement" by recrystallization or by solution and reprecipitation in formation waters.

The Silica Cycle

We can now proceed to outline the silica cycle, as shown diagrammatically in Fig. 2. We start with the silicate minerals that are the ultimate source of silica in solution. Through the weathering process the silicate minerals contribute silica in solution to surface waters and may be concomitantly altered to colloidal alumino-silicates (the clay minerals). The silica in surface waters, being far under the concentrations necessary to precipitate amorphous silica and not having sufficient time available to precipitate crystalline quartz, is carried to either the oceans or to formation waters. In the ocean, via biochemical precipitation by siliceous organisms, the silica is precipitated as amorphous silica or opaline silica. The concentration of silica in the sea is controlled by silica-secreting organisms. During diagenesis the amorphous silica deposited in the oceans recrystallizes to quartz and the silica in solution in formation waters gradually comes to equilibrium with quartz by precipitation of secondary overgrowths, authigenic crystals, etc. During diagenesis, either early (penecontemporaneous) or late, the clay minerals originally formed as weathering products may alter to different species and, depending on the specific transformation involved, as described previously, will either contribute to or take away silica in solutions.

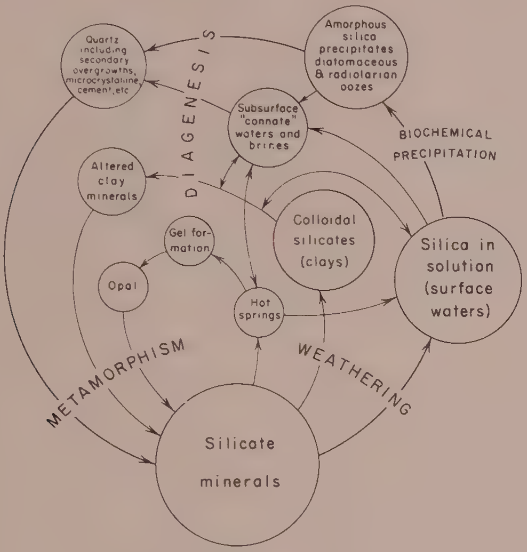
Quartz including secondary overgrowths, microcrystalline, cement, etc
Amorphous silica precipitates diatomaceous & radiolarian oozes
DIAGENESIS
Subsurface "connate" waters and brines
BIOCHEMICAL PRECIPITATION
Altered clay minerals
Colloidal silicates (clays)
Silica in solution (surface waters)
Gel formation
Opal
Hot springs
METAMORPHISM
WEATHERING
Silicate minerals

FIG. 2. The silica cycle.

Hot spring waters (White, Brannock, and Murata, 1956) derive their silica content by solution and alteration of silicate minerals plus a background amount of silica that may have been present in the original unheated ground-waters. Some juvenile water may be included. The hot spring waters then contribute back to formation waters, or to surface waters. Hot spring waters precipitate silica, as they cool at the surface and become supersaturated, forming opaline or siliceous sinters through intermediate stages of gel formation. Thermal waters may also circulate without emerging as hot springs and so precipitate silica in pore spaces as the waters cool in near surface rocks. The full cycle is then completed by metamorphism of the sedimentary silicate minerals and reorganization into minerals stable at high temperatures and/or pressures.

The Silica Cycle in the Past

We may ask whether the silica cycle, at least that part of it involved in the sedimentary cycle, operated in the same way throughout the known history of the earth. Certainly the general flow pattern outlined must have started after the beginning of the weathering process and the accumulation of the primitive oceans sometime early in the pre-Cambrian. The concentration of silica in surface waters may have been quite different from today, however. We can suppose that the extensive weathering of silicate rocks by rain waters with an amount of CO_2 dissolved somewhat higher than at present (Rubey, 1951, p. 1124) would contribute much more silica to solution (or at a faster rate) than at present. At the same time there may have been no large population of silica-secreting organisms that would biochemically precipitate silica and maintain low concentrations of silica in the oceans. The presence of algal structures in some pre-Cambrian siliceous rocks might be taken as tenuous evidence of the early evolution of silica-secreting organisms, at least in the later pre-Cambrian, but all of the definitely documented algae from the pre-Cambrian seem to have been lime-depositers (Whittard, 1953). It is also possible that the algae in these siliceous rocks have been diagenetically silicified. The diatoms and radiolaria had not yet evolved, and it is uncertain how early the siliceous sponges developed. Hence, depending on the uncertainties of silica-secreting organism development, and further depending on the difficulty of estimating the absolute amount of silica contributed to the oceans per unit time, we may postulate a primitive ocean that was saturated with $Si(OH)_4$ (in acid or near-neutral ocean water). As additional silica was added amorphous silica must have started to precipitate inorganically. The inorganic precipitation must have continued to keep pace with addition of silica derived from weathering until the population of siliceous organisms increased to the point where they could reduce concentrations to below saturation levels. The evidence from the rock column seems to indicate that this development took place at least as early as the later pre-Cambrian. Primary silica deposits, such as some bedded cherts of inorganic origin, may be slightly more abundant in the pre-Cambrian than in the younger rock columns but the difficulty of arriving at some kind of valid statistical estimate is so great that no firm arguments can be based on present knowledge. Paleozoic columns do not seem to have a greater proportion of inorganic primary siliceous rocks than younger rocks. We do know that radiolaria and siliceous sponges had evolved by the early Paleozoic; these organisms were probably responsible for holding down silica concentrations in sea water and thus preventing inorganic silica precipitation, at least from the

Paleozoic on. Much later, in the Mesozoic, the diatoms appeared and from this time on the cycle must have operated much as today.

According to this argument, most bedded cherts formed since the early Paleozoic (or possibly even later pre-Cambrian) must have originated in much the same way as Bramlette (1946) suggested for the Monterey chert, a diagenetic reorganization of a biochemical silica precipitate (diatomite). The abundance of diatoms in this case, as perhaps in most cases, was related to silica produced by alteration of pyroclastic material. This is not to say that there cannot have been inorganic silica deposits at some times and places. The extensive marine alteration of waterlaid volcanic materials during periods of intense volcanism would have liberated large amounts of silica to solution, and if the waters did not rapidly mix with the open ocean reservoir and if siliceous organisms were not present in large numbers, an inorganic silica precipitate would form. This is similar in general outline to the origin proposed by Rubey (1929, p. 168) for the siliceous Mowry shale, which involved the subaqueous decomposition of volcanic glass into amorphous silica.

SUMMARY

We have seen that the silica-water system is properly considered in terms of two subsystems, a metastable amorphous silica-water system and a stable crystalline quartz-water system. Most natural surface and near-surface waters do not have enough silica dissolved to precipitate amorphous silica inorganically; the only significant exceptions to this are the thermal spring waters, which precipitate siliceous and opaline sinters. Many surface waters are supersaturated with respect to quartz, and though, theoretically, quartz should precipitate, no deposits of crystalline quartz have been observed in rivers, lakes, or the oceans, probably the result of the very long times needed to reach equilibrium at low temperatures. A large amount of amorphous silica is precipitated from the oceans by diatoms, radiolaria, sponges, etc., and as these materials are buried in the sediment, the amorphous silica dissolves and eventually becomes reprecipitated as quartz. All lines of evidence point to interstitial formation waters, originally trapped in the sediment and later modified by chemical processes and groundwater movement, as the solution that precipitates crystalline quartz in the diagenetic stage of the history of a sedimentary rock. This implies that almost all primary silica deposits were originally in the form of amorphous silica.

REFERENCES

ALEXANDER, G. B., HESTON, W. M., AND ILER, R. K. (1954), The solubility of amorphous silica in water: *J. Phys. Chem.*, **58**, 453–455.

Bezrukov, P. L. (1955), Distribution and rate of sedimentation of silica silts in the Sea of Okhotsk: *Dokl. Akad. Nauk S.S.S.R.*, **103,** 473–476.

Bramlette, M. N. (1946), The Monterey formation of California and the origin of its siliceous rocks: *U. S. Geol. Survey*, Prof. Paper **212**.

Bruevich, S. V. (1953), Geochemistry of silicon in the sea: *Akad. Nauk S.S.S.R., Izvest., Ser. Geol.*, No. **4,** 67–69.

Buehler, E. J., and Walker, A. C. (1949), Growing quartz crystals: *Sci. Monthly*, **49,** 148–155.

Buerger, M. J. (1935), The silica framework crystals and their stability fields: *Zeits. Krist.*, **90,** 186–192.

——— (1954), The stuffed derivatives of the silica structures: *Am. Mineral.*, **39,** 600–614.

Clarke, F. W. (1924), Data of geochemistry: *U. S. Geol. Survey*, Bull. **770**.

Correns, C. W., and Nagelschmidt, G. (1933), Über Faserbau und Optische Eigenschaften von Chalzedon: *Zeits. Krist.*, **85,** 199–213.

Corwin, J. F., Herzog, A. H., Owen, G. E., Yalman, R. G., and Swinnerton, A. C. (1953), The mechanism of the hydrothermal transformation of silica glass to quartz under isothermal conditions: *J. Am. Chem. Soc.*, **75,** 3933–3934.

Donnay, J. D. H. (1936), La birefringence de forme dans la calcedoine: *Soc. Geol. Belgique Annales*, **59,** 289–302.

Emery, K. O., and Rittenberg, S. C. (1952), Early diagenesis of California basin sediments in relation to origin of oil: *Am. Assoc. Petrol. Geol. Bull.*, **36,** 735–806.

Folk, R. L., and Weaver, C. E. (1952), A study of the texture and composition of chert: *Am. J. Sci.*, **250,** 498–510.

Fothergill, C. A. (1955), The cementation of oil reservoir sands and their origin: *Proc. Fourth Petr. Cong.*, Sect. **1/8,** 301–314.

Frye, J. C., and Swineford, A. (1946), Silicified rock in the Ogallala formation: *Kansas Geol. Survey*, Bull. **64,** Pt. 2.

Gardner, L. U. (1938), Reaction of the living body to different types of mineral dusts: *Am. Inst. Min. Metallurg. Eng.*, Tech. Pub. **929,** 1–15.

Garrels, R. M. (1957), Some free energy values from geologic relations: *Am. Mineral.*, **42,** 780–791

———, and Howard, P. F. (1957), Reactions of mica and feldspar with water at low temperatures: *1957 Clay Conference, Berkeley, California*, in press.

Goldsmith, J. R. (1953), A "simplexity principle" and its relation to "ease" of crystallization: *J. Geol.*, **61,** 439–451.

Grim, R. E. (1953), Clay mineralogy: McGraw-Hill, New York.

———, Dietz, R. S., and Bradley, W. F. (1949), Clay mineral composition of some sediments from the Pacific Ocean off the California coast and the Gulf of California: *Geol. Soc. Am. Bull.*, **60,** 1785–1808.

———, and Bradley, W. F. (1955), Structural implications in diagenesis: *Geol. Rundschau*, **43,** 469–474.

Heald, M. T. (1956), Cementation of Simpson and St. Peter sandstones in parts of Oklahoma, Arkansas, and Missouri: *J. Geol.*, **64,** 16–30.

Iler, R. K. (1955), The colloid chemistry of silica and silicates: Cornell University Press, Ithaca.

———, and Dalton, R. L. (1956), Degree of hydration of particles of colloidal silica in aqueous solution: *J. Phys. Chem.*, **60,** 955–957.

Jander, G., and Jahr, K. F. (1934), Das System der Kieselsauren: *Kolloid-Beihefte*, **41,** 48–57.

JOHNSON, R. H. (1920), The cementation process in sandstone: *Am. Assoc. Petrol. Geol. Bull.*, **4,** 33–35.

KENNEDY, G. C. (1950), A portion of the system silica-water: *Econ. Geol.*, **45,** 629–653.

KRAUSKOPF, K. B. (1956), Dissolution and precipitation of silica at low temperatures: *Geochim. Cosmochim. Acta*, **10,** 1–26.

LATIMER, W. M. (1952), Oxidation potentials: Prentice-Hall , New York, Second Edition.

LENHER, V. (1921), Silicic acid: *J. Am. Chem. Soc.*, **43,** 391–396.

LISITSYN, A. P. (1955), Distribution of authigenic SiO_2 in the bottom sediments of the western Bering Sea: *Dokl. Akad. Nauk S.S.S.R.*, **103,** 479–482.

MAXWELL, J. C., AND VERRALL, P. (1954), Low porosity may limit oil in deep sands: *World Oil*, **138,** No. 6, 102–104.

MEENTS, W. F., BELL, A. H., REES, O. W., AND TILBURY, W. G. (1952), Illinois oil-field brines, their geologic occurrence and chemical composition: *Illinois Geol. Survey*, Illinois Petroleum **66.**

MIDGLEY, H. G. (1951), Chalcedony and flint: *Geol. Mag.*, **88,** 179–184.

MILLOT, G. (1949), Relations entre la constitution et la genese des roches sedimentaires argileuses: Geol. Appliq. et Prosp. Min., University of Nancy (France), Vol. II.

MOHR, E. C. J., AND VAN BAREN, F. A. (1954), Tropical soils: Interscience Pub., New York.

MURATA, K. J. (1946), Significance of internal structure in gelatinizing silicate minerals: *U. S. Geol. Survey*, Bull. **950.**

PELTO, C. R. (1956), A study of chalcedony: *Am. J. Sci.*, **254,** 32–50.

PETTIJOHN, F. J. (1957), Sedimentary rocks: Harper and Brothers, New York, Second Edition.

ROLLER, P. S., JR., AND ERVIN, GUY, JR. (1940), The system calcium oxide-silica-water at 30°. The association of silicate ion in dilute alkaline solution: *J. Am. Chem. Soc.*, **62,** 461–471.

ROY, C. J. (1945), Silica in natural waters: *Am. J. Sci.*, **243,** 393–403.

RUBEY, W. W. (1929), Origin of the siliceous Mowry shale of the Black Hills region: *U. S. Geol. Survey*, Prof. Paper **154.**

——— (1951), Geologic history of sea water: *Geol. Soc. Am. Bull.*, **62,** 1111–1147.

SOSMAN, R. B. (1927), The properties of silica: Am. Chem. Soc. Monograph Series No. 37, Chemical Catalogue Co., New York.

SVERDRUP, H. U., JOHNSON, M. W., AND FLEMING, R. H. (1942), The oceans: Prentice-Hall, New York.

TAYLOR, J. M. (1950), Pore space reduction in sandstones: *Am. Assoc. Petrol. Geol. Bull.*, **34,** 701–716.

WALDSCHMIDT, W. A. (1941), Cementing materials in sandstones and their influence on the migration of oil: *Am. Assoc. Petrol. Geol. Bull.*, **25,** 1839–1879.

WALKER, T. R. (1957), Frosting of quartz grains by carbonate replcaement: *Geol. Soc. Am. Bull.*, **68,** 267–268.

WARREN, B. E., AND BISCOE, J. (1938), The structure of silica glass by X-ray diffraction studies: *J. Am. Ceram. Soc.*, **21,** 49–54.

WEITZ, E., FRANCK, H., AND SCHUCHARD, M. (1950), Silicic acid and silicates: *Chem. Ztg.*, **74,** 256–257.

WHITE, D. E., BRANNOCK, W. W., AND MURATA, K. J. (1956), Silica in hot-spring waters: *Geochim. Cosmochim. Acta*, **10,** 27–59.

WHITTARD, W. F. (1953), The enigma of the earliest fossils: *Bristol Naturalist's Soc. Proceedings*, **28,** Pt. 4, 289–304.

THE AMERICAN MINERALOGIST, VOL. 42, NOVEMBER–DECEMBER 1957

THE GRAPHICAL ANALYSIS OF MINERAL ASSEMBLAGES IN PELITIC SCHISTS*

JAMES B. THOMPSON, JR., *Harvard University, Cambridge, Massachusetts.*

ABSTRACT

The principal minerals used as metamorphic indicators in pelitic schists are, to a first approximation, phases in the system: SiO_2-Al_2O_3-MgO-FeO-K_2O-H_2O. At a given pressure, temperature and humidity (activity of H_2O), quartz-bearing assemblages in this system are dependent on the relative amounts of Al_2O_3, MgO, FeO, and K_2O. These assemblages may be shown three-dimensionally in the tetrahedron: Al_2O_3-MgO-FeO-K_2O. Assemblages which include muscovite as well as quartz may be represented successfully in two dimensions by projecting the compositions of minerals onto some suitable plane with the composition KAl_3O_5 as point of projection. This projection is applicable to rocks over a wide range in bulk composition and through wide range of metamorphic conditions. It also provides a unique characterization of the mineral facies observed in pelitic schists. The principal variation in composition of most of the minerals involved is given by the ratio MgO/MgO+FeO. This ratio may commonly be determined with sufficient accuracy by simple measurements of optical or other physical properties.

INTRODUCTION

In the classic work of Barrow (1893, 1912) in the Scottish Highlands, and in numerous field and petrographic studies since that time, regional metamorphic zoning has been described and mapped in terms of the successive appearance of certain minerals or mineral assemblages in aluminous schists. Such schists are generally formed by the metamorphism of pelitic sediments. The principal indicator minerals in the order of their appearance in the area studied by Barrow, are: chlorite, biotite, almandite, staurolite, kyanite and sillimanite. Other minerals of pelitic schists have been used as indicators by various authors. A chloritoid isograd has been drawn in the Taconic area by Balk (1953; see also Tilley, 1925). Heald (1950) has drawn an isograd on the first appearance of the pair: orthoclase+sillimanite.

A pelitic schist is not a simple chemical system and the mineralogic variations that have been observed do not lend themselves readily to graphical analysis. Certain components such as ZrO_2, CO_2, S or P_2O_5 are not present in the above mentioned "indicators" in measurable amounts and may be dismissed if we simply omit from consideration those phases in which such components appear in measurable amounts—regarding these latter phases, in effect, as the crucible in which the others react. Even with eliminations of this sort, however, we are still faced with a polyphase, multicomponent system and rather arbitrary simplification is necessary. Possible consequences of this simplification will be discussed at the end of this paper.

---

* Contribution from the Department of Mineralogy and Petrography, Harvard University No. 382.

THE CHOICE OF COMPONENTS

To a first approximation the indicator minerals listed above may be regarded as phases in the six-component system: SiO_2-Al_2O_3-MgO-FeO-K_2O-H_2O, a system which also includes minerals such as muscovite, quartz, andalusite, cordierite and others commonly associated with the above indicators. It is apparent that this is but an approximation when we consider the known content of Fe_2O_3 or TiO_2 in a typical biotite, CaO or MnO in garnet, or Na_2O in muscovite or potassic feldspar, even though in many instances it is possible to give the compositions of these minerals in terms of the six components listed above and leave very little of their substance unaccounted for. The success of such an approximation may be measured by its applicability which will be discussed more fully below. However, it must be remembered that in any specific natural occurrence an apparently anomalous mineral association may be related to an unusual abundance, in one or more of the minerals, of some neglected component.

It may seem of little value that the system is now narrowed down to six components, since even at a specified temperature and pressure a three-dimensional model is needed to represent completely the phase assemblages in a system of as few as four components. Though this is true enough, we can profit from the fact that we are not interested in *all possible* assemblages in the system, but in only those that occur in rocks under present consideration. Specifically, the schists and gneisses in which mineral zones have been mapped almost invariably contain quartz, and we are not seriously restricting our field of observation if we omit from the present discussion all assemblages where quartz is not present. Now, since quartz is virtually pure SiO_2, it is clear that an increase or decrease in the amount of SiO_2 in a quartzose rock will be reflected simply in an increase or decrease of quartz, other things being equal, and that the minerals present other than quartz are dependent on the relative amounts of components other than SiO_2.

THE GRAPHICAL STATUS OF H_2O

The restriction that quartz be present thus has the effect of reducing the compositional variables by one so that we are left, for graphical purposes, with a five-component system: Al_2O_3-FeO-MgO-K_2O-H_2O. Were a phase corresponding to any of these other components commonly present we could eliminate it as we did SiO_2, but this does not appear to be the case. It is possible that a fluid phase made of nearly pure H_2O was present in such rocks at one time or another, but it is not a phase that we observe in typical thin sections of a schist or gneiss, nor are there "holes" where such a phase might have been. There is to be sure, even in a schist or gneiss, evidence of H_2O in excess of that combined in the crystalline phases, and evidence that this extra H_2O is concentrated along the grain boundaries, but it would be unwarranted to assume from this that such an intergranular film may be regarded, even approximately, as either pure H_2O chemically or like a bulk aqueous fluid in its physical properties. We shall, however, eliminate H_2O from our graphical analysis, but for rather different reasons.

It is apparent, from comparison of chemical analyses of pelitic sediments (Clarke, 1924, pp. 516–518 and p. 552) with those of typical schists and gneisses derived therefrom (Clarke, p. 553 and pp. 625–626) that such rocks lose H_2O when metamorphosed, and, from consideration of the minerals involved, that the higher the grade of the metamorphism, the greater the loss.

Whether a rock will tend to gain or lose H_2O at a given pressure and temperature is dependent on the activity, a_{H_2O}, or chemical potential, μ_{H_2O}, of H_2O in the rock (or its intergranular film) relative to its immediate surroundings.

If a_{H_2O} or μ_{H_2O}, or the humidity η,[1] in the rock is higher than in its surroundings, the rocks will tend to lose H_2O, and vice versa. In an open system of this sort the stable phase-assemblage will be dependent on the

---

[1] $a_{H_2O} = e^{\frac{\mu_{H_2O} - \mu_{H_2O}^*}{RT}}$ where $\mu_{H_2O}^*$ is the chemical potential of H_2O in some standard or reference state. The *relative humidity of* meteorologists may be regarded as an activity of H_2O expressed in per cent (rather than on a fractional basis as is usual in chemical literature) and where the standard state is water-saturated air (or distilled water) at the P and T in question. A more useful standard state, for geologic purposes, would be the stable form of pure H_2O at the P and T in question. This would be virtually identical with the meteorological standard state at low pressures and temperatures and have the advantage of being independent of other components present at high temperatures and pressures. The activity of H_2O with standard state so defined will be referred to henceforth as simply the "humidity." More formally:

$$\eta \equiv e^{\frac{\mu_{H_2O} - \mu_{H_2O}^0}{RT}}$$

where $\mu_{H_2O}^0$ is μ_{H_2O} for the stable form of pure H_2O at P, T. There are no other "humidities" in standard geological parlance with which it may be confused, and it is virtually identical with the meteorological relative humidity in a surface or near-surface environment. Furthermore, the intuitive connotations commonly associated with the word "humidity" are qualitatively correct with respect to η but not with respect to μ_{H_2O}. Specifically: a rise in temperature at constant P and η will, in general, tend to dehydrate the system and a rise in temperature at constant P and μ_{H_2O} will tend to hydrate the system.

temperature and pressure, the *activities* or *chemical potentials* of those components to which the system is open, and upon the *relative amounts* of those components to which the system is closed, or, in our specific case, on P, T, η, and the relative amounts of Al_2O_3, MgO, FeO and K_2O. This includes as a limiting case, the possible occurrence of pure H_2O as a separate phase. Such an occurrence would correspond to unit (or 100 per cent) humidity at any given pressure and temperature. This would be the practical maximum value for the humidity at the given pressure and temperature owing to the choice of the stable form of the pure substance (at P, T) as standard state. A humidity less than unity (or 100 per cent) might be visualized, graphically, as the situation which would prevail if a hypothetical form of H_2O, more stable than the actual stable one at the P and T in question, were present in the system. In general the graphical analysis of mineral assemblages neglecting the amount of H_2O relative to other components seems to work. This is consistent either with the presence of pure H_2O as a phase at the time the assemblage formed, or with the assemblage having reached its final state in accord with some externally controlled humidity.

THE TETRAHEDRON: Al_2O_3-MgO-FeO-K_2O

Compositions with respect to the remaining four components, Al_2O_3, MgO, FeO, and K_2O, may be plotted in the tetrahedron of Fig. 1. The portion Al_2O_3-$KAlO_2$-FeO-MgO or "A-K-F-M" has been employed by Barth (1936, also Osberg, 1952) for the illustration of mineral assem-

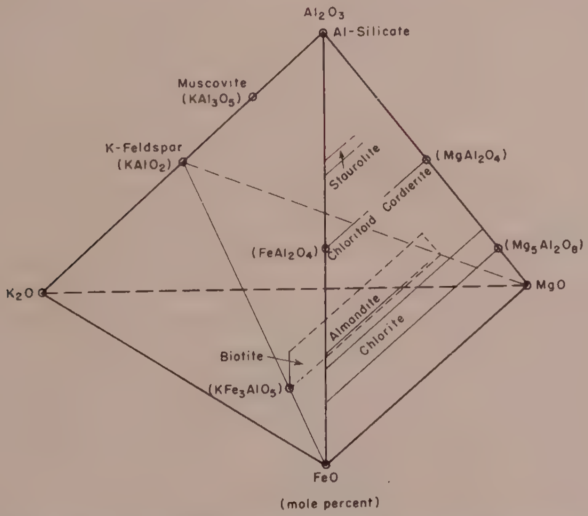

FIG. 1. The system SiO_2-Al_2O_3-MgO-FeO-K_2O-H_2O showing phases stable with quartz at P, T, η, as plotted in tetrahedron Al_2O_3-MgO-FeO-K_2O.

blages in schists. The "A-K-F" diagram of Eskola (1915) is similar but treats (MgO+FeO) as one component. Barth (p. 819) gives practical convenience as the reason for disregarding H_2O, but not without misgivings (p. 822). Eskola and Osberg assume H_2O to have been in excess. We have justified its elimination on a different basis which includes the latter as a limiting case.

A tetrahedral diagram is cumbersome for written presentation. Barth employed a perspective view developed by H. von Philipsborn (1928), and Osberg showed the Al_2O_3-FeO-MgO face with biotite projected onto the line FeO-MgO, the point of projection apparently being indefinitely removed from FeO-MgO in the plane $KAlO_2$-FeO-MgO. Barth's diagram is difficult to visualize particularly if several assemblages are to be shown, and Osberg's diagram, which resembles one that we shall describe below, does not clarify the relationships of potash feldspar when it appears in association with aluminous minerals such as almandite or cordierite.

The usefulness of the "A-K-F" diagram of Eskola, as extensively employed by Turner (1948) and other authors, is impaired by the lumping of MgO and FeO as one component. Though Fe^{++} and Mg substitute for each other readily (and perhaps nearly ideally) in solid solutions, they definitely do not behave as one component. Eskola (1915, p. 123) was, to some extent, aware of this, and the point has been clarified and emphasized by Bowen (1925). The ratios MgO/(MgO+FeO), in pairs of coexisting mineral phases typically differ by easily measurable amounts. Furthermore the nature of any system of the type: X-MgO, at any given P and T is commonly quite different from the analogous system: X-FeO. One may, for example, compare the systems: SiO_2-MgO (Bowen and Andersen, 1914) and SiO_2-FeO (Bowen and Schairer, 1932) at any P and T where both are not entirely liquid.

The approach outlined below will make use of the fact that muscovite, like quartz, is nearly ubiquitous in metamorphosed pelites and rocks of comparable composition. The principal exceptions occur in the inner parts of certain contact aureoles and in the highest grades of regional metamorphism. Consequently we have relatively little interest in assemblages which do not include muscovite. Muscovite, however, is unlike quartz in that its composition is not that of a simple limiting component such as SiO_2. The solution of the problem is thus more complicated and may be regarded, graphically, as a projection onto some appropriate surface of the compositions of phases in equilibrium with muscovite.

The Representation of Phases Occurring with Muscovite

The compositions of most natural muscovites, with respect to the components considered, lie at or very near the point labeled "KAl_3O_5"

in Fig. 1. At any given P, T and η the range of composition of muscovite will thus be a small volume at and near "KAl_3O_5," the surface of which will be terminus to all tie lines, compatibility triangles and compatibility tetrahedra for those assemblages in this system which include muscovite in addition to quartz. The surface of the volume for muscovite compositions should resemble, in general features, that of a wind-faceted pebble, and be characterized by smooth surfaces (termini of tie lines), edges (termini of triangles) and corners (termini of tetrahedra). The opposite ends of the tie lines, opposite edges of the triangles, and opposite faces of the tetrahedra will also constitute a surface giving the compositions of phases compatible with muscovite. The latter surface, consisting of three-phase triangles (three phases, that is, in addition to quartz and muscovite), bundles of two-phase tie lines, and one-phase areas, will be topologically like an ordinary three-component compatibility diagram except that points upon it will not, as a rule, be co-planar. We may, however, construct a map of such a surface by some suitable projection of it. An important consideration in so doing is to avoid, as far as possible, points of projection that would lead to overlapping of different portions of the projected surface. Thus in a simplified, two-dimensional analogue (Fig. 2), F would be a suitable point of projection for phases in equilibrium with phase α, but Q would not. In some instances it may not be possible to avoid overlap in projection. As shown in Fig. 2 this is most likely where the ubiquitous phase has a wide range of compositional variability. Fortunately, muscovite, in terms of the components considered shows but minor variation in composition from $KAl_3Si_3O_{10}(OH)_2$, or "KAl_3O_5" in the tetrahedron of Fig. 1. This means that tie lines from other phases to muscovite will be very nearly radial to "KAl_3O_5," and that the choice of this as point of projection will make any overlap highly unlikely.

A convenient surface to receive the projection is the plane: Al_2O_3-MgO-FeO. Many of the indicator minerals have compositions already lying in or very near it. The essential features of the projection are shown in Fig. 3. Compositions in the sub-tetrahedron A-P-F-M will project onto the area A-F-M, those in the volume N-O-P-F-M onto the extension of the plane A-F-M beyond the line F-M, and those in the sub-tetrahedron B-N-O-P onto the extension of the plane AFM beyond A. Compositions in the plane N-O-P will project to points indefinitely removed from A. We might, for convenience, define compositions in the volume A-F-M-N-O-P as projecting in the *positive* sense onto A-F-M and those in the volume B-N-O-P as projecting in the *negative* sense onto A-F-M. Though Fig. 3 aids in visualization the actual operation is more readily accomplished by formula as indicated in Fig. 4. Mineral assemblages typical of the lower sillimanite zone in west-central New Hampshire are shown in Fig. 5. Nearby rocks in the kyanite zone have similar assemblages with kyanite taking the place of sillimanite. The "negative" part of the projection has been shown in Fig. 5, but is trivial, for many purposes, since each possible assemblage is represented in the positive part even though all bulk compositions are not.

Another convenient plane upon which to project is the plane that includes the edge MgO-FeO and is parallel to the edge Al_2O_3-K_2O (Fig. 6).

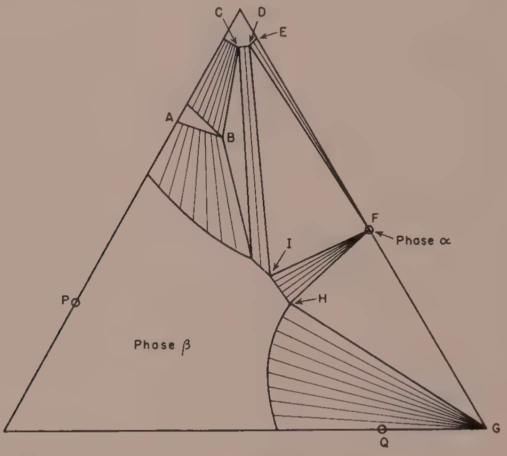

Fig. 2. The phases in equilibrium with phase α, a fixed compound, are shown by the line running G-H-I-D-E. If the compositions of these phases are projected through point F into some straight line, no portions of G-H-I-D-E will be superimposed in the projection. Phases in equilibrium with β, a solution, are given by the line running A-B-C-D-F-G. Projection through a point such as P would result in the portions A-B and B-C being partly superimposed. If a phase has an extreme range of solution it may not be possible in some instances to choose a point such that there will be no overlap. If the phase is a fixed compound, lying on the periphery of the triangle (or surface of the tetrahedron as in the example in the text), then no difficulty can arise if the point of projection be chosen as the composition of the compound, as all tie lines must then be radial to that point.

In this case all compositions in the tetrahedron project in the positive sense, but the lack of resemblance to a standard triangular diagram is perhaps confusing. The method of plotting is shown in Fig. 7 with the projected fields of several minerals indicated, as in Fig. 4. In Fig. 8 the sets of assemblages shown in Fig. 5 are plotted again in the alternative projection. The two projections are entirely equivalent, the first more easily adapted to triangular coordinates and the second to orthogonal coordinates. The first provides relatively more "working room" in the

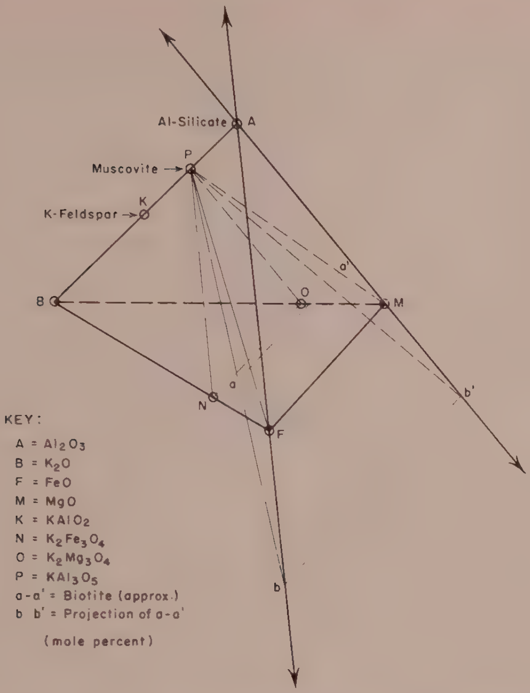

FIG. 3. The tetrahedron Al_2O_3-K_2O-FeO-MgO showing projection through idealized muscovite composition onto plane determined by Al_2O_3, FeO and MgO.

less aluminous range of composition, and the second does the same for the more aluminous range of composition.[1]

Although our concern has been mainly with plotting the compositions of coexistent minerals, a rock composition may also be plotted provided the content of all mineral phases not appearing in the projection has first been subtracted from the total bulk composition. This may be

---

[1] In a way the above procedures are analogous to the conventional method of presenting high-temperature experimental data in a system such as "FeO"-SiO_2 (Bowen and Schairer, 1932). Actually, as the authors emphasize, this study was of ternary equilibria in the system Fe-Si-O, and the "binary" diagram represents phases in equilibrium with an iron crucible. Both wustite and liquid, in this system, contain more oxygen than in a purely ferrous system, and their compositions are projected, by calculation, onto the line FeO-SiO_2. The calculation of Bowen and Schairer is equivalent to projection along lines parallel to the edge Si-O. Allen and Snow (1955), use a different calculation in their work in the system Ca-Fe-Si-O, and their "ternary" diagram is a projection, through oxygen, onto the plane CaO-FeO-SiO_2, of phases in equilibrium with iron. The relative amount of "Fe_2O_3" in the phases in the above systems is commonly small, hence the method of projection makes little practical difference. A closer analogy to our procedure would be to project through Fe as that is the composition of the ubiquitous phase.

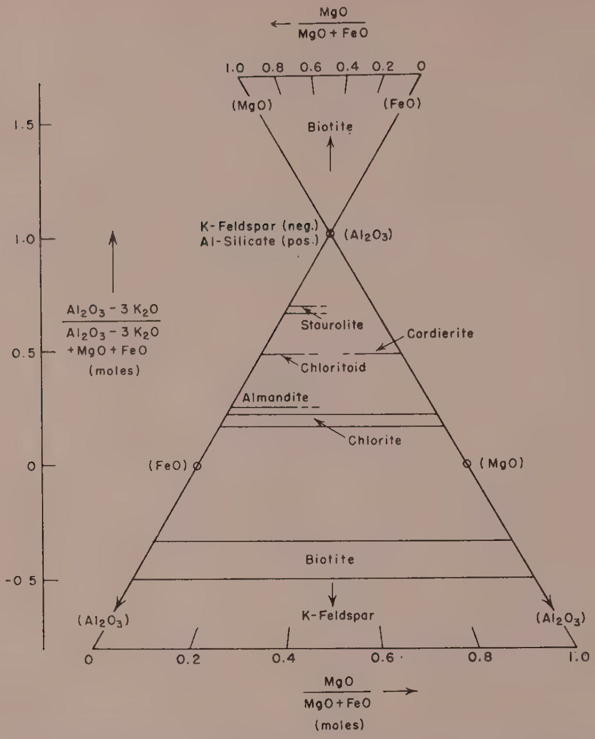

FIG. 4. System SiO_2-Al_2O_3-MgO-FeO-K_2O-H_2O showing possible phases in equilibrium with quartz and muscovite at P, T, η. Projection is through point KAl_3O_5 of Fig. 1 onto plane Al_2O_3-MgO-FeO.

accomplished by direct calculation from the mode, or by making a norm-like calculation based on an assumed distribution of the pertinent components. Though previous authors have emphasized calculations of this sort, the value of making them is doubtful except perhaps for purposes of "predicting" the mineral composition of a rock under metamorphic conditions other than those observed. We can see, in thin section, what phases and assemblages are actually present and, if necessary, can calculate the bulk composition from the mode. For purposes of finding out about the physical environment during metamorphism, however, the important consideration is with regard to the relative compositions of coexisting phases, not their relative amounts. The bulk composition of a given assemblage or the relative modal abundance of the phases, may thus, for present purposes at least, be regarded as simply a pre-metamorphic accident (except with regard to H_2O), though admittedly of prime importance in determining the pre-metamorphic nature of the rock.—A plea might also be inserted at this point for the reporting, in petrographic

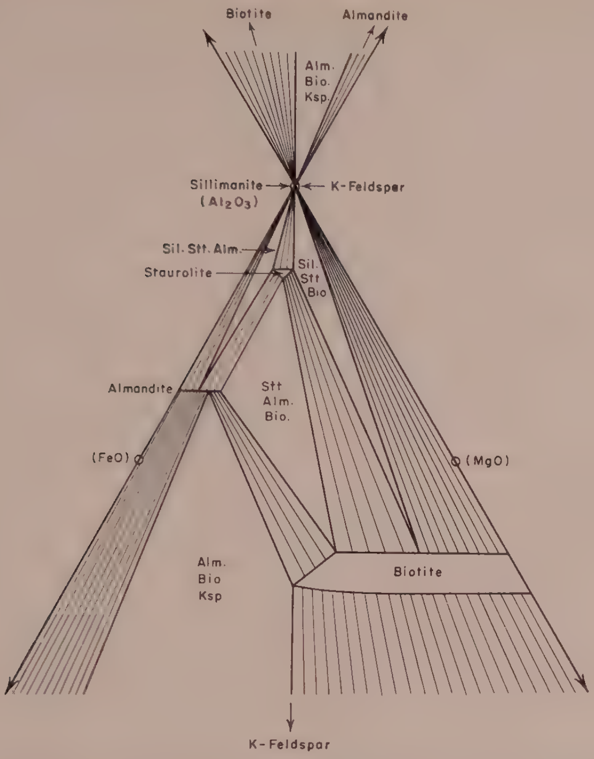

FIG. 5. Phases with muscovite and quartz in the system SiO_2-Al_2O_3-MgO-FeO-K_2O-H_2O as observed (schematically) in the lower sillimanite zone of west-central New Hampshire. Projection as in Figure 4.

descriptions of metamorphic rocks, of specific assemblages rather than just averaged modes. Slides from several specimens may contain mutually incompatible assemblages and much information of physico-chemical value may be lost in the averaging.

THE EFFECTS OF OTHER COMPONENTS

There are two possibilities with regard to a component not considered in the above analysis. One possibility is that the extra component is not present in measurable proportions in any of the phases with which we have been concerned. In this case the mutual equilibrium among these phases is not affected by the presence of the extra component. This component must then be present in some other phase or phases than those appearing in our projection. The total number of coexisting phases containing SiO_2-Al_2O_3-MgO-FeO-K_2O-H_2O and any one other component is limited by the phase rule. Hence, if more than one of these phases contains the extra component, the possible number of phases pertinent to our projection must be correspondingly limited. As long as any of the phases in the projection remain, however, their mutual equilibria are independent of the presence of the extra component and the phases that contain it.

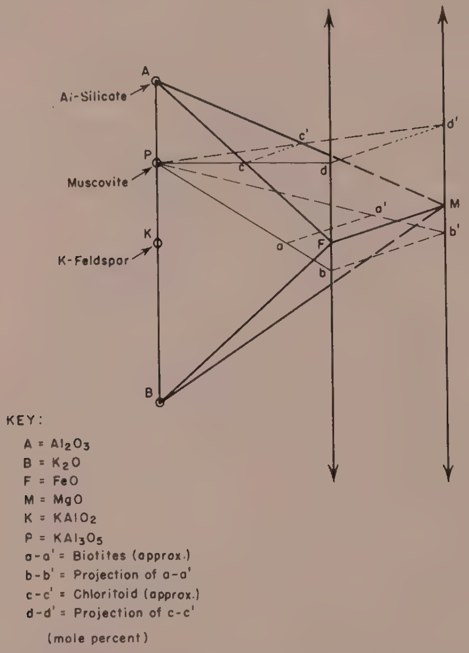

FIG. 6. The tetrahedron Al_2O_3-K_2O-FeO-MgO showing projection through idealized muscovite composition onto plane passing through FeO and MgO and parallel to the line Al_2O_3-K_2O.

The other possibility is that the neglected component *does* enter one of the phases of concern. In this case the mutual equilibria of these phases are affected, and those phases that incorporate the extra component may be stabilized so as to appear in assemblages where they would not otherwise be present. The most likely offenders will be discussed individually.

Na_2O may occur in significant proportions in either potassic feldspar or muscovite and to a lesser and perhaps negligible extent in biotite. The point at which the feldspar would project would not, however, be altered by this substitution, and the other projected phases contain little or no Na_2O. The problem of anomalous stabilization of muscovite or potassic feldspar is also cancelled by the fact that Na_2O is commonly sufficiently abundant that a fundamentally sodic phase is present. This is typically albite in high-grade assemblages or low-grade assemblages poor in alumina, and typically paragonite in the more highly aluminous low-grade assemblages. Where the albite or paragonite contains no extraneous component other than soda the variance of the assemblage is the same as it would be if no soda were present. Quantitatively, however, equilibria involving muscovite or potassic feldspar would be somewhat displaced relative to the corresponding equilibria in a soda-free system.

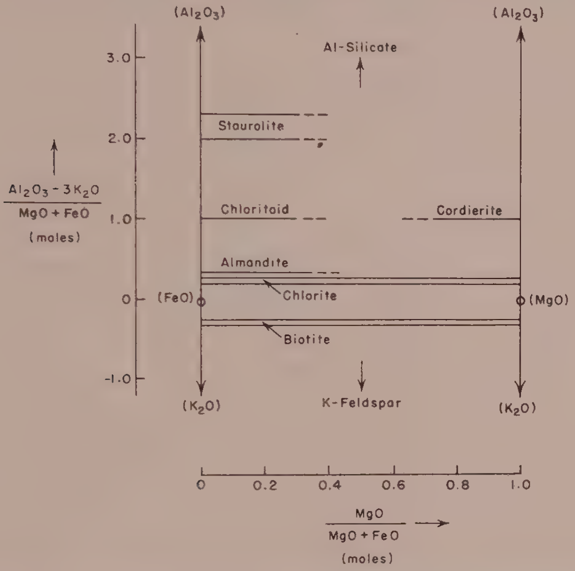

FIG. 7. System SiO_2-Al_2O_3-MgO-FeO-K_2O-H_2O showing possible phases in equilibrium with quartz and muscovite at P, T, η. Projection is through point KAl_3O_5 of Fig. 1 onto plane parallel to edges Al_2O_3-K_2O and MgO-FeO.

The principal difficulty arises with the occurrence of a calcic plagioclase rather than albite.

CaO is also troublesome through the occurrence of a grossularite component in the garnet, and MnO may be significant in either garnet or chloritoid. Occurrences of four of the projected phases in one assemblage are known, though not common, and several examples are known to the writer. In some of these the garnets have been shown to have a significant content of CaO, or MnO, or both. It is probably best, for purposes of the projections discussed herein, to either disregard, or at least treat with caution, any garnet in which the sum of components other than pyrope and almandite is more than a few per cent.

In plotting compositions of minerals containing extraneous components the writer does not simply subtract the CaO or MnO, but also Al_2O_3, K_2O, etc. such that the material subtracted represents an inde-

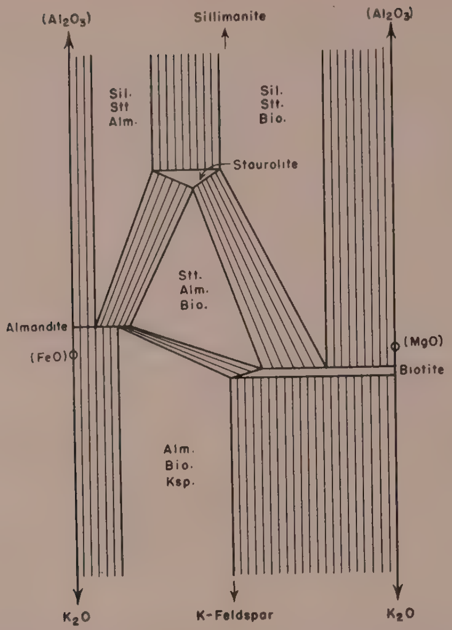

FIG. 8. Phases with muscovite and quartz in the system SiO_2-Al_2O_3-MgO-FeO-K_2O-H_2O as observed (schematically) in the lower sillimanite zone of west-central New Hampshire. Projection as in Fig. 7 and equivalent to Fig. 5.

pendently variable component of the mineral itself. Thus in a garnet analysis[1] yielding:

(*a*)	$Ca_3Fe_2^{+++}(SiO_4)_3$	2.4	mole per cent
(*b*)	$Ca_3Al_2(SiO_4)_3$	5.5	mole per cent
(*c*)	$Mn_3Al_2(SiO_4)_3$	2.1	mole per cent
(*d*)	$Fe_3^{++}Al_2(SiO_4)_3$	71.7	mole per cent
(*e*)	$Mg_3Al_2(SiO_4)_3$	18.3	mole per cent

the plotted composition would be on the basis of (*d*) and (*e*) recalculated to 100 per cent.

It might be pointed out that if the systems were closed to H_2O and that component not present in excess, then coexistence of four of the projected phases should be much more common than it is. As a rule it is not possible to vary the H_2O-content of most mineral assemblages without the appearance of a new phase. This is not consistent with an inherited bulk-content of H_2O, but is consistent with an externally controlled humidity.

---

[1] The garnet from the Gassetts schist, Chester, Vermont.

IRON OXIDES

Fe_2O_3, as a component, has been omitted from consideration though typically present in small amounts in most ferromagnesian minerals. Ferric or partly ferric phases such as magnetite, hematite, or stilpnomelane are also fairly common in metamorphosed pelites.

The writer has considered the possibility that the activity of oxygen might, like the humidity, be externally controlled. In such a case Fe_2O_3 would behave graphically like FeO, and both magnetite and hematite could be treated as phases in the projection, plotting at the point marked "FeO" in either Fig. 4 or Fig. 7. Stilpnomelane would then project somewhere between the line "FeO-MgO" and the range of chlorite. In general, however, the analysis of pelitic assemblages has been more successful when the system has been treated as closed to oxygen, and Fe_2O_3 kept as a separate component graphically. This is emphatically the case in the common occurrence reported by James and Howland (1955) of *both* magnetite and hematite in metamorphosed iron formation. In any occurrence of this sort the activity of oxygen at any given pressure and temperature is fixed internally, not externally, owing to the presence of two phases in the two-component system Fe-O.

MINERAL FACIES IN PELITIC SCHISTS

In order to construct a complete projection for the indicator minerals at any locality it is necessary that the rocks at that locality show enough variation in bulk composition that all three-phase assemblages are represented (five-phase assemblages counting quartz and muscovite). Owing to the normal variation, from bed to bed, in many clastic sediments, it is quite commonly possible to construct a major portion of such a projection on the basis of one outcrop or group of adjacent outcrops, and it is indeed wise in attempting to do so to find an area where rocks of considerable heterogeneity are intimately interstratified. Where a complete or nearly complete construction can be made it can be said to characterize the *mineral facies* for the pelitic schists at that locality. It is thus not any one assemblage but the set or "ensemble" of assemblages that defines the facies. Only then can we specify that any two rocks of identical composition (except for H_2O) from separated isofacial localities, will have the same mineral composition as required by the definition of Eskola (1915, p. 114). Clearly, many assemblages may occur in more than one facies, and one assemblage is in general insufficient to determine the facies other than within gross limits.

The compositions at the corners of the three-phase fields will, in general, show *continuous variation* from place to place in response to variation in P, T and η at the time of formation of the rocks. In addition

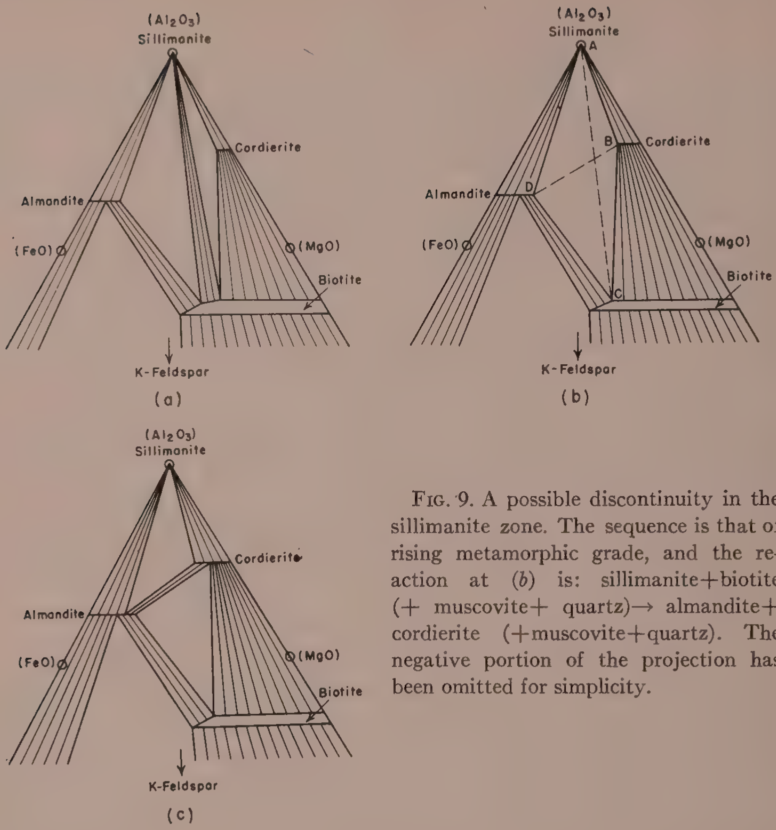

FIG. 9. A possible discontinuity in the sillimanite zone. The sequence is that of rising metamorphic grade, and the reaction at (*b*) is: sillimanite+biotite (+ muscovite+ quartz)→ almandite+ cordierite (+muscovite+quartz). The negative portion of the projection has been omitted for simplicity.

to such continuous variation in facies there will be discontinuities in facies involving changes in the basic topology of the projection. These may involve the appearance of a new phase, the disappearance of an old one, or a change in the compatible associations as in Fig. 9.

The discontinuities in facies are probably the most suitable changes upon which to draw isograds since they are independent, if observed at all, of local variation in the ratios of the critical components. In Fig. 9b all compositions in the quadrilateral A-B-C-D would show the discontinuity. An isograd based on the simple shift of the boundary of a three-phase field across some specific bulk composition, on the other hand, is clearly dependent on the composition selected as well as on the externally controlled variables: P, T and η.

A discontinuity in facies in this system represents conditions of either univariant or bivariant equilibrium. Where H_2O is gained or lost, as is commonly the case, the equilibrium is bivariant. The dependence of bivariant equilibria upon the externally controlled variables has been discussed by the author in a previous paper (Thompson, 1955). Where H_2O is not actively involved the equilibrium is univariant. Examples of univariant equilibria would be a change from kyanite to sillimanite or a reaction such as: sillimanite+biotite (+quartz+muscovite)→almandite+cordierite (+quartz+muscovite). In the latter example almandite or cordierite but not both (barring extraneous components) may be present on the left hand side (Fig. 9*a*), and biotite or sillimanite, but not both, on the right hand side (Fig. 9*c*). This equilibrium is univariant because muscovite and biotite are the only hydrous phases involved as well as the only potassic phases. In both, to a first approximation, H_2O is equal to $2K_2O$, hence, no water is gained or lost in the above reaction.

A complete sequence of projections representing all changes from the chlorite zone to the sillimanite zone in a metamorphic area must clearly, on geometric grounds, involve many independent discontinuities in facies. Furthermore, the sequence determined in one area should not be taken as one that should necessarily be applicable to any other metamorphic terrane. A different path with respect to P, T and η is quite likely to pass through a different sequence of facies.

The number of possible facies is certainly large, even if we regard as topologically "the same" those which may be transformed into one another by continuous variation, and it is not possible to indicate them all without more knowledge than we now have of the compositions of coexisting minerals. Knowledge of the relative values of the ratio $MgO/(MgO+FeO)$ in coexisting pairs limits the topological possibilities and a partial listing in order of increasing tendency to concentrate FeO is:

(1) Cordierite
(2) Biotite
(3) Staurolite
(4) Almandite

Chlorite is probably more "siderophile" than cordierite and less so than biotite. Chloritoid is definitely more siderophile than biotite, chlorite, or cordierite, but is of uncertain status relative to staurolite and almandite. Even if it were known that chloritoid came between staurolite and almandite in the above series, however, the relative topology of these three phases would still be ambiguous, as the chloritoid composition could still lie on either side of the tie line joining the staurolite and garnet occurring with it. Inversions in siderophile tendency are unlikely owing to the near ideality of the substitution of Fe^{++} for Mg. Once the topologic relationships have been determined it will be possible, at least in principle, to establish the possible facies and clarify their sequential relations to one another. The author will present chemical data bearing on this matter in a subsequent paper.

ACKNOWLEDGMENTS

The ideas contained herein were presented in part at a symposium on the role of volatiles in geological processes, at Luray, Virginia, in October, 1955, and in part at a symposium on metamorphic facies at Washington, D. C., in March, 1956. Both symposia were sponsored by the Geophysical Laboratory. The writer is grateful to the participants for their stimulating comment and discussion. Recent students of the writer have uncovered much pertinent petrographic information, and have detected many flaws with their questions. The writer is also indebted to John L. Rosenfeld and Marland P. Billings for critical review of the manuscript.

REFERENCES

ALLEN, W. C., AND SNOW, R. B. (1955), The orthosilicate-iron oxide portion of the system CaO-"FeO"-SiO_2: *Jour. Amer. Ceram. Soc.*, **38,** 264–280.

BALK, R. (1953), Structure of graywacke areas and Taconic Range, east of Troy, New York: *Bull. Geol. Soc. Amer.*, **64,** 811–864.

BARROW, G. (1893), On an intrusion of muscovite-biotite gneiss in the south-east Highlands of Scotland: *Geol. Soc. London, Quart. Jour.*, **49,** 330–358.

BARROW, G. (1912), On the geology of lower Dee-side and the southern Highland border: *Geol. Assoc. Proc.*, **23,** 268–284.

BARTH, T. F. W. (1936), Structural and petrologic studies in Dutchess County, New York, Pt. II: *Geol. Soc. Amer. Bull.*, **47,** 775–850.

BOWEN, N. L. (1925), The mineralogical phase rule: *Jour. Wash. Acad. Sci.*, **15,** 280–284.

BOWEN, N. L., and ANDERSEN (1914), The binary system MgO-SiO_2: *Amer. Jour. Sci.*, 4th ser., **37,** 487–500.

BOWEN, N. L., AND SCHAIRER, J. F. (1932), The system FeO-SiO_2: *Amer. Jour. Sci.*, 5th ser., **24,** 177–213.

CLARKE, F. W. (1924), The data of geochemistry, fifth edition: U. S. Geol. Survey Bull. **770,** 841 pp.

ESKOLA, P. (1915), On the relation between chemical and mineralogical composition in the metamorphic rocks of the Orijärvi region: *Comm. Géol. Finlande*, Bull. **44,** 145 pp.

HARKER, A. (1939), Metamorphism, second edition, revised: Methuen, London, 362 pp.

HEALD, M. T. (1950), Structure and petrology of the Lovewell Mountain quadrangle, New Hampshire: *Geol. Soc. Amer. Bull.*, **61,** 43–90.

JAMES, H. L., AND HOWLAND, A. L. (1955), Mineral facies in iron- and silica-rich rocks: *Geol. Soc. Amer. Bull.*, **66,** 1580–1588.

JUURINEN, A. (1956), Composition and properties of staurolite: *Ann. Acad. Sci. Fennicae:* Ser. A-III, **47,** 53 pp.

OSBERG, P. H. (1952), The Green Mountain anticlinorium in the vicinity of Rochester and East Middlebury, Vt.: *Vermont Geol. Surv.*, Bull. **5,** 127 pp.

PHILIPSBORN, H. VON (1928), Zur graphischen Behandlung quartenär systeme: *N. Jahrb. f. Min. Geol. Paläont.* Beil-Bd. **57,** Abt. A. 973–1012.

THOMPSON, J. B. (1955), The thermodynamic basis for the mineral facies concept: *Am. Jour. Sci.*, **253,** 65–103.

TILLEY, C. E. (1925), Petrographical notes on some chloritoid rocks: *Geol. Mag.*, **62,** 309–318.

TURNER, F. J. (1948), Mineralogical and structural evolution of the metamorphic rocks: *Geol. Soc. Amer.* Memoir **30,** 342 pp.

THE AMERICAN MINERALOGIST, VOL. 42, NOVEMBER-DECEMBER 1957

IONIC DIFFUSION AND THE PROPERTIES OF QUARTZ*

I. THE DIRECT CURRENT RESISTIVITY

Henry E. Wenden, *Harvard University, Cambridge, Massachusetts.*†

Abstract

The direct current resistivity of a number of Z-cut plates of natural quartz has been measured and the dependence of the axial resistivity upon temperature, field intensity, crystallographic orientation and time of passage of current investigated. The history of investigation of this property is summarized and previous results tabulated. The current flowing in a quartz plate under the influence of an electric field is complex, consisting of parts having characteristic time dependence and activation energies. The anomalous charging and discharging currents were investigated, and are considered to be the result of a reversible interfacial polarization having a relaxation frequency near 0.01–0.001 cycle/sec. The early surge current is connected with the migration of impurity ions and decays as a result of irreversible trapping and electrolytic exclusion of these ions. During the period of dominance of this current, quartz displays semiconductor behavior. Room temperature resistivity during this phase of conduction is of the order of 10^{13}–10^{19} ohm-cm, resistivity at 500° C. is of the order of 10^{5} ohm-cm, and activation energy lies in the range 20–25 kcal./mole. After passage of current for over 500 hours, the steady-state mechanism is unmasked, yielding an activation energy of 35–40 kcal./mole, room temperature resistivity of the order of 10^{27} ohm-cm, and resistivity at 500° C. of about 5×10^{9} ohm-cm. Quartz is shown to have a marked voltage coefficient of resistivity which varies with temperature and time of passage of current. This complex interdependence of the factors affecting the resistivity of quartz arises out of the common connection with the migration of impurity ions. Resistivity is a vectorial property but the exact nature of the dependence has not been completely investigated. Ionic diffusion in the equatorial direction has been observed, and has been demonstrated to play a part in the equatorial conductivity. Existing discrepancies and contradictions in reported values for the resistivity of quartz are shown to have their origin in the neglect of the factor of time of passage of current. When current is passed for a sufficiently long time to exhaust impurity ion connected mechanisms of conduction, the difference between axial and equatorial resistivity and the difference between different samples of quartz is of the same magnitude as the experimental error.

Introduction

Quartz is outstanding among minerals for the constancy of its physical properties. Except in those cases where numerous voids or inclusions are present, the density, indices of refraction and unit cell dimensions of clear quartz, and even of most colored varieties, show a remarkable consistency from sample to sample and locality to locality. A Harvard group (Frondel and Hurlbut (1953)), studying variations in these properties of quartz, found differences so minute as to require instrumental

---

* Contribution No. 383, Department of Mineralogy and Petrography, Harvard University, Cambridge, Massachusetts.

† Present Address: Department of Mineralogy, The Ohio State University, Columbus, Ohio.

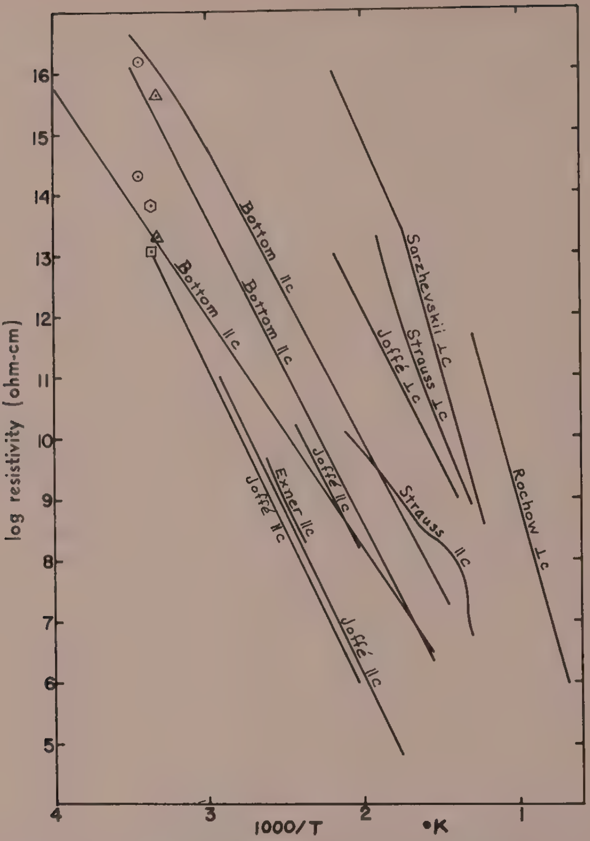

Fig. 1. Summary of published resistivity data, 1901–1956. Measurements over a range of temperature plotted as log resistivity vs. reciprocal of absolute temperature. Measurements at a single temperature by Thornton (circles), Curtis (hexagon), Richardson (triangles) and Klarmann (square).

techniques of the highest precision for their certain detection. Chemical analyses made in the course of that study revealed very low total impurity content (Table 3) and left considerable uncertainty as to the proper correlation of observed variations in physical properties with the impurities detected by analysis. Prof. C. S. Hurlbut suggested to the author in the fall of 1953 that light might be shed on these problems by the diffusion into quartz of impurity ions. Exploratory experiments yielded positive results, and a program to study the effects on the properties of quartz of impurity ions introduced by ionic diffusion was initiated.

In the course of this work precise information on the direct current resistivity of natural quartz became necessary in order to evaluate the contribution to the total conductivity of the introduced impurity ions undergoing diffusion. The data available in the literature presented a picture of inconsistency and contradiction quite at variance with the remarkable constancy of most of the other properties of quartz. Figure 1 summarizes the existing information up to the time of the present investigation. It will be noted that the values of axial resistivity* reported by different authors for any given temperature range over two decades. The slopes of the curves likewise show a wide range, indicating lack of agreement as to the energy of activation of the mechanism of conduction. As a result of the variation in slope of the curves, room temperature resistivities obtained by extrapolation (Table 1) show very large discrepancies. The agreement concerning the equatorial resistivity is only slightly better.

TABLE 1. SUMMARY OF EXPERIMENTAL METHODS

Author	Date	Temp (° C.)	Time of passage of current	Field intensity (volts/cm)	Electrode material	Resistivity (25° C.) (ohm-cm)	
						Axial	Equat.
Curie	1886–89	7–300	10s–11d	1–6000	Pt	1×10^{14}	3×10^{16}
Exner	1901	100–150	—	270–600	Na amalgam	1×10^{15}*	—
Thornton	1910	17	1m–144d	0.09–0.75†	none	2×10^{14}	1.5×10^{16}
Curtis	1912	26.5	0.5–1.0s	—	metallic	6.9×10^{13}	—
Richardson	1915–25	26.5	10s–20m	—	silver	2×10^{13}	4.3×10^{15}
Joffé	1928	26–500	to 190h	to 10,000	metal or graphite	1×10^{13}*	1×10^{19}*
Rochow	1938	500–1200	—	25	Pt foil	—	1×10^{29}*
Klarmann	1938	room	—	$1\text{–}2\times10^{5}$	silver	1.2×10^{13}	—
Sarzhevskii	1952	300–500	—	28000	—	—	1×10^{2} *
Verhoogen	1952	300–500	to 10d	350–1750	Pt	1×10^{20}*	—
Bottom	1953	−42–416	15 m	—	aluminum	6.4×10^{13} 1.6×10^{16}	—
King	1955–56	85–462	to 600h	500	Pt	1×10^{26}* 1×10^{28}*	—
Strauss	1956	200–500	1–20m	1000(?)	stainless steel	1×10^{17}*	1×10^{23}*
Wenden	1955–57	25–535	to 1400h	to 2000	Pt	1×10^{27}*	

* Extrapolated value, given as an order of magnitude.
† e.s.u.

Differences between axial and equatorial resistivity reported by any one author are as great as 10^6, if curves are extrapolated to room temperature. Moreover, if the least value for axial resistivity is compared with the largest value for equatorial resistivity, both reduced to room temperature, the difference is greater than 10^{15}. There is no basis in theory for such enormous differences in axial and equatorial resistivity of pure, ordered quartz. It is very probable that this effect is dependent upon impurities, and indeed it was suggested as early as 1887 (Warburg and Tegetmeier) that the migration of sodium through quartz in the direction of the c axis might account for the large observed difference in axial and equatorial resistivity. This is a reasonable postulate, and indicates that the resistivity is extraordinarily sensitive to impurity content, and hence is of peculiar significance in the study of the effect of such ions on the properties of quartz. For this reason, as well as to obtain reliable numerical values for this property, a series of careful measurements of the direct current resistivity were undertaken. This paper is a report on this phase of the problem.

---

* "Axial resistivity" is considered to be the resistivity of a quartz crystal for current flowing parallel to the c axis.

Historical Note

The first significant measurements of the direct current resistivity of quartz were made by Jacques Curie as a part of a thesis on the electrical properties of crystals, and were reported in 1886, 1888 and 1889. At the same time research on the electrical resistivity of quartz was being carried out by Warburg and Tegetmeier (1887, 1888). These pioneer efforts were remarkably successful, and most of the important features of the direct current conductivitiy of quartz were clearly indicated. For example, Curie recognized the dependence of the resistivity on the time of passage of current, and made a quantitative statement of the current-time relation in exponential form. Likewise, Warburg and Tegetmeier clearly demonstrated the axial transport of charge by sodium ions through quartz plates, and correctly inferred that the greater part of the short-term conduction is electrolytic. However, these observations, valid in themselves, did not lead to correct inferences concerning the general mechanism of conduction in quartz, and the subsequent history of investigation of this property is one of disagreement and inconsistency, arising in the main from neglect by the experimenters of the factor of time of passage of current.

Experimental Methods

The block diagram (Fig. 2) shows the essential elements of the apparatus used in the present study. Figure 4 shows the layout of the equipment and identifies the components.

A Z-cut disc of optical grade Brazilian quartz, polished on both surfaces, is placed in a vertical muffle furnace between platinum foil electrodes, and upon the upper electrode, insulated from it by a one-inch quartz cylinder, are placed stainless steel weights to maintain good contact. Another quartz cylinder insulates the lower electrode from the stainless steel block on which it rests, and the self-supporting leads from the electrodes leave the furnace through oversize clearance holes in the ceramic base. Figure 3 shows the holder assembly and furnace construction. A regulated power supply furnishing 0–1500 volts in 150 volt steps is connected in series with the test sample and the decade shunt of a

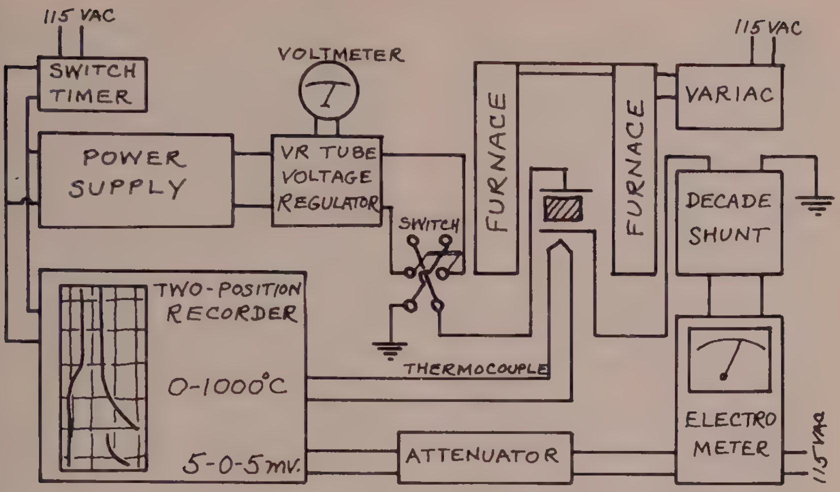

FIG. 2. Block diagram of apparatus for resistivity measurement.

Keithley Model 210 electrometer. A potential is impressed across the sample and a current flows through the shunt. The voltage across the shunt is read by the electrometer, whose output drives the 0–5 millivolt range of a two-position Leeds-Northrop Model G Speedomax recorder through a suitable attenuator. A thermocouple in the stainless steel block beneath the sample holder actuates the second range of the Speedomax recorder, which is directly calibrated in degrees C., so that a continuous record of furnace temperature and current flowing in the plate under test are kept on the same strip chart. A switch permits reversal of polarity of the applied voltage.

The furnace is counterweighted and slides up and down easily on stainless steel rods. The support framework of the furnace is designed to accommodate the electrometer beneath the furnace so that the critical lead from the sample to the high side of the electrometer shunt may be kept short. Furnace temperature is set by means of a General Radio V5 Variac, and line voltage fluctuations are suppressed by use of Raytheon voltage stabilizers.

The overall precision of the measurements is low, plus or minus 10 per cent, but is adequate for the purposes of this investigation. The general accuracy of the instruments was checked at regular intervals by comparison of the reading of the Speedomax against two different portable potentiometers, and by calibration of the voltage scales of the electrometer against standard cells. No guard electrode was used, as Rochow (1938) and others have shown that the error resulting from surface conduction is negligible above about 200° C.

Study of the ionic conductivity of quartz and of the mobility of ions

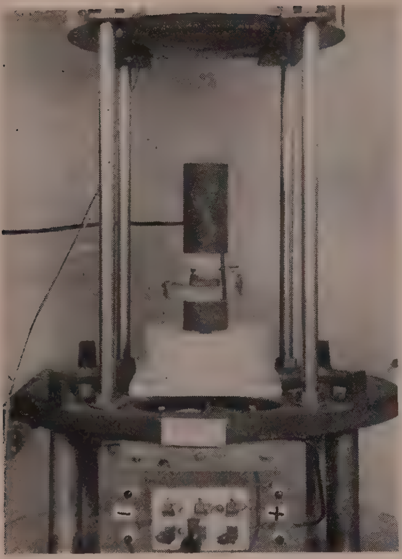

Fig. 3. Sample holder arrangement and furnace construction. Polarity reversing switch at lower center.

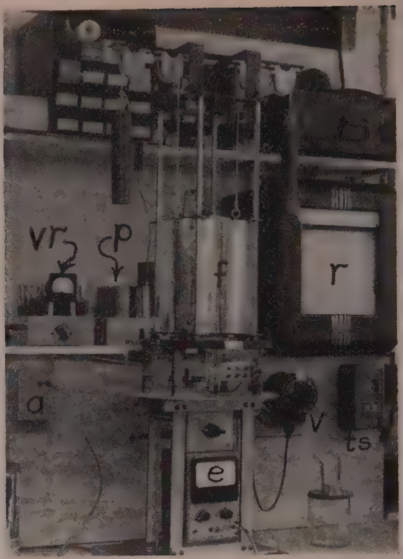

Fig. 4. Resistivity apparatus. *a*, attenuator; *e*, electrometer; *f*, furnace; *r*, recorder; *p*, power supply; *vr*, voltage regulator; *v*, variac; *ts*, time switch.

in quartz may be carried out simply by inserting between the quartz plate and the platinum anode a pressed pellet of a non-volatile, non-hygroscopic salt of the ion of interest. In Fig. 3, such a pellet of sodium chloride may be seen in place above the quartz disc. Ionic diffusion aspects of this study will be discussed in a later publication.

Dependence of the Resistivity on Time of Passage of Current

Of the many factors which determine the resistivity of quartz, the length of time during which the current flows in the sample is that which produces the largest effect, and which has the most complex relationship with the numerical value of the resistivity. For example, passage of current through a plate of quartz for over 500 hours produced an increase in resistivity of 10^8 ohm-cm.

Whenever a potential is applied to a plate of quartz a current flows which is large at first and diminishes rapidly with time. This current consists of four parts, each of which has its own time dependence. These are, in the order of their appearance:

(*a*) the normal dielectric charging current
(*b*) the anomalous charging current
(*c*) the surge current
(*d*) the steady-state direct conduction current

(*a*) The normal dielectric charging current, or displacement current, appears as an instantaneous "kick" of the galvanometer as the capacitor formed by the platinum electrodes, leads and switch gear charges. This current is generally interpreted as displacement in an applied electric field either of electrons in the electronic superstructure of ions, or of cations and anions relative to each other in the structure. The relative importance of the two types of displacement depends on the frequency of the exciting field (Mott and Gurney (1948)). In direct current measurements, where the capacitance of the circuit yields a time constant of a fraction of a second, this mechanism is of no practical importance.

(*b*) The anomalous currents are small currents which make their appearance whenever potential is changed, a charging current if the potential is increased, a discharging current if the potential is decreased. These currents are of short duration, having a relaxation time of the order of minutes, and are superposed on the currents resulting from other modes of conduction. Hence, when the currents due to other modes of conduction are very small the anomalous currents form a significant part of the total current, and the Law of Superposition, as stated by Curie (1889) and generalized by Jacquerod and Mugeli (1922) holds. This law may be stated: "The total quantity of electricity transported by the anomalous charging current is equal to that transported by the anomalous discharge current." This may be stated:

$$Q_{\text{charging}} = \int_0^t \mathrm{I}_c dt = Q_{\text{discharging}} = \int_t^\infty \mathrm{I}_d dt$$

Q is the quantity of charge in coulombs, I_c and I_d are the charging and discharging currents in amperes, respectively, t is time in seconds, and if it is supposed that the circuit is closed at time 0, charging current flows until time t, upon which the potential is removed or shorted out, and discharge current then flows until time ∞. Essentially complete charge and discharge, as measured with a practical electrometer, is reached in 5–15 minutes.

In an effort to isolate the mechanism of conduction responsible for the anomalous charging and discharging currents some experiments were undertaken using manually switched square-wave alternating current at frequencies of 1/900, 1/300 and 1/60 cycles per second.

At the time these experiments were made current had flowed in the test plate for a total of 108 hours at elevated temperature, so that further decrease of current during the short period of the tests was negligible. The tests were made at 100° C., a temperature at which the direct conduction current was too small to measure on the Keithley electrometer.

Polarity was reversed every 15 minutes, 5 minutes and 1 minute in

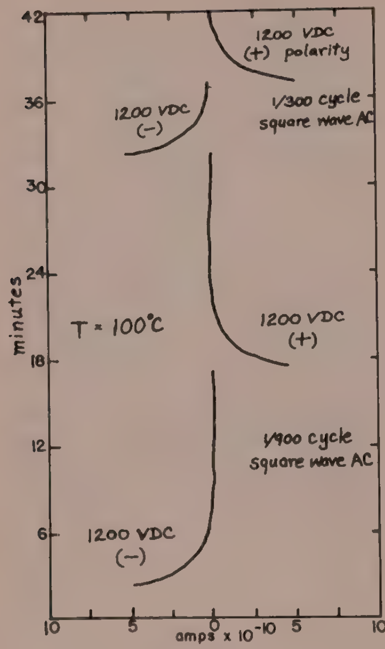

Fig. 5. Current-time curves for square wave alternating current at 100° C. Traced directly from the Speedomax strip chart.

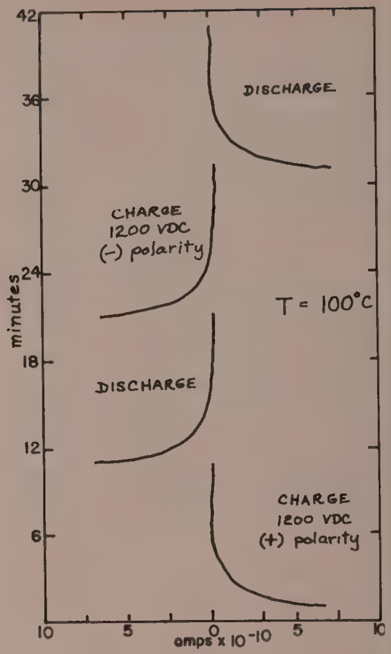

Fig. 6. Current-time curves for anomalous charging and discharging currents at 100° C. Traced directly from the Speedomax strip chart.

succession, recording several cycles at each frequency. Figure 5 is a tracing of the strip chart record for the 1/900 and 1/300 cycle/sec frequencies. Each half cycle is entirely symmetrical with the half cycles preceding and following. The mode of current decay for each half cycle can be closely approximated by Curie's formula

$$\rho = At^n \quad \text{where} \quad \left.\begin{matrix} A = 10^{12} \\ n = 1.4 \end{matrix}\right\} \text{at } 100^\circ \text{ C.}$$

and ρ is resistivity in ohm-cm, t is time in seconds, and A and n are constants for a given temperature.

Hence, although there is, strictly speaking, no measurable direct current flowing, if the time t above is small compared to the relaxation time of 6–7 minutes observed, there will be an alternating current flow that is appreciable due entirely to the anomalous charging current. In this way, the anomalous phenomenon acts to store and return energy into the external circuit just as a capacitor does. The question may arise, is this not in fact a capacitative effect? The capacitance of the platinum electrodes may be computed from the formula for a parallel plate capacitor as 0.7 $\mu\mu fd$ with air dielectric ($K=1$) for one inch diameter electrodes spaced 0.25 inch apart. But the capacitance of the system required to yield the charging current curve observed may be found from the formula

$$C = \frac{t}{R \log_e (E_0/E_t)} \text{ farads}$$

where t is time in seconds, E_0 the initial voltage read on the electrometer across shunting resistor R, and E_t the voltage read at time t. This formula is valid for capacitors either charging or discharging through a resistor, in this case the entire capacitance of the system discharging through the shunt in the decade box, 10^{10} ohms. Solving,

$$C = \frac{120}{10^{10} \log_e (5.2/1.5)} = 9650\ \mu\mu fd$$

This capacitance requires a dielectric constant for quartz of 13786. Whereas this is not an impossible value for dielectric constant, it is larger by a factor of 3000 than the customary value of 4.6 for the axial dielectric constant of quartz. Furthermore, if similar measurements are made at higher temperature, the value of K required becomes even greater. However, for alternating currents having higher frequencies, over 0.1 cycle /sec, the mechanism considered here does not operate, as the rise time of this current is of the order of a few seconds.

Joffé (1928) discards the concept of a change of dielectric constant of this magnitude as implying viscous processes in crystals for which no evidence exists. Field (1944), following Maxwell's theory of layered dielectrics, suggests that such an increase in dielectric constant results from the accumulation of charge carriers, either ions or electrons, at domain interfaces and submicroscopic defects in the lattice, constituting a reversible polarization which he terms interfacial polarization.

Field (1944) points out that if we consider the dielectric constant for optical frequencies, which is equal to the square of the index of refraction, as the result of electronic polarization and come down the scale of frequency, each new type of polarization encountered will produce an increase in the dielectric constant. Each type of polarization has associated with it a relaxation time T at which the polarization is within $1/e$ of completion, and a relaxation frequency f_m connected with the relaxation time T by the equation

$$f_m = \frac{1}{2\pi T}$$

at which frequency the loss factor has a maximum value. Entering this equation with values of T derived from the experiments described we find values for f_m in the range 0.01–0.001 cycle for the anomalous currents.

In the case of quartz, the mean dielectric constant for optical frequencies is about 2.4. For radio frequencies, the mean dielectric constant is about 4.6 for all frequencies from power to UHF. Hence, a relaxation frequency must lie somewhere in the microwave-infrared region, associated with the excitation of a new type of polarization, probably ionic displacement of lattice ions. We have just seen that there is evidence for another increase in dielectric constant in the 0.01–0.001 cycle/sec region. This increase must reflect the appearance of still another type of polarization. Field (1944) and Murphy and Morgan (1937) consider this to be interfacial polarization in the case of various commercial ceramic dielectric materials. Figure 7 shows the behavior of the dielectric constant and loss factor of quartz with frequency.

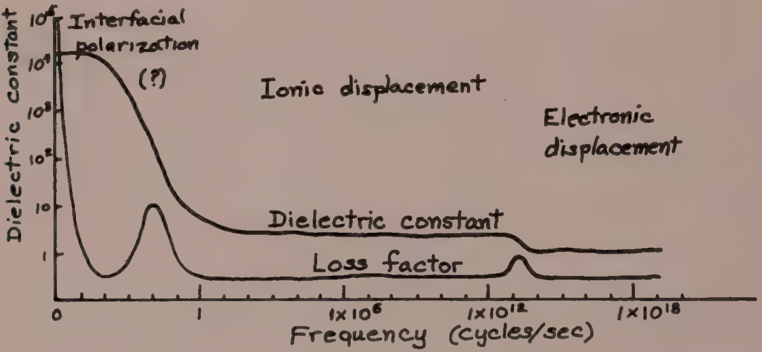

FIG. 7. Dielectric constant and loss factor of quartz over a wide range of frequency.

A series of charging and discharging curves were also recorded at 100° C. (Fig. 6) by applying a potential for 10 minutes, short circuiting the power supply for 10 minutes, applying potential with reversed polarity for 10 minutes, then shorting the power source for another 10 minutes. Charge and discharge curves are identical within the limits of precision of the method, indicating that the Law of Superposition holds, and that the phenomenon is completely reversible. The relation

$$Q_{\text{charging}} = Q_{\text{discharging}}$$

holds, and no direct current flow has taken place.

When this experiment is repeated at a higher temperature, the Law of Superposition holds for the anomalous part of the current, but does not for the entire observed current because the direct conduction current is large compared with the anomalous current. For this reason, charging and discharging curves taken at 280° C. are not symmetrical nor identical. In Fig. 8 note that the scales for charge and discharge currents are not the same. The discharge current for either polarity is identical in

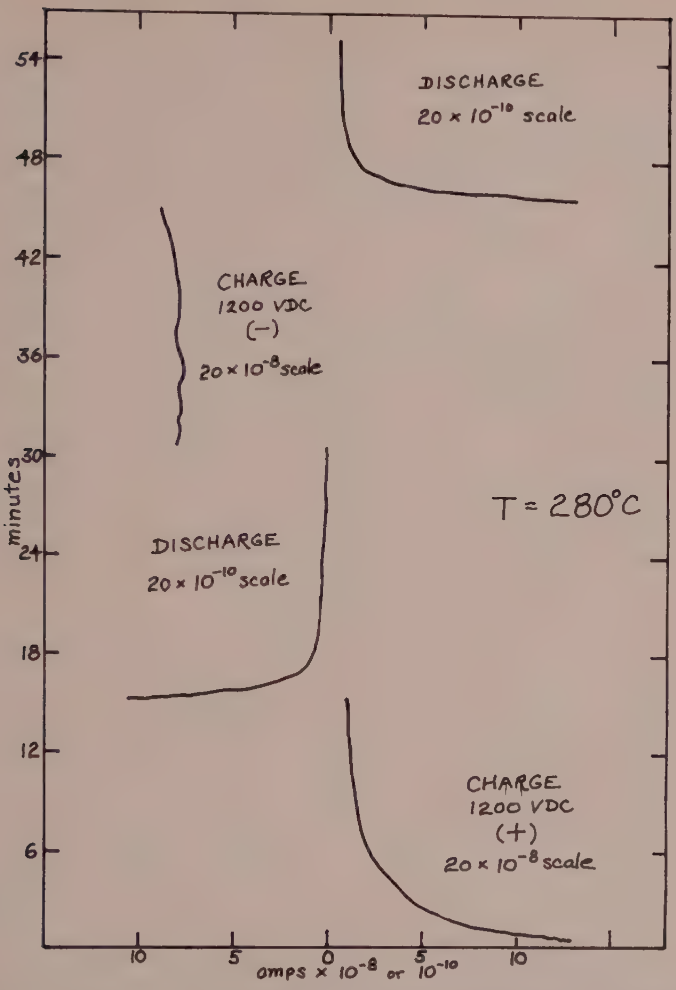

FIG. 8. Current-time curves showing charging and discharging current at 280° C. Note that the scale for the charging current is not the same as that for the discharging current. Traced directly from the Speedomax strip chart.

magnitude and waveform to that yielded after charging with opposite polarity at the same temperature for the same time, although the charging current curves display an asymmetry resulting from the semiconductor behavior of quartz discussed later in this paper.

This experiment indicates clearly that the anomalous charging currents are independent of, and superposed on those currents carried by other mechanisms. The anomalous currents increase with increase in temperature, but at a much smaller rate than the direct conduction current. When the temperature was increased from 100° C. to 280° C. in the preceding experiment, the increase in peak value of charging current was only about 0.3 per cent of the increase in direct conduction current. Thus, the anomalous currents seem to be present at all temperatures but relatively insensitive to temperature changes. They probably contribute little to the net conduction. They are not a significant source of error in measurements of resistivity unless the current is read within a few minutes after application of potential. We may consider that these currents are caused by displacement of non-lattice ionic and possible electronic charge carriers, and that the decay of the charging current is the result of the reversible trapping of charge carriers at domain interfaces and lattice imperfections. The discharge current is the result of equalization of distribution of charges after the removal of the exciting potential. Sarzhevskii (1952) has shown that free electrons exist in quartz at temperatures below 300° C. and these may play a part in the anomalous currents at these temperatures, but the dominant role of cations seems to be established by Joffé's (1928) observation that the density of the space charges which appear in quartz in an electric field is always greatest near the cathode, regardless of polarity.

(*c*) The third part of the current is one which constitutes the largest part of the total current for several hours after application of potential, and which because of its behavior I shall call surge current. Upon application of *e.m.f.* for the first time at any given temperature, current rises rapidly to a maximum, reaching peak value in less than three minutes, and in many cases in less than one second. Thereafter, current decreases with passage of time.

The decrease is rapid for the first hour, generally to one per cent or less of the initial peak current. For the next 5–7 hours the current decays less rapidly, reaching about 50 per cent of the one hour current at 6–8 hours from the start of the run. The current then falls much more slowly, the rate of change of current with time decreasing slowly as current decreases. This trend continues for over 500 hours.

For time of flow of current up to one hour, the rate of decay of current, ratio of peak current to one hour current, and form of the decay curve differ from run to run, temperature to temperature, and sample to sample (Fig. 9). However, after the first hour, a pattern is well established. From about the end of the first hour to the sixth or eighth hour, if the logarithm of the resistivity is plotted against the reciprocal of the time, this portion of the curve is almost a straight line (Fig. 10). About the sixth to the eighth hour, a fairly sharp inflection in the log reciprocal curve indicates a decrease in rate of change of current with time. Beyond 24 hours, the curve becomes asymptotic.

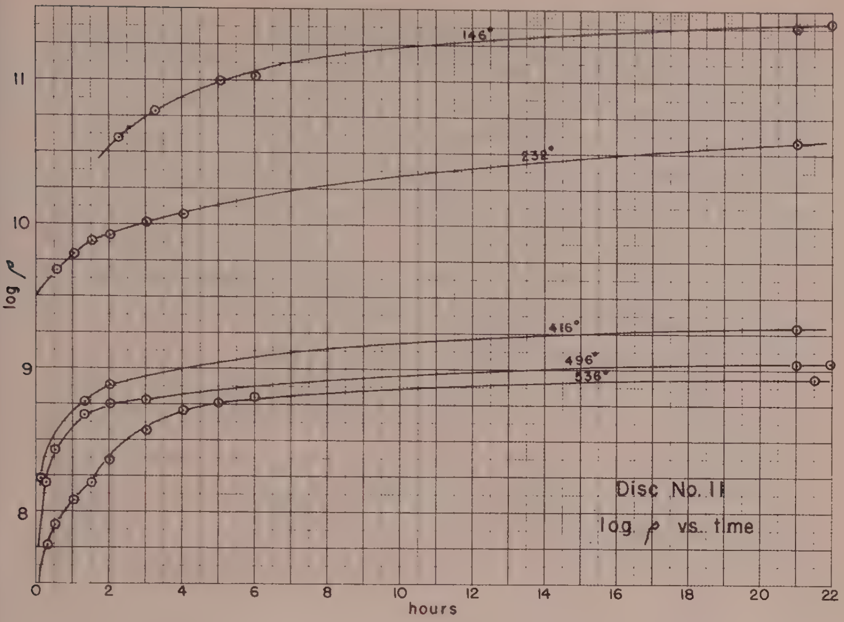

FIG. 9. Logarithm of resistivity in ohm-cm. vs. time in hours.

Thus, the resistivity-time relation may be divided into three fairly distinct phases:

(1) rapid and rather erratic increase in resistivity during the first hour
(2) more gradual increase in resistivity approximating to an exponential function of time from one hour to 6–8 hours
(3) still slower increase of resistivity from 6–8 hours to over 500 hours, becoming negligible

This threefold division of the current-time relation was observed also by Thornton (1910) using a wholly different method of experimentation. Note that this threefold division does not include the anomalous current. The surge current is, for temperatures above 200° C. during the time that it is dominant, orders of magnitude greater than the anomalous current. The surge current has a very marked temperature dependence, leading to activation energies in the range 10–30 kcal/mole, whereas the anomalous currents increase only slightly with temperature. The polarization causing the anomalous currents is completely reversible, whereas the mechanism causing the surge current is almost completely irreversible.

It is of interest to note that Curie (1889) stated the relation between resistivity and time in the form

$$\rho = aT^n$$

where ρ is the resistivity, T is the time, a and n are constants, a depending chiefly on temperature, and n roughly constant for a given specimen.

This equation was tested and found to fit reasonably well that portion of the time-resistivity curve between one and eight hours. The generalization fails for longer runs, and Curie's constants a and n for runs which exceeded one day are markedly different from those for runs of three hours or less. The decay curve of the anomalous current has the same general form, a circumstance which has probably given rise to a great many misunderstandings. Most authors fail to distinguish between the surge current and the anomalous current on the one hand, or between the surge current and the steady-state conduction current on the other. The surge current is a transitory, but perfectly definite phase of the conduction process in dielectrics. The empirical data accumulated during the present study concerning the surge currents can be fitted only by an expression containing additive terms, which may themselves be complex functions. An example of such a general expression is that derived by Jacquerod and Mugeli (1922) for the anomalous resistivity, and has the form

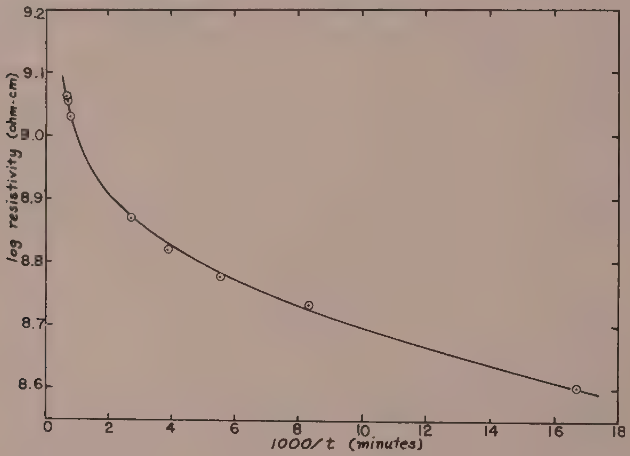

FIG. 10. Log resistivity vs. reciprocal of time in minutes. Disc No. 11 at 499° C.

$$\rho = \rho_0 e^{at} + \rho_1 e^{bt} + \rho_2 e^{ct}$$

where ρ_0, ρ_1, and ρ_2; a, b, and c are constants.

If, after the passage of current in a given direction and at a fixed temperature for 24 hours, the polarity is suddenly reversed, the resistivity-time relation for the new polarity is not symmetrical with the first run. Repeated reversals of polarity produce runs adhering to the same pattern. The maxima of current are always higher for the runs whose polarity corresponds with that first selected, and the time of rise to maximum is shorter, whereas for all subsequent runs on the opposite polarity, alternating with those of the first polarity, the maxima are lower and the rise times longer. In all cases, after less than four hours, these initial effects have disappeared and current declines slowly, the absolute value depending only on the total time elapsed since the beginning of the first run, and not on polarity or sequence of polarity changes. Table 2 gives current and time values for two temperatures.

TABLE 2. POLARITY SENSITIVE EFFECTS IN ELECTRICAL CONDUCTION IN QUARTZ

Temp (° C.)	Run	Polarity	Maximum current (amps)	Rise time (mins)	24-hour current (amps)
418	1	+	3.7×10^{-3}	1	5.0×10^{-6}
	2	−	3.1×10^{-4}	18	3.8×10^{-6}
	3	+	8.3×10^{-4}	10	3.2×10^{-6}
	4	−	2.0×10^{-4}	26	2.5×10^{-6}
499	1	+	4.1×10^{-3}	2	8.3×10^{-6}
	2	−	2.8×10^{-4}	17	7.8×10^{-6}
	3	+	1.0×10^{-3}	6	6.3×10^{-6}
	4	−	2.5×10^{-4}	20	5.2×10^{-6}

This simply means that quartz, for the short-term surge current, behaves as a semiconductor, in which the first application of potential determines the polarity of the forward, or easy, direction of conduction, so that the magnitude of the current flowing at any time thereafter depends not only on the potential and the temperature, but also on the direction of flow.

Up to the current maximum and for a few hours thereafter the dominant mechanism of conduction is one whose activation energy is low and varies from sample to sample. While this mechanism dominates, the sample may show semiconductor characteristics. After the disappearance in 4–8 hours of polarity sensitive effects, the conduction is dominated by a mechanism of higher energy of activation which operates progressively, so that current becomes a function only of total time of passage of current for a given temperature and potential.

This large initial current, the surge current, is almost certainly attributable to the mobilization of non-lattice impurity ions acting as charge carriers. These may, upon continued maintenance of an electric field, become irreversibly trapped in lattice defects or migrate to the surface of the test sample and there plate out, so as to become unavailable for further transfer of charges. At any given temperature, the trapping and exclusion of ionic carriers at the surface of the plate or in lattice defects during the initial current surge introduces a polarity-sensitive or semiconductor behavior apparent in all later runs at that temperature. The carriers involved in this mechanism are those impurity ions most favorably placed to participate immediately in conduction with a low energy of activation. As these become exhausted by irreversible trapping or removal, the initial surge current decays, giving way to the more slowly decreasing current (long-term surge current) carried by interstitial impurity ions less favorably placed for conduction. These latter ions probably move through the celebrated "tunnels" or "pores" parallel to the c axis, whereas the ions contributing to the early surge current may be located along domain boundaries, growth lines or other imperfections and hence are less firmly bound.

The reality of this process of exclusion and plating out of impurity ions is attested by the visible deposit of salts found at the cathode surface of every plate of natural quartz that underwent a long resistivity run. Although too scanty for analysis, these cathode deposits yield a qualitative test for sodium, and Verhoogen (1952) describes the collection of detectable amounts of boron at the cathode after measurement of an Arizona quartz crystal. If such a plate is cleaned and rerun at a later time, the resistivity remains high and surge current effects are much less marked than during the first run.

(*d*) The fourth part of the current is the long-term, steady-state current which becomes manifest only after the disappearance of the short-term effects. Decay of the masking impurity ion currents seems to be complete at 1200 hours, and may in some cases, be complete at 500.

Mott and Gurney (1948) suggest that this current may be due, at the higher temperatures, to mobilization of all the ions in a crystal, or all the ions of one sign. Demonstration of the electrolysis of quartz is difficult, since the total amount of silicon that would be liberated by a current of 10×10^{-6} amperes is

$$m = \frac{It(7.01)}{96{,}485} = 6.3 \times 10^{-5} \text{ gms./day}$$

Slightly more than half as much oxygen would be produced. At the rate computed more than three months would be required to accumulate 6 mg. of silicon at the cathode. The current postulated above is approximately that which would flow through a one-quarter inch plate of quartz at a potential of 1500 volts during a lengthy run. Electrolytic dissociation of the quartz could certainly account for the observed currents without visible deterioration of the plate. It may well be, however, that only oxygen ions, or oxygen ions and holes, are mobile.

Sarzhevskii (1952) has shown by the absence of the Hall magnetoresistance effect above 300° C. that the conductivity is primarily ionic above that temperature. The number of free conduction electrons below 300° C., where a Hall effect was noted, is 10 to 10^5 electrons/cm^3. This small number indicates that the conductivity of quartz at all temperatures is predominantly ionic. Sarzhevskii's work was done on equatorial plates, and consequently the conductivity he discusses is chiefly the characteristic, or steady-state, conductivity, since short-term surge current effects are much less marked in equatorial plates.

The question of the ability of impurity ions to carry the current observed to flow up to the point where the steady-state mechanism becomes dominant may be settled by reference to analyses of quartz made during a Harvard study (Frondel and Hurlbut (1953)) which are presented in Table 3.

TABLE 3. ANALYSES OF QUARTZ (WEIGHT PER CENT)

Sample	Ti	Mn	Fe	Al_2O_3	Na	K	Li
1	0.0001	0.00002	—	0.0008	0.0004	0.0002	0.0005
2	.0002	.00002	.0003	.0008	—	—	.0004

1. Colorless quartz (C105), Arkansas.
2. Dark smoky quartz (S101), Brazil.

These analyses are taken as representative of clear quartz, and hence of the optical grade material used in this study. Total impurities do not, in general, exceed 0.1 per cent, even in strongly colored and visibly impure material. Calculating on the basis that all ions except aluminum, which is considered to be in tetrahedral coordination, are mobile and free to participate in conduction, the impurities listed for Sample Number 1 in Table 3 are capable of transferring 0.638 coulombs of charge. In terms of a typical current-time curve, such as that shown for 496° C. in Fig. 9, this means that the impurity ions are capable of carrying the total integrated current up to 10.5 hours from the beginning of the run. Since the steady-state mechanism is also participating, the effects consequent upon the presence of impurities may be expected to die away in 12–24 hours, a figure in good agreement as to order of magnitude with suppositions based on the nature of current decay and the disappearance of semiconductor effects. At the end of this time, the current must be carried entirely by the steady-state mechanism. If the temperature is raised, a new current surge is to be expected, since ions irreversibly trapped at the lower temperature may be freed to participate in the short-term conduction again at a higher temperature.

Even if we assume a figure for the total mobile impurities ten times greater than that given by analyses 1 and 2, the capacity of these impurity ions to transfer charges could still be exhausted within the duration of the runs made in this study. Since Sarzhevskii's work seems to indicate that this current cannot be electronic, we are forced to the conclusion that the long term, steady-state current must arise from electrolysis of the quartz itself.

Variation of Resistivity with Temperature

Perhaps the most fruitful approach to the mechanism of conduction in quartz is through variation of resistivity with temperature. In this study, the upper limit of temperature was arbitrarily set at about 540° C. The resistivity of high quartz was not considered. The lower limit was set by the sensitivity of the electrometer at about 25° C.

The chief problem in studying the variation of resistivity with temperature is the separation of the effects of temperature from the effects of elapsed time and applied potential.

Some experimenters have used alternating current, which involves a frequency-sensitive polarization and yields small values for the resistivity compared with direct current measurements made over long periods of time. Other experimenters have used direct current, but have applied potential at a given temperature for only short periods, reversing polarity after a few minutes, and taking the average of the readings made on opposite polarities as the current for that temperature. The potential is then removed while the plate is brought to a new temperature. In this way an entire sequence of measurements over a wide temperature range may be made without exceeding a few hours total time of passage of current. Thus, all measurements are made within the period of dominance of the short-term surge current. If readings are taken after 15 minutes or more, the anomalous current is excluded; if after a shorter time interval, a portion of this current is also included. If a regular procedure is followed at all temperatures, a self-consistent body of data may be obtained, yielding the activation energy for the short term mechanism. This seems to have been the procedure followed by most early investigators. Disc No. 12 (Fig. 12) was measured in this way and yields, for the resistivity, good agreement with the mean of Bottom's (1953) results, (Fig. 1) and for the activation energy, good agreement with the mean of all earlier investigators for axial resistivity. Measurements made in this way plot as straight lines on the conventional arith-log display of log resistivity vs. reciprocal of absolute temperature, provided all measurements were made the same length of time after application of potential.

Investigators differed widely in their practice as to time of reading current after application of potential. Curie (1889) recommended one minute, F. Braun suggested 24 hours. Others have attempted to read instantaneous peak current at the moment of application of potential. Strauss (1955) read current every minute, reversing polarity every 20 minutes, while increasing temperature uniformly. Other investigators maintain potential at all times and cycle temperature, reading current whenever thermal equilibrium is established. Unless current is first allowed to pass through the test plate for a period of hundreds of hours, measurements of this kind result in an inextricable mingling of the effects of temperature and time. Such measurements plot on the log resistivity vs. reciprocal temperature graph as curved rather than straight lines.

The principal reason for the diversity of results and lack of agreement among these investigators lies in the different methods of dealing with the factor of time.

In order to separate the effects of temperature and time it is necessary to allow current to pass through the plate until further changes of current with time are negligible. The temperature may then be cycled with potential continuously applied, and measurements of current made whenever thermal equilibrium is reached. A total of 70 current measurements was made on one such plate (Disc No. 11) through which current had been passed for over 500 hours.

A plot of these 70 points (Fig. 11) reveals two straight line segments joined at an inflection point at about 350° C. This test plate, through which current had been passed with positive polarity for nearly 600 hours, was removed from the furnace for about four weeks. It was then thoroughly cleaned and reassembled in the furnace with clean platinum electrodes. A new series of measurements was then made with negative polarity from 26° C. to 525° C. The values of resistivity obtained were in close agreement with the earlier values, but were slightly higher. A final series of measurements were taken on this plate after the total cumulative time reached 1400 hours (Fig. 11). This series is best represented as a straight line without inflections on the log resistivity-reciprocal temperature plot.

The overall tendency in this last experiment was to straighten out the resistivity temperature curve, and increase all values of resistivity. This indicates that quartz which has been electrically treated does not regain its initial conductivity by standing for a time comparable with the time of passage of current, as claimed by Curie (1889). Both high and low temperature portions of this curve move toward higher resistivity with time. The low temperature branch changes somewhat in slope with passage of time and the inflection appears to migrate to lower temperatures, finally disappearing, whereas the high temperature portion moves more nearly parallel to itself.

The work of King (1955, 1956) has strikingly confirmed these findings. In King's experiments the factor of time has been effectively separated from that of temperature, following Wenden (1955), by passing current through the plate for a period of weeks before making measurements. Accordingly, his results are directly comparable with those reported here, and afford excellent numerical agreement both as to absolute resistivity and activation energy (Fig. 12 and Table 5). Since King's observations embody some at temperatures lower than were possible with the Keithley electrometer, they extend the results of this study in a most interesting way. It appears that the knee, or inflection point of the two-branched curve described above does not disappear with continued passage of current, but migrates to lower and lower temperatures. Hence, we may conceive of a family of curves resulting from a series of measurements of resistivity at different times during a very long run like those shown in Fig. 13.

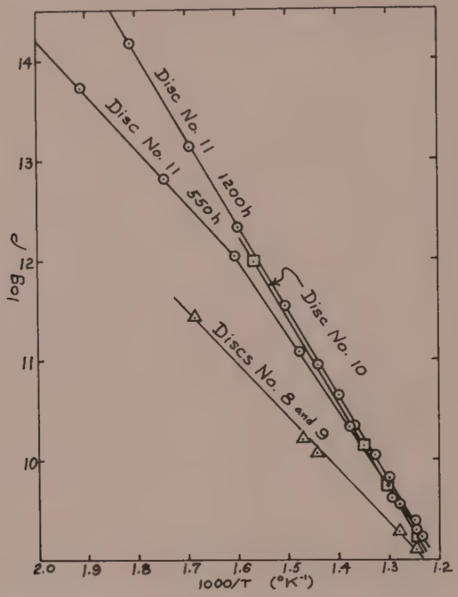

FIG. 11. Logarithm of resistivity vs. reciprocal of absolute temperature for Discs 8 and 9, 10, and Disc No. 11 after passage of current for 550 hours, and again after passage of current for 1200 hours. See Table 5a for identification of disc numbers. All are Z-cut discs of natural quartz.

Considering separately the two portions of the two-branched curve obtained after three weeks (Disc No. 11, Fig. 11), it is found that each may be represented within the limits of error of the method by an expression having the form

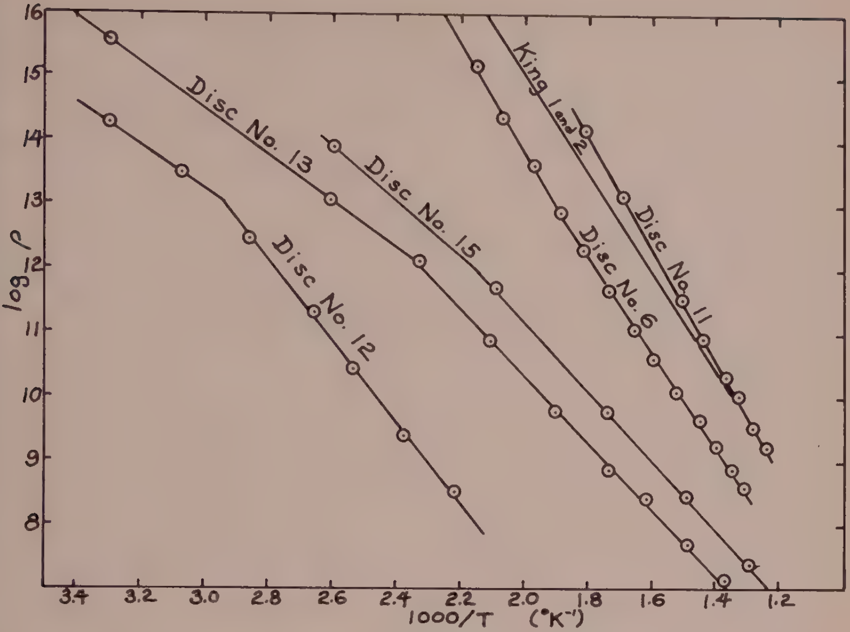

FIG. 12. Log resistivity vs. reciprocal temperature. Discs 11, 12 and 13 are Z-cut, Disc No. 6 is inclined 51°40′ and Disc No. 15 is X-cut. Discs No. 13 and 15 were run with NaCl anodes. Discs 11 and 6 passed current for 1400 and 2000 hours, Disc No. 12 for about 3½ hours. King's (1956) curve for natural quartz is included for comparison.

$$\rho_1 = A_1 e^{U_1/RT}$$

If T is given values lying between 298° and 623° K., ρ_1 is the resistivity over that range of temperature, U_1 is the activation energy of the dominant mechanism of conduction over that range, R is the molar gas constant equal approximately to 2.0, and A_1 is a constant which fixes the absolute values of resistivity. Similarly, for the upper branch of the curve

$$\rho_2 = A_2 e^{U_2/RT}$$

where the symbols have the same meaning as before except that T has values between 623° and 809° K., and ρ_2, U_2 and A_2 apply to this temperature range.

Calculation of the constants from the measured values of resistivity yield

Temperature Range	U	A
298°–623° K.	26.0 kcal./mole	910
623°–809° K.	34.0 kcal./mole	1.47

Calculation of the activation energy from the values of resistivity measured after passage of current for over eight weeks yields only one value, which affords a good fit for all observations recorded. The inflection point present in the earlier observations made on this same sample has migrated to lower temperature, beyond the range of sensitivity of the electrometer.

Temperature Range	*U*	*A*
279°–808° K.	39.5 kcal./mole	24.55

The activation energy *U* is notably higher, reflecting an increase in slope for the curve as a whole.

Many experimenters have found that similar expressions may be used to represent the conductivity of ionic crystals (Mott and Gurney (1948), pp. 36 63; Jost (1952), pp. 179–197). Two-branched curves, the higher temperature branch having the greater activation energy, have been observed in NaCl, LiCl, LiF, KBr and most of the other alkali halides, and also in PbI_2 and other salts of lead, silver and copper. These curves are represented by Smekal, Lehfeldt and Seith by formulas having the form

$$\sigma = A_1 e^{-U_1/RT} + A_2 e^{-U_2/RT}$$

consisting of additive terms of exponential form, where the symbols A, U, R, etc., have the same meaning as in the discussion immediately preceding, and σ is the conductivity.

Interpretation of these terms is varied. Smekal considers the first term (in NaCl) to correspond to conduction by surface particles, whereas the second represents electrolytic conduction in the normal lattice. Seith interprets the first term in PbI_2 as the conductivity of the Pb ions, and the second term as the conductivity due to the I ions. Jost suggests the first term may represent the influence of interstitial impurity ions, whereas the second term reflects the "correct conductivity" of the crystal. Mott and Gurney, in commenting on Smekal's results for NaCl, reject Smekal's interpretation of the first term as surface conductivity, and remark that (p. 39): "Clearly the first term gives the conductivity due to a small number of ions in special places, which can be released easily, while the second term is that due to a large number; all the ions in the crystal, or all the ions of one sign, which can only be released with greater difficulty." Mott and Gurney refer to the first term as the "structure-sensitive" part of the conductivity.

The calculated activation energy for the low temperature mechanism in Disc No. 11 above, and the activation energy for Disc No. 12, which was measured so as to obtain the activation energy of the short term mechanism, are both very close to that found for the diffusion of alkali metal ions in quartz (Tables 4 and 5). Table 5 shows, for purposes of comparison, the activation energies for conduction mechanisms in quartz.

There is, in the data presented in Tables 4 and 5, a very strong suggestion that all investigators prior to Wenden (1955) and King (1955, 1956) have been measuring, not the axial resistivity of quartz, but the mobility in quartz of impurity ions; from the activation energies reported, probably alkali metal ions.

Activation energies and absolute magnitudes both suggest that the equatorial resistivities of earlier workers were more nearly a measure of the actual resistivity of pure quartz, but the wide spread to be found in the published results, coupled with experimental evidence from this study (Fig. 12), indicate that ionic diffusion and lattice defects influence the equatorial resistivity as well. Compare curves for Discs 13 and 15.

VOLTAGE DEPENDENCE OF RESISTIVITY

It has long been recognized that quartz, like many other dielectrics, does not rigorously obey Ohm's Law. That is, the relation between voltage and current for a given temperature is not linear, and the apparent resistivity of a sample held at constant temperature varies with the intensity of the electric field applied to it (Fig. 13). Shaposhnikov (1910) stated that quartz obeys Ohm's Law up to a field intensity of 4000 volts /cm for short periods, with the resistivity decreasing for more intense fields or longer times of flow. Frenkel (1938) suggested for the relation of

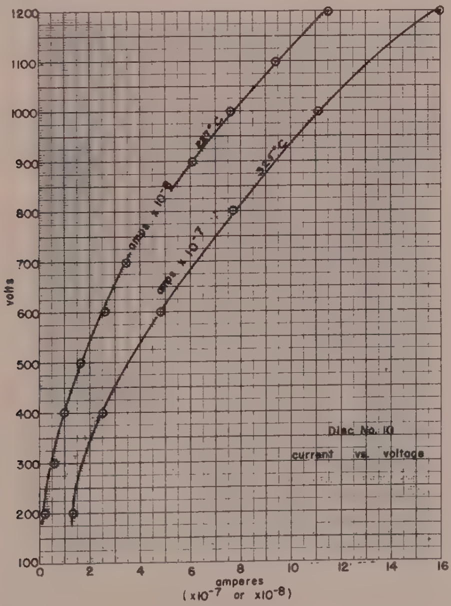

Fig. 13. Non-linear relation between voltage and current for quartz.

TABLE 4. ACTIVATION ENERGIES OF ALKALI METAL IONS IN QUARTZ

Ion	Activation energy	Author	Date
Li	20.4 kcal./mole	Verhoogen	1952
Li	17.7 kcal./mole	Stuart	1955
Na	22–25 kcal./mole	Vogel & Gibson	1950
Na	24 kcal./mole	Verhoogen	1952
Na	24.1 kcal./mole	Wenden	1957
K	31.7 kcal./mole	Verhoogen	1952

resistivity to field intensity the expression

$$\rho = \rho_0 e^{-\beta\sqrt{E}}$$

where ρ_0 is a constant determining the absolute magnitude of the resistivity and β is a constant depending on the orientation of the sample. E is the field intensity in volts/cm.

Sarzhevskii (1952) incorporated Frenkel's formula into a two-term expression for the dependence of resistivity on both temperature and voltage

$$\rho = \rho_1 e^{B_1/T} + \rho_2 e^{B_2/T}$$

where ρ_1 and ρ_2 are constants for the particular sample, B_2 depends on the thermal activation energy of the principal conduction mechanism, and

$$B_2 = \frac{U}{R}$$

where R is the gas content, U the activation energy in cal/mole. B_1 is a complex function depending both upon orientation and voltage

$$B_1 = B_0 - \beta\sqrt{E}$$

where B_0 is a constant for a given sample, β depends on the orientation and E is the field strength in volts/cm. If the temperature is made constant for a given sample, Sarzhevskii's equation reduces to Frenkel's.

A number of measurements of resistivity were made at different temperatures, varying the voltage in 150 volt steps from 150 to 1200 volts while holding the temperature constant. One set of measurements was made on a quartz plate through which current had been passed for only a few days. Another set was later made on the same plate after current had passed through it for over two months. These measurements are plotted in Figs. 14 and 15 as the common logarithm of the resistivity vs. the square root of the field strength in volts/cm.

For the short term mechanism; that is, those modes of conduction that depend on the presence of impurity ions, Fig. 13 indicates that the resis-

TABLE 5. ACTIVATION ENERGIES OF THE CONDUCTION MECHANISMS IN QUARTZ, AND ABSOLUTE VALUES OF THE RESISTIVITY

Author	Temp (° C.)	Resistivity (ohm-cm.)		Ratio $\frac{eq}{ax}$	Activation energy (kcal./mole)				Constant A
		Axial	Equat.		Axial		Equat.		
					High	Low	High	Low	
Curie	20	1×10^{14}	3×10^{16}	300					
Thornton	17	2×10^{14}	1.53×10^{16}	131					
Richardson	26.5	2×10^{13}	4.3×10^{15}	215					
Joffé	25	1×10^{13}	$1 \times 10^{19*}$	1×10^{6}					
	500	1.6×10^{2}	5.6×10^{8}	3.5×10^{6}		24.4		22.5	7.26×10^{-4}
Rochow	500	—	4.75×10^{11}						
	1200	—	9.1×10^{5}				42.9		2.36
Verhoogen	500	2×10^{9}	—			23			
Sarzhevskii	560	—	3.81×10^{8}				42		
	302	—	2.51×10^{13}						
	178	—	1.0×10^{16}					21	2.63×10^{5}
Bottom (Clear)	25	2.24×10^{13}				17.7			2.86
	500	2.9×10^{5}							
Bottom (Smoky)	12	1.26×10^{16}				22.9			0.0405
	298	2.09×10^{7}							
Bottom (Synthetic)	12	4.17×10^{16}				20.9			4.66
	417	1.78×10^{7}							
King Natural	107	9.12×10^{17}			35.5				2.33
	177	6.03×10^{16}				13.4			1.95×10^{10}
	461	1.45×10^{10}							
King (Synthetic)	111	5.76×10^{17}			39.0				
	230	2.40×10^{15}				11.1			2.2×10^{11}
	460	1.00×10^{10}							
Strauss	203	1.0×10^{10}	4.0×10^{14}	4.0×10^{4}		18.4			42.6
	496	6.3×10^{6}	7.96×10^{8}	127				31.3	1.17
Wenden (Disc 9)	529	1.28×10^{9}				24.2			362
	321	2.58×10^{11}							
Wenden (Disc 10)	528	1.64×10^{9}			39.9				0.025
	365	9.57×10^{11}							
Wenden (Disc 11)	535	1.65×10^{9}			39.5				24.55
	390	3.42×10^{11}							
	279	1.54×10^{14}							
Wenden (Disc 12)	177	3.30×10^{8}				25.0			0.0024
	121	2.73×10^{10}							
	76	2.99×10^{12}							
Wenden (Disc 13)	500	4.65×10^{6}				24.2			1.34
	156	1.32×10^{12}							
Wenden (Disc 15)	499	—	2.25×10^{7}					25.1	1.97
	205	—	4.98×10^{11}						
Wenden (Disc 6)	490	3.88×10^{8}			36.0				0.0205
	302	4.78×10^{11}							
	168	1.18×10^{16}							

TABLE 5A. EXPLANATION OF DISC NUMBERS IN TABLE 5

Disc No.	Cut	Electrodes		Field strength (volts/cm)	Time of passage of current
		Cathode	Anode		
6	51°40′	Au	Pt	2450	2000h
8	Z	Pt	Pt	1880	100h
9	Z	Pt	Pt	1880	100h
10	Z	Pt	Pt	1880	282h
11	Z	Pt	Pt	1880	1400h
12	Z	Ag	Ag	1880	15m
13	Z	Pt	NaCl	156	108h
15	X	Pt	NaCl	156	60h

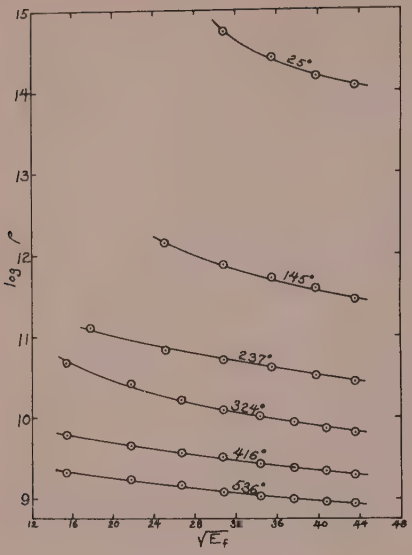

FIG. 14. Logarithm of resistivity vs. the square root of the field strength in volts/cm for a number of temperatures. Disc No. 11 after passage of current for 100 hours.

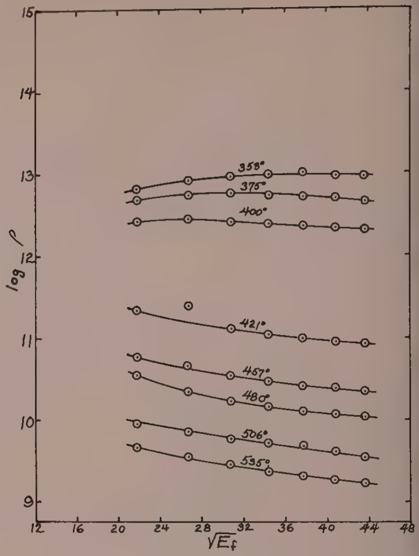

FIG. 15. Logarithm of resistivity vs. the square root of the field strength in volts/cm for a number of temperatures. Disc No. 11 after passage of current for 1400 hours.

tivity is decreased with increased field intensity at all temperatures. This observation is in agreement with the findings of Shaposhnikov, Klarmann and Mühlenpfordt (1938), Strauss (1955) and almost all investigators who have commented on the voltage dependence of the resistivity.

In the series of measurements made on the sample after passage of current for two months, it appears, below 375° C., that increase in field strength produces an increase in resistivity, whereas for higher temperatures there is an apparent decrease in resistivity for increased field strength. In no case do the plotted values indicate a strictly constant value for β in Frenkel's formula, although both Frenkel's and Sarzhevskii's equations yield close approximations to the measured resistivities at most temperatures. Agreement with Frenkel's formula is closest at the higher temperatures in both the short term and long term measurements. The factor of time clearly enters this relationship as it does all other aspects of the resistivity.

Frenkel has attributed the decrease in resistivity at higher field intensities to the excitation of an electronic mode of conduction by the freeing of electrons in the vicinity of lattice defects or interstitial impurity ions. Since the ejection of electrons in this way depends on the presence of impurity ions, it is reasonable to suppose that passage of current for long periods of time, reducing the number of such ions, may well produce the observed diminution or reversal of the effect of increased field strength.

VARIATION OF RESISTIVITY WITH CRYSTALLOGRAPHIC ORIENTATION

One of the most frequently repeated statements concerning the resistivity of quartz is that the axial resistivity is thousands of times smaller than the equatorial resistivity. This statement is, however, true only for axial resistivities that have been measured a short time after the application of potential, and which measure the mobility of impurity ions rather than the resistivity of quartz. The facts seem to indicate that when the measuring potential has been applied for a sufficiently long time the axial resistivity increases to the same order of magnitude as the equatorial resistivity. Figure 12 shows this clearly. Disc No. 12, as explained above, was deliberately measured in such a way as to obtain the values of resistivity and activation energy associated with the short-term ionic surge current. The axial resistivities found for Disc No. 12 are between three and four orders of magnitude smaller than Sarzhevskii's values for equatorial resistivity. On the other hand, Disc No. 11, after passage of current for eight weeks afforded values of axial resistivity that are almost identical with Sarzhevskii's for equatorial resistivity, and lie near the mean of Strauss' and Rochow's values for equatorial resistivity. There is as much difference between different investigators' values for equatorial resistivity as there is between the mean of the nearly identical axial resistivities of King and Wenden, and the mean of the various curves for equatorial resistivity. The difference between the axial and equatorial resistivity seems to be about of the same magnitude as the experimental error.

There is evidence that ionic diffusion may take place in directions other than parallel to *c*, and may well enter into the recorded values for equatorial resistivity. The actual relation between axial and equatorial resistivity will only be clarified when both quantities have been measured with a precision higher than that of the present study, and with equally careful precautions against inclusion of impurity-connected currents. There seems to be at least an indication that the difference between axial and equatorial resistivity is really small, comparable with the birefringence and the difference in other vectorial properties of quartz.

An interesting outgrowth of the present study has been the measurement of the resistivities of a series of quartz plates cut at different angles to the *c* axis. These slices were prepared by the Cambridge Thermionic Corp. and the orientation checked by a combination of optical and *x*-ray methods. Electrodes of Du Pont Liquid Bright Platinum #6455 were fired on and the resistivity measured at 500° C. Twelve such samples were measured, the temperature and voltage being held constant and the current noted after twenty-four hours. Table 6 records the results of this experiment. Although it is too early to express a firm opinion, there seems to be a systematic relationship between orientation and resistivity that will probably become clearer and more consistent when longer runs are made and the effect of impurity ions more clearly delineated.

Table 6. Variation of Resistivity with Crystallographic Orientation

Disc No.	Orientation (angle ∧ *c*)	Resistivity at 500° C. (ohm-cm.)		
		4 hrs.	8 hrs.	24 hrs.
1	0°	6.65×10^6	6.65×10^6	7.98×10^6
2	10°15′	2.63×10^6	2.85×10^6	3.15×10^6
3	20°10′	2.52×10^6	2.78×10^6	3.52×10^6
4*a*	30°	2.26×10^6	2.60×10^6	4.06×10^6
4*b*	29°50′	2.52×10^6	2.85×10^6	4.35×10^6
5	42°	2.12×10^6	2.66×10^6	3.52×10^6
6	51°40′	6.0×10^6	6.0×10^6	6.0×10^6
7	60°	—	1.20×10^7	1.50×10^7
8*a*	70°	3.52×10^7	4.13×10^7	5.09×10^7
8*b*	73°	7.25×10^7	7.72×10^7	8.55×10^7
9*a*	80°	2.18×10^8	2.39×10^8	2.69×10^8
9*b*	80°	2.37×10^8	2.55×10^8	2.92×10^8

For short times of passages of current the resistivity is, as Mott and Gurney say, "structure-sensitive"; that is, the current that is carried chiefly by impurity ions is greatly influenced as to magnitude and direction by the structure of the quartz. Examination of a carefully constructed model (Fig. 16) of the low-quartz structure reveals that, in addition to the often-described "tunnels" or "pores" parallel to the *c* axis, there are similar continuous openings through the structure parallel to the *a* axes, and in directions inclined about 59° to the *c* axis, nearly perpendicular to the sheets of tetrahedra underlying the major rhombohedron. These two latter sets of "pores" have an opening area in projection somewhat smaller than those parallel to *c*, and in the case of the *a* axis tunnels, have about the same center to center spacing. In the case of the inclined openings, however, the center to center spacing in projection is about 1.75 Å, as contrasted with about 2.5 Å for the *c* axis channels projected on the base. It is difficult to believe that these openings are wholly without influence on the short-term, or structure-sensitive, part of the resistivity-time relationship in equatorial and inclined sections. Experiments now in progress, as well as Disc No. 13, which was

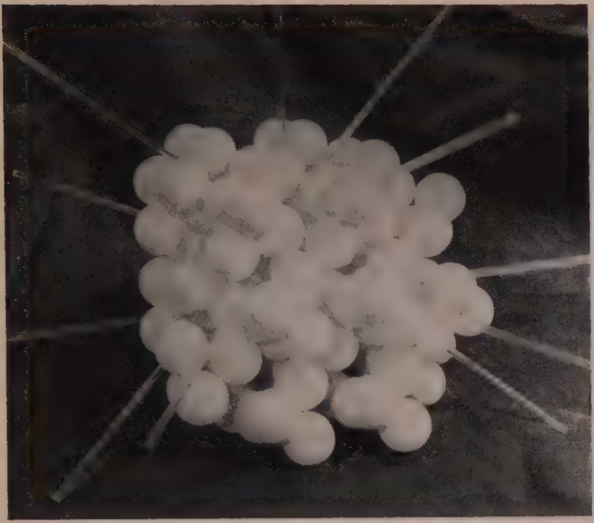

FIG. 16. Packing model of low quartz. Rods indicate the position of channels through the structure. The center vertical rod is parallel to the c axis. Model constructed by Ivan Barnes.

an ionic diffusion run using an X-cut plate, indicate that these channels do permit some ionic diffusion in directions other than parallel to c.

One very long run of over 2000 hours total duration was made using a test plate inclined 51°40′ to the c axis. The results of this run are given in Table 5 and Fig. 12 as Disc. No. 6. The high activation energy and uniform slope of the resistivity-temperature curve for this disc indicate that short-term ionic mechanisms do not play a significant part in the plotted values. The long duration of the run further guarantees exclusion of impurity ion connected effects. Nevertheless, the resistivity of this disc is less by one to two decades than the resistivity of Disc No. 11 which had passed current for a comparable length of time, but was Z cut. Since this is an isolated measurement unsupported by other long-term measurements on inclined plates, it is not safe to generalize from the results, but there is at least the suggestion that some directions in quartz conduct more readily than the c axis.

ACKNOWLEDGMENTS

It is a pleasure to acknowledge my indebtedness to Prof. C. S. Hurlbut, for his kind help and counsel at all stages of the research, for his critical reading of the manuscript and his many constructive suggestions. I wish also to thank Mr. Richard Collette for many helpful suggestions respecting laboratory practice, and Mr. Ivan Barnes for his assistance with some of the calculations. Financial support for a part of the work was furnished by the U. S. Army Signal Corps under contract DA 36-039-sc-56689.

REFERENCES

BOTTOM, V. E. *et al.* (1953), Final Report; Signal Corps Contract DA 36-039-sc-66, Colo. A & M Coll., Ft. Collins, Colo.

FIELD, R. F. (1944), Interpretation of current-time curves, General Radio Co., Cambridge, Mass. (Privately dupl. report)

FRONDEL, C., AND HURLBUT, C. S. (1953), Final Report: Signal Corps Contract DA 36-0390sc-15350, Harvard Univ., Cambridge, Mass.

GIBSON, G., AND VOGEL, R. C. (1950), Migration of lithium and several multicharged ions through quartz plates in an electric field II, *J. Chem. Phys.*, **18,** 1094–1097.

HARRIS, P. M., AND WARING, C. E. (1937), Diffusion of lithium ions through quartz in an electric field, *Jour. Phys. Chem.*, **41,** 1077.

JOFFÉ, A. F. (1928), The physics of crystals, McGraw-Hill, New York.

JOST, W. (1952), Diffusion in solids, liquids and gases, Academic Press.

KING, J. C. (1955), Second Interim Report: Signal Corps Contract DA 36-039-sc-64586, Bell Telephone Labs., Inc., Whippany, N.J.

KING, J. C. (1956), Fifth Interim Report: Signal Corps Contract DA 36-039-sc-64586, Bell Telephone Labs., Inc., Whippany, N. J.

MOTT, N. F. AND GURNEY, R. W. (1948), Electronic processes in ionic crystals, Oxford.

ROCHOW, E. G. (1938), Electrical conductivity in quartz. *Jour. App. Phys.*, **9,** 664–669.

SARZHEVSKII, P. E. (1952), *Doklady Akad. Nauk SSRR*, **82,** 571–574 (In Russian) Reviewed by J. M. Hough in *Sci. Abst.*, **55,** (1952).

SOSMAN, R. B. (1927), The properties of silica, Chemical Catalog Co., New York. All references prior to 1927 are reviewed in this work.

STRAUSS, S. W. *et al.* (1956), Fundamental factors controlling electrical resistivity in vitreous ternary lead silicates, *J. Res. Nat. Bur. Stand.*, **56,** 135–142.

STUART, M. R. (1955), Dielectric constant of quartz as a function of frequency and temperature, *J. App. Phys.*, **26,** 1399–1404.

VERHOOGEN, J. (1952), Ionic diffusion and electrical conductivity in quartz, *Am. Mineral.*, **37,** 637–655.

VOGEL, R. C., AND GIBSON, G. (1950), Migration of sodium ions through quartz plates in an electric field, *J. Chem. Phys.*, **18,** 490–494.

WENDEN, H. E. (1954), Second Quarterly Report: Signal Corps Contract DA 36-039-sc-56689, Harvard Univ., Cambridge, Mass.

WENDEN, H. E. (1954a), Third Quarterly Report: Signal Corps Contract DA 36-039-sc-56689, Harvard Univ., Cambridge, Mass.

WENDEN, H. E. (1955), Interim Report; Signal Corps Contract DA-36-039-sc-56689, Harvard Univ., Cambridge, Mass.

WENDEN, H. E. (1956), Final Report: Signal Corps Contract DA 36-039-sc-56689, Harvard Univ., Cambridge, Mass.

THE AMERICAN MINERALOGIST, VOL. 42, NOVEMBER-DECEMBER 1957

PRELIMINARY REPORT ON THE MINERALOGY AND PETROLOGY OF SOME MARINE BOTTOM SAMPLES OFF THE COAST OF PERU AND CHILE[1]

E-AN ZEN, *Woods Hole Oceanographic Institution, Woods Hole, Massachusetts.*

ABSTRACT

Marine bottom core samples from the coast of Peru and Chile were studied by x-ray and optical methods. For the fourteen cores included in this report, the following minerals are definitely identified: quartz, plagioclase, illite, chlorite, kaolinite, montmorillonite, calcite, aragonite, pyroxene, amphibole (both exclusively detrital), and an oxide of iron. The distribution of the minerals in a given core, as well as their textural relations, tends to remain constant, although considerable differences exist among the cores.

Volcanic glass is a common phase in many samples. Much of the glass is partially or completely devitrified; the products of devitrification include the clay minerals and calcite and demonstrate the exchange of material between the glass and the surroundings. Detailed study of such mineral assemblages should shed light on the equilibrium relations among these minerals in sediments.

INTRODUCTION

During the last months of 1955, the research vessel *Atlantis* of the Woods Hole Oceanographic Institution, under the leadership of B. Kummel and the late H. C. Stetson, undertook a cruise (no. 221) off the Pacific coast of Peru and northern Chile, to collect hydrographic data and bottom sediment samples from this part of the continental margin of South America. A free-running, Stetson-type coring tube was used, and eighty-four cores were recovered. The mineralogy and petrology of these cores have been studied since the autumn of 1956; this paper is a preliminary report of the investigations to date.

The west central coast of South America had been chosen for the investigation for various reasons. Study of the modern sediments from this area have been confined to reconnaissances (Revelle, 1944). The area, however, possesses a combination of both shallow and deep bottoms close to land, strong subaerial relief, and extensive Tertiary and modern volcanism. Sedimentological studies here thus might yield information useful in the interpretation of ancient sediments. Bottom profiles along the coring traverses are being prepared by J. M. Zeigler of the Woods Hole Oceanographic Institution. In addition, broad surveys of the coastal geology may be found in the works of Jenks (1946; 1956), Cristi (*in* Jenks, 1956), and Rüegg (1957); of the bottom topography by Schweigger (1947); and of the surface hydrography by Gunther (1936).

---

[1] Contribution No. 384 from the Department of Mineralogy and Petrography, Harvard University; No. 913 from the Woods Hole Oceanographic Institution.

Laboratory Procedure

Identification of the minerals in the core samples was principally by means of the Norelco recording Geiger-counter diffractometer, aided by the petrographic microscope with oil-immersion lens. As results using the diffractometer are highly sensitive to experimental methods, a description of the procedure follows.

Samples were taken from a given core at intervals of about 10 centimeters, or wherever visible variations of lithology occur such as color, grain size, and reactivity with HCl. The sample was dried, ground fine, and divided into several portions. One part was saved for heat-treatment and another part used directly for *x*-ray study. Copper radiation with nickel filter was used at 45 KV and 20 ma. A typical instrumental setting was as follows: goniometer speed, 1° 2θ per minute; chart speed, $\frac{1}{2}''$ per minute; scale factor, 4; multiplier, 1; time constant, 4 or 8 seconds; and divergent, scatter, and receiving slits, 1°, 1°, and 0.003″, respectively.

The diffraction patterns were compared with standards for identification. For samples suspected of kaolinite and/or chlorite, a second portion was heated in a muffle furnace to between 550 and 600° C. for $\frac{1}{2}$ hour and *x*-rayed under identical conditions (Brindley and Robinson, *in* Brindley, 1951, p. 188); for samples suspected of montmorillonite, an additional portion was saturated with glycerin and *x*-rayed (MacEwan, *in* Brindley, 1951, p. 115).

Samples were mounted for *x*-ray work using a small hand press. Although this method of sample preparation is liable to uncontrolled orientation effects for some minerals, for routine identification work this effect is an advantage, since commonly the platy minerals occur only in small amounts and without preferred orientation their presence in a crude sample might be undetected.

Identification of Minerals

To avoid any possible confusion, the nomenclature used for the various platy minerals is set out below. It should be emphasized that the names do not necessarily correspond to distinct mineral phases, many of which cannot be differentiated by the adopted techniques.

Illite

This name is used in the sense of Grim (1953, p. 35), and applies to all platy minerals in the samples with a strong reflection at about 10 Å. Although much of this is probably related to muscovite, phases such as glauconite and biotite, with 10 Å basal spacings, are possibly present and not distinguished. Nagelschmidt (1937, p. 519) suggests the use of the

(060) line to distinguish the dioctahedral from the trioctahedral micas, a criterion which Grim, Bradley, and Brown (*in* Brindley, 1951, p. 159) point out does not apply to glauconite. Moreover, the criterion is unsuitable for samples with minerals such as kaolinite and quartz with interfering diffraction lines (see, e.g., Brindley and MacEwan, *in* Brindley, 1951, Table XIV, 1, II). Nagelschmidt also suggests (1937, p. 519) that the relative weakness or absence of the 5 Å basal reflection is suggestive of trioctahedral micas. Most of the 10 Å micas from the cores show this relationship. However, this does not seem to be a reliable criterion, as prolonged grinding of natural, coarsely crystalline muscovite has resulted in the complete obliteration of the 5 Å line while the 10 Å line remains strong.

The possibility exists that the 10 Å "illite" in some samples represents intergrowth of muscovite and montmorillonite. Such interlayering may be detected by the angular displacement of the basal reflection spacings of the untreated samples (Brown and MacEwan, *in* Brindley, 1951, p. 277), and by additional displacements upon thermal and organic complexation treatments (MacEwan, *op. cit.*, pp. 118–121; Yoder and Eugster, 1955, p. 249). Detailed studies on a few cores (cores nos. 70 and 74) so far have failed to show the existence of such interlayering.

Kaolinite

This is applied to platy minerals with a ca. 7 Å line, that becomes destroyed by heating to 550–600° C. for ½ hour (Brindley and Robinson, *op. cit.*, p. 188).[2] Although probably predominantly kaolinite, other phases with the same structure cannot be distinguished.

Chlorite

This name applies to a non-swelling platy mineral with a 14 Å line, or, in those cases where this is too weak to be resolved, a 7 Å line which is not destroyed by heating. This criterion is subject to the reservations already discussed in the previous paragraph.

Montmorillonite

This is defined by the presence of a diffraction line between 10 and 14 Å, which swells to ca. 17 Å upon saturation with glycerin (MacEwan, *op. cit.*, p. 115), and collapses to 10 Å upon heating to 550–600° C. Montmorillonite is found in several cores as an important clay-mineral phase; however, as remarked earlier, there is no conclusive evidence for the existence of its intergrowth with muscovite-type layers.

---

[2] Johns, Grim, and Bradley (1954, p. 243) suggest that the loss of diffraction lines after heating to 450° C. is attributable to chlorite, whereas their retention is due to kaolinite. Bradley's suggestion (1954, p. 328) of partial replacement of brucite-layers by "hydrous layers" in some sedimentary chlorites may eventually explain the apparently contradictory observations. The applicability of Brindley and Robinson's criterion to the Peruvian samples is being studied.

Many of the samples have been examined microscopically. Such optical studies yield information on the textural relations in the samples, as well as the presence of fossils and material amorphous to the x-ray, such as certain siliceous microfossils and volcanic glass. They also conveniently check the x-ray results on mineral identification.

Description of the Cores

The course of cruise 221 of the *Atlantis* was so arranged that seven coring traverses were made roughly normal to the shore line, and one long traverse parallel thereto. The traverses span the region between the coastline and the Peru-Chile trench, a submarine deep running roughly parallel to the west coast of South America (Schweigger, 1947). Not all the cores are yet studied; instead two or three cores from each transverse cruise, one from each end and one from the middle, were taken for the reconnaissance work. The locations of the fourteen cores reported here are given in Fig. 1; in Table 1 the results are summarized in terms of the megascopic lithology (somewhat generalized) and x-ray and microscopic mineralogy of the corresponding intervals.

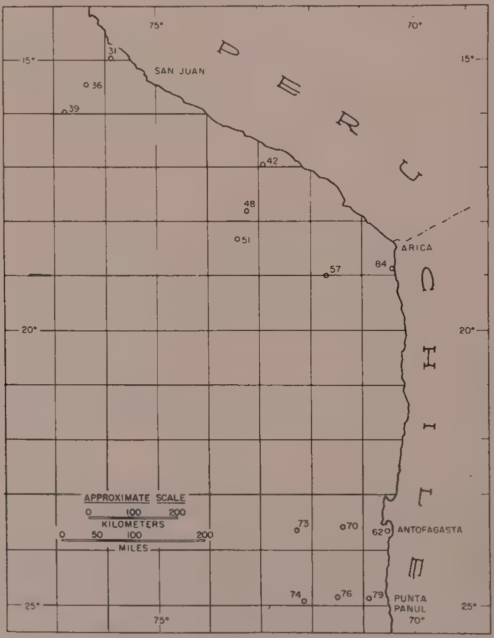

FIG. 1. Map showing locations of the fourteen cores.

TABLE 1. DATA ON THE CORES

Depth interval from top of core, cm.	Megascopic description	Mineralogy
	Core no. 31–3. Depth of water: 225 meters	
0–12	Empty	
12–17	Dark olive-brown, homogeneous clayey mud. Weak HCl reaction	Quartz: present but subsidiary Plagioclase: local, subsidiary Illite: trace to absent Kaolinite: rare trace Samples are largely microfossils showing no x-ray pattern and optically isotropic
17–23	Grades down from above through light brown silt to white, friable, sandy layer (2 cm.). No HCl reaction	Same as above
23–42	Sharp contact above; fine brown clayey mud. No HCl reaction	Same as above
42–48	Grading down into yellowish white sandy layer (2 cm.) with irregular bodies of brown mud. No HCl reaction	Same as above
48–62	Sharp upper contact; brown mud with light-coloured sandy layers 1 mm. thick, locally crossbedded. No HCl reaction	Same as above
62–77	Brown clayey mud. No HCl reaction	Same as above
77–90	Alternation of 1 mm. layers of brown clayey and pale sandy layers, with planar beddings. No HCl reaction	Same as above
90–107	Brown clayey mud with occasional shell remains. Weak HCl reaction	Abundant quartz at 97 cm., otherwise same as above
107–115	Like 77–90, but strongly crossbedded. Weak HCl reaction	Same as above
115–174	Brown mud, with thin white layers at irregular intervals. The latter type becoming rarer towards the bottom. No HCl reaction except locally	Same as top of core, with rare calcite. (124–162 cm. levels: abundant quartz, variable amount of plagioclase)
174–183	Like 77–90. Weak to no HCl reaction	Same as top of core
	Core no. 36–3. Depth of water: 4,435 meters	
0–199	Deep olive brown, clayey mud. Uniform textured, without visible grains. Occasional irregular patches varying in colour from pale brown to dark brown. Rare white ovoids scattered throughout the core. No reaction with HCl except in depth intervals between 45 and 120 cms	Quartz and plagioclase: predominant Kaolinite Illite Pyroxene and amphibole: detrital Calcite: an added phase between 45 and 120 cm. levels Glass: fairly common, mostly devitrified Fossils: abundant throughout the core

TABLE 1. *(continued)*

Depth interval from top of core, cm.	Megascopic description	Mineralogy
Core no. 39–3. Depth of water: 2,600 meters		
0–30	Brown, friable silt with scattered white and black spots. Vigorous HCl reaction	Calcite: predominant, mostly organic remains Quartz and plagioclase: subsidiary; partly detrital Illite Kaolinite or chlorite Glass: abundant
30–36	Grades down to white silty loam, with sharp contact at the bottom. Moderate to weak HCl reaction	Plagioclase: predominant Quartz: trace Illite (possibly biotite) Glass: abundant No calcite
36–63	Brown silt with interspersed layers of white chalky silt in the upper part; otherwise same as 0–30 cm. Sharp contact at the bottom, changing to	Calcite: predominant, organic remains Quartz and plagioclase: abundant Illite Kaolinite: local Pyroxene and amphibole: rare, detrital Glass: abundant
63–90	Pale, chalky silt, with vigorous HCl reaction, grading down to	Calcite: predominant, organic remains Quartz and plagioclase: trace Illite: trace Glass: abundant
90–185	Pure white chalk, without stratification. Vigorous HCl reaction	Calcite: nearly pure sample; organic remains Quartz: very rare
Core no. 42–4. Depth of water: 1,152 meters		
0–40	Unconsolidated, medium sand. Massive and homogeneous, dark olive-green in colour. Rare 1 mm. laminae of white sand. Vigorous HCl reaction except for the top 10 cm.	Quartz and plagioclase: predominant. Mostly as angular (detrital?) grains but partly probably as devitrification product Illite Kaolinite: above 30 cm. level Chlorite: below 30 cm. level Calcite: present except in the top 10 cm; as large rhombs and as devitrification product Pyroxene and amphibole: angular, detrital Glass: abundant, in various stages of devitrification
40–80	Gradationally changes from above downward into olive-yellow colour with local brown stain; otherwise no change in lithology. Vigorous HCl reaction	Same as above, with chlorite Aragonite: between 40 and 60 cm. levels; probably shell fragments
80–86	Gradationally changes from above into light gray, fine silt with dark green partings. Vigorous HCl reaction	Same as 0–40 cm., with chlorite

TABLE 1. (*continued*)

Depth interval from top of core, cm.	Megascopic description	Mineralogy
	Core no. 48–4. Depth of water: 6,146 meters	
0–14	Sticky, fine clayey mud, mostly olive to brown, with local black layers. No HCl reaction	Quartz and plagioclase: predominant; at least partly detrital Illite Kaolinite Pyroxene and amphibole: detrital Biotite: rare, detrital (?) Iron oxide (hydrous?) Glass: abundant Microfossils
14–16	Light brown, friable layer with oölitic texture. No HCl reaction	Quartz and plagioclase: predominant Illite and kaolinite: subsidiary Glass Microfossils
16–80	Same as 0–14 cm.; below 32 cm. level largely olive brown with faint, irregular layering due to colour variation. No HCl reaction	Quartz and plagioclase Illite Chlorite down to 56 cm. Kaolinite below 56 cm. Pyroxene and amphibole: detrital Glass Microfossils: very abundant
80–82	Yellowish-olive, silty clay. No HCl reaction	Same as above, with kaolinite
82–151	Same as 16–80 cm. No HCl reaction	Same as above
	Core no. 51–4. Depth of water: 4,456 meters	
0–18	Empty	
18–80	Deep brown, plastic clayey mud, uniform and homogeneous, nonstratified, with rare white, tiny ovoids. Gradually becomes brownish-gray towards the bottom. No HCl reaction	Quartz: very abundant Plagioclase: abundant Illite Kaolinite Montmorillonite (?) Pyroxene and amphibole: detrital Glass: rare Microfossils: present, but not abundant
80–91	Same as above, except that the mud is hard and non-plastic	Same as above
91–254	Brown plastic mud as above, gradually becoming olive-brown below 200 cm. level. Very local HCl reaction	Same as above
	Core no. 57–5. Depth of water: 4,106 meters	
0–60	Dull whitish green-gray mud, fine, compact, hard, with irregular, thin films of a green colour criss-crossing the sample at intervals of a few mms. No HCl reaction	Quartz: predominant Plagioclase: important Illite and kaolinite: in appreciable amounts Pyroxene and amphibole: scattered Glass: abundant, partly devitrified Microfossils: abundant

TABLE 1. (*continued*)

Depth interval from top of core, cm.	Megascopic description	Mineralogy
60–62	Angular fragments of fine white silty matter in green argillaceous matrix. No HCl reaction	Same as above
62–118	Same as 0–60 cm. levels	Same as above
118–138	Olive brown, unconsolidated, well sorted sand with pale, argillaceous cement; sharp contacts. No HCl reaction	Plagioclase: predominant Quartz: important Illite and kaolinite: absent to barely detectable Glass: abundant Microfossils: abundant
138–175	Same as 62–118 cm. levels	Same as above 118 cm. level
Core no. 62–6. Depth of water: 79 meters		
0–30	Massive, olive coloured, well sorted, unconsolidated sand, grains about 0.5 mm. across. Scattered shells of complete or fragmentary gastropods and pelecypods; locally concentrating into layers. Vigorous HCl reaction	Calcite: predominant Plagioclase: important Quartz: variable in amount, generally subsidiary Illite: only between 60 and 90 cm. levels Kaolinite and/or chlorite: in small amounts, not differentiated Aragonite: probably shell fragments, locally important Amphibole and pyroxene Glass: present in small amounts Fossils: very abundant, including considerable foraminifera
30–90	Same as above but with dark brown argillaceous layers interspersed, up to 2 cm. thick, at irregular intervals	Same as above
90–122	Same as above, but the sand becomes finer-grained approaching silt; core well stratified by colour variation (coarser, olive-colour vs. finer, brown colour)	Same as above
Core no. 70–6. Depth of water: 6,999 meters		
0–70	Fine, sticky, dark brown, homogeneous clayey mud with only occasional colour variations to suggest layering. No HCl reaction	Quartz and plagioclase: predominant. Most of these are large, angular, probably detrital grains Chlorite and illite Kaolinite: local Montmorillonite: local only. With illite, chlorite, and possibly kaolinite Pyroxene and amphibole: detrital, subsidiary Biotite: rare, may be detrital Iron oxide (hydrous?) Glass: moderate in amount, in various stages of devitrification Microfossils: rare

TABLE 1. *(continued)*

Depth interval from top of core, cm.	Megascopic description	Mineralogy
70–131	Gradual change from above; slowly becomes a clay-mud of steel gray colour but with the same texture. No HCl reaction	Same as above; no evidence for montmorillonite
131–134	Gray, friable, fine silt with gradational upper and sharp lower contacts. No HCl reaction	Same as above; grains well sorted Glass: abundant
134–138	Steel gray fine clayey mud as before. No HCl reaction	Same as 0–131 cm. levels
138–141	Same as 131–134 cm., with gradational upper and sharp lower contacts. No HCl reaction	Same as above; much volcanic glass. Grains well sorted
141–145	Olive gray-green clayey mud. No HCl reaction	Same as 0–131 cm. levels
	Core no. 73–6. Depth of water: 4,279 meters	
0–31	Empty	
31–107	Deep chocolate brown, sticky, clayey mud. Uniform and homogeneous, without stratification. Locally (67–72 cm.) vaguely layered due to slight colour differences, or motley-coloured (78–88 cm.). Colour grades downwards into pale choc. brown. No HCl reaction	Quartz: moderately abundant Plagioclase: present, locally abundant Illite Kaolinite Chlorite: locally present Pyroxene and amphibole: detrital Glass Microfossils: present
107–110	Yellowish brown silty mud, with sharp contacts. No HCl reaction	Same as above, with abundant fresh colourless glass
110–279	Same as above 107 cm. level, except that a 2 mm. silty layer exists at 111 cm. level. Colour is predominantly chocolate brown near the top, grading downwards through yellow-brown to gray brown. No HCl reaction	Same as above 107 cm. level; kaolinite more common than chlorite Much glass, mostly devitrified
	Core no. 74–7. Depth of water: 3,968 meters	
0–98	Deep brown, fine, hard mud, with thin, faint layerings at 1–5 mm. intervals due to colour variations. HCl reaction: above 36 cm., none; 36–70 cm., moderate; 70–98 cm., none	Quartz and plagioclase: abundant Illite: abundant Kaolinite: in small amounts Montmorillonite: present Chlorite: in small amounts Calcite: in moderate amounts between 36 and 70 cm. levels Glass: abundant, in various stages of devitrification Microfossils: abundant
98–108	Same as above, with faint, irregular layers of buff mud. HCl reaction: moderate	Same as above, with abundant calcite

TABLE 1. *(continued)*

Depth interval from top of core, cm.	Megascopic description	Mineralogy
108–121	Same as 0–98 cm. levels. HCl reaction: moderate	Same as 0–98 cm. levels
121–141	Same as 98–108 cm. levels. HCl reaction: moderate	Same as 98–108 cm. levels, with abundant glass
141–149	Same as 108–121 cm. levels. HCl reaction: weak to none	Same as 0–98 cm. levels, with chlorite and montmorillonite
149–160	Same as 121–141 cm. levels. HCl reaction: moderate to good	Same as above, with abundant calcite
160–173	Deep brown clayey mud with numerous fine, even layers of light buff mud. HCl reaction: vigorous	Calcite: predominant Plagioclase: abundant Quartz: subsidiary Kaolinite and chlorite: subsidiary, undifferentiated Glass: abundant Microfossils
	Core no. 76–7. Depth of water: 5,669 meters	
0–6	Empty	
6–8	Dark brown mud, uniform and homogeneous. No HCl reaction. (type "A")	Plagioclase: predominant Quartz: in moderate amounts Microcline: possibly present locally Illite Kaolinite Pyroxene and amphibole: detrital Calcite: very rare Glass: abundant Microfossils
8–18	Same, with about equal amounts of irregular patches of fine, buff mud (type "B"); the two types in sharp contact. No HCl reaction	Same as above
18–30	Like type A, but with HCl reaction	Calcite: predominant (organic remains) Quartz and plagioclase: subsidiary Kaolinite Illite: in small amounts Pyroxene and amphibole: rare Glass: rare but present
30–35	Type B, with HCl reaction	Same as above
35–40	Type A, with HCl reaction	Same as above
40–61	A and B in about equal amounts, forming layers or with B in irregular patches. HCl reaction	Same as above
61–70	A, with HCl reaction	Same as above

TABLE 1. (*continued*)

Depth interval from top of core, cm.	Megascopic description	Mineralogy
70–78	A and B in about equal amounts, with B in irregular patches. HCl reaction	Same as above
78–103	A, with HCl reaction	Same as above
	Core no. 79-7. Depth of water: 1,856 meters	
0–2	Empty	
2–26	Olive green, medium-fine, massive sand, with mud matrix. Local shell fragments. Vigorous HCl reaction	Quartz, plagioclase, and calcite: predominant Kaolinite Illite Chlorite Pyroxene and amphibole: detrital Glass: abundant, some very fresh Microfossils: abundant
26–30	Same as above, with 3–5 mm. white sand layers at 3–5 mm. distance apart	Same as above
30–82	Same as 2–26 cm. levels	Same as above
82–85	Gray unconsolidated, well-sorted sand, medium-coarse, without matrix material. Gradational upper, and sharp lower contacts	Quartz, plagioclase, and calcite: predominant Platy minerals: accessory only Pyroxene and amphibole No glass Microfossils: abundant, mostly foraminifera Note: all the microscopically resolved mineral grains are angular and apparently detrital
85–118	Fine brown clayey silt, uniform but for one pale, sandier layer between 94 and 96 cm. levels. Visible quartz and mica grains rarely present	Same as between 2–26 cm. levels
118–131	Intimate interlayering of brown, muddy and white, sandy silt, grading down to uniform fine muddy silt	Same as above
131–138	Slightly coarser silt, same as above 118 cm. level	Same as above
138–140	Same as between 82–85 cm. levels; gradational upper and sharp lower contacts	Same as between 82–85 cm. levels Montmorillonite (?)
140–150	Same as above 138 cm. level, with two thin sandy layers near the upper contact	Same as between 131–138 cm. levels
150–152	Same as between 138–140 cm. levels; gradational upper and sharp lower contacts	Same as between 138–140 cm. levels
152–156	Same as above 150 cm. level	Same as between 140–150 cm. levels

TABLE 1. *(continued)*

Depth interval from top of core, cm.	Megascopic description	Mineralogy
156–158	Same as between 150–152 cm. levels; gradational upper contact	Same as between 150–152 cm. levels
	Core no. 84–5. Depth of water: 933 meters	
0–76	Deep olive-brown, unconsolidated, nonclayey sand. Uniform, nonstratified. Scattered calcareous shell remains throughout. HCl reaction: moderate to weak	Quartz and plagioclase: predominant, mostly detrital Illite: trace Kaolinite: subsidiary Chlorite: found at 40 cm. level only Pyroxene and amphibole: detrital Calcite: small amounts, as product of devitrification Glass: abundant Microfossils: abundant
76–156	Much like above, but with numerous small (about 2 mm. × 4 mm.) irregular light-coloured patches scattered in the core, locally concentrated to suggest layering. Moderate HCl reaction	Same as above

DISCUSSION AND INTERPRETATION

The detrital portions of the cores studied are generally well-sorted. The detrital grains consist largely of volcanic glass in various stages of devitrification, angular grains of quartz, feldspar (plagioclase), pyroxene, amphibole, and also grains comprised of exceedingly fine mineral aggregates, possibly representing fragments of pre-existing rocks. Nevertheless, for a given core at a given depth level, the grains show good sorting, suggesting current action, even though a sample may be largely volcanic glass. This point is supported by observed graded bedding, cross-bedding, and fine-scale interlamination of different lithologies in many of the cores, even one (no. 31) composed nearly exclusively of tests of microfossils.

The gross lithology as well as mineralogy of any given core tends to be constant. Although the contrast amongst cores may be great, samples from a given core, with a few exceptions, tend to have the same minerals in comparable proportions, including the micaceous portions. There seems to be little difference in the x-ray patterns between the top of a core, presumably fresh sediment, and the lower, better indurated parts, such as reported by Murray and Harrison (1956, p. 36). True enough, the cores are extremely superficial samples of the sedimentary columns, nonetheless the relative constancy remains striking.

Volcanic glass is commonly encountered. As noted previously, these glass fragments are fairly well-sorted and at places finely interlaminated with other lithologic types—for instance calcitic layers. Quite possibly, these represent ash beds which, as far as microscopic determinations permit, are remarkably free of other types of material, except microfossils, although in this grain-size range it is admittedly difficult to detect rock fragments with any degree of certainty. The fragments of glass in a given sample show very different degrees of devitrification. Some fragments are fresh, the only crystalline phases being occasional unaltered phenocrysts, chiefly plagioclase (usually labradorite to andesine) and pyroxene or amphibole; but other fragments are partly or completely devitrified. Indices of refraction of the unaltered glass commonly yield values near or slightly greater than 1.56 and suggest basaltic composition, although rarely the index may be down to 1.51 and suggests a highly siliceous glass (Williams, Turner, and Gilbert, 1955, p. 28).

The difference in the extent of devitrification may be due to differences in the ages of the fragments, brought together through fluviatile agents. On the other hand, it may also be due to variations in the rates of devitrification, reflecting differences in the thermal history of the fragments, such as the degree of annealing and rate of chilling. Such a phenomenon is known to occur in rhyolitic flows (Boyd, 1957, p. 52); however, few laboratory data exist on this problem.

The most common, and nearly ubiquitous product of devitrification is a non-swelling mica which gives a well-defined reflection at about 10 Å. This is probably closely related to muscovite. A second common product is a 7 Å micaceous mineral, presumably kaolinite. Chlorite is relatively rare, montmorillonite is scarce; but calcite is fairly common. Quartz and an oxide of iron complete the list; whether any other phase results from devitrification is not established.

The formation of calcite and kaolinite, through hydration and carbonation of volcanic glass, is interesting in that it demonstrates the existence of interaction between the glass and its surroundings. Through the intimate association of these two minerals in a matrix of volcanic glass, as determined optically, they are probably stable together, and exclude, under the specific conditions, anorthite as a stable phase. Many samples, on the other hand, have only kaolinite and no recognizable calcite or any other diagenetic essential calcium phase; calcium may have been leached out of these samples.

Another point of interest is the role of iron and magnesium in the devitrification process. At least part of the iron goes to an "oxide" as noted. Apart from this, however, the only recognized essentially ferromagnesian phase is occasional chlorite. While it is possible that part of the magnesium goes into a 10 Å mica, a good proportion of the iron and magnesium may have become dissolved in the surrounding water and lost to the sediment. In general, the more devitrified a volcanic glass is, the lighter its color tends to be.

SUMMARY

Preliminary mineralogical examination of cores collected from the coast of Peru and Chile has revealed some features of mineralogical interest. Chief among these is the presence of abundant volcanic glass in many of the cores. Devitrification of the glass, in contact with sea water, results in minerals whose intimate association suggests approach towards chemical equilibrium; study of the detailed nature of these mineral associations therefore should yield data on the phase relations at the lowest end of the spectrum of diagenetic-metamorphic conditions. On the other hand, it should be emphasized that the very presence of volcanic glass indicates that the samples, as a whole, are not equilibrium systems although portions of them may locally be so.

The principal limitations in a mineralogical-petrological study of sediments lie in the fine grain size and the identification of clay minerals. While the use of modern *x*-ray diffractometers considerably reduces the size problem, it appears that for many sediments even *x*-rays are too coarse a probe, which must be supplemented by techniques such as electron microscopy and differential thermal analysis. On the other hand, conventional optical methods can also yield information valuable in the interpretation of the sediment samples.

The principles and methods of clay-mineral identification have been summarized elsewhere (Brindley, 1951; Grim, 1953; Weaver, 1956). Work is currently in progress on the detailed and specific identification of the clay-fraction of the core samples. Results to date, however, do indicate that the clay mineral phases listed in this report are essentially correct.

The geological interpretation of the mineralogical results cannot be made without a comprehensive study of the regional geology, as well as an understanding of the oceanography around the depositional site. Such an interpretation will be deferred to a later date.

ACKNOWLEDGMENTS

I wish to thank Drs. E. H. Smith and C. O. Iselin, past and present Directors, respectively, of the Woods Hole Oceanographic Institution, for their administrative support of the study. The Faculty of the Division of Geological Sciences at Harvard University has generously made available to me all the laboratory facilities. Discussions with Professors B. Kummel and J. B. Thompson, Jr., have been stimulating; their encouragement is gratefully acknowledged. The manuscript was critically reviewed by Professors C. Frondel, B. Kummel, R. Siever, and J. B. Thompson, Jr., all of Harvard University.

REFERENCES

BOYD, F. R. (1957), Geology of the Yellowstone rhyolite plateau. Harvard University Ph.D. Thesis. 134 pp.

BRADLEY, W. F. (1954), X-ray diffraction criteria for the characterization of chloritic material in sediments. *In* Clays and clay minerals, Publ. no. 327, Nat. Acad. Sci. and Nat. Res. Council. pp. 324–334.

BRINDLEY, G. W., ed. (1951), X-ray identification and crystal structures of clay minerals. London: The Mineralogical society. 345 pp.

GRIM, R. E. (1953), Clay mineralogy. New York: McGraw-Hill Book Co., 384 pp.

GUNTHER, E. R. (1936), A report on oceanographical investigations in the Peru coastal current. *Discovery* Reports, **13**, pp. 107–276.

JENKS, W. F. (1946), Preliminary note on geologic studies of the Pacific slope on southern Peru. *Amer. Jour. Sci.*, **244**, 367–372.

JENKS, W. F., ed. (1956), Handbook of South American geology. *Geol. Soc. Amer., Mem.* **65,** 378 pp.

JOHNS, W. D., GRIM, R. E., AND BRADLEY, W. F. (1954), Quantitative estimations of clay minerals by diffraction methods. *Jour. Sed. Pet.*, **24,** 242–251.

MURRAY, H. H., AND HARRISON, J. L. (1956), Clay mineral composition of recent sediments from Sigsbee Deep. *Jour. Sed. Pet.*, **26,** 363–368.

NAGELSCHMIDT, G. (1937), X-ray investigation on clays, Pt. III. *Zeit. Krist.*, **97,** 514–521.

REVELLE, R. R. (1944), Marine bottom samples collected in the Pacific Ocean by the Carnegie on its seventh cruise. *Carnegie Inst. Wash. Publ.* **556,** Pt. I. pp. 1–180.

RÜEGG, W. (1957), Geologie zwischen Cañete-San Juan 13°00′–15°24′ Südperu. *Geol. Rundschau*, **45,** 775–858.

SCHWEIGGER, E. (1947), La fosa de Lima. *Bol. Soc. Geol. del Peru*, **20,** 35–50.

WEAVER, C. E. (1956), The distribution and identification of mixed-layer clays in sedimentary rocks. *Am. Mineral.*, **41,** 202–221.

WILLIAMS, H., TURNER, F. J., AND GILBERT, C. M. (1955), Petrography. San Francisco: W. H. Freeman and Co., 406 pp.

YODER, H. S., AND EUGSTER, H. P. (1955), Synthetic and natural muscovites. *Geoch. et Cosmoch. Acta*, **8,** 225–280.

THE AMERICAN MINERALOGIST, VOL. 42, NOVEMBER-DECEMBER 1957

NOTES AND NEWS

HYDROTHERMAL SYNTHESIS OF MONAZITE

JOHN W. ANTHONY, *Department of Mineralogy and Petrography, Harvard University, Cambridge, Massachusetts.**

Monazite was first synthesized by Radominski in 1875. His method consisted in fusing $CePO_4$ in an excess of $CeCl_3$. Recent syntheses have been reported. Mooney (1948) worked with powders of the rare earth phosphates whose method of preparation was not specified. Karkhanavala (1956) produced $CePO_4$ by heating $Ce(NO_3)_3 \cdot 4H_2O$ and $(NH_4)_2HPO_4$ to about 200° C. The washed product when sintered at 700° C. gave the monoclinic dimorph of $CePO_4$ corresponding to monazite. The size of crystals was not specified.

In the present investigation single-crystals of monazite have been synthesized hydrothermally in bombs at temperature as low as 200° C. Cerium hydroxide gel was precipitated from an aqueous solution of ceric ammonium nitrate with an excess of ammonium hydroxide and thoroughly washed. A charge consisting of the dried gel and an excess of 85 per cent phosphoric acid was heated in a lead-sealed, stainless steel bomb equipped with a Teflon liner and cap. Teflon was found to provide an excellent liner material at the temperatures used because of its chemical inertness and good machining characteristics. Runs of 48 hours at 300° C. produced crystals up to 0.7 mm. measured along the *c* axis. The majority of crystals occur as clumped masses clinging to the liner walls, but many doubly-terminated, untwinned individuals having clean, bright faces have been observed.

Preliminary results suggest that thorium can be introduced into solid solution in synthetic monazite. Crystals have been grown by the method outlined with Si present in the form of $Na_2SiO_3 \cdot 9H_2O$ solution and the Th present as ThO_2 gel. The unit cell dimensions of the resulting crystals were determined by the powder method and showed significant variations from those of pure synthetic monazite. The content of Th in the crystals is not known, however, and this aspect of the study is being continued.

REFERENCES

KARKHANAVALA, M. D. (1956), The synthesis of huttonite and monazite: *Current Science*, No. **5**, 166–167.

MOONEY, ROSE, C. L. (1948), Crystal structures of a series of rare earth phosphates: *J. Chem. Physics*, **16**, 1003.

RADOMINSKI, M. F. (1875), Reproduction artificielle de la monazite et de la xenotime: *Compt. Rend.*, **80**, 304–307.

---

* Present address, Dept. of Geology, University of Arizona, Tucson, Arizona.

THE AMERICAN MINERALOGIST, VOL. 42, NOVEMBER-DECEMBER 1957

STUDIES OF URANIUM MINERALS (XXIII): TORBERNITE, ZEUNERITE AND URANOSPHERITE.[1]

ROBERT BERMAN, *Harvard University Cambridge, Mass., and U. S. Geological Survey, Washington, D. C.*[2]

TORBERNITE

An attempt was made to synthesize the fully hydrated (8–12 H_2O) form of torbernite, as no account of its synthesis could be found in the literature. Two solutions were made: 4.83 g. of $Cu(NO_3)_2 \cdot 3H_2O$ and 21.68 g. of $(UO_2)(NO_3)_2 \cdot 6H_2O$ were dissolved in 500 ml. of water; 5.52 g. of $NaH_2PO_4 \cdot H_2O$ was dissolved in another 500 ml. of water. Both solutions were chilled with distilled-water ice cubes before and during mixing. The two solutions were combined, and the mixture was stored in a regrigerator at 5° C. A green precipitate formed in the course of several days. It was kept in the refrigerator as a damp slurry and was used in that form as far as possible.

Under the petrographic microscope the precipitate was seen to be microcrystalline, with low birefringence and extinctions visible on some of the grains. Only a mean index of refraction could be obtained; it was measured as 1.590.

The *d*-spacings were obtained on an *x*-ray spectrometer and are given in Table 1. They are analogous to the spacings of fully hydrated zeunerite and autunite and bear the same relationship to the less hydrated forms as do the other species of the torbernite group. The cell dimensions are $a_0 = 7.025$ Å± 0.005, $c_0 = 20.63$ Å± 0.02.

ZEUNERITE

Zeunerite is the arsenate analogue of torbernite. Fully hydrated zeunerite was synthesized by J. W. Frondel (1951) but hitherto has not been reported with certainty in nature.

Some specimens with transparent green crystals were obtained from the Natural History Museum of Vienna. The labels identified the specimens as zeunerite from the Weisser Hirsch mine, Schneeberg, Saxony. The indices of refraction are as follows: $nO = 1.610$, $nE = 1.582$ (± 0.001, 25° C). The specific gravity was measured on the Berman Balance. Several grains gave values close to 3.47.

The zeunerite occurs as orthogonal crystals as much as 2 mm. in diameter, bounded by prisms and basal planes. Some of the rectangular

---

[1] Publication authorized by the Director, U. S. Geological Survey.

[2] Present address, Westinghouse Bettis Plant, Pittsburgh 30, Pa.

Table 1. Interplanar Spacings for Torbernite, Zeunerite and Uranospherite. Cu Kα Radiation, Ni Filter

Torbernite, artificial $a_0=7.025$ Å, $c_0=20.63$			Zeunerite, Schneeberg $a_0=7.18$ Å, $c_0=21.06$		Uranospherite, Schneeberg	
d (Å)	I	*hkl*	*d* (Å)	I	*d* (Å)	I
10.30	10	002	10.20	10	5.25	8
6.61	4	101	6.75	5	4.74	3
5.17	3	004	5.25	1	4.37	4
4.94	9	110	5.06	8	4.15	1
4.476	4	112	4.606	2	3.87	7
3.674	4	114			3.47	7
3.578	9	200	3.611	9	3.16	10
3.512	8	202	3.384	7	3.05	3
3.097	1	211	3.167	2	2.71	1
		212	3.064	1	2.60	1
2.904	3	204	2.946	4	2.54	1
2.853	2	213	2.885	4	2.46	2
2.731	1	214	2.753	3	2.39	2
2.665	1	205			2.35	1
2.477	1	220	2.533	4	2.16	2
2.412	2	222	2.457	4	2.08	2
2.237	1	224			2.03	1
			2.366	1	1.97	8
			2.321	2	1.90	7
			2.263	3	1.83	8
			2.201	4	1.80	1
			2.075	5	1.73	2
			1.978	1	1.66	4
			1.932	6	1.59	1
			1.870	1	1.56	1
			1.795	5	1.52	1

blocks are truncated by the (011) form; on some of the larger crystals these pyramids result in a lozenge shape. The pyramids are striated parallel to the base. There are good cleavages parallel to the base and prisms. The basal cleavage is by far the best. The crystals typically break into rectangular tabular fragments. Incipient dehydration, presumably due to metazeunerite, has taken place along some of the rectangular edges of the base, outlining the crystals with light-green matte material. The unaffected material gives an *x*-ray pattern virtually identical with that of fully hydrated zeunerite. The spacings of the natural material are listed in Table 1. The unit cell dimensions are $a_0=7.18\pm0.01$Å, $c_0=21.06\pm0.02$Å.

Miss M. E. Thompson (personal communication) states that a copper uranyl arsenate having similar indices of refraction occurs as a coating on black coaly material from the Dexter Mine, Calf Mesa, San Rafael Swell, Utah. When the samples were first studied, the optical properties were as follows: $nO = 1.610 \pm 0.002$, $nE = 1.583 \pm 0.002$. Pleochroism O = pale blue-green, E = very pale green. No pleochroism was observed in the Schneeberg samples. The Calf Mesa material dehydrated very quickly. The x-ray pattern, obtained a few weeks later, matches meta-zeunerite, and the indices changed to $nO = 1.642$, $nE = 1.610$.

URANOSPHERITE

Uranospherite was described by Weisbach (1873) from the Walpurgis vein of the Weisser Hirsch mine at Neustädtl, near Schneeberg, Saxony. It is a secondary mineral, formed with various arsenates in the oxidized zone of a vein carrying uraninite, native bismuth, and cobalt-nickel arsenides. It is associated with walpurgite, uranospinite, troegerite, zeunerite, erythrite, and black cobalt oxide. It is known only from the original locality. Very few authentic specimens appear to be extant, and x-ray powder data have not been available.

Uranospherite is a hydroxide or hydrated oxide of bismuth and hexavalent uranium. The formula is uncertain, perhaps $Bi_2O_3 \cdot 2UO_3 \cdot 3H_2O = (BiO)(UO_2)(OH)_3$. The only reported analysis is given in Table 2.

TABLE 2. ANALYSIS OF URANOSPHERITE

	Bi_2O_3	UO_3	H_2O	Total
1.	42.66	52.39	4.95	100.00
2.	44.34	50.88	4.75	99.97

1. Theoretical weight percentage, $Bi_2O_3 \cdot 2UO_3 \cdot 3H_2O$.
2. Uranospherite, Schneeberg, Saxony; Winkler, analyst, in Weisbach (1873).

The mineral is orange in color, and occurs as drusy, radial aggregates up to 0.5 mm. in diameter. When these are broken apart, the radial laths of the material almost always rest on a cleavage. The laths usually have somewhat irregular terminations, giving the drusy appearance to the exterior of the radial group. Occasionally, the laths are terminated by one or two small oblique edges. The edges make angles of 40° and 140° with the sides of the lath. In the cases where two terminal edges meet, forming an arrowlike point on the lath, the angle of the point is 80°. Faint striations can be observed parallel to the direction of the lath. Spectrographic and thermal analyses are lacking. On heating, the mineral decrepitates and falls to pieces composed of brown, silky needles.

An authentic specimen was obtained from the Natural History Museum, Vienna, through the courtesy of Dr. A. Schiener, curator. The

TABLE 3. OPTICAL PROPERTIES OF URANOSPHERITE

	Orientation	New data	Larsen (1921)
X	*a*	1.959	1.955
Y	*b*	1.981	1.985
Z	*c*	2.060	2.05

optics were measured, using phosphorus and Larsen-Meyrowitz index liquids, and the results are in agreement with those reported by Larsen (1921) on a specimen from the Roebling collection. The values obtained are given in Table 3.

Z is parallel to the elongation of the laths and X is normal to the cleavage. The optic sign is positive, and 2V is calculated as 56°. Larsen observed strong dispersion, $r<v$. There is no marked absorption or pleochroism. The mineral is probably orthorhombic. A U. S. National Museum specimen, no. R-5892, labelled uranospherite, was examined optically and its identity was verified. The *x*-ray diffraction pattern of the Vienna specimen is given in Table 1.

Fletcher (1913) attempted to measure the melting point of supposed uranospherite from Sabugal, Portugal. He states that small particles "lose body" at 1170° C., and that larger particles melt with iridescence at 1320° C. His material is from an undescribed locality for this mineral, and its authenticity is very doubtful.

This study is part of a program conducted by the U.S. Geological Survey on behalf of the Division of Raw Materials of the U. S. Atomic Energy Commission.

REFERENCES

FLETCHER, A. L. (1913), *Proc. Roy. Dublin Soc.* **13,** 443.
FRONDEL, J. W. (1951), *Am. Mineral.* **36,** 259.
LARSEN, E. S. (1921), *U.S.G.S. Bull.* **679.**
WEISBACH, A. (1873), *Jb. Min.* **1873,** 315.

THE AMERICAN MINERALOGIST, VOL. 42, NOVEMBER-DECEMBER 1957

IDENTITY OF PILBARITE WITH THOROGUMMITE AND KASOLITE

RUSSELL M. HONEA, *Harvard University, Cambridge, Massachusetts.*[*]

Pilbarite was described by Simpson (1910) from the Wodgina area of the Pilbara goldfields, Western Australia. The mineral occurs as small nodules enclosed in albite in weathered outcrops of tantalite-rich pegmatites. Occasional residual cores of thorogummite indicate that the

[*] Present address, Dept. of Geology, University of Texas, Austin, Texas.

pilbarite is pseudomorphous after a primary thorium mineral, probably uranoan thorite. Weathering or hydrothermal alteration of the original thorium mineral yielded what Simpson (1930) considered a chemically related series of distinct species maitlandite, nicolayite, pilbarite, and hydrothorite. Frondel (1953) has shown that maitlandite, nicolayite, and hydrothorite are minor chemical variants of the phase thorogummite. In a later paper Frondel (1956) mentions pilbarite as an ill-defined substance which needs further study.

The present study was undertaken as part of a broad research into the mineralogy of the uranium and thorium silicates. Two specimens of pilbarite were available for study: a U. S. National Museum specimen originally from Simpson, and a specimen from the O. I. Lee collection originally from the Government Museum, Western Australia. Both specimens match the description of Simpson in all respects. The mineral is bright yellow with the rims of nodules bleached somewhat lighter, and their surfaces coated by iron oxide. Luster earthy. Hardness 2½ to 3. Specific gravity 4.15 to 4.95, with most fragments giving a value near 4.68. The wide range is due to variable porosity of the earthy aggregates, and to varying proportions of the component minerals.

X-ray powder patterns of both specimens prove the pilbarite to be a mixture of thorogummite and kasolite. All lines of standard patterns of both minerals are present. Optical examination under high magnification shows the material to be a microcrystalline aggregate of apparently isotropic grains with an average index of refraction of 1.74, and minute anisotropic grains with a mean index of 1.9. This latter value is near that to be expected from kasolite with $n\text{X} = 1.877$, $n\text{Y} = 1.880$, $n\text{Z} = 1.935$. The apparent isotropism of the thorogummite results from the submicroscopic size of the component crystallites.

Simpson described pilbarite as a hydrated silicate of lead, uranium, and thorium with the composition shown in Table 1. From this Simpson derived the empirical formula $ThO_2 \cdot UO_3 \cdot PbO \cdot 2SiO_2 \cdot 4H_2O$. It is

TABLE 1. COMPOSITION OF PILBARITE

SiO_2	12.72	MnO	nil	ThO_2	31.34
P_2O_5	1.08	FeO	nil	Ce_2O_3	0.19
K_2O	0.09	Fe_2O_3	0.20	Y_2O_3	0.49
Na_2O	0.04	Al_2O_3	0.15	H_2O (−)	3.50
CaO	0.57	Ta_2O_5	0.47	H_2O (−)	4.16
PbO	17.26	UO_3	27.09	CO_2	nil
MgO	0.21	UO_2	nil		99.56

Simpson, E. S. (p. 465, 1928).

readily seen that thorogummite, $Th(SiO_4)_{1-x}(OH)_{4x}$, and kasolite, $Pb(UO_2)(SiO_3)(OH)_2$, can account for the stated composition. The proportions of the two minerals in the mixture cannot be ascertained from the analysis because it is not known how much of the PbO is present in kasolite and how much is present in the thorogummite from radioactive disintegration of uranium and thorium. The optical and *x*-ray study suggests that the two minerals are present in approximately equal amounts.

The writer gratefully acknowledges the many helpful criticisms of Professor Clifford Frondel in the course of the present investigation.

References

Frondel, Clifford (1953), Hydroxyl substitution in thorite and zircon: *Am. Mineral.*, **38,** 1007–1018.

——— (1956), Mineralogy of thorium: *U. S. Geol. Survey Prof. Paper*, **300,** 567–579.

Simpson, E. S. (1910), Pilbarite, a new mineral from the Pilbara goldfields, W. A.: *Chem. News*, **102,** 283–284.

——— (1928), Famous mineral localities: Wodgina, North West Australia: *Am. Mineral.*, **13,** 457–458.

——— (1930), Contributions to the mineralogy of Western Australia: *Royal Soc. Western Australia Jour.*, **16,** 33–35.

——— (1952), *Minerals of Western Australia*, Perth, Vol. **3,** 139–142.

THE AMERICAN MINERALOGIST, VOL. 42, NOVEMBER-DECEMBER 1957

UNIT CELL AND SPACE GROUP OF LARSENITE, $PbZnSiO_4$

Frederic G. Layman, *Harvard University, Cambridge, Massachusetts.*

Larsenite from Franklin, New Jersey was described in 1928 by Palache, Bauer, and Berman, and a summary description was given by Palache in 1935. On morphological and chemical data, the mineral was placed in the Olivine Group and has been so accepted by later writers. No single-crystal or powder *x*-ray diffraction work has been reported thus far. Recently, samples of larsenite were supplied by the Harvard Mineralogical Museum to Dr. Heinrich Neumann of the University of Oslo, who drew our attention to the fact that powder photographs of the mineral are not of the general olivine type.

An *x*-ray single-crystal study of type larsenite from Franklin has been made by the rotation, Weissenberg, and precession methods using Cu and Mo radiation. This work has shown that larsenite is not isostructural with the Olivine Group, but is related dimensionally thereto. The *a* and *b* axes of larsenite are approximately double those of olivine and the *c* axes of the two minerals are approximately the same. Both minerals are orthorhombic, but the space groups are different. A summary of the x-ray data follows:

$a_0 = 8.23 \pm .01$ A $a_0 : b_0 : c_0 = .435 : 1 : .267$
$b_0 = 18.94 \pm .01$ Space group: *Pnam* or *Pna*
$c_0 = 5.06 \pm .01$ Unit cell contents 8 [$PbZnSiO_4$]

The cell dimensions were obtained from Weissenberg O-layer photographs. Closely conformable values were obtained from the rotation and precession photographs. The powder photograph data in Cu radiation for larsenite are given in part in Table 1.

As no doubly terminated crystals of larsenite have been found, it is uncertain whether the mineral belongs in the orthorhombic *mmm* class (space group *Pnam*) or in the orthorhombic *mm* class (space group *Pna*). The orientation of the structure cell is identical with that of the morphological cell orginally described, but the *a* and *b* axes are doubled with respect to the morphological unit.

The aid of Dr. Clifford Frondel is gratefully acknowledged.

TABLE 1

Line No.	Intensity	*d* meas.	$1/d^2$ meas.	$1/d^2$ calc.	*hkl*
1	2	7.47	.0179	.0176	110
2	1	6.23	.0258	.0260	120
3	7	4.87	.0423	.0419	011
4	2	4.71	.0451	.0448	040
5	5	4.20	.0568	.0567	111
6	4	4.00	.0625	.0620	210
7	1	3.90	.0659	.0651	121
8	2	3.78	.0701	.0704	220
9	1	3.55	.0795	.0791	131
10	2	3.44	.0846	.0844 .0848	230 150
11	10	3.19	.0984	.0983 .0987	201 141
12	9	3.03	.1090	.1091 .1095	051 221
13	1	2.95	.1150	.1156	160
14	9	2.85	.1230	.1239 .1235	151 231
15	5	2.79	.1285	.1292	250
16	5	2.72	.1350	.1360	310
17	1	2.65	.1425	.1431	241

BIBLIOGRAPHY

1. Palache, Charles, Bauer, L. H., and Berman, Harry (1928), Larsensite, Calcium Larsenite, and the associated Minerals at Franklin, N. J. *Am. Mineral.*, **13,** 334–340.
2. Palache, Charles (1935), The Minerals of Franklin and Sterling Hill, Sussex County, New Jersey, *U.S.G.S. Professional Paper*, **180,** 80–81.

THE AMERICAN MINERALOGIST, VOL. 42, NOVEMBER-DECEMBER 1957

NOTES ON A PERALKALINE GRANITE FROM CASHES LEDGE, GULF OF MAINE

Priestley Toulmin III, *Harvard University, Cambridge 38, Massachusetts.*

The writer has recently had the opportunity to examine a specimen of granite from Cashes Ledge, a submarine prominence in the Gulf of Maine. The specimen was collected by Dr. John M. Zeigler of Woods Hole Oceanographic Institution. Although the precise location of the specimen is not available, reference to topographic maps of the area (Murray, 1947, Fig. 7) indicates that the position must be approximately 42° 54′ N. Lat., 68° 56′ W. Long.

The hand specimen is a roughly rectangular slab approximately $5\times4\times1$ cm. Bryozoans and algae encrust one of its larger sides; the side opposite is freshly broken. Megascopically one can recognize quartz, alkali feldspar, black amphibole, and a little dark green pyroxene, all having an average grain size of about three millimeters. Under the hand lens, tiny crystals of iron-rich olivine may be discerned. The minerals appear quite fresh; the only sign of weathering is an occasional speck of limonite in the amphibole.

Under the microscope, the rock is seen to be holocrystalline, hypautomorphic granular. *Quartz* occurs in anhedral grains averaging 1–3 mm. in diameter, ranging up to 5 mm. The quartz shows very slightly wavy and irregular extinction, and carries many tiny clear inclusions. *Microperthite* subhedra have about the same size range as the quartz, and are composed of elongate and more or less equant irregular areas of albite in an untwinned microcline host. Apparent differences of shape between albite masses probably reflect different orientations of host crystals relative to the plane of the thin section. Plagioclase is concentrated slightly at the margins of perthite grains, but no independent extra-perthitic plagioclase crystals were seen. Tiny specks of clay minerals disseminated through the microcline give it a "dusty" appearance in thin section. A specimen of microperthite was homogenized by heating at 910° C. ± 10° C. for about fifty hours; an *x*-ray powder pattern was prepared on a Norelco Geiger-counter diffraction spectrometer using CuKα radiation. The bulk composition of the homogenized material was determined from measurements of $d_{(20\bar{1})}$, using quartz as an internal standard, and referring the d—spacing to the chart of Bowen and Tuttle (1950, Fig. 2). The average of five measurements of $d_{(20\bar{1})}$ is 4.14 Å, corresponding to $Or_{56}(Ab+An)_{44}$ (wt.%). The accuracy of the determination is of the order of ±5% Or.

There are two amphiboles in the rock. *Hornblende*, apparently iron-rich, occurs in subhedral grains up to 4 mm. across. The hornblende is strongly absorbing and pleochroic, varying from yellow-green to very dark brownish green or black; no useful interference figure was obtained. Strikingly pleochroic *riebeckite*, varying from deep blue or black to light yellow-brown, occurs principally in sheaf-like aggregates of very thin needles 0.1–0.5 mm. long. The aggregates are clustered in several areas in the slide, where they are associated with hornblende, aegirite, iron-rich olivine, astrophyllite, aenigmatite (?), and quartz. Riebeckite also forms larger crystals, one of which is 0.1×0.4 mm. and is in contact with hornblende, aegirite, quartz, and aenigmatite (?).

Aegirite, or aegirite-rich pyroxene, forms 0.1 mm. irregular grains associated with hornblende, riebeckite, and aenigmatite (?). The mineral has a moderate negative 2V, birefringence about 0.05, and X is very nearly parallel to *c*. The pleochroism is rather strong, with Z′ yellow-green and X′ deep grass green.

Iron-rich *olivine* occurs in several small (0.05 mm.) grains and in one large (0.3 mm.) broken euhedron associated with clusters of riebeckite needles in the section studied. $2V_x$ was determined by universal stage to be 60°±5°, corresponding approximately to Fa_{85} (ferrohortonolite) (Tröger, p. 37).

Astrophyllite occurs in a 0.2×0.5 mm. irregularly shaped grain enclosed in the hornblende of a hornblende-aegirite intergrowth. Many small red-brown to yellow fibrous aggregates associated with aenigmatite (?) and riebeckite may also be astrophyllite.

A strongly absorbing, pleochroic mineral, referred to in this note as *aenigmatite* (*?*), occurs as a few remnants of euhedral crystals one to five mm. long; the mineral is highly fractured, and much of it was lost in preparation of the thin section. The color varies from dark chestnut brown (X′) through dark red-brown to black (Z′). The extinction is at 45° to the elongation. The mineral is very similar to that which Washington (1898, pp. 792–793) described as allanite in a granite from Gloucester, Massachusetts, but the pleochroism and extinction angle of the material in the Cashes Ledge specimen are more nearly those of aenigmatite. Unfortunately, sufficient pure material for *x*-ray determination has not been obtained. Small red-brown granules, probably of the same mineral, are associated with the clusters of riebeckite needles.

Zircon is quite rare in the section examined; the few tiny crystals seen are enclosed in amphibole grains. A small amount of an opaque mineral, probably *magnetite*, seems to have formed by alteration of hornblende.

Although no banded structure is apparent in the hand specimen, quartz and feldspar are concentrated in different parts of the thin section. For this reason, and because of the small size of the thin section (1×3 cm.), no quantitative modal analysis has been attempted. In general, the amounts of quartz and of feldspar are about equal, and the color index is about 10.

The mineralogy of the rock clearly reflects its peralkaline character; petrographically it resembles many of the alkaline granites of New England that generally have been assigned to, or correlated with, the White Mountain magma series (Billings, 1945; Greenwood, 1951, pp. 1171–1178; Chapman and Williams, 1935). Like these rocks, it shows little or no cataclastic or gneissic structure. It is quite similar to certain granites of Cape Ann, Massachusetts, in which fayalite and allanite (the latter "very rare") are reported as accessory minerals (Warren and McKinstry, 1924, p. 332). The absence or rarity of extraperthitic plagioclase, association of hastingsitic and riebeckitic amphiboles and aegiritic pyroxenes, and the occurrence of accessory iron-rich olivine and astrophyllite are all characteristics of the more alkaline granites of the Cape Ann area; the bulk composition of the microperthite is within the rather narrow range found by the writer for the microperthites of granites and quartz syenites in the southwestern part of the Cape Ann granitic body. These microperthites range from Or_{48} to Or_{60} (wt. %), corresponding to a range of 4.13 A. to 4.15 A. in $d_{(20\bar{1})}$.

Recent zircon-age studies (Webber *et al.*, 1956; Tilton *et al.*, 1957; Lyons *et al.*, 1957; Quinn *et al.*, 1957) suggest that at least two unrelated groups of alkaline intrusive rocks of late Paleozoic to early Mesozoic (?) age may exist in the new England area. The rocks of Cape Ann and Peabody, Massachusetts, appear to be about 85 million years older than the rocks of the White Mountain magma series in New Hampshire. If this apparent age difference is real, it seems unlikely that the two groups are genetically related. Petrographic criteria by which rocks of the two series can be distinguished with certainty are not available at present.

Cashes Ledge is approximately 75 miles east-northeast of Rockport, Massachusetts, and about the same distance east-southeast of the Mt. Agamenticus area, Maine, the two nearest shore points where similar rocks are exposed. Dr. Zeigler, who obtained the specimen, states definitely that it was broken from bedrock. This occurrence thus implies a considerably greater souteastward extent for rocks of this type than has been indicated by earlier data. It should be noted that certain granites of eastern Maine are petrographically similar to the rocks under consideration (Chapman, 1956; Wing, 1953); to the writer's knowledge, however, the relationship of these rocks to the White Mountain magma series has not yet been the subject of a detailed study.

Professor M. P. Billings suggested the examination of this specimen to the writer. Dr. Zeigler kindly provided the specimen and consented to publication of this description. Professor J. B. Thompson, Jr., read the manuscript and made a number of helpful suggestions.

REFERENCES

BILLINGS, M. P. (1945), Mechanics of igneous intrusion in New Hampshire: *Amer. Jour. Sci.*, **243**-*A* (Daly Vol.), 40–68.

BOWEN, N. L., AND TUTTLE, O. F. (1950), The system $NaAlSi_3O_8$-$KAlSi_3O_8$-H_2O: *Jour. Geol.*, **58,** 489–511.

CHAPMAN, C. A. (1956), A pseudo-ring dike, Mt. Desert Island, Maine: *Illinois State Acad. Sciences, Trans.*, **49,** 133–136.

CHAPMAN, R. W., AND WILLIAMS, C. R. (1935), Evolution of the White Mountain magma series: *Am. Mineral.*, **20,** 502–530.

GREENWOOD, ROBERT (1951), Younger intrusive rocks of Plateau Province, Nigeria, compared with alkalic rocks of New England: *Bull. Geol. Soc. Amer.*, **62,** 1151–1178.

LYONS, J. B., JAFFE, H. W., GOTTFRIED, D., AND WARING, C. L. (1957), Lead-alpha ages of some New Hampshire granites: *Amer. Jour. Sci.*, **255,** 527–546.

MURRAY, H. W. (1947), Topography of the Gulf of Maine: *Bull. Geol. Soc. Amer.*, **58,** 153–196.

QUINN, A. W., JAFFE, H. W., SMITH, W. L., AND WARING, C. L. (1957), Lead-alpha ages of Rhode Island granitic rocks compared to their geologic ages: *Amer. Jour. Sci.*, **255,** 547–560.

TILTON, G. R., DAVIS, G. L., WETHERILL, G. W., AND ALDRICH, L. T. (1957), Isotopic ages of zircon from granites and pegmatites: *Amer. Geophysical Union, Trans.*, **38,** 360–371.

TRÖGER, W. E. (1956), Optische Bestimmung der gesteinsbildenden Minerale—Teil I, Bestimmungstabellen: E. Schweizerbart'sche Verlagsbuchhandlung, Stuttgart.

WARREN, C. H., AND MCKINSTRY, H. E. (1924), The granites and pegmatites of Cape Ann, Massachusetts: *Proc. Amer. Acad. Arts and Sciences*, **59,** 313–368.

WASHINGTON, H. S. (1898), The petrographical province of Essex County, Mass., Part I: *Jour. Geol.*, **6,** 787–808.

WEBBER, G. R., HURLEY, P. M., AND FAIRBAIRN, H. W. (1956), Relative ages of eastern Massachusetts granites by total lead ratios in zircon: *Amer. Jour. Sci.*, **254,** 574–583.

WING, L. A. (1953), Preliminary report on eastern Maine granites: *Rept. State Geologist of Maine,* **1951–1952,** 47–51.

The next Conference of the *X*-ray Analysis Group of the British Institute of Physics will be held in Manchester, England, on April 18–19, 1958. Full details will be available in January, 1958, from Dr. R. L. Gordon, Safety in Mines Research Establishment, Portobello St., Sheffield 1, England.

The National Science Foundation aided in the publication of the recently issued Index to Volumes 31–40 of *The American Mineralogist.* Notice of the decision to assist was received after the Index had been printed, so it was not possible to acknowledge this aid in the index itself. The Council of the Mineralogical Society, therefore, wishes to take this means of acknowledging with thanks the substantial financial assistance rendered by the National Science Foundation in publishing this decennial index.

BOOK REVIEW

HANDBUCH DER MIKROSKOPIE IN DER TECHNIK. Volume IV, Mikroskopie der Silikate. Part 1. Mikroskopie der Gesteine. Edited by HUGO FREUND with the collaboration of C. W. CORRENS, D. HOENES, S. MATTHES, H. VON PHILLIPSBORN, H. PILLER, AND W. E. TRÖGER. 796 + LIV pp., 490 photomicrographs, drawings, and tables, 2 colored photomicrographs. Umschau Verlag, Frankfurt am Main, Germany. 1955(?) Price 98 DM.

This is just one book of an encyclopedic series in which there are eight volumes, several with two or even three parts. The series, called *A Manual of Microscopy in Technology* is intended to be all-embracing, dealing with all major fields of industrial technology to which the microscope has specific application. It is typical, of course, that the German editors should entitle such an enormous series a "Handbuch," i.e., a handbook or manual. In size and weight the series apparently will be nothing approaching a work that can be transported in toto with facility by hand. The entire series, when completed, will consist of the following volumes (all in German, titles in translation):

Vol. I. Optical principles, instruments, and accessories for microscopy in technology. Two parts, one on the transmitting, the other on the reflecting microscope.
Vol. II. Microscopy of economic mineral deposits. Three parts: 1) Coal, coke, lignite; 2) Ores, concentrated ores, slag; 3) Petroleum and potash salts.
Vol. III. Microscopy of colored metal alloys, light metal alloys, and iron-carbon alloys.
Vol. IV. Microscopy of silicates. Two parts: 1) Rocks (here reviewed); 2) Ceramic raw materials.
Vol. V. Microscopy of wood and paper. Two parts: 1) Anatomy of wood; 2) Microscopy of paper and technology of wood preparation.
Vol. VI. Microscopy of textile fibers, textiles, and leather.
Vol. VII. Microscopy of chemical technology.
Vol. VIII. Microscopy of human nourishment and luxury materials as well as animal food and fertilizer material.

Vol. IV, Part 1, has five sections, following an introduction by Freund: Section 1, by Phillipsborn, is entitled "The historical development of microscopic methods in mineralogy and their significance to general microscopy and technology"; Section 2, by Tröger, "Optical properties and determination of the most important rock-forming minerals"; Section 3, by Hoenes, "Fundamentals of microscopy in rock technology"; Section 4, by Correns and Piller, "Microscopy of the fine-grained silicate minerals"; and Section 5, by Matthes, "Microscopy of technologically useable asbestos."

The first part, dealing with the history of mineralogical and petrographical microscopy, is one of the most complete syntheses of this subject that the reviewer has ever encountered. It has the added virtue of containing 47 figures (2 in color) of micro-drawings and photomicrographs of historical significance, including pictures of crystals and rocks by such pioneers of microscopy as Hooke (1665), Leeuwenhoek (1684–1688), Capeller (1723), Brewster (1823), Sorby (1858), Zirkel (1863) and many others. Pictures of many of these individuals also are included. It is interesting to recall that, although thin sections of fossil wood were prepared by Nicol in 1831, it was not until 1849 that Sorby made the first rock thin sections (of calcareous sandstone). This section also has an outstanding bibliography.

Section 2, on optical determination of minerals, begins with a brief general treatment of techniques; i.e., immersion mounts and thin sections, followed by descriptions of individual species, series or groups, about 60 in all. The choice of minerals important as rock-forming species is judicious, but their arrangement is by three "genetic" groups, namely those of magmatic paragenesis, those of sedimentary paragenesis, and those of metamorphic paragenesis. Obviously, as Tröger also recognizes, this would lead to considerable repetition if carried to completion, and thus many species or groups are placed arbitrarily. The listing of topaz as a metamorphic mineral certainly is dubious. For determinative purposes is provided a chart (in a rear pocket) which is essentially a plot of birefringence against γ index with (+) minerals in the top half separated from (−) minerals of the lower half by a central band of isotropic species. By itself the diagram is hardly adequate as a substitute for a series of tables that would include many of the other optical properties. This section is well illustrated with photomicrographs, variation diagrams, and optical orientation diagrams. Many of the last two types stem from Tröger's book, Tabellen zur optischen Bestimmung der gesteinsbildenden Minerale (reviewed in *Am. Mineral.*, **38,** 144–45, 1953). Unfortunately the section still retains a mishmash of mineral varietal names of which many European mineralogists seem so pedantically fond: anomite, grothite, mesitinspar, pistomesite, oligonspar, quarzine, and pseudozoisite, among others.

The largest section (ca. 350 pp.) treats the relations between the microscopic characteristics of rocks and their technological employment. This is practically an independent volume, dealing with the mineralogy of rocks and quantitative mineralogical measurements; rock textures, their precise delineation, including petrofabric methods and interpretations, and their significance in the quarrying or mining of rocks and in the structural employment of rock; the weathering and weather resistivity of rocks; the relations between petrographic and technological characteristics of rocks, and finally an exhaustive description of examples—igneous (plutonic, dike, and flow rock), sedimentary and metamorphic. Some first-class photomicrographs of special features of rocks adorn this section. One cannot help but wonder to what extent technologists of the stone industry or tunnel engineers will concern themselves with such concepts as the "geneity" (Genität) and "tropy" (Tropie) of textures, or R-tectonites. Doubtless rocks as structural materials remain more widely used in Europe than in the United States, but it is to be hoped that Part 2 of Volume IV deals in at least equal detail with the petrography of concrete, brick, synthetic lightweight aggregate, and other fabricated structural materials of far greater quantitative importance today.

The descriptions of the properties of the fine-grained silicate minerals and the special problems attendant upon their determination are excellently presented by Correns and Piller. Minerals included are the clays, hydromicas, chlorites, and aluminum hydroxide minerals. The final short section on asbestos is concerned with microscopic determinations of types of asbestos, their special microscopic characteristics, microscopic control of quality, and microscopic characteristics of synthetic asbestos.

The book is difficult to evaluate as a whole; in fact it hardly is a whole but is just a collection of parts. Each section contains material of value to specialists in those particular subfields of mineralogy and petrography, but its jolting price tag of nearly $25 makes it impossible to recommend its purchase to students and other threadbare cohabitants of universities. Thus, doubtless it will be acquired chiefly by foundation libraries, petroleum geologists, and book reviewers.

E. Wm. Heinrich
University of Michigan
Ann Arbor, Michigan

NEW MINERAL NAMES

Ezcurrite

SIEGFRIED MUESSIG AND ROBERT D. ALLEN. Ezcurrite ($2Na_2O \cdot 5B_2O_3 \cdot 7H_2O$), a new sodium borate from Argentina; occurrence, mineralogy, and associated minerals. *Econ. Geol.*, **52,** 426–437 (1957).

Ezcurrite occurs in cleavable masses that have a bladed fibrous structure sometimes radiating; masses are up to 7 cm. long and 1.5 cm. wide. Chem. analyses by Ralph Mathieson and Henry Kramer gave, resp., B_2O_3 58.86, 59.34; Na_2O 20.67, 20.37; H_2O (20.47) (by diff.), 20.89; sum 100.00, 100.60%. Soluble in water, easily soluble in acids. When heated swells to an opaque white mass, then fuses to a clear glass.

Ezcurrite is colorless, transparent, luster vitreous to satiny. H. about 2.5, G. 2.153. Optically biaxial, neg., *n*s (Na) α 1.472, β 1.506, γ 1.526, all ± 0.002, 2V $73\frac{1}{2}°$ (calcd.), elongation positive, γ; elongation 42.6°. There are two cleavages, one perfect, one less so, which intersect at 71° 18.5′. The optical data suggest that ezcurrite is triclinic. *X*-ray powder data are given; the strongest lines are in Å: 6.94 10, 3.08 6, 2.77 3, 4.48 2, 3.31 2, 3.13 2; 45 weaker lines are listed.

Differential thermal analysis curves show a large endothermic reaction beginning at 160–170° with a low of the trough at 260–265°.

The mineral occurs at the Tincalayu borax mine, Salta province, Argentina, associated with borax and kernite. Ulexite and inderite occur elsewhere in the deposit.

The name is for Juan Manuel de Ezcurra, manager of the Compania Productora de Boratos, S. A., which owns the deposit.

MICHAEL FLEISCHER

Wölsendorfite

JEAN PROTAS. La wölsendorfite, nouvelle espèce uranifère. *Compt. rend.*, **244,** 2942–2944 (1957).

The mineral, previously confused with fourmarierite, occurs in crystalline red masses in fissures in fluorite at Wölsendorf, Bavaria, in orange-red crystalline incrustations on pitchblende from Great Bear Lake, in orange-red spherulites with the pitchblende of Kerségalec, Lignol, France, and in small carmine red nodules with secondary uranium minerals at Shinkolobwe, Katanga. Analysis made on 120 mg. gave UO_3 69.80, PbO 23.14, CaO 1.24, H_2O 4.30, insol. in HNO_3 0.48, sum 98.96%, corresponding to $(Pb, Ca)U_2O_7 \cdot 2H_2O$, with Pb:Ca = 5:1

X-ray study indicates the mineral to be orthorhombic, with *a* 11.95±0.05, *b* 13.99 ±0.07, *c* 7.02±0.05Å. The unit cell contains $CaPb_5U_{12}O_{42} \cdot 12H_2O$. There is one good cleavage (001). The *x*-ray powder pattern gave (in A.) for the strongest lines 3.09, 3.47, 6.93, 3.51, 14 more lines are given. D. 6.8±0.1; *n*s on a cleavage flake, determined in S-Se melts, were n_1 2.09±0.01, n_2 2.05±0.03.

The name is for the locality.

DISCUSSION.—The *x*-ray pattern is very close to that of "Mineral C" of Frondel, *Am. Mineral.* **41,** 539–568 (1956), but the optics and analyses are quite different. Frondel states that the same pattern was given by a sample of synthetic hydrated lead diuranate.

M. F.

Kašparite

ALOIS DUBANSKÝ. Přispěvky k Poznani geochemie sekundarnich sulfatu. III. Sulfaty z Dubniku u Prešova. *Chem. Listy*, **50,** 1347–1361 (1956).

Analysis of the fibrous mineral gave MgO 2.52, CoO 1.52, CaO 0.08, MnO 0.21, FeO 0.01, NiO, CuO tr., ZnO 0.11, Al_2O_3 13.37, Fe_2O_3 0.32, SO_3 35.45, H_2O 45.54, insol. 0.71, sum 99.84%. This corresponds to $(Mg, Co)Al_3(SO_4)_5(OH) \cdot 28H_2O$. A dehydration curve shows the loss of about 24 H_2O up to 300°, of 3 H_2O up to about 350°, and of SO_3 above 600°.

The mineral is monoclinic or triclinic. It has *ns* α 1.481, β 1.485, γ 1.487, $\gamma{:}c$ 30°. *X*-ray powder data are given and compared with those of pickeringite; the spacings and intensities check very closely for 21 of 24 lines, but kašparite shows extra lines at 5.84 and 4.12 (the latter strong) and does not show a weak line at 5.38.

The name is for Professor Jan Kašpar of Prague.

Discussion—Further work is needed, but the mineral would appear to be a cobaltoan pickeringite, perhaps with an admixed aluminum sulfate.

M. F.

Childro-Eosphorite

H. Strunz and Margarete Fischer. Childro-eosphorit, Tavorit, und Fairfieldit von Hagendorf. *Neues Jahrb. Mineral., Monatsh.*, **1957**, 78–88.

The name childro-eosphorite is given to a member of the childrenite-eosphorite series containing equal amounts of MnO and FeO. The analysis shows FeO 14.86, MnO 15.17, which gives MnO:FeO=1.034:1. It is therefore a ferroan eosphorite and the name is unnecessary.

M. F.

NEW DATA

Becquerelite

Jean Protas. Propriétés et synthèse d'un oxyde hydraté d'uranium et de calcium de Shinkolobwe, *Katanga Compt. rend.*, **244**, 91–93 (1957).

All samples (20) of becquerelite examined were found by *x*-ray study to be identical with a synthetic compound $CaO \cdot 6UO_3 \cdot 11H_2O$. Analysis of material from Shinkolobwe (on 160 mg.) gave UO_3 86.57, CaO 2.78, H_2O 10.16, sum 99.51%. D.T.A. study showed two breaks, at 160° and 360°.

X-ray study showed the mineral to be orthorhombic, *a* 13.86±0.03, *b* 12.42±0.03, *c* 14.96±0.03A. $Z=4$. G. 5.12±0.02 (natural), 5.10±0.02 (synthetic). Optically biaxial, negative, with *ns* α 1.725, β 1.815, γ 1.825, 2V 32°, X colorless, Y and Z yellow. *X*-ray powder patterns of the natural and synthetic compounds had the strongest lines 3.55, 3.55; 3.21, 3.20; 7.54, 7.48A.

Discussion—The *x*-ray and optical data agree well with those of Frondel and Cuttitta, *Am. Mineral.* **38**, 1019–1024 (1953), who found no CaO, and gave the formula as $7UO_3 \cdot 11H_2O$, but found $BaO \cdot 6UO_3 \cdot 11H_2O$ for the closely related billietite.

M. F.

Gunnbjarnite (=a ferrian sepiolite)

H. Strunz. Gunnbjarnit, ein Ferri-Sepiolith. *Neues Jahrb. Mineral.*, Monatsh., **1957**, 75–77.

Gunnbjarnite, described in 1951 as a nontronite (*Am. Mineral.*, **37**, 1070 (1952)) is shown by *x*-ray study to be a member of the sepiolite group. Rotation photographs around [100] gave a_0 5.30, b_0 27.00, c_0 13.42. The unit cell contains 2

$$[(Mg_{2.27}Fe''_{0.10}Mn_{0.01}Ca_{0.45}Fe'''_{0.75})_{3.58}(Si_{5.03}Al_{0.45}Fe'''_{0.52})O_{15}(H_2O)_3(OH)_2 \cdot 3H_2O.]$$

M.F.

DISCREDITED MINERALS

Laubanite (=Natrolite)

H. Strunz. Laubanit, ein Natrolith, *Neues Jahrb. Mineral.*, Monatsh. **1957,** 116–118.

Laubanite was described in 1887 by Traube as a zeolite. Analyses by Traube and by Brendler in 1955 agree well: SiO_2 47.84, 47.91; Al_2O_3 16.74, 16.60; FeO 0.56, trace; MgO 1.35, 1.46; CaO 16.07, 16.80; H_2O 17.08, 17.22; sum 99.74, 99.99%. G. 2.29, 2.24. The original samples were lost during the war, but samples from the type locality that corresponded to the original description were obtained from seven collections.

These showed G. 2.20–2.26, *ns* α 1.477, γ 1.489. Spectrographic analyses of several samples showed much Na, little Ca, very little Mg. Flame photometer determinations showed CaO 0.5–1.0%, Na_2O 6.88–6.94%. *X*-ray powder photographs agreed with that of natrolite.

Laubanite therefore appears to be a natrolite that has lost about half its Na_2O, perhaps by exchange for H^+ or $(H_3O)^+$. No explanation can be given for the two erroneous analyses.

M. F.

Galapektite (=Montmorillonite)

G. T. Faust. A study of the montmorillonite variety galapektite. *J. Wash. Acad. Sci.*, **47,** 143–146 (1957).

Galapektite was described by Breithaupt in 1832 as a clay mineral from Angleur, Belgium. Since then, it has been referred to montmorillonite and also to halloysite, both of which occur at Angleur. An analysis, published by Ross and Hendricks (1945), and new *x*-ray and D.T.A. data show that galapektite is a montmorillonite. The name should be dropped.

M. F.

Nocerite (=Fluoborite)

Cesare Brisi and Wilhelm Eitel. Identity of nocerite and fluoborite. *Die Naturwissenschaften*, **21,** 496 (1956).

Nocerite, supposedly $Ca_3Mg_3F_8O_2$ (see Dana's *System*, 7th Ed., Vol. **2,** p. 85), is shown by spectrographic analysis to be a fluoborate, the F end-member of the fluoborite series, as shown by the optical data and unit cell determinations (see Dana's *System*, 7th Ed., vol. **2,** p. 369). Presumably the high Ca reported in nocerite was due to admixed fluorite or limestone (but no CO_2 was reported).

See *Am. Mineral.*, **42,** 288–293. M. F.

INDEX TO VOLUME 42

Leading articles are in **bold face** type; notes, abstracts and reviews are in ordinary type. Only minerals for which definite data are given are indexed.

Abernathyite (Thompson, Ingram, Gross) 443
Absorption spectra of some silicates in the visible and near infrared (Clark) 732
Administration Report of the Ceylon Government Mineralogist for 1955 (Fernando) 439
Ahlfeld, F., and Reyes, J. M. Las Especies Minerales de Bolivia (Book Review) 304
Allen, R. D. 919
———, and Kramer, H. Ginorite and sassolite from Death Valley, California 56
———, with Muessig, S. The hydration of kernite 699
Alluaudites and varulites (Fisher) 661
"Alterite," use of the term (Carroll) 110
Aluminian ferroanthophyllite from the Kitakami Mountainland, Northeastern Japan (Seki, Yamasaki) 506
Alumoferroascharite (Serdyuchenko) 582
Alushtite (=dickite+hydrous mica) (Logvinenko, Frank-Kamenetskii) 122
Andalusite- and corundum-bearing pegmatites in Yosemite National Park, California (Rose) 635
Anderson, George Harold, memorial of (Gillson) 240
Angular aperture, and useful interference figures (Windhell) 570
Ankinovich, E. A. 583
Anthony, J. W. Hydrothermal synthesis of monazite 904
Anthophyllite and hornblende from the Bancroft area, Ontario, paragenesis of (Tilley) 412
Appleman, D. E., with Coleman, R. G. Umohoite from the Lucky Mc Mine, Wyoming 657
Arizona's Meteorite Crater, Past-Present-Future (Nininger) (Book Review) 576
Arsenate-belovite, phosphate-belovite (Yakhontova, Sidorenko) 583
Arsentsumebite (=duftite-α) (Guillemin) 122
Auraria: The Story of a Georgia Gold-Mining Town (Coulter) (Book Review) 438
Avalite (=chromian illite) (Stangatchilovitch) 122
Avelinoite (=cyrilovite) (Lindberg) (Strunz) 586
Avelinoite, cyrilovite and wardite, relationship of the minerals (Lindberg) 204
Axelrod, J. M. 581

β-Ga_2O_3 and its alumina isomorph, θ-Al_2O_3, characterization of (Kohn, Katz, Broder) 398
Barker Index of Crystals: A Method for the Identification of Crystalline Substances. Vol. II, Monoclinic System (Porter, Spiller) (Book Review) 575
Barnes, H. L. How to Prospect for Uranium (Book Review) 579
Bass, M. N. Effects of gamma irradiation on physical properties of minerals 100
Bassett, W. A., and Lapham, D. M. A thermal increment diffractometer 548
Bau und Bildung der Kristalle. Die Architektonik der Stofflichen Welt (Raaz, Köhler) (Book Review) 436
Baumann, H. N., Jr. The preparation of petrographic sections with bonded diamond wheels 416
Baur, G. S., Larsen, W. N., and Sand, L. B. Image projection by fibrous minerals 697
———, and Sand, L. B. *X*-ray powder data for ulexite and

halotrichite 676
Becquerelite (Protas) 920
Berger, R. W., with Tennant, C. G. *X*-ray determination of the dolomite-calcite ratio of a carbonate rock 23
Berman, R. M. The role of lead and excess oxygen in uraninite 705
——— Some physical properties of naturally irradiated fluorite 191
——— Studies of uranium minerals (XXIII); torbernite, zeunerite and uranospherite 905
Bibliography of Hardness and Hardness Testing (Book Review) 303
Bikitaite, $LiAlSi_2O_6 \cdot H_2O$, a new mineral from Southern Rhodesia (Hurlbut) 792
Billings, M. P. The Geology of New Hampshire, Part 2: Bed Rock Geology 439
Birnessite (Jones, Milne) 440
Bismutotantalite from Brazil (Hurlbut) 178
Bobkovite (Kazitsyn) 440
Bohnshtedt-Kupletskaya, E. M. 308
Boltwoodite (Frondel, Ito) 307
Bondareva, A. M. 585
Borazon 301
Borgniezite (de Bethune, Meyer) 443
Borgstromite (=jarosite) 586
Borodin, L. S. 581
Bowen, N. L. The Evolution of the Igneous Rocks (Book Review) 435
Bowen, Norman L., memorial of (Schairer) 242
Brannerite from San Bernardino County, California (Hewett, Stone, Levine) 30
Brindley, G. W. 585
———, with Zussman, J. Serpentine with 6-layer ortho-hexagonal cells 666
———, and Zussman, J. A structural study of the thermal transformation of serpentine minerals to forsterite 461
———, with Zussman, J., and Comer, J. J. Electron diffraction studies of serpentine minerals 133
Brisi, C., and Eitel, W. Identity of norcerite and fluoborite 288, 921
Broder, J. D., with Kohn, J. A., and Katz, G. Characterization of β-Ga_2O_3 and its alumina isomorph, θAl_2O_3 398
Buddington, A. F. Acceptance of the Roebling Medal 259
Buerger, M. J. Elementary Crystallography (Book Review) 305
Butler, J. R. Rare earths and thorium in lyndochite 671

Caillère, S. 586
Calcite-aragonite equilibrium, note on (Clark) 564
Caley, E. R., and Richards, J. F. S. Theophrastus on Stones (Book Review) 437
Carobbiite (Strunz) 117
Carphosiderite, borgstromite, utahite, cyprusite (all=jarosite or natrojarosite) (Moss) 586
Carroll, D. Use of the term "alterite" 110
Cerite, crystallography of (Gay) 429
Chayes, F. Petrographic Modal Analysis (Book Review) 574
———, and MacKenzie, W. S. Experimental error in determining certain peak locations and distances between peaks in *x*-ray powder diffractometer patterns 534
Chemical Analyses of Igneous Rocks, Metamorphic Rocks, and Minerals, 1931–1954 (Guppey) 439
Childro-Eosphorite (Strunz, Fischer) 920
Christ, C. L. (Book Reviews) 305, 575
Chukhrov, F. V. 440
Claringbull, G. F. 444, 580
Clark, S. P., Jr. Absorption spectra of some silicates in the visible and near infrared 732
——— A note on calcite-aragonite equilibrium 564

Clay mineral, identification of the 14 Å component (Tamura)... 107
Clay Minerals Bulletin, Vol. 3, No. 15, Oct. 1956... 439
Clay minerals, determination of (060) reflections of by means of counter type *x*-ray diffraction instruments (Rich)... 569
Clay minerals, separation of from carbonate rocks (Ray, Gault, Dodd)... 681
Clays and Clay Minerals (Swineford, Editor) (Book Review)... 305
Clifford, T. N. Fuchsite from a Silurian (?) quartz conglomerate, Acworth Township, New Hampshire... 566
Clino-chrysotile (Whittaker, Zussman) (Zussman, Brindley, Comer)... 585
Cochran, M., and King, A. G. Two new types of holders used in grinding thin sections... 422
Coffinite (Stieff, Stern, Sherwood)... 443
Coleman, R. G., and Appleman, D. E. Umohoite from the Lucky Mc Mine, Wyoming... 657
Collette, R. L., with Frondel, C. Hydrothermal synthesis of zircon, thorite, and huttonite... 759
——— Synthesis of tourmaline by reaction of mineral grains with NaCl-H_3BO_3 solution, and its implications in rock metamorphism... 754
Comer, J. J.... 585
———, with Zussman, J., and Brindley, G. W. Electron diffraction studies of serpentine minerals... 133, 585
Coulter, E. M. Auraria: The Story of a Georgia Gold-Mining Town (Book Review)... 438
Cryphiolite (=mixture) (Claringbull, Hey)... 444
Crystallographic Data for the Calcium Silicates Heller, Taylor) (Book Review)... 436
Cuproplumbite (=bayldonite) (Guillemin)... 123
Curien, H.... 119
Cyprusite (=jarosite) (Moss)... 586
Cyrilovite, avelinoite and wardite, relationship of the minerals (Lindberg)... 204
Cyrtolite, *x*-ray fluorescence as applied to (Norton)... 492

de Bethune, P.... 443
Delahay, P. Instrumental Analysis (Book Review)... 702
Denning, R. M. The grinding hardness of diamond in a principal cutting direction... 362
———, (Book Reviews)... 303, 435
———, Giardini, A. A., Poindexter, E., Slawson, C. B. Piezobirefringence in diamond: further results... 556
Diamond (Hahn) (Book Review)... 304
Diamond, the grinding hardness in a principal cutting direction (Denning)... 362
Diamond, piezobirefringence in: further results (Denning, Giardini, Poindexter, Slawson)... 556
Diamond, a spectrographic study of the minor element content of (Raal)... 354
Diamond, thermal expansion of (Skinner)... 39
Diamonds, synthetic, hardness of (Slawson)... 299
Diderichite (=rutherfordine) (Frondel, Meyrowitz)... 444
Differential thermal analysis, a new method employing multiple thermocouples (Lodding, Sturm)... 78
Discredited minerals... 121, 444, 586, 921
Dodd, C. G., with Ray, S., and Gault, H. R. The separation of clay minerals from carbonate rocks... 681
Dolomite-calcite ratio of a carbonate rock, *x*-ray determination of (Tennant, Berger)... 23
Dolomite, zincian and plumbian, from Tsumeb, South-West Africa (Hurlbut)... 798

Doloresite, a new vanadium oxide mineral from the Colorado plateau (Stern, Stieff, Evans, Sherwood) 587

Dubanský, A. 919

Duftite (Guillemin) 123

Duttonite, a new quadrivalent vanadium oxide from the Peanut Mine, Montrose County, Colorado (Thompson, Roach, Meyrowitz) 455

Eckelmann, W. R., with Kulp, J. L. Discordant U-Pb ages and mineral type 154

Eitel, W., with Brisi, C. Identity of norcerite and fluoborite . . . 288

Elementary Crystallography (Buerger) (Book Review) 305

Emerson, D. O., and Wright, H. D. Secondary uranium minerals at the W. Wilson Mine in the Boulder batholith, Montana . . 222

Engelhardt, W. v. 120

Epidote from Hawleyville, Connecticut (Lapham) 62

Erd, R. C. (Book Review) 578

———, Evans, H. T., Jr., and Richter, D. H. Smythite, a new iron sulfide, and associated pyrrhotite from Indiana 309

Eunicite (Paiva Hetto) 441

Evans, H. T., Jr., with Erd, R. C. and Richter, D. H. Smythite, a new iron sulfide, and associated pyrrhotite from Indiana 309

———, with Robinson, S. C., Schaller, W. T., and Fahey, J. J. Nolanite, a new iron-vanadium mineral from Beaverlodge, Saskatchewan 619

———, with Stern, T. W., Stieff, L. R., and Sherwood, A. M. Doloresite, a new vanadium oxide mineral from the Colorado Plateau 587

Evolution of the Igneous Rocks (Bowen) (Book Review) 435

Ezcurrite (Muessig, Allen) 919

Fahey, J. J., with Robinson, S. C., Evans, H. T., Jr., and Schaller, W. T. Nolanite, a new iron-vanadium mineral from Beaverlodge, Saskatchewan 619

Fairbairn, H. W. (Book Review) . . 574

Famatinite (Gaines) 766

Fassaite from near Helena, Montana (Knopf, Lee) 73

Faust, G. T. (Book Reviews) . . . 435, 436

——— 921

Fernando, L. J. D. Administration Report of the Ceylon Government Mineralogist for 1955 . . . 439

Ferritungstite from Nevada, new data on (Richter, Reichen, Lemmon) 83

Ferroferrimargarite (Ginzburg) 582

Fibrous minerals, image projection by (Sand, Baur, Larsen) 697

Fischer, M. 920

Fisher, D. J. Alluaudites and varulites 661

Fisher, E. 121

Fluoborite and norcerite, identity of (Brisi, Eitel) 288

Fluorite, some physical properties of naturally irradiated (Berman) 191

Foshag, William Frederick, memorial of (Schaller) 249

Franck, M. L., with Smith, W. L., and Sherwood, A. M. U and Th in accessory allanite of igneous rocks 367

Frank-Kamenetskii, V. A. 122

Free energy values from geologic relations, some (Garrels) 780

Freirinite (=lavendulan) Guillemin 123

Frondel, C. Mineralogy of uranium 125

———, Presentation of Certificate of Appreciation to the retiring editor of the American Mineralogist, Walter F. Hunt 265

——— 307, 443

———, and Collette, R. L. Synthesis of tourmaline by reaction of mineral grains with NaCl-H_3BO_3 solution, and its implications in rock metamorphism 754

——— Hydrothermal synthesis of zircon, thorite, and huttonite.. 759

———, and Ito, J. The geochemistry of germanium in the oxidized zone of the Tsumeb Mine, South-West Africa.... 743

Fuchsite from a Silurian (?) quartz conglomerate, Acworth Township, New Hampshire (Clifford)...................... 566

Füchtbauer, H................. 120

Gabrielson, O.................. 581

Gaines, R. V. Luzonite, famatinite, and some related minerals... 766

Galapektite (=montmorillonite) (Faust)................... 921

Gamma irradiation, effects on physical properties of minerals (Bass).................... 100

Garnets, diagrams for the correlation of unit cell edges and refractive indices with the chemical composition of (Sriramadas)................... 294

Garrels, R. M. Some free energy values from geologic relations 780

Gault, H. R., with Ray, S., and Dodd, C. G. The separation of clay minerals from carbonate rocks...................... 681

Gay, P. The crystallography of cerite...................... 429

Genthelvite from Cookstove Mt., El Paso Co., Col. (Scott)..... 425

Geología de las Cuencas Sedimentarias de Venezuela y de sus Campos Petrolíferos (Young, Bellizzia, Renz, Johnson, Robie, Mas Vall) (Book Review)..................... 579

Geology of New Hampshire, Part 2: Bed Rock Geology (Billings) 439

Gerasimovsky, V. I.............. 307

Germanium in the oxidized zone of the Tsumeb Mine, South-West Africa, geochemistry of (Frondel, Ito).................. 743

Gerstleyite (Frondel, Morgan).... 443

Getseva, R. V.................. 442

Giardini, A. A., with Denning, R. M., Poindexter, E., and Slawson, C. B. Piezobirefringence in diamond: further results..................... 556

Gillson, J. L. Memorial of George Harold Anderson........... 240

Ginorite and sassolite from Death Valley, California (Allen, Kramer).................. 56

Ginzburg, A. I.................. 582

Ginzburgites (Chukhrov)......... 440

Girhard, M. N.................. 443

Grawe, O. R.................... 443

Grimaldi, F. S. (Book Review).... 702

Gross, E. B..................... 443

Gruner, J. W., with Smith, D. K., Jr., and Lipscomb, W. N. The crystal structure of uranophane $[Ca(H_3O)_2](UO_2)_2(SiO_4)_2 \cdot 3H_2O$............... 594

Guillemin, C......119, 122, 123, 124, 444

Gunnbjarnit (Strunz)............ 920

Guppey, E. M. Chemical Analyses of Igneous Rocks, Metamorphic Rocks, and Minerals, 1931–1954................. 439

Hahn, E. Diamond (Book Review) 304

Halloysite and montmorillonite, a technique for the isolation of (Loughnan)................ 393

Halotrichite, *x*-ray powder data for (Baur, Sand)............... 676

Handbuch der Mikroskopie in der Technik (Freund, Editor) (Book Review)............. 917

Hand-picking mineral grains, an apparatus for (Murthy)...... 694

Hanes, M. E., with McIntosh, L. Lineation protractor......... 432

Heidornite (Engelhardt, Füchtbauer).................... 120

Heinrich, E. W. (Book Reviews)... ....439, 578, 917

Heller, L., and Taylor, H. F. W. Crystallographic Data for the Calcium Silicates (Book Review)..................... 436

Henderson, E. P. (Book Review) 576, 578

Hénin, S....................... 586

Henriques, A................... 586

Hess, H. H. Presentation of the Roebling Medal to Arthur F. Buddington 256
Hewett, D. F., and Stone, J. Uranothorite near Forest Home, San Bernardino County, California 104
———, and Levine, H. Brannerite from San Bernardino County, California 30
Hey, M. H. 444, 580
Heyl, A. V. 581
Hibonite (Curien, Guillemin, Orcel, Sternberg) 119
Honea, R. M. Identity of pilbarite with thorogummite and kasolite 908
Honessite (Heyl, Milton, Axelrod) 581
How to Prospect for Uranium (Barnes) (Book Review) 579
Howlite from California, crystallography and *x*-ray measurements of (Murdoch) 521
Huang, W. T. Titanclinohumite from the Wichita Mountains, Oklahoma 686
Hull-Davey chart, modified, for high values of *c/a* (Schneer) . . 282
Hunt, Walter F., retiring editor of the American Mineralogist, presentation of Certificate of Appreciation to (Frondel) 265
Hurlbut, C. S., Jr. Bikitaite, $LiAlSi_2O_6 \cdot H_2O$, a new mineral from Southern Rhodesia 792
——— Bismutotantalite from Brazil 178
——— The wurtzite-greenockite series 184
——— Zincian and plumbian dolomite from Tsumeb, South-West Africa 798
Hutton, C. O. Kobeite from Paringa River, South Westland, New Zealand 342
——— Sengierite from Bisbee, Arizona 408
Huttonite, hydrothermal synthesis of (Frondel, Collette) 759
Hydrocuprite discredited (Switzer) 115
Hydrogrossular from Tokatoka, New Zealand (Mason) 379
Hydronasturan (Getseva) 442

Iddingsite in some basaltic rocks of New Mexico, the nature of (Sun) 525
Ingerson, E. (Book Reviews) . . . 304, 579
Ingram, B. 443
Instrumental Analysis (Delahay) (Book Review) 702
Introduction to Crystallography (Phillips) (Book Review) 435
Istisuite (Kashkai, Mamedov) 117
Ito, J. 307
———, with Frondel, C. The geochemistry of germanium in the oxidized zone of the Tsumeb Mine, South-West Africa 743

Jones, L. H. P. 440

Kalousek, G. L., and Muttart, L. E. Studies on the chrysotile and antigorite components of serpentine 1
Kalsilite, order-disorder in (Smith, Sahama) 287
Karpatite (Piotrovsky) 120
Karpinskite (Ruskavishnikova) . . . 584
Karpinskyite (Shilin) 119
Kashkai, M. A. 117
Kašparite (Dubanský) 919
Katz, G., with Kohn, J. A., and Broder, J. D. Characterization of β-Ga_2O_3 and its alumina isomorph, θ-Al_2O_3 398
Kazitsyn, Y. V. 440
Kennedy, G. C. Acceptance of the Mineralogical Society of America Award 264
Kernite, hydration of (Muessig, Allen) 699
Kerr, P. F., with Kopp, O. C. Differential thermal analysis of sulfides and arsenides 445
Kettnerite (Zak, Syneček) 121
King, A. G. Pyrite-uraninite polycrystal 648
——— Technique for thinned polished sections 689

———, with Cochran, M. Two new types of holders used in grinding thin sections........ 422
Kingite (Norrish, Rogers, Shapter) 580
Klingsberg, C., and Roy, R. Synthesis, stability and polytypes of nickel and gallium phlogopite........................ 629
Knopf, A., and Lee, D. E. Fassaite from near Helena, Montana.. 73
Kobeite from Paringa River, South Westland, New Zealand (Hutton).................. 342
Kohn, J. A., Katz, G., and Broder, J. D. Characterization of β-Ga_2O_3 and its alumina isomorph, θAl_2O_3.............. 398
Kopp, O. C., and Kerr, P.F. Differential thermal analysis of sulfides and arsenides.......... 445
Kramer, H., with Allen, R. D. Ginorite and sassolite from Death Valley, California..... 56
Kraus, E. H. (Book Review)..... 304
Kulp, J. L., and Eckelmann, W. R. Discordant U-Pb ages and mineral type................ 154
Kupletskite (Semenov).......... 118
Kurath, S. F. Storage of energy in metamict minerals.......... 91
Kurumsakite (Ankinovich)....... 583

Lapham, D. M. Epidote from Hawleyville, Connecticut......... 62
———, with Bassett, W. A. A thermal increment diffractometer....................... 548
Larnite, scawtite and hydrogrossular from Tokatoka, New Zealand (Mason)............... 379
Larsen, W. N., with Baur, G. S., and Sand, L. B. Image projection by fibrous minerals...... 697
Larsenite, $PbZnSiO_4$, unit cell and space group of (Layman)..... 910
Las Especies Minerales de Bolivia (Ahlfeld, Reyes) (Book Review)..................... 304
Lattice constants from Weissenberg patterns (Pabst)............ 664
Laubanite (=natrolite) (Strunz).. 921
Lavendulan (freirinite=lavendulan) (Guillemin)............ 123
Layman, F. G. Unit cell and space group of larsenite, $PbZnSiO_4$.. 910
Lee, D. E., with Knopf, A. Fassaite from near Helena, Montana.. 73
Lemmon, D. M., with Richter, D. H., and Reichen, L. E. New data on ferritungstite from Nevada.................... 83
Lepp, H. Stages in the oxidation of magnetite.................. 679
Lesserite (Frondel, Morgan, Waugh)................... 443
Leucophosphite from the Sapucaia pegmatite mine, Minas Gerais, Brazil (Lindberg)....... 214
Levine, H., with Hewett, D. F., and Stone, J. Brannerite from San Bernardino County, California..................... 30
Lindackerite (Guillemin)......... 124
Lindberg, M. L................. 586
——— Leucophosphite from the Sapucaia pegmatite mine, Minas Gerais, Brazil........ 214
——— Relationship of the minerals avelinoite, cyrilovite and wardite...................... 204
Lineation protractor (McIntosh, Hanes).................... 432
Lipscomb, W. N., with Smith, D. K., Jr., and Gruner, J. W. The crystal structure of uranophane $[Ca(H_3O)_2](UO_2)_2(SiO_4)_2 \cdot 3H_2O$.............. 594
Lithiophosphate (Matias, Bondareva).................... 585
Lizardite, ortho-chrysotile, clinochrysotile, para-chrysotile (Whittaker, Zussman) (Zussman, Brindley, Comer)...... 585
Lodding, W., and Sturm, E. A new method of differential thermal analysis employing multiple thermocouples............. 78
Lodochnikite (lodochnikovite), ufertite (uferite), obruchevite (Melkor, Gerasimovsky)..... 307
Logvinenko, L. V................ 122
Loughnan, F. C. A technique for the

isolation of montmorillonite and halloysite 393
Luzonite, famatinite and related minerals (Gaines) 766
Lyndochite, rare earths and thorium in (Butler) 671

MacKenzie, W. S., with Chayes, F. Experimental error in determining certain peak locations and distances between peaks in *x*-ray powder diffractometer patterns 534
Magnetite, stages in the oxidation of (Lepp) 679
Magnussonite (Gabrielson) 581
Mamedov, A. I. 117
Mandy, T. 704
Marine bottom samples off the coast of Peru and Chile, preliminary report on the mineralogy and petrology of some (Zen) 889
Mason, B. Larnite, scawtite and hydrogrossular from Tokatoka, New Zealand 379
Matias, V. V. 585
Mauritzite (Tokody, Mandy, Nemes-Varga) 704
McConnell, D. (Book Reviews) . 305, 437
McIntosh, L., and Hanes, M. E. Lineation protractor 432
McKinstry, H. E. (Book Review) . 437
Mertie, J. B., Jr. (Book Review) .. 438
Meta-autunite I 226
Meta-torbernite 228
Meta-uranocircite 228
Meta-zeunerite 230
Metamict minerals, storage of energy in (Kurath) 91
Metatyuyamunite (Stern, Stieff, Girhard, Meyrowitz) 443
Meteorites in the Collections of Yale University, Postilla No. 27, Yale Peabody Museum, Kurt Servos (Book Review) .. 578
Meyer, A. 443
Meyrowitz, R. 117, 443
———, with Thompson, M. E., and Roach, C. H. Duttonite, a new quadrivalent vanadium oxide from the Peanut Mine, Montrose County, Colorado 455
Millerite, a new occurrence of (Woodhouse, Norris) 113
Milne, A. A. 440
Milton, C. 581
Mineralogical Society of America Award, acceptance of (Kennedy) 264
Mineralogical Society of America Award, presentation to George C. Kennedy (Schairer) 262
Mineralogical Society of America, proceedings of the thirty-seventh annual meeting at Minneapolis, Minnesota 267
List of papers of special mineralogical interest presented at annual meeting 278
Miyashiro, A. 443
Moleva, V. A. 308
Monazite, hydrothermal synthesis of (Anthony) 905
Montgomery, A. Three occurrences of high-thorian uraninite near Easton, Pennsylvania 804
Montmorillonite and halloysite, a technique for the isolation of (Loughnan) 393
Morgan, V. 443
Moss, A. A. 586
Muessig, S., and Allen, R. D. The hydration of kernite 699
Muessiz, M. 919
Murdoch, J. Crystallography and *x*-ray measurements of howlite from California 521
Murthy, M. V. N. An apparatus for hand-picking mineral grains .. 694
Muttart, L. E., with Kalousek, G. L. Studies on the chrysotile and antigorite components of serpentine 1

Nazarenko, I. I. 581
Nemes-Varga, S. 704
Nenadkevite (Polykarpova) 441
New data 123, 443, 586, 920
New mineral names 117, 307, 440, 580, 704, 919
Nickel, E. H. 443

Nickel and gallium phlogopite, synthesis, stability and polytypes of (Klingsberg, Roy) 629
Nininger, H. H. Arizona's Meteorite Crater, Past-Present-Future (Book Review) 576
Niocalite (Nickel) 443
Nolanite, a new iron-vanadium mineral from Beaverlodge, Saskatchewan (Robinson, Evans, Schaller, Fahey) 619
Norcerite and fluoborite, identity of (Brisi, Eitel) 288, 921
Norris, R. M., with Woodhouse, C. D. A new occurrence of millerite 113
Norrish, K. 580
Norton, D. A. *X*-ray fluorescence as applied to cyrtolite 492

Obruchevite (Melkor, Gerasimovsky) 307
Offretite (=phillipsite) (Strunz) . . 444
Olivine *x*-ray determinative curve (Yoder, Sahama) 475
Orcel, J. 119, 586
Ortho-chrysotile (Whittaker, Zussman) (Zussman, Brindley, Comer) 585
Osumilite (Miyashiro) 443

Pabst, A. (Book Review) 436
——— Lattice constants from Weissenberg patterns 664
Painite (Claringbull, Hey, Payne) . 580
Paiva Hetto, J. E. 441
Parabayldonite (=plumboan conichalcite) (Guillemin) 123
Para-chrysotile (Whittaker, Zussman) (Zussman, Brindley, Comer) 585
Payne, C. J. 580
Pearl, R. M. Rocks and Minerals (Book Review) 578
Pelitic schists, the graphical analysis of mineral assemblages in (Thompson) 842
Peralkaline granite from Cashes Ledge, Gulf of Maine, notes on (Toulmin) 912
Periclase, thermal expansion of (Skinner) 39
Petrographic Modal Analysis (Chayes) (Book Review) 574
Petrographic sections, preparation with bonded diamond wheels (Baumann) 416
Pettijohn, F. J. Sedimentary Rocks (Book Review) 578
Phillips, F. C. An Introduction to Crystallography (Book Review) 435
Phosphate-belovite (Yakhontova, Sidorenko) 583
Pilbarite, identity of, with thorogummite and kasolite (Honea) 908
Piotrovsky, G. L. 120
Plagioclase feldspars, determination of the composition of by means of infrared spectroscopy (Thompson, Wadsworth) 334
Poindexter, E., with Denning, R. M., Giardini, A. A., and Slawson, C. B. Piezobirefringence in diamond: further reresults 556
Polished sections, thinned, technique for (King) 689
Polykarpova, V. A. 441
Porter, M. W., and Spiller, R. C. The Barker Index of Crystals: A Method for the Identification of Crystalline Substances. Vol. II, Monoclinic System (Book Review) 575
Preobrazhenskite (Yarzhemskii) . . 704
Progress in Economic Geology 439
Prokofjew, A. P. Vorratsberechnung Mineralischer Rohstoffe (Book Review) 437
Protas, J. 919, 920
Pyrite-uraninite polycrystal (King) 648

Quartz, ionic diffusion and the properties of. (1) The direct current resistivity (Wenden) . . 859

Raal, F. A. A spectrographic study of the minor element content of diamond 354
Raaz, F., and Köhler, A. Bau und Bildung der Kristalle. Die Architektonik der Stofflichen Welt (Book Review) 436

Ramdohr, P. 584

Ray, S., Gault, H. R., and Dodd, C. G. The separation of clay minerals from carbonate rocks 681

Reichen, L. E., with Richter, D. H., and Lemmon, D M. New data on ferritungstite from Nevada. 83

Rich, C. I. Determination of (060) reflections of clay minerals by means of counter type *x*-ray diffraction instruments. 569

Richards, J. F. C., with Caley, E. R. Theophrastus on Stones (Book Review). 437

Richter, D. H., with Erd, R. C., and Evans, H. T., Jr. Smythite, a new iron sulfide, and associated pyrrhotite from Indiana. 309

———, Reichen, L. E., and Lemmon, D. M. New data on ferritungstite from Nevada. 83

Richter, T. L. 581

Roach, C. H. 117

———, with Thompson, M. E., and Meyrowitz, R. Duttonite, a new quadrivalent vanadium oxide from the Peanut Mine, Montrose County, Colorado. . 455

Robinson, S. C., Evans, H. T., Jr., Schaller, W. T., and Fahey, J. J. Nolanite, a new iron-vanadium mineral from Beaverlodge, Saskatchewan. 619

Rocks and Minerals (Pearl) (Book Review). 578

Roebling Medal, acceptance of (Buddington). 259

Roebling Medal, presentation to Arthur F. Buddington (Hess). 256

Rogers, L. E. R. 580

Romo, L. A., and Roy R. Studies of the substitution of OH^- by F^- in various hydroxylic minerals 165

Rose, R. L. Andalusite- and corundum-bearing pegmatites in Yosemite National Park, California. 635

Roy, R., with Klingsberg, C. Synthesis, stability and polytypes of nickel and gallium phlogopite. 629

———, with Romo, L. A. Studies of the substitution of OH^- by F^- in various hydroxylic minerals 165

Rukavishnikova, I. A. 584

Sahama, T. G., and Smith, J. V. Tri-kalsilite, a new mineral. . . 286

———, with Smith, J. V. Order-disorder in kalsilite. 287

———, with Yoder, H. S., Jr. Olivine *x*-ray determinative curve 475

Sand, L. B., with Baur, G. S. *X*-ray powder data for ulexite and halotrichite. 676

———, and Larsen, W. N. Image projection by fibrous minerals. 697

Sassolite and ginorite from Death Valley, California (Allen, Kramer). 56

Scawtite from Tokatoka, New Zealand (Mason). 379

Schairer, J. F. Memorial of Norman L. Bowen. 242

———, Presentation of the Mineralogical Society of America Award to George C. Kennedy. 262

Schaller, W. T. Memorial of William Frederick Foshag. 249

———, with Robinson, S. C., Evans, H. T., Jr., and Fahey, J. J. Nolanite, a new iron-vanadium mineral from Beaverlodge, Saskatchewan. 619

Schneer, C. J. A modified Hull-Davey chart for high values of *c/a*. 282

Scott, G. R. Genthelvite from Cookstove Mountain, El Paso County, Colorado. 425

Sedimentary Rocks. 2d ed. (Pettijohn) (Book Review). 578

Seki, Y., and Yamasaki, M. Aluminian ferroanthophyllite from the Kitakami Mountainland, Northeastern Japan. 506

Semenov, E. I. 118, 308

Sengierite from Bisbee, Arizona (Hutton). 408

Serdyuchenko, D. P. 582

Serpentine minerals, electron dif-

fraction studies of (Zussman, Brindley, Comer)........... 133
Serpentine minerals, structural study of the thermal transformation to forsterite (Brindley, Zussman).................. 461
Serpentine, studies on the chrysotile and antigorite components of (Kalousek, Muttart)....... 1
Serpentines with 6-layer orthohexagonal cells (Zussman, Brindley).................. 666
Shapter, R. E.................... 580
Sherwood, A. M................. 443
———, **with Smith, W. L., and Franck, M. L. U and Th in accessory allanite of igneous rocks**...................... 367
———, **with Stern, T. W., Stieff, L. R., and Evans, H. T., Jr. Doloresite, a new vanadium oxide mineral from the Colorado plateau**................ 587
Shilin, L. L...................... 119
Shorsuite (Vinnichenko)......... 441
Sidorenko, G. A.................. 583
Siever, R. The silica budget in the sedimentary cycle........... 821
Silica budget in the sedimentary cycle (Siever)............... 821
Simplotite (Thompson, Roach, Meyrowitz)................ 117
Skinner, B. J. The thermal expansions of thoria, periclase and diamond................... 39
Slawson, C. B. Hardness of synthetic diamonds............. 299
———, **with Denning, R. M., Giardini, A. A., and Poindexter, E. Piezobirefringence in diamond: further results**....... 556
Sludskaya, N. N.................. 308
Smith, D. K., Jr., Gruner, J. W., and Lipscomb, W. N. The crystal structure of uranophane $[(Ca(H_3O)_2](UO_2)_2(SiO_4)_2\cdot 3H_2O$ 594
Smith, J. V., and Sahama, T. G. Order-disorder in kalsilite.... 287
———, with Sahama, T. G. Trikalsilite, a new mineral...... 286
Smith, W. L., Franck, M. L., and Sherwood, A. M. U and Th in accessory allanite of igneous rocks...................... 367
Smolianinovite (Yakhontova)..... 307
Smythite, a new iron sulfide, and associated pyrrhotite from Indiana (Erd, Evans, Richter).. 309
Sriramadas, A. Diagrams for the correlation of unit cell edges and refractive indices with the chemical composition of garnets...................... 294
Stangatchilovitch, D. (Stangačilović, D.)..................... 122
Starkeyite (Grawe).............. 443
Staszicite (=olivenite?) (Guillemin)...................... 122
Stead, F. W. (Book Review)...... 579
Stern, T. W..................... 443
———, **Stieff, L. R., Evans, H. T., Jr., and Sherwood, A. M. Doloresite, a new vanadium oxide mineral from the Colorado plateau**................. 587
Sternberg, M..................... 119
Stieff, L. R...................... 443
———, **with Stern, T. W., Evans, H. T., Jr., and Sherwood, A. M. Doloresite, a new vanadium oxide mineral from the Colorado plateau**........ 587
Stilleite (Ramdohr).............. 584
Stone, J., with Hewett, D. F. Uranothorite near Forest Home, San Bernardino County, California......... 104
Stone, J., with Hewett, D. F., and Levine, H. Brannerite from San Bernardino County, California...................... 30
Structure Reports for 1940–1941, Vol. 8 (Wilson, Editor) (Book Review)..................... 435
Strunz, H.......117, 444, 586, 920, 921
Sturm, E., with Lodding, W. A new method of differential thermal analysis employing multiple thermocouples.............. 78
Substitution of OH^- **by** F^- **in vari-**

ous hydroxylic minerals, studies by (Romo, Roy) ... 165

Sulfides and arsenides, differential thermal analysis of (Kopp, Kerr) ... 445

Sun, M. S. The nature of iddingsite in some basaltic rocks of New Mexico ... 525

Switzer, G. Hydrocuprite discredited ... 115

Syneček, V. ... 121

Talktriplite (=ferroan wagnerite) (Henriques) ... 586

Tamura, T. Identification of the 14 Å clay mineral component ... 107

Tennant, C. B., and Berger, R. W. *X*-ray determination of the dolomite-calcite ratio of a carbonate rock ... 23

Termierite (=mixture) (Orcel, Hénin, Caillère) ... 586

Theophrastus on Stones (Caley, Richards) (Book Review) ... 437

Thermal expansions of thoria, periclase and diamond (Skinner). 39

Thermal increment diffractometer (Bassett, Lapham) ... 548

Thin sections, two new types of holders used in grinding (Cochran, King) ... 422

Thompson, C. S., and Wadsworth, M. E. Determination of the composition of plagioclase feldspars by means of infrared spectroscopy ... 334

Thompson, J. B., Jr. The graphical analysis of mineral assemblages in pelitic schists ... 842

Thompson, M. E. ... 117, 443

———, Roach, C. H., and Meyrowitz, R. Duttonite, a new quadrivalent vanadium oxide from the Peanut Mine, Montrose County, Colorado ... 455

Thoria, thermal expansion of (Skinner) ... 39

Thorite, hydrothermal synthesis of (Frondel, Collette) ... 759

Tilley, C. E. Paragenesis of anthophyllite and hornblende from the Bancroft area, Ontario ... 412

Titanclinohumite from the Wichita Mountains, Oklahoma (Huang) ... 686

Tokody, L. ... 704

Torbernite, zeunerite and uranospherite (Berman) ... 905

Toulmin, P., III. Notes on a peralkaline granite from Cashes Ledge, Gulf of Maine ... 912

Tourmaline, synthesis of by reaction of mineral grains with $NaCl\text{-}H_3BO_2$ solution, and its implications in rock metamorphism (Frondel, Collette). 754

Trichalcite (=tyrolite) (Guillemin) 123

Tri-kalsilite, a new mineral (Sahama, Smith) ... 286

Tsuboi Commemorative Volume .. 439

U and Th in accessory allanite of igneous rocks (Smith, Franck, Sherwood) ... 367

U-Pb, discordant ages and mineral type (Kulp, Eckelmann) ... 154

Ufertite (uferite) (Melkor, Gerasimovsky) ... 307

Ulexite and halotrichite, *x*-ray powder data for (Baur, Sand). 676

Umohoite from the Lucky Mc Mine, Wyoming (Coleman, Appleman) ... 657

Uraninite, high-thorian, three occurrences near Easton, Pennsylvania (Montgomery) ... 804

Uraninite, the role of lead and excess oxygen in (Berman) ... 705

Uranium, mineralogy of (Frondel). 125

Uranium minerals, secondary, at the W. Wilson Mine in the Boulder batholith, Montana (Emerson, Wright) ... 222

Uranium minerals, studies of (XXIII): torbernite, zeunerite and uranospherite (Berman) .. 905

Uranophane $[Ca(H_3O)_2](UO_2)_2(SiO_4)_2 \cdot 3H_2O$, the crystal structure of (Smith, Gruner, Lipscomb) ... 594

Uranothorite near Forest Home, San Bernardino County, California (Hewett, Stone)....... 104
Urgite (Getseva)................ 442
Utahite (=jarosite) (Moss)....... 586

Varulites and alluaudites (Fisher). 661
Vesbine (=volborthite) (Guillemin) 444
Vinnichenko, N. T............... 441
Vinogradovite (Semenov, Bohnshtedt-Kupletskaya, Moleva, Sludskaya).................. 308
Vorratsberechnung Mineralischer Rohstoffe (German trans. by O. Oelsner and E. Peukert) (Prokofjew) (Book Review) . 437

Wadsworth, M. E., with Thompson, C. S. Determination of the composition of plagioclase feldspars by means of infrared spectroscopy................ 334
Waltherite (=walpurgite) (Fisher) 121
Wardite, avelinoite and cyrilovite, relationship of the minerals (Lindberg)................ 204
Waugh, J. T. L.................. 443
Wenden, H. E. Ionic diffusion and the properties of quartz. (1) The direct current resistivity. 859
Whittaker, E. J. W............... 585
Winchell, H. Large angular aperture and useful interference figures..................... 570
Wolsendorfite (Protas)........... 919
Woodhouse, C. D., and Norris, R. M. A new occurrence of millerite................... 113
Wright, H. D., with Emerson, D. O. Secondary uranium minerals at the W. Wilson mine in the Boulder batholith, Montana.. 222
Wurtzite-greenockite series (Hurlbut)...................... 184

X-ray powder diffractometer patterns, experimental error in determining certain peak locations and distances between peaks in (Chayes, MacKenzie) 534

Yakhontova, L. K.............307, 583
Yamasaki, M., with Seki, Y. Aluminian ferroanthophyllite from the Kitakami Mountainland, northeastern Japan......... 506
Yarzhemskii, Y. Y............... 704
Yoder, H. S., Jr., and Sahama, T. G. Olivine *x*-ray determinative curve.................. 475
Young, G. A., Bellizzia, A., Renz, H. H., Johnson, F. W., Robie, R. H., and Mas Vall, J. Geología de las Cuencas Sedimentarias de Venezuela y de sus Campos Petrolíferos (Book Review)................... 579

Zak, L.......................... 121
Zen, E-an. Preliminary report on the mineralogy and petrology of some marine bottom samples off the coast of Peru and Chile...................... 890
Zircon, thorite and huttonite, hydrothermal synthesis of (Frondel, Collette)............... 759
Zirconolite (Borodin, Nazarenko, Richter)................... 581
Zussman, J..................... 585
———, and Brindley, G. W. Serpentines with 6-layer orthohexagonal cells............. 666
———, with Brindley, G. W. A structural study of the thermal transformation of serpentine minerals to forsterite........ 461
———, Brindley, G. W., and and Comer, J. J. Electron diffraction studies of serpentine minerals.................. 133